

2013-07-10

# Modulation of Human Rhinovirus-Induced Epithelial Responses by Cigarette Smoke

Hudy, Magdalena

---

Hudy, M. (2013). Modulation of Human Rhinovirus-Induced Epithelial Responses by Cigarette Smoke (Doctoral thesis, University of Calgary, Calgary, Canada). Retrieved from <https://prism.ucalgary.ca>. doi:10.11575/PRISM/26978

<http://hdl.handle.net/11023/781>

*Downloaded from PRISM Repository, University of Calgary*

UNIVERSITY OF CALGARY

Modulation of Human Rhinovirus-Induced Epithelial Responses by Cigarette Smoke

by

Magdalena Hanna Hudy

A THESIS

SUBMITTED TO THE FACULTY OF GRADUATE STUDIES  
IN PARTIAL FULFILMENT OF THE REQUIREMENTS FOR THE  
DEGREE OF DOCTOR OF PHILOSOPHY

DEPARTMENT OF MEDICAL SCIENCE

CALGARY, ALBERTA

JULY, 2013

© Magdalena Hanna Hudy 2013

## Abstract

Human rhinovirus (HRV) is the major viral pathogen associated with exacerbations of asthma and chronic obstructive pulmonary disease (COPD). Cigarette smoke is the predominant risk factor for the development of COPD and approximately 25% of asthmatics smoke. Moreover, smokers experience longer and more severe respiratory tract infections compared to non-smokers, but the mechanisms responsible have not been delineated. Since the airway epithelial cell is the only cell type shown to be infected with HRV *in vivo*, and is one of the first cells in contact with cigarette smoke, the aim of this thesis was to investigate if and how cigarette smoke modulates epithelial responses to HRV infection using an *in vitro* tissue culture model system in conjunction with HRV and cigarette smoke extract (CSE).

HRV-induced expression of CXCL10, a chemokine linked to antiviral immunity, was potently inhibited by CSE via multiple mechanisms. CSE suppressed HRV-induced transcription of CXCL10 via inhibition of nuclear factor- $\kappa$ B (NF- $\kappa$ B), interferon regulatory factor (IRF)-1 and signal transducer and activator of transcription (STAT)-1 pathways. CSE also suppressed HRV-induced expression of the viral sensors melanoma differentiation-associated protein 5 (MDA5) and retinoic acid-inducible gene-I (RIG-I), but only MDA5 was shown to be directly involved in HRV-induced CXCL10 production. CSE also suppressed HRV-induced chromatin accessibility around the CXCL10 transcriptional start site.

By contrast, epithelial production of the neutrophil chemoattractant CXCL8, was induced by CSE or HRV infection alone, and was further enhanced by the combination of these stimuli. This enhancement was mediated via mRNA stabilization and involved the mRNA stabilizing protein human antigen R (HuR).

This study provides the first demonstration that CSE differentially modulates HRV-induced chemokine responses in airway epithelial cells and provides insights into the underlying mechanisms of altered chemokine production. HRV-induced CXCL10 was suppressed by CSE via a combination of multiple mechanisms, while CXCL8 enhancement was mediated via mRNA stabilization. These results provide potential insights into how cigarette smoke alters HRV-induced inflammatory responses *in vivo* and how this could lead to more severe clinical outcomes in COPD patients and asthmatics who smoke during HRV-induced disease exacerbations.

## Acknowledgements

This thesis would not be possible without the guidance and support of many people. I would like to take this opportunity to thank all those that have contributed to my journey as a PhD student, allowing me to grow as a person and a scientist.

Thank you to my supervisor David Proud, for his exceptional guidance. Although he accepted me with no previous research experience, he still let me learn, make mistakes, and succeed without having to hold my hand every step of the way. He has taught me that the best way to learn is by overcoming failure and finding your own solutions. He encouraged my passion for science and exemplified the first-rate researcher that I aspire to be.

Thank you to my PhD Committee for encouraging me with both positive and constructive feedback, and by always making me strive to be a better scientist. Thank you to Richard Leigh for his support, interest and thought-provoking questions. It would be an honor and a privilege to have colleagues of your caliber one day.

Thank you to the members of the Proud-Leigh lab, both past and present. You have all contributed to this project in some way. In particular, thank you to all those that contributed to the gene array study. Moreover, thank you for encouraging me, supporting me, listening to me vent, helping me with experiments (or helping with trouble-shooting when they didn't work) and, most of all, thank you for the stimulating conversations and making me laugh. I could not have asked for a better group of people to work with and will always remember these last 5+ years fondly.

I would like to express a huge thank you to those that have provided the funding for the research that went into this thesis: Alberta Innovates - Health Solutions, The Lung Association of Alberta and NWT, University of Calgary and the Canadian Institutes of Health Research.

I would also like to express my thanks to all of my family and friends for their unwavering love, support and encouragement throughout my whole academic career. Thank you to my parents, Ewa and Arek, for letting me find my own way, even though it took well over a decade. Bet you never thought I would stop being a student, and really, I never will!

Lastly, thank you to my wonderful husband, Ben. You were there for me every step of the way for the last 15 years and were my rock in the toughest year of my life. I could never have done this without you.

## Table of Contents

Abstract.....	ii
Acknowledgements.....	iv
List of Tables .....	x
List of Figures and Illustrations .....	xi
List of Symbols, Abbreviations and Nomenclature.....	xv
Epigraph.....	xx
CHAPTER ONE: INTRODUCTION.....	1
1.1 COPD.....	3
1.1.1 Definition.....	3
1.1.2 Burden of Disease.....	5
1.1.3 Etiology and Pathogenesis.....	7
1.1.4 Exacerbations .....	8
1.2 Asthma.....	10
1.2.1 Definition.....	10
1.2.2 Burden of Disease.....	11
1.2.3 Etiology and Pathogenesis.....	12
1.2.4 Asthma and Cigarette Smoking.....	13
1.2.5 Exacerbations .....	14
1.3 HRV .....	16
1.3.1 Prevalence, Incidence, Pathogenesis and Symptoms .....	16
1.3.2 Infection of Airway Epithelium.....	17
1.3.3 Classification .....	19
1.3.4 Receptor Usage and Cell Entry .....	22
1.3.5 Replication.....	22
1.3.6 Immune Response .....	23
1.4 Cigarette Smoke.....	25
1.4.1 Cigarette Smoke and Respiratory Infections.....	27
1.4.2 Airway Epithelium and Cigarette Smoke.....	28
1.5 Airway Epithelium.....	29
1.5.1 Structure and Function .....	29
1.5.2 Airway Epithelium in COPD.....	31
1.5.3 Airway Epithelium in Asthma.....	32
1.6 Chemokines .....	32
1.6.1 Classification and Function .....	32
1.6.2 CXCL10 .....	34
1.6.2.1 CXCL10: Role during HRV infections .....	35
1.6.2.2 CXCL10: Role in smokers, COPD and asthma.....	36
1.6.3 CXCL8 .....	37
1.6.3.1 CXCL8: Role during HRV infections .....	38
1.6.3.2 CXCL8: Role in smokers, COPD and asthma.....	38
1.7 Gene Regulation .....	39
1.7.1 Transcriptional Regulation.....	42

1.7.1.1 NF- $\kappa$ B .....	42
1.7.1.2 IRFs.....	44
1.7.1.3 STATs.....	45
1.7.2 Post-Transcriptional Regulation.....	49
1.7.2.1 mRNA stability .....	50
1.7.3 Epigenetic Regulation .....	53
1.8 Objective.....	56
1.9 Hypothesis .....	56
1.10 Thesis Aims .....	57
1.10.1 Aim 1 .....	57
1.10.2 Aim 2 .....	57
1.10.3 Aim 3 .....	57
<b>CHAPTER TWO: MATERIALS AND METHODS .....</b>	<b>58</b>
2.1 Materials .....	59
2.2 Human Epithelial Cell Culture .....	63
2.2.1 Primary human bronchial epithelial (HBE) cell isolation and culture .....	63
2.2.2 Bronchial epithelial cell line (BEAS-2B) culture.....	64
2.3 HRV Propagation and Purification.....	65
2.3.1 HRV-16 .....	65
2.3.2 HRV-1A .....	66
2.3.3 Viral titre .....	66
2.4 HRV Infection of Airway Epithelial Cells .....	67
2.5 Transfection of Cells with Synthetic dsRNA .....	67
2.6 Preparation of CSE .....	68
2.7 Treatment of Cells with Nicotine.....	69
2.8 Measuring Cell Viability .....	70
2.8.1 3-(4,5-dimethylthiazol-2-yl)-2,5-diphenyltetrazolium bromide (MTT) assay.....	70
2.8.2 Lactate dehydrogenase (LDH) assay.....	70
2.9 Viral Titre Assay.....	71
2.10 Flow Cytometry .....	72
2.11 Gene Array Analysis.....	73
2.12 RNA Isolation, DNase Treatment, cDNA Preparation and Real-Time RT-PCR.....	74
2.12.1 RNA isolation.....	74
2.12.2 DNase treatment .....	75
2.12.3 cDNA preparation .....	75
2.12.4 Real-time RT-PCR .....	76
2.13 Enzyme Linked Immunosorbent Assay (ELISA).....	79
2.13.1 CXCL10 .....	79
2.13.2 CXCL8 .....	80
2.14 Western Blotting.....	81
2.14.1 Whole cell lysate extraction .....	81
2.14.2 Protein assay .....	81
2.14.3 Sodium dodecyl sulphate – polyacrylamide gel electrophoresis (SDS-PAGE) and protein transfer .....	82

2.14.4 Immunoblotting .....	82
2.14.5 Assessment of equal protein loading.....	86
2.14.6 Densitometry .....	86
2.15 Luciferase Reporter Assay.....	87
2.15.1 CXCL10 promoter constructs.....	87
2.15.2 CXCL8 promoter constructs.....	89
2.15.3 Transient transfection and luciferase assay .....	90
2.16 Actinomycin D Chase Assay .....	91
2.17 Inhibitors and siRNA .....	91
2.17.1 IKK $\beta$ inhibitor .....	91
2.17.2 JAK inhibitor .....	92
2.17.3 p38 MAPK inhibitor.....	92
2.17.4 siRNA .....	93
2.18 Electrophoretic Mobility Shift Assay (EMSA) .....	95
2.18.1 Nuclear extraction and protein quantification .....	95
2.18.2 Oligonucleotide generation, annealing and end-labelling .....	96
2.18.3 EMSA binding reaction and non-denaturing PAGE .....	97
2.18.4 Supershift assays .....	98
2.19 Chromatin Accessibility Assay.....	99
2.19.1 In situ chromatin digestion.....	100
2.19.2 Genomic DNA isolation .....	100
2.19.3 Primer design and real-time PCR analysis .....	101
2.20 Chromatin Immunoprecipitation (ChIP) Assay .....	103
2.20.1 Cell fixation .....	103
2.20.2 Chromatin shearing by sonication.....	104
2.20.3 DNA clean-up and concentration determination.....	105
2.20.4 ChIP.....	106
2.20.5 PCR analysis.....	108
2.20.5.1 Conventional PCR .....	108
2.20.5.2 Real-Time PCR.....	109
2.21 H & E.....	110
2.22 Statistical Analyses .....	111
<b>CHAPTER THREE: CSE DIFFERENTIALLY MODULATES HRV-INDUCED CHEMOKINE RESPONSES IN AIRWAY EPITHELIAL CELLS.....</b>	<b>112</b>
3.1 Background.....	113
3.1.1 Effects of cigarette smoke on HRV-induced CXCL10 .....	114
3.1.2 Effects of cigarette smoke on HRV-induced CXCL8 .....	114
3.2 Hypothesis .....	115
3.3 Results.....	115
3.3.1 CSE alone or in combination with HRV-16 is not overtly cytotoxic to airway epithelial cells .....	115
3.3.2 CSE inhibits HRV-16-induced CXCL10 in airway epithelial cells .....	118
3.3.3 CSE and HRV-16 each induce CXCL8 alone and at least additively increase CXCL8 in combination in airway epithelial cells.....	126

3.3.4 CSE modulates HRV-1A-induced CXCL10 and CXCL8 from airway epithelial cells .....	131
3.3.5 Inhibition of CXCL10 and induction of CXCL8 is unaffected by “aging” of CSE. ....	132
3.3.6 Nicotine does not mimic the modulating effects of CSE on HRV-16-induced CXCL10 and CXCL8 .....	135
3.4 Discussion.....	137
CHAPTER FOUR: MODULATION OF HRV-INDUCED CHEMOKINE PRODUCTION BY CSE IS INDEPENDENT OF EFFECTS ON RECEPTOR EXPRESSION AND VIRAL REPLICATION .....	139
4.1 Background.....	140
4.2 Hypothesis .....	140
4.3 Results.....	140
4.3.1 CSE alone or in combination with HRV-16 does not alter the number of airway epithelial cells expressing the HRV-16 receptor, ICAM-1.....	140
4.3.2 CSE does not affect HRV-16 titre in airway epithelial cells.....	142
4.3.3 CSE inhibits poly [I:C]-induced CXCL10 and poly [I:C]+CSE enhance CXCL8 above either stimulus alone in airway epithelial cells. ....	143
4.4 Discussion.....	146
4.5 Future Studies .....	149
CHAPTER FIVE: MECHANISMS OF HRV-INDUCED CXCL10 INHIBITION BY CSE ...	150
5.1 Background.....	151
5.1.1 Regulation of CXCL10 expression by HRV .....	151
5.1.2 Regulation of CXCL10 expression by cigarette smoke .....	152
5.2 Hypothesis .....	152
5.3 Results.....	152
5.3.1 CSE suppresses HRV-induced and poly [I:C]-induced CXCL10 promoter activation.....	152
5.3.2 HRV-16-induced CXCL10 promoter activation is suppressed by CSE but not dependent on activator protein 1 (AP-1).....	155
5.3.3 Inhibition of HRV-16-induced CXCL10 by CSE is partially dependent on inhibition of NF- $\kappa$ B.....	157
5.3.4 Inhibition of HRV-16-induced CXCL10 by CSE is partially dependent on inhibition of IRF-1 .....	164
5.3.5 Induction of HRV-16-induced CXCL10 and its inhibition by CSE is partially dependent on STAT-1.....	168
5.3.6 ChIP of HRV-induced CXCL10 with NF- $\kappa$ B and IRF-1 .....	179
5.3.7 Induction of HRV-16-induced CXCL10 and its inhibition by CSE is partially dependent on MDA5.....	181
5.3.8 Inhibition of HRV-16-induced CXCL10 by CSE is, in part, regulated epigenetically .....	189
5.4 Discussion.....	190
5.5 Future Studies .....	202

CHAPTER SIX: MECHANISMS OF CXCL8 ENHANCEMENT BY THE COMBINATION OF HRV AND CSE.....	204
6.1 Background.....	205
6.1.1 Transcriptional regulation of CXCL8 .....	205
6.1.1.1 Transcriptional Regulation of CXCL8 by HRV .....	206
6.1.1.2 Transcriptional Regulation of CXCL8 by Cigarette Smoke.....	207
6.1.2 Post-transcriptional regulation of CXCL8.....	208
6.1.2.1 Post-Transcriptional Regulation of CXCL8 by HRV.....	210
6.1.2.2 Post-Transcriptional Regulation of CXCL8 by Cigarette Smoke .....	210
6.2 Hypothesis .....	211
6.3 Results.....	211
6.3.1 HRV-16-induced CXCL8 enhancement by CSE is not regulated transcriptionally	211
6.3.2 The combination of HRV-16 and CSE stabilizes CXCL8 mRNA.....	213
6.3.3 The p38 MAPK pathway is involved in CSE-induced and HRV-16+CSE-induced CXCL8.....	215
6.3.4 CSE, HRV-16 and HRV-16+CSE all fail to alter the expression of AUF-1, KHSRP or HuR.....	218
6.3.5 HuR is involved in enhancement of CXCL8 by the combination of HRV-16+CSE	222
6.4 Discussion.....	229
6.5 Future Studies .....	234
CHAPTER SEVEN: GENERAL DISCUSSION, LIMITATIONS, FUTURE DIRECTIONS AND CLINICAL RELEVANCE .....	235
7.1 General Discussion .....	236
7.1.1 Rationale of study.....	236
7.1.2 CSE differentially modulates HRV-induced chemokine expression in airway epithelial cells .....	237
7.1.3 CSE inhibits HRV-induced CXCL10 via multiple mechanisms.....	241
7.1.4 CSE enhances HRV-induced CXCL8 via mRNA stabilization .....	245
7.2 Limitations .....	247
7.3 Future Directions .....	251
7.4 Clinical Relevance .....	253
7.5 Overall Conclusions.....	256
REFERENCES .....	259
APPENDIX A: PUBLICATIONS LIST .....	302
APPENDIX B: COPYRIGHT PERMISSION .....	304

## List of Tables

Table 1.1: GOLD Defined Stages of COPD.....	4
Table 1.2: Inflammatory, Host-Defense and Anti-Viral Mediators Induced by HRV in the Airway Epithelium.....	19
Table 2.1: Treatment Groups for Flow Cytometry Experiments.....	72
Table 2.2: Real-Time RT-PCR Primers and Probes.....	77
Table 2.3: Real-Time RT-PCR Standard Sequences.....	78
Table 2.4: Western Blotting Antibodies.....	83
Table 2.5: CXCL10 Promoter Point Mutation Primer Sequences.....	89
Table 2.6: siRNA Information.....	94
Table 2.7: EMSA Oligonucleotide Sequences.....	96
Table 2.8: Supershift Assay Antibodies.....	99
Table 2.9: ChIP Reaction Components.....	106
Table 2.10: Antibodies Used in the ChIP Reaction.....	107

## List of Figures and Illustrations

Figure 1.1: Viral pathogens associated with exacerbations of COPD.....	10
Figure 1.2: Viral pathogens associated with exacerbations of asthma in adults.....	14
Figure 1.3: Schematic diagram of the HRV genome.....	20
Figure 1.4: Human airway structure. ....	31
Figure 1.5: Simplified mammalian MAPK signalling pathway. ....	42
Figure 1.6: Canonical NF- $\kappa$ B signalling pathway. ....	44
Figure 1.7: The canonical JAK-STAT pathway and its negative regulation.....	46
Figure 1.8: The IFN-mediated JAK/STAT pathways.....	48
Figure 2.1: 3R4F research grade cigarettes and syringe apparatus used to generate CSE. ....	69
Figure 3.1: CSE alone or in combination with HRV-16 does not overtly affect cell viability of airway epithelial cells at concentrations of $\leq 50\%$ CSE.....	117
Figure 3.2: Time-course of HRV-16-induced CXCL10 in airway epithelial cells.....	119
Figure 3.3: CSE inhibits HRV-16-induced CXCL10 in airway epithelial cells as assessed by gene microarray. ....	121
Figure 3.4: CSE inhibits HRV-16-induced CXCL10 in airway epithelial cells.....	123
Figure 3.5: At a variety of concentrations CSE inhibits HRV-16-induced CXCL10 in airway epithelial cells. ....	124
Figure 3.6: Even at low concentrations, CSE inhibits HRV-16-induced CXCL10 in airway epithelial cells. ....	125
Figure 3.7: Time-course of CSE-induced CXCL8 in airway epithelial cells. ....	127
Figure 3.8: CSE and HRV-16 each induce CXCL8 alone and at least additively increase CXCL8 in combination in airway epithelial cells.....	128
Figure 3.9: Time-course of CSE-induced and HRV-16-induced CXCL8 protein release from airway epithelial cells. ....	129
Figure 3.10: CSE concentration-dependently induces CXCL8 alone and in combination with HRV-16 in airway epithelial cells.....	130

Figure 3.11: CSE modulates HRV-1A-induced CXCL10 and CXCL8 from airway epithelial cells. ....	132
Figure 3.12: The effects of freshly prepared versus “aged” CSE alone or in combination with HRV-16 on CXCL10 and CXCL8 production in airway epithelial cells. ....	134
Figure 3.13: The effects of nicotine alone or in combination with HRV-16 on airway epithelial cell viability and chemokine production. ....	136
Figure 4.1: CSE alone, HRV-16 alone or the combination of HRV-16+CSE do not alter the number of airway epithelial cells expressing ICAM-1 but both HRV-16 alone and HRV-16+CSE increase the number of ICAM-1 receptors per cell. ....	141
Figure 4.2: CSE does not affect HRV-16 titre in airway epithelial cells.....	142
Figure 4.3: CSE alone or in combination with poly [I:C] does not overtly affect airway epithelial cell viability.....	144
Figure 4.4: CSE inhibits poly [I:C]-induced CXCL10 in airway epithelial cells. ....	145
Figure 4.5: CSE and poly [I:C] each induce CXCL8 alone and further increase CXCL8 in combination in airway epithelial cells. ....	146
Figure 5.1: Schematic diagram of the putative CXCL10 promoter.....	151
Figure 5.2: CSE inhibits both HRV-16-induced and poly [I:C]-induced CXCL10 promoter activation in airway epithelial cells.....	154
Figure 5.3: Effects of point mutations on CXCL10 promoter activation in airway epithelial cells. ....	156
Figure 5.4: Induction of CXCL10 protein by HRV-16 is partially dependent on transcriptional activation by NF- $\kappa$ B.....	158
Figure 5.5: CSE inhibits HRV-16-induced promoter activation of two CXCL10-specific NF- $\kappa$ B recognition sequences. ....	159
Figure 5.6: CSE inhibits HRV-16-induced NF- $\kappa$ B translocation/binding to the CXCL10-specific NF- $\kappa$ B recognition sequences.....	161
Figure 5.7: HRV-16-induced phosphorylation of I $\kappa$ B $\alpha$ is inhibited by CSE in airway epithelial cells. ....	163
Figure 5.8: CSE inhibits HRV-induced IRF-1 translocation/binding to the CXCL10-specific ISRE recognition sequence.....	165
Figure 5.9: CSE inhibits HRV-16-induced IRF-1 expression in airway epithelial cells.....	167

Figure 5.10: IRF-2 expression is not altered by CSE, HRV-16 or the combination in airway epithelial cells. ....	168
Figure 5.11: Effects of CXCL10 promoter truncation on activation by HRV-16 in airway epithelial cells. ....	169
Figure 5.12: Effects of STAT site point mutations on CXCL10 promoter activation in airway epithelial cells. ....	171
Figure 5.13: CSE inhibits HRV-induced transcription factor translocation/binding to the CXCL10-specific STAT recognition sequence. ....	173
Figure 5.14: CSE inhibits HRV-16-induced p-STAT-1 in airway epithelial cells. ....	175
Figure 5.15: HRV-16 induces p-STAT-1 as early as 9 h post-treatment and this induction is inhibited in the presence of CSE in airway epithelial cells.....	176
Figure 5.16: HRV-16-induced CXCL10 is concentration-dependently inhibited in the presence of a specific JAK inhibitor. ....	177
Figure 5.17: Effects of STAT-1-targeting siRNA on p-STAT-1 knock-down and CXCL10 protein expression in airway epithelial cells. ....	179
Figure 5.18: ChIP Optimization.....	180
Figure 5.19: CSE inhibits HRV-16-induced RIG-I and MDA5 in airway epithelial cells. ....	184
Figure 5.20: Time-course of RIG-I and MDA5 induction by HRV-16 and inhibition in the presence of CSE in airway epithelial cells.....	184
Figure 5.21: Knock-down of HRV-16-induced RIG-I does not affect CXCL10 protein expression in airway epithelial cells. ....	187
Figure 5.22: Knock-down of HRV-16-induced MDA5 results in suppression of CXCL10 protein expression in airway epithelial cells. ....	188
Figure 5.23: HRV-induced chromatin accessibility of the CXCL10 promoter region is partially suppressed by CSE. ....	190
Figure 6.1: Schematic diagrams of the putative CXCL8 promoter and mRNA transcript. ....	208
Figure 6.2: HRV-16-induced CXCL8 enhancement by CSE is not regulated transcriptionally in airway epithelial cells. ....	213
Figure 6.3: The combination of HRV-16 and CSE stabilizes CXCL8 mRNA in airway epithelial cells. ....	215

Figure 6.4: The p38 MAPK pathway is involved in CSE-induced and HRV-16+CSE-induced CXCL8 production in airway epithelial cells. ....	218
Figure 6.5: CSE alone, HRV-16 alone or the combination of the two stimuli does not alter the expression of ARE-binding proteins AUF-1, KHSRP and HuR at early time-points in airway epithelial cells. ....	220
Figure 6.6: CSE alone, HRV-16 alone or the combination of the two stimuli does not alter the expression of ARE-binding proteins AUF-1 and HuR at later time-points in airway epithelial cells. ....	221
Figure 6.7: CXCL8 protein production is enhanced by HRV-16+CSE compared to CSE or HRV-16 alone in airway epithelial cells. ....	223
Figure 6.8: Effects of AUF-1-targeting siRNA on CXCL8 protein expression in airway epithelial cells. ....	226
Figure 6.9: Effects of KHSRP-targeting siRNA on CXCL8 protein expression in airway epithelial cells. ....	227
Figure 6.10: Effects of HuR-targeting siRNA on CXCL8 protein expression in airway epithelial cells. ....	228
Figure 7.1: CSE differentially regulates HRV-induced chemokine production in human airway epithelial cells. ....	258

## List of Symbols, Abbreviations and Nomenclature

<u>Symbol</u>	<u>Definition</u>
ABTS	2,2'-azino-bis (3-ethylbenzthiazoline-6-sulphonic acid)
AHR	Airway hyperresponsiveness
ALI	Air-liquid interface
ANOVA	Analysis of variance
AP-1	Activator protein-1
ARE	Adenine and uridine-rich elements
ARE-BP	ARE-binding protein
ASF	Airway surface fluid
AUF-1	Adenine and uridine-rich factor-1
BAL	Bronchoalveolar lavage
BEAS-2B	Bronchial epithelial cell line
BEBM	Bronchial epithelial basal medium
BEGM	Bronchial epithelial growth medium
BSA	Bovine serum albumin
CARD	Caspase activation and recruitment domain
CARDIF	CARD adapter inducing IFN- $\beta$
C/EBP- $\beta$	CCAAT/enhancer-binding protein- $\beta$
ChIP	Chromatin immunoprecipitation
CL	Clover leaf
COPD	Chronic obstructive pulmonary disease
CSE	Cigarette smoke extract
DAMP	Danger-associated molecular pattern
DARC	Duffy antigen receptor for chemokines
DC	Dendritic cell
DMEM	Dulbecco's modified eagle medium
DMSO	Dimethyl sulfoxide
dsRNA	Double stranded RNA

DTT	Dithiothreitol
ECL	Enhanced chemiluminescent
EDTA	Ethylenediaminetetraacetic acid
ELAV	Embryonic lethal, abnormal vision
ELISA	Enzyme-linked immunosorbent assay
EMSA	Electrophoretic mobility shift assay
ERK	Extracellular signal-regulated kinase
FBS	Fetal bovine serum
FEV <sub>1</sub>	Forced expiratory volume in one second
FVC	Forced vital capacity
GAPDH	Glyceraldehyde-3-phosphate-dehydrogenase
GAS	IFN- $\gamma$ -activated site
GINA	Global Initiative for Asthma
GOLD	Global Initiative for Chronic Obstructive Lung Disease
GPCR	G-protein-coupled receptor
HAT	Histone acetyltransferase
HBE	Human bronchial epithelial
HBSS	Hank's balanced salt solution
HDAC	Histone deacetylase
H & E	Haematoxylin and eosin
HEPES	4-(2-hydroxyethyl)-1-piperazineethanesulfonic acid
hnRNPD	Heterogeneous nuclear ribonucleoprotein D
HRP	Horseradish peroxidase
HRV	Human rhinovirus
HSA	Human serum albumin
HuR	Human antigen R
ICAM	Intracellular adhesion molecule
IFN	Interferon
Ig	Immunoglobulin
I $\kappa$ B	Inhibitor of NF- $\kappa$ B

IKK	I $\kappa$ B kinase
IL	Interleukin
IP-10	IFN- $\gamma$ -inducible protein of 10 kDa
IPS-1	IFN- $\beta$ promoter stimulator-1
IRES	Internal ribosomal entry site
IRF	Interferon regulatory factor
ISG	Interferon-stimulated gene
ISGF3	Interferon-stimulated gene factor 3
ISRE	Interferon-stimulated response element
JAK	Janus kinase
JNK	c-Jun amino terminal kinase
KC	Keratinocyte-derived chemokine
KHSRP	K-homology domain splicing regulatory protein
LB	Luria-Bertani
LDH	Lactate dehydrogenase
LDL	Low density lipoprotein
LPS	Lipopolysaccharide
MAF	Mammary gland factor
MAPK	Mitogen-activated protein kinase
MAVS	Mitochondrial antiviral signaling protein
MDA5	Melanoma differentiation-associated gene 5
MDNCF	Monocyte-derived neutrophil chemotactic factor
MIP-2	Macrophage inflammatory protein-2
miRNA	Micro RNA
MK2	p38-MAPK-activated kinase 2
MMP	Matrix metalloproteinase
MTT	3-(4,5-dimethylthiazol-2-yl)-2,5-diphenyltetrazolium bromide
NAF	Neutrophil-activating factor
NAP-1	Neutrophil-activating peptide 1
NEMO	NF- $\kappa$ B essential modulator

NF- $\kappa$ B	Nuclear factor-kappa B
NIH	National Institutes of Health
NK	Natural killer
PAMP	Pathogen-associated molecular patterns
PARN	Poly (A) ribonuclease
PBS	Phosphate-buffered saline
P-bodies	Processing bodies
PEF	Peak expiratory flow
PIAS	Protein inhibitor of activated STAT
PIC	Protease inhibitor cocktail
PIPES	Piperazine-N,N-bis (2-ethanesulfonic acid)
PKR	Protein kinase R
PMSF	Phenylmethanesulfonylfluoride
Poly [I:C]	Polyionosinic-polycytidylic acid
PRR	Pathogen recognition receptors
PTP	Protein tyrosine phosphatase
RIG-I	Retinoic acid-inducible gene-I
RLR	RIG-like receptor
RLU	Relative light units
ROS	Reactive oxygen species
RSV	Respiratory syncytial virus
RT	Room temperature
RT-PCR	Reverse transcription-polymerase chain reaction
SEM	Standard error of the mean
SDS-PAGE	Sodium dodecyl sulphate – polyacrylamide gel electrophoresis
SH2	Src-homology 2
SIRT	Sirtuin/silent information regulator
SOCS	Suppressor of cytokine signalling
ssRNA	Single stranded RNA
STAT	Signal transducer and activator of transcription

TAD	Transcriptional activation domains
TBE	Tris/borate/ethylenediaminetetraacetic acid
TBS	Tris-buffered saline
TCID <sub>50</sub>	50% tissue culture-infective dose
Th	T helper
TIR	Toll/IL-1 receptor
TLR	Toll-like receptor
TNF- $\alpha$	Tumor necrosis factor alpha
TRIF	TIR domain containing adaptor inducing IFN- $\beta$
TTBS	Tween-20 1X TBS
TTP	Tristetraprolin
UTR	Untranslated region
VISA	Virus-induced signaling adapter
VP	Viral capsid protein
VPg	Virion protein, genome-linked
WHO	World Health Organization
ZFP36	Zinc finger protein 36
7TM	Seven trans-membrane

## **Epigraph**

*There are no facts, only interpretations.*

-Friedrich Nietzsche, from *The Will to Power*

## Chapter One: **Introduction**

The lungs are among the most important major organs in the human body. Proper lung functioning is essential for effective gas exchange, protection from insults inhaled from the external environment and ultimately, survival. Lung diseases, such as chronic obstructive pulmonary disease (COPD) and asthma are associated not only with compromised lung function, but also with altered host inflammatory and functional responses to inhaled pathogens, allergens and pollutants. Understanding the mechanisms responsible for the underlying inflammatory response and impaired lung function is critical for future effective treatment of these diseases.

Human rhinovirus (HRV) is responsible for the majority of virally-induced exacerbations of COPD and asthma<sup>1-6</sup>. Cigarette smoking is the main risk factor associated with the development of COPD in developed countries and approximately a quarter of asthmatics smoke<sup>7-10</sup>. Smoking asthmatics tend to have worse respiratory symptoms, require more hospitalizations, are less responsive to conventional treatments and generally have a decreased quality of life compared to non-smoking asthmatic individuals<sup>11-23</sup>. Moreover, healthy smokers tend to experience upper respiratory tract infections of prolonged duration and increased severity compared to non-smokers<sup>24-29</sup>. *In vivo*, the human airway epithelium is the primary cell to be infected with HRV<sup>30</sup>, and this cell is also the first point of contact for inhaled cigarette smoke. The inflammatory responses induced in the airway epithelium by HRV have been rigorously studied, but surprisingly, if and how cigarette smoke modulates these responses has not been investigated in much detail. Thus, **the overall aim of this thesis was to investigate if and how cigarette smoke modulates HRV-induced inflammatory responses in the airway epithelium.** This would not only be

relevant to further understanding the inflammatory response induced in HRV-infected smokers, but particularly, and most importantly, in COPD patients and smoking asthmatics during HRV-induced exacerbations.

## 1.1 COPD

### *1.1.1 Definition*

COPD is defined by the Global Initiative for Chronic Obstructive Lung Disease (GOLD) as:

*“COPD, a common preventable and treatable disease, is characterized by persistent airflow limitation that is usually progressive and associated with an enhanced chronic inflammatory response in the airways and the lung to noxious particles or gases. Exacerbations and comorbidities contribute to the overall severity in individual patients”<sup>31</sup>*

The definition put forth by GOLD is extremely broad, as COPD is a complex and heterogeneous disease that encompasses a spectrum of conditions and disease severity. In terms of the pulmonary component, COPD includes varying degrees of chronic bronchitis, obstructive bronchiolitis and emphysema. Chronic bronchitis is defined as the presence of cough and sputum for a duration of at least three months in two or more consecutive years<sup>31</sup>. Obstructive bronchiolitis is also termed small airways disease and involves both components of inflammation and remodelling. Emphysema is defined as:

*“Abnormal permanent enlargement of air spaces distal to terminal bronchioles, accompanied by destruction of their walls without obvious fibrosis.”<sup>32</sup>*

Emphysema results from the destruction of the lung parenchymal tissue leading to a loss of alveolar attachments and a decrease in the elastic recoil of the lungs. Two types of emphysema have been identified, including centrilobular emphysema, which manifests predominantly in the upper lobes of the lung typically around the central lobules, and panlobular emphysema, which manifests more uniformly and predominantly involves the lower lobes of the lung<sup>33</sup>. The remodelling components of both obstructive bronchiolitis and emphysema are major contributors to airflow limitation in COPD resulting in a decline of forced expiratory volume in 1 second (FEV<sub>1</sub>), decreased lung volume expiration, gas trapping and hyperinflation. Extra-pulmonary components and comorbidities are also important factors in COPD<sup>34</sup>, some of the most common being hypertension, diabetes, coronary heart disease, cancer, pulmonary vascular disease and cachexia. Over two thirds of COPD patients report one or more comorbidities<sup>35</sup>.

The GOLD guidelines distinguish COPD into four stages based on the severity of airflow obstruction, as diagnosed by spirometry (**Table 1.1**).

**Table 1.1: GOLD Defined Stages of COPD**

Stage	Severity	FEV <sub>1</sub> /FVC	FEV <sub>1</sub>
I	Mild	<0.70	≥ 80% predicted
II	Moderate	<0.70	50% ≤ FEV <sub>1</sub> < 80% predicted
III	Severe	<0.70	30% ≤ FEV <sub>1</sub> < 50% predicted
IV	Very Severe	<0.70	< 30% predicted

FEV<sub>1</sub> = forced expiratory volume in 1 second.

FVC = forced vital capacity.

Chronic airway inflammation is a major component of COPD and is characterized by an increased abundance of inflammatory cells<sup>36</sup> including neutrophils, activated macrophages and activated CD8+ T-lymphocytes<sup>37-39</sup> along with a release of a variety of inflammatory mediators including various chemokines, cytokines, lipids and growth factors<sup>39</sup>. Proteolytic enzymes released from neutrophils and activated macrophages, including neutrophil elastase and matrix metalloproteinases (MMPs), lead to emphysematous destruction.

### ***1.1.2 Burden of Disease***

COPD is rapidly increasing in prevalence and is a huge burden to health care systems throughout the world. In a report released by the World Health Organization (WHO) in 2004, 63.6 million people were documented to be affected by symptomatic COPD<sup>40</sup> but a variety of studies suggest that it could be as high as 10% of the world's entire population<sup>41,42</sup>. The reason the number of those affected with COPD is likely to be much higher than currently reported by the WHO, is that a predicted 60-85% of patients remain undiagnosed, particularly those with mild disease<sup>43,44</sup>. Moreover, this disease accounted for 3 million deaths in 2004, making it the 4<sup>th</sup> leading cause of death worldwide<sup>45</sup>. Even in high-income countries like Canada, COPD is a major problem, being the 5<sup>th</sup> leading cause of death and the 10<sup>th</sup> leading cause of disability<sup>45</sup>. The Public Health Agency of Canada estimates that over 770,000 Canadians, or about 4% of the total population, have been diagnosed with COPD<sup>46</sup>, but the Conference Board of Canada reports that this number is actually much higher and, in fact, the number of people in

Canada affected with COPD was over 1.6 million in 2010 and is projected to increase to over 2.5 million by 2030<sup>47</sup>.

The economic burden of COPD is enormous, accounting for billions of health care dollars around the world<sup>35</sup>. In 2003, it was estimated that the combined direct and indirect costs of COPD in the USA alone were over 23 billion dollars<sup>48</sup>. In Canada, COPD exacerbations are the leading cause for hospital admission with an average cost of \$10,000 per patient, per visit<sup>49</sup>, and the total annual healthcare cost is estimated to be over 4 billion dollars and projected to increase to 9.5 billion dollars by 2030<sup>47</sup>. The exact numbers are hard to pin down due to under-diagnosis of this disease and the difficulty in calculating both the direct costs, including hospitalization and medication, and indirect costs, including lost work, long-term disability and premature death associated with this disease<sup>48</sup>. Nonetheless, it is estimated that hospitalization resulting from exacerbations account for the majority of costs associated with this disease, representing approximately 40-60% of the total direct costs<sup>50</sup>.

The prevalence and burden of COPD are projected to increase due to the continued exposure to COPD risk factors, such as cigarette smoking, and the changing age demographic of the world's population. Deaths due to COPD are projected to increase by more than 30% in the next 10 years<sup>51</sup> and it is predicted that by 2030, COPD will be the third leading cause of death and the fifth leading cause of disability world wide<sup>45,52</sup>. With the continued rise in prevalence of this disease the economic costs will, undoubtedly, keep increasing.

### ***1.1.3 Etiology and Pathogenesis***

Risk factors associated with the development of COPD include prolonged exposure to atmospheric pollutants, including cigarette smoke, smoke from burning biomass fuels, outdoor air pollution, occupational exposures in the form of dust, fumes and/or chemical irritants, as well as, very rarely, an  $\alpha_1$ -antitrypsin deficiency<sup>53,54</sup>.

The most common risk factor associated with the development of COPD is cigarette smoking<sup>10</sup>. In developed countries it accounts for more than 95% of cases<sup>39</sup>. In fact, most patients with COPD are current or ex-cigarette smokers, with at least a 15-20 pack-year smoking history. It has been previously thought that only about 10% of smokers go on to develop COPD<sup>41</sup>. Recently, it has been suggested that this is an underestimation and that over 25% of smokers may actually go on to develop this disease<sup>41,55</sup>. COPD usually takes decades to develop, and previous longitudinal studies looking at the development of COPD in smokers have only gone out as far as 5-10 years, whereas the aforementioned study followed a cohort of subjects for 25 years<sup>55</sup>. Interestingly, those subjects who were continuous smokers, as opposed to those who had quit at various points throughout this 25 year study, had a 35.5% incidence for the development of COPD. In addition to the extended time period of this study, these new statistics may also be reflective of the extended lifespan of the general population; the longer people live, the more time there is to develop COPD. Nevertheless, it still remains unclear as to why only a minority of cigarette smokers go on to develop COPD. The exact mechanisms as to how cigarette smoking can result in COPD are not yet clearly defined. Both a dysregulation in the natural balance of oxidants: antioxidants and proteases: anti-proteases have been suggested<sup>56-59</sup>.

One of the genetic risk factors associated with the development of COPD, namely  $\alpha$ 1-antitrypsin deficiency, supports the concept that a protease: anti-protease imbalance can contribute to the development of this disease. The incidence of  $\alpha$ 1-antitrypsin deficiency is fairly common in the general population with 1 in 2000-5000 individuals being affected<sup>60-62</sup> but only approximately 1-2% of COPD patients are reported to have  $\alpha$ 1-antitrypsin deficiency<sup>60,62</sup>. The deficiency of the gene coding for  $\alpha$ 1-antitrypsin results in an increased risk for the development of COPD with a major panlobular emphysematous component<sup>62,63</sup>. Normally,  $\alpha$ 1-antitrypsin is produced in the liver and distributed via the bloodstream and locally in the lung by macrophages and bronchial epithelial cells<sup>62</sup>. It is a very potent inhibitor of serine proteases, hence lack of this inhibitor plays a role in the dysregulation of the protease: anti-protease balance, resulting in the build-up of neutrophil elastase that is released from activated neutrophils, which ultimately leads to the destruction of surrounding tissue in the lung, including alveolar walls<sup>36,62</sup>. Importantly, cigarette smoking further increases the risk for developing COPD in individuals with  $\alpha$ 1-antitrypsin deficiency<sup>60,61</sup>.

#### ***1.1.4 Exacerbations***

Exacerbations of COPD are a major cause of hospital admission and are associated with a large proportion of health care costs related to this disease<sup>64-66</sup>. An exacerbation of COPD is defined as an event in the natural course of the disease that is characterized by changes in the patient's baseline dyspnea, cough and/or sputum production that is beyond normal day-to-day variations<sup>67</sup>. This event is usually acute in onset and may warrant a

change in the patient's medication<sup>67</sup>. The major symptoms include breathlessness, wheezing, chest tightness and an increase in cough and sputum production<sup>64,68</sup>. A significant decline in FEV<sub>1</sub>, forced vital capacity (FVC) and peak expiratory flow (PEF) are commonly associated with acute exacerbations of COPD<sup>64</sup>. It has been convincingly shown that the frequency of exacerbations correlates with disease progression in COPD<sup>69</sup>. Exacerbations lead to increased disease severity, decrease the patient's quality of life and increase the risk of disease-related mortality<sup>64,68,70,71</sup>.

The majority of COPD exacerbations (60-80%) are caused by respiratory infections<sup>43</sup>. Non-infectious causes of exacerbations include, but are not limited to, cardiac dysfunction, pulmonary embolism, pneumothorax, and exposure to air pollution or allergens<sup>43</sup>. Of the COPD exacerbations that are caused by pulmonary infections about half (40-60%) of those are associated with viruses<sup>1,2,72,73</sup>. Importantly, upper respiratory tract virus infections in COPD are associated with more frequent and severe exacerbations<sup>1,74</sup>. The main pathogen associated with viral exacerbation of COPD is HRV, which accounts for more than 50% of all viral exacerbations (**Figure 1.1**)<sup>1-4</sup>. Additional viruses associated with exacerbations of COPD include respiratory syncytial virus (RSV), coronavirus, influenza virus, parainfluenza virus, and very rarely other viruses such as adenovirus and human metapneumovirus<sup>64,75,76</sup>.

During an exacerbation of COPD, the underlying smoking-related airway inflammation is further exaggerated by the infective stimulus, resulting in an increase in infiltrating inflammatory cells into the lung including neutrophils and CD8+ T

lymphocytes<sup>77</sup>. However, the exact mechanisms underlying virus-induced exacerbations of COPD are still under investigation.

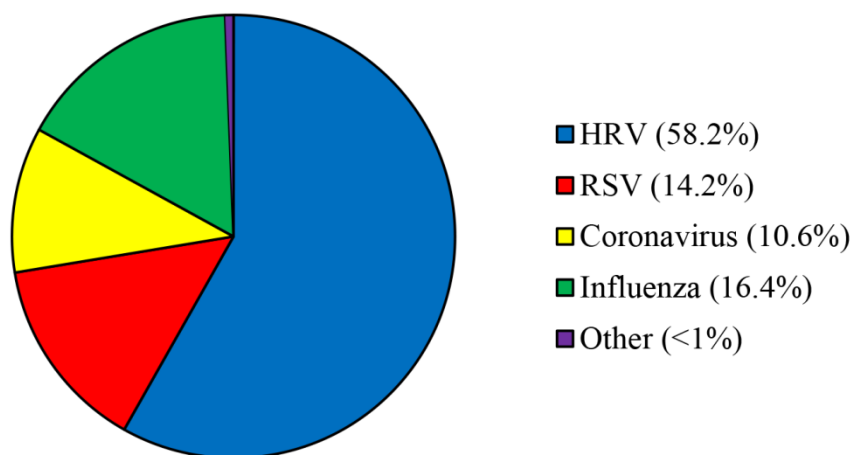


**Figure 1.1: Viral pathogens associated with exacerbations of COPD.**

Data are derived from<sup>1</sup>.

## 1.2 Asthma

### 1.2.1 Definition

Asthma is described by the Global Initiative for Asthma (GINA) as:

*“a chronic inflammatory disorder of the airways in which many cells and cellular elements play a role. The chronic inflammation is associated with airway hyperresponsiveness that leads to recurrent episodes of wheezing, breathlessness, chest tightness, and coughing, particularly at night or in the early morning. These episodes are usually associated with widespread, but variable, airflow obstruction within the lung that is often reversible either spontaneously or with treatment.”*<sup>78</sup>

Not unlike COPD, asthma is a heterogeneous disease that is difficult to define but it is generally characterized by chronic inflammation of the airways, airway hyperresponsiveness (AHR), variable airflow obstruction and varying degrees of structural changes, known as airway remodelling.

### ***1.2.2 Burden of Disease***

Asthma is considered to be one of the most common chronic diseases in the world and is, in fact, the most common chronic disease in children and young adults<sup>7,79</sup>. This disease affects more than an estimated 300 million people worldwide and prevalence continues to increase, with an expected 400 million people affected by 2025<sup>80,81</sup>. Clinical asthma affects around 4.5% of adults (aged 18-45) worldwide<sup>7</sup>. The prevalence of asthma is high in North America compared to the rest of the world, with the disease affecting approximately 11% of the total population<sup>78</sup>. Specifically in Canada, it has recently been reported that about 13% of children and 8.6% of adults have been diagnosed with asthma<sup>82</sup>. Cumulatively over 3.2 million Canadians have asthma, and this number is expected to increase to over 3.9 million by 2030<sup>47</sup>. As in COPD, the total economic burden of asthma is hard to calculate as it also involves both direct and indirect costs<sup>83</sup>. To provide a sense of the economic burden of asthma in Canada, the combined direct and indirect costs are estimated to be around 2.2 billion dollars and projected to increase to 4.2 billion dollars by 2030<sup>47</sup>.

### ***1.2.3 Etiology and Pathogenesis***

Causes linked to the development of asthma are as diverse as the disease itself. Both genetic and environmental components have been implicated in the subsequent development of this disease and particularly, interplay between gene-environment interactions. Thus far, a family history of atopic disease is the strongest risk factor for the development of asthma. Additionally, a history of wheezing illness induced by HRV infections in genetically predisposed children is also a strong predictor for the subsequent development of asthma<sup>84,85</sup>.

Airway inflammation, AHR and airway remodelling contribute to airflow obstruction and ultimately, difficulty breathing. Chronic airway inflammation is one of the hallmarks of asthma and involves a variety of cell types and mediators. Classically, asthma is thought of as a CD4+ T helper type 2 (Th2)-mediated disease, associated with increased levels of Th2 cytokines, including interleukin (IL)-4, IL-5, IL-9 and IL-13, along with increased immunoglobulin (Ig)E levels and eosinophilic inflammation. It is now known that asthmatics can have a range of inflammatory phenotypes, including eosinophilic, neutrophilic, mixed granulocytic and even 'pauci-granulocytic' inflammation. Recent evidence implicates other Th subsets, including Th9, Th17 and T regulatory cells, as also having a role in modulating these disease phenotypes<sup>79</sup>. AHR involves an aberrant increase in the 'twitchiness' of the airways in response to inhalation of common airway irritants such as allergens, pollutants or respiratory viruses and is confirmed clinically using a methacholine or histamine challenge test<sup>79</sup>. Airway remodelling is a term used to collectively describe the structural changes that occur in the lungs of asthmatics. These

changes are typically characterized by epithelial disruption, goblet cell metaplasia, goblet cell hyperplasia and hypertrophy, an increase in smooth muscle mass, vascular angiogenesis, mucus gland hypertrophy, and increased matrix protein deposition that results in reticular basement membrane thickening<sup>86</sup>.

#### ***1.2.4 Asthma and Cigarette Smoking***

Around 25-35% of asthmatics smoke, which is surprisingly no different than the percentage of smokers in the general population<sup>7-9</sup>. The prevalence of asthmatics who smoke is largest in Europe and South East Asia, where over a third of asthmatics smoke cigarettes<sup>7</sup>. Asthmatics who smoke are reported to have an increase in morbidity and mortality rates compared to those asthmatics who do not smoke<sup>87</sup>. They have more severe respiratory symptoms, are less responsive to conventional anti-inflammatory treatments (corticosteroids), have more frequent exacerbations and generally have a decreased quality of life compared to asthmatics who do not smoke<sup>11-23</sup>.

The increased respiratory symptoms in asthmatics who smoke are partly due to lower FEV<sub>1</sub>, increased mucus production and increased sub-epithelial thickness<sup>11</sup>. Moreover, cigarette smoking accelerates the decline in lung function in asthmatic patients<sup>20,88-90</sup>. Cigarette smoke has also been shown to enhance allergic inflammation<sup>91</sup> and facilitate allergen penetration through the respiratory epithelium leading to an increased severity of allergic inflammation<sup>92</sup>. Many studies have shown that smoking asthmatics are less responsive to corticosteroid treatment and one study has shown that they also require more frequent use of rescue medication<sup>93</sup>. Cigarette smoke has been shown to change the

typical eosinophilic inflammatory profile in asthmatics to a neutrophilic phenotype, more typical of that seen in COPD<sup>87</sup>. This altered inflammatory profile is characterized by increased neutrophilic inflammation, increase of CD8+ T lymphocytes, infiltration of activated macrophages and a decrease in eosinophilic inflammation<sup>87</sup>.

### 1.2.5 Exacerbations

Up to 80% of asthma exacerbations in children and about 50% of asthma exacerbations in adults are associated with viral infections<sup>5,6</sup>. Virus-induced exacerbations of asthma are associated with increased neutrophilic inflammation in the airways, an increase in neutrophil degranulation and generally more severe disease symptoms<sup>94</sup>. The virus most frequently associated with virally-induced exacerbations of asthma is HRV<sup>5,6</sup> (**Figure 1.2**). Other viruses associated with exacerbations of asthma include coronavirus, RSV, influenza, parainfluenza and adenovirus<sup>95</sup>.

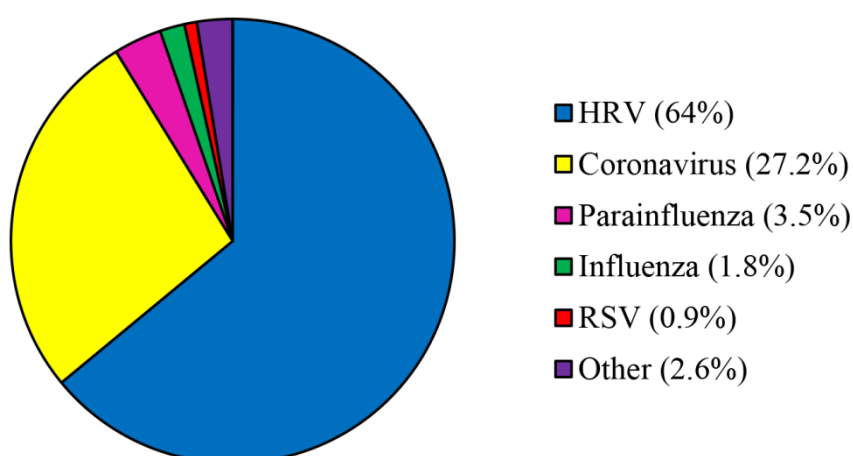


**Figure 1.2: Viral pathogens associated with exacerbations of asthma in adults.**

Data are derived from<sup>6</sup>.

It has been shown that, although asthmatic subjects are no more susceptible to HRV infection and do not differ in the severity and duration of upper respiratory tract infection compared to healthy subjects, they do display more severe and prolonged lower respiratory tract symptoms<sup>96</sup>. In a study where asthmatic and control healthy subjects were experimentally infected with HRV, asthmatic subjects displayed lower respiratory tract symptoms consistent with a mild exacerbation<sup>97</sup>. Asthmatics had a decrease in both PEF and FEV<sub>1</sub> as well as an increase in AHR compared to healthy subjects. Using an *in vitro* cell culture model, one study suggests that bronchial epithelial cells derived from asthmatics display increased levels of HRV replication compared to bronchial epithelial cells derived from healthy individuals<sup>98</sup>. In contrast, another study has shown that *in vivo*, there is no difference in peak HRV titres between mild asthmatics and otherwise healthy subjects following experimental HRV infection<sup>99</sup>.

It has been proposed that asthmatics may respond unfavourably to HRV infections compared to healthy individuals due to an over-exuberant pro-inflammatory response<sup>100-102</sup> and/or a deficiency in their innate immune response<sup>95,98,103</sup>. The over-exuberant inflammatory response has mainly been attributed to enhanced activation of the pro-inflammatory transcription factor nuclear factor- $\kappa$ B (NF- $\kappa$ B), which would, presumably, result in the activation of many pro-inflammatory genes that are regulated by this ubiquitous transcription factor. There have been studies attributing a deficiency in the innate immune response in asthmatics, but these remain controversial<sup>98,103</sup>. These studies claim that both type I interferon (IFN)- $\beta$  and type III IFN- $\lambda$  production are deficient

following HRV infection in asthmatic subjects compared with otherwise healthy controls. In contrast, other studies have shown that IFN- $\beta$  expression is not altered between airway epithelial cells derived from asthmatics and normal<sup>104,105</sup>, as well as in stable asthma IFN- $\lambda$  production is not deficient<sup>106</sup>.

In addition to asthmatics who smoke being reported to have a higher frequency of exacerbations compared to those who do not smoke, it has also been reported that asthmatics hospitalized for exacerbations are more likely to be current smokers<sup>14</sup>.

### 1.3 HRV

#### *1.3.1 Prevalence, Incidence, Pathogenesis and Symptoms*

The common cold is the most frequent acute respiratory illness in humans<sup>107</sup> and the National Institutes of Health (NIH) report that there are over a billion cases per year of the common cold in the USA alone<sup>108</sup>. Adults usually experience between 2-4 colds/year, whereas children usually experience between 6-10 colds/year<sup>109</sup>. HRV infections are the predominant cause of the 'common cold', being the virus responsible in 80% of cases<sup>107</sup>, and therefore, it is often referred to as the common cold virus<sup>30,107</sup>. In a minority of cases the common cold can also be caused by RSV, parainfluenza virus, coronavirus, adenovirus, paramyxovirus, orthomyxovirus or echovirus<sup>110</sup>.

HRV has a high degree of species specificity, as efficient replication occurs only in humans and higher primates<sup>30</sup>. Chimpanzees and gibbons have been infected but no overt illness was observed in these animals<sup>30</sup>. The infection rate of HRV in humans is between

70-80%<sup>111,112</sup>. Interestingly, in the northern hemisphere, HRV infection tends to be seasonal with the largest peaks of infection seen in the fall and spring<sup>113,114</sup>.

Infection with HRV causes vasodilation, increased vascular permeability and increased glandular secretion in the nasal mucosa, and these, in turn, lead to common symptoms including nasal obstruction and rhinorrhea<sup>111</sup>. The clinical symptoms are primarily caused by the inflammatory response of the host to the virus infection and not by a cytopathic effect<sup>115</sup>. Typical symptoms include nasal stuffiness, discharge, sneezing and cough but frequent symptoms can also include hoarseness of the throat, headache, malaise and lethargy<sup>107</sup>.

Ordinarily, after 8-10 h following intranasal inoculation, shedding of infectious virions can be detected<sup>112</sup>. During experimental HRV infections the onset of symptoms is observed 10-12 h following intranasal inoculation<sup>112</sup>. Virus shedding peaks on the 2<sup>nd</sup> to 3<sup>rd</sup> day after infection and decreases rapidly thereafter<sup>112,116</sup>. The median duration of a symptomatic HRV infection is 7 days but detectable levels of virus and viral RNA can persist for up to 3 weeks<sup>116,117</sup>.

### ***1.3.2 Infection of Airway Epithelium***

The human airway epithelium is the primary site of HRV infection and replication. Although many cell types can be infected with HRV *in vitro*, the airway epithelial cell is, thus far, the only cell type in which HRV infection has been detected *in vivo* via both *in situ* hybridization and immunohistochemistry<sup>30,118</sup>. There is some suggestion that the basal epithelial cell is the most susceptible epithelial cell type and this may be due to the

relatively higher expression of the major group HRV receptor intracellular adhesion molecule-1 (ICAM-1) on basal epithelial cells compared to non-basal epithelial cells<sup>119</sup>. Additionally, HRV has been shown to infect epithelial cells in both the upper and lower airways<sup>104,118,120-126</sup>. Using *in situ* hybridization, a handful of studies suggest that HRV may be detected in a limited number of cells in the sub-epithelial layer, but the cell type(s) infected in this region has not, to date, been identified<sup>125,127</sup>.

In contrast to some other respiratory viruses, HRV infections do not lead to overt epithelial cell cytotoxicity, either *in vivo* or *in vitro*<sup>128,129</sup>. This implies that HRV must initiate disease exacerbations by altering epithelial cell biology in a manner that increases airway inflammation and thus causes disease worsening, rather than through cytotoxicity-mediated effects<sup>130</sup>. There is now strong evidence indicating that HRV infection of human airway epithelial cells leads to the production of a variety of molecules, some of which would be expected to enhance airway inflammation. Specifically, upon HRV infection the airway epithelium had been shown to up regulate a variety of inflammatory, host-defense and anti-viral molecules (**Table 1.2**)<sup>131-133</sup>. This thesis project will focus on two of these chemokines, namely CXCL10 and CXCL8, for reasons that will be outlined in section **1.6**.

**Table 1.2: Inflammatory, Host-Defense and Anti-Viral Mediators Induced by HRV in the Airway Epithelium.**

Category	Mediator
<i>Chemokines</i>	CXCL1 (GRO- $\alpha$ ), CXCL3 (GRO- $\gamma$ ), CXCL5 (ENA-78), <b>CXCL8</b> (IL-8), <b>CXCL10</b> (IP-10), CCL2 (MCP-1), CCL3 (MIP-1 $\alpha$ ), CCL5 (RANTES), CCL11 (Eotaxin), CCL20 (MIP-3 $\alpha$ ), CCL24 (Eotaxin-2), HBD-2
<i>Cytokines</i>	IL-1, IL-6, IL-11, IL-16, TNF- $\alpha$
<i>Interferons</i>	IFN- $\beta$ , IFN- $\lambda$
<i>Anti-virals</i>	Viperin, ISG56, ISG15
<i>Colony Stimulating Factors</i>	G-CSF, GM-CSF
<i>Growth Factors</i>	VEGF, TGF- $\beta$ , FGF, EGF, amphiregulin, activin A

Adapted from<sup>134</sup>. GRO: growth related oncogene, ENA: epithelial cell-derived neutrophil-activating peptide, IL: interleukin, MCP: monocyte chemotactic protein, MIP: macrophage inflammatory protein, RANTES: Regulated on Activation, Normal T cell Expressed and Secreted, HBD: human beta defensin, TNF: tumor necrosis factor, ISG: interferon stimulated gene, G-CSF: granulocyte colony-stimulating factor, GM-CSF: granulocyte macrophage colony-stimulating factor, VEGF: vascular endothelial growth factor, TGF; transforming growth factor, FGF: fibroblast growth factor, EGF: epidermal growth factor.

### 1.3.3 Classification

HRVs are members of the family *Picornaviridae* and the genus *Enterovirus*, and are, as the name implies, small RNA viruses<sup>135</sup>. Picornaviruses are non-enveloped, positive sense single-stranded (+ss) RNA viruses with an icosahedral capsid<sup>135</sup>. HRV has a diameter of 30 nm<sup>135</sup>, a mass of  $\sim 8.5 \times 10^6$  Daltons and a 7.2-7.5 kilo base (kb) genome<sup>107,136</sup>. The HRV genome contains a single open reading frame encoding a long polypeptide chain, the

polyprotein, which is normally cleaved during translation (**Figure 1.3**)<sup>135,137</sup>. The 3' terminus is polyadenylated and there is a small protein called the viral protein genome-linked (VPg) at the 5' end instead of a 7-methyl guanosine cap structure<sup>135</sup>. The 5' VPg is the protein primer for RNA synthesis and is involved in the initiation of viral replication<sup>135</sup>. Adjacent to the VPg is a 5'-terminal cloverleaf-like motif (CL), also necessary for RNA replication, which binds viral and cellular proteins for the initiation of RNA synthesis and helps to convert infecting genomes from translation to replication templates<sup>135</sup>. Associated with the CL is the internal ribosomal entry site (IRES) which is responsible for the initiation of translation of the viral genome and is essentially a 'landing pad' for ribosomes<sup>108</sup>. The adjacent genome codes for viral capsid proteins (VP1-4) and additional non-structural proteins including 2A-C and 3A-D<sup>137</sup>.

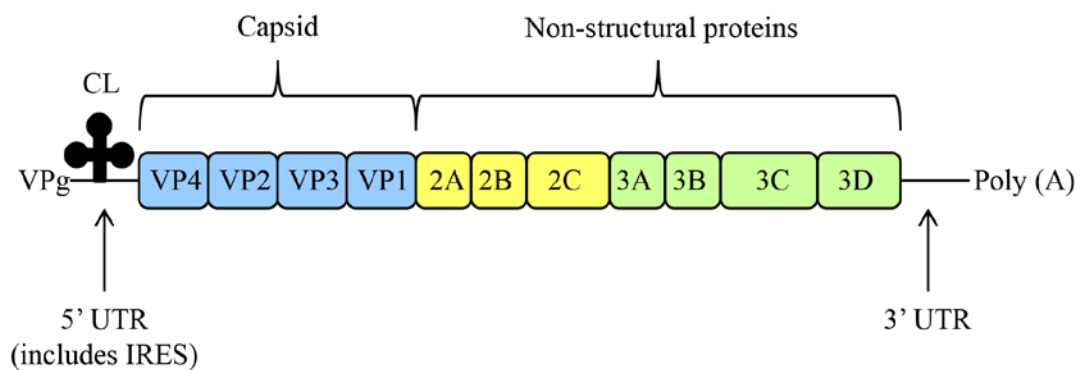


**Figure 1.3: Schematic diagram of the HRV genome.**

The VP1-4 proteins make up 60 protomers, with VP1-3 being exposed on the surface having a star shaped plateau at the fivefold axis of symmetry<sup>135</sup>. At the surface

junction of each VP1-3 protomer are deep canyons with a hydrophobic pocket beneath the canyon floor and this is where the receptor binding site is located<sup>135</sup>. The viral 2A protein is a protease involved in cleaving the HRV polyprotein and also cleaves factors involved in cap-dependent translation initiation, shutting down host cell translation<sup>108,135</sup>. The 2B protein inhibits cellular secretory pathways (endoplasmic reticulum and Golgi apparatus), and is suggested to have roles in viral RNA synthesis while 2C is involved in vesicle formation and has nucleoside triphosphatase (NTPase) activity<sup>135,137</sup>. The 3A protein is involved in the inhibition of intracellular transport<sup>135</sup>. Subsequent VPg's are coded by 3B<sup>135,137</sup>. The 3C protease is responsible for processing events to generate replication proteins from the viral genome, and also inhibits host transcription<sup>135,137</sup>. The 3D protein is the viral encoded RNA-dependent RNA polymerase<sup>135,137</sup>.

There are over 150 genomically distinct HRV strains known to date that are divided into three clades, namely HRV-A, HRV-B and HRV-C<sup>138-140</sup>. Recently there is suggestion of an additional clade within HRV-A; the HRV-D clade<sup>138,139</sup>. Around 100 serotypes within the HRV-A and HRV-B species have been identified<sup>138</sup>. A serotype is defined by the ability of a mono-specific antiserum to neutralize viral infectivity. Members of the HRV-C species have not yet been serotyped due to difficulties with growing in cell culture<sup>138,141,142</sup>.

HRVs are acid labile, where inactivation occurs below pH 6 for all serotypes<sup>135</sup>. They are relatively stable at 24-37 °C<sup>30</sup>. HRVs can survive hours, and even days, on environmental surfaces and can be stable for years at freezing temperatures<sup>30</sup>.

### ***1.3.4 Receptor Usage and Cell Entry***

The serologically distinct HRVs (clades A and B) are divided into two groups based on receptor usage. Major group HRVs (91 serotypes), such as HRV-16, utilize ICAM-1 as their cellular receptor, while minor group HRVs (10 serotypes), such as HRV-1A, utilize members of the low density lipoprotein (LDL) receptor family for cell entry<sup>143-145</sup>. ICAM-1 (CD54) has 5 immunoglobulin-like domains, with a transmembrane portion and a small cytoplasmic tail<sup>146</sup>. The main function of ICAM-1 is as an adhesion molecule, mediating binding between endothelial cells and leukocytes. As such, it plays a major role in the migration of leukocytes from the blood to the sites of inflammation. The receptor(s) for members in the HRV-C clade is/are yet to be identified but is/are speculated to be more closely related to ICAM-1 than to the LDL receptor<sup>115,138</sup>.

Most HRV serotypes enter the host cell by receptor mediated endocytosis<sup>135</sup>. It is suggested that subsequent un-coating is triggered by mild endosomal acidification, and the RNA genome is released when a pH of ~6.5 is reached in the endosomal compartment<sup>135</sup>. In contrast, upon receptor binding of some HRV serotypes, including HRV-3 and HRV-14, the HRV capsid is said to expand by 4% due to the mere interaction with the receptor, allowing the viral capsid to directly release the RNA genome into the cytoplasm of the host cell<sup>135</sup>.

### ***1.3.5 Replication***

Following attachment to its cognate receptor and internalization of the RNA genome, HRV replication, like other +ssRNA viruses, occurs in association with

intracellular membranes<sup>147</sup>. Specifically, HRV replication of some serotypes is suggested to occur on membranes derived from the endoplasmic reticulum or on membranes of fragmented golgi<sup>108,135,148</sup>. Once the +ssRNA is released into the cytoplasm, the VPg is removed and the IRES promotes binding of the 40S ribosomal subunit initiating translation<sup>135</sup>. The polyprotein is then subsequently cleaved by the viral 2A and 3C proteases, producing individual viral proteins<sup>108,137</sup>. HRV +ssRNA is then replicated by the viral RNA-dependent RNA polymerase to a –ssRNA form, using membrane vesicles as a scaffold<sup>135</sup>. The –ssRNAs are then copied to more +ssRNAs which can then be used for further translation into more viral proteins or used for packaging into new virion particles, which is a process called morphogenesis<sup>135</sup>. Due to the generation of –ssRNA, double stranded (ds) RNA is formed during the viral replication cycle.

The optimal condition for growth and replication for HRVs is 33-34°C at a pH of 7-7.2 making the upper airway an ideal candidate for HRV propagation<sup>30</sup>. Since replication has also been shown to occur at 37°C, the lower airways also can support productive replication of HRV<sup>126</sup>.

### ***1.3.6 Immune Response***

The innate immune response utilizes pattern recognition receptors (PRRs) to detect and respond to pathogen-associated molecular patterns (PAMPs)<sup>149</sup>. During HRV replication a dsRNA intermediate is formed that acts as a PAMP which can be detected by PRRs such as Toll-like receptor (TLR)-3, the cytoplasmic retinoic acid-inducible gene-I (RIG-I)-like receptors (RLRs) including RIG-I and melanoma differentiation-associated

gene 5 (MDA5) and protein kinase R (PKR). All of these receptors have been shown to be expressed by airway epithelial cells<sup>150-154</sup>. TLR3, RIG-I and MDA5 have all been implicated in pro-inflammatory gene production during HRV infection<sup>154-158</sup> but there is controversy in the literature about the relative role of these PRRs in HRV-induced signalling. Although PKR-dependent induction of pro-inflammatory cytokine production has been shown following HRV infection<sup>159,160</sup>, the role of PKR in the detection of HRV is still uncertain. Additionally, the importance of PKR in the induction of anti-viral responses is questionable, since PKR knock-out mice have been shown to maintain normal anti-viral responses<sup>161</sup>. The role of TLR3 in the induction of anti-viral responses is also uncertain because TLR3 knock-out mice also maintain effective anti-viral responses following a variety of viral infections<sup>162</sup>. In a murine model of HRV infection, TLR3 null mice demonstrated unchanged IFN induction and no alterations in viral titre<sup>156</sup>. TLR3 is important, however, at least in part, for anti-viral responses to other viruses<sup>163,164</sup>. Both RIG-I and MDA5-deficient mice have been shown to have impaired anti-viral responses<sup>165</sup>.

Signalling induced through TLR3, RIG-I and MDA5 leads to an antiviral immune response triggering the type I IFN response, interferon-inducible genes (ISGs) and the induction of inflammatory cytokines<sup>149,166</sup>. In airway epithelial cells TLR3 is predominantly located on intracellular endosomal membranes<sup>150,151</sup>. TLR3 signalling can activate both canonical and non-canonical NF- $\kappa$ B pathways, as well as interferon regulatory factor (IRF)-3 and IRF-7 via the adapter molecule Toll/IL-1 receptor (TIR) domain containing adaptor inducing IFN- $\beta$  (TRIF)<sup>149,167</sup>. RIG-I and MDA5 are both cytoplasmic proteins that bind dsRNA via their DExD/H box RNA helicase domains located adjacent to two caspase

recruitment domains (CARDs) which are responsible for activating downstream signalling<sup>149,166</sup>. CARD binds to a mitochondrial-associated adapter protein which has four names, the CARD adapter inducing IFN- $\beta$  (CARDIF) / IFN- $\beta$  promoter stimulator-1 (IPS-1) / virus-induced signaling adapter (VISA) / mitochondrial antiviral signaling protein (MAVS), which can then induce a plethora of downstream signalling events, including both canonical and non-canonical NF- $\kappa$ B signalling, as well as mitogen-activated protein kinase (MAPK) signalling and IRF activation<sup>168-171</sup>.

Although adaptive immune responses are observed in response to HRV infections, as neutralizing antibodies can be detected in approximately 50-90% of individuals<sup>25,172-175</sup>, the presence of neutralizing antibodies, or virus specific T cells, are not detectable until some 2-3 weeks post infection<sup>176</sup>. Thus, it is assumed that innate immune responses play the dominant role in regulating symptomatic responses. It is thought that adaptive immunity can offer protection against subsequent infections with that particular strain of HRV. Unfortunately, since there are such a large number of known circulating HRV serotypes and HRV has a high mutation rate, repeated infection can still occur in any individual.

#### 1.4 Cigarette Smoke

It is estimated by the WHO that there are around 1.25 billion smokers worldwide<sup>15</sup>. Cigarette smoking has been linked to a plethora of diseases including a variety of squamous cell cancers, ischemic heart disease, cerebro- and vascular disease, diabetes, and other diseases related to the reproductive, gastrointestinal, and immune systems<sup>177-179</sup>. Additionally, cigarette smoke has detrimental effects on teeth and skin such as aging,

wrinkles and poor wound healing. Not surprisingly, tobacco smoke is the second major cause of death in the world<sup>177</sup>, as about half of all smokers will develop a serious smoking-related illness<sup>179</sup>. It is estimated that smokers rate of mortality is tripled compared to non-smokers and smokers lose, on average, 10 years of life<sup>180</sup>.

There are two phases of cigarette smoke, namely the tar or particulate phase and the vapour or gas phase<sup>181</sup>. Although the major inducer of tobacco dependence is nicotine, cigarette smoke contains over 4000 compounds<sup>182,183</sup> and, thus far, over 100 of them have been shown to be harmful including tar, nitrogen oxides, hydrogen cyanide and volatile aldehydes<sup>183,184</sup>. At least 50-60 of these compounds are known carcinogens<sup>183</sup> and 1 puff of a cigarette results in the production of  $10^{16}$  oxygen radicals or reactive oxygen species (ROS)<sup>181,185</sup>. Although it has been reported that the ROS in cigarette smoke itself are not capable of passing through the plasma membranes of cells<sup>186-188</sup>, cigarette smoke also contains lipid soluble components, such as phenolic compounds, aldehydes and polycyclic aromatic hydrocarbons, which are capable of inducing ROS inside cells<sup>186</sup>. Generation of ROS such as superoxide ( $O_2^{\bullet-}$ ), hydroxyl radicals ( $\bullet OH$ ) and hydrogen peroxide ( $H_2O_2$ ) leads to a disruption in cellular homeostasis resulting in impaired physiological function, random cellular damage, activation of signalling pathways, triggering repair and apoptotic cascades, and defective host defenses<sup>189</sup>. This oxidative stress is ultimately a result of an imbalance between ROS production and detoxification with anti-oxidants<sup>189</sup>.

Most commercial cigarettes include filters made of cellulose acetate tow with added plasticizers<sup>183</sup>. More than 50% of filters have rows of small perforations slowing the

velocity of the smoke stream which apparently leads to more complete combustion and a reduction of select volatile agents<sup>183</sup>. It has been argued that this does not necessarily make cigarette smoking 'safer' but, in fact, makes it more dangerous, since smokers will inhale more deeply and tend to smoke more in order to compensate for the decreased volume of cigarette smoke flow<sup>183,190</sup>.

Cigarette smoking is associated with an increase in airway inflammation in otherwise healthy smokers without airway obstruction as evidenced by an increase of neutrophils, macrophages and CD8+ lymphocyte numbers in the blood and bronchoalveolar lavage (BAL) fluid<sup>191-196</sup> as well as increased numbers of inflammatory cells (neutrophils, eosinophils, macrophages and mast cells) in the bronchial wall<sup>193,194,197</sup>. Cigarette smoke not only increases the number of neutrophils and alveolar macrophages, but also activates them to produce pro-inflammatory mediators, ROS and proteolytic enzymes<sup>179,196</sup>. Cigarette smoking is also associated with features that are characteristic of airway remodelling as evidenced by an increase in remodelling factor deposition, such as laminin and tenascin, under the basement membrane<sup>197</sup>. In addition to pro-inflammatory effects, cigarette smoke had also been shown to have immune suppressive effects as evidenced by a decrease in natural killer (NK) cell number and activity in smokers compared to non-smokers<sup>198-201</sup>.

#### ***1.4.1 Cigarette Smoke and Respiratory Infections***

Numerous studies suggest that cigarette smoke generally impairs innate immune responses<sup>202,203</sup>. Although the exact mechanisms are not completely known, cigarette

smoke may both enhance pro-inflammatory, remodelling and apoptotic responses, and suppress anti-viral defenses. Specifically, there is evidence indicating that cigarette smoke impairs and/or modulates immune responses to infection with influenza<sup>204–208</sup> and RSV<sup>209,210</sup>. Moreover, it has been reported that cigarette smokers experience more frequent acute respiratory tract infections and both the severity and duration of these infections is greater than in non-smokers<sup>24–29</sup>. It is still unclear whether this is due to increased susceptibility to infection, inability to effectively clear the infection, an exaggerated pro-inflammatory response to the infecting agent, or a combination of all three.

#### ***1.4.2 Airway Epithelium and Cigarette Smoke***

The airway epithelial cell is one of the first cell types to come into direct contact with inhaled cigarette smoke. With over 4000 chemical components, it undoubtedly has modulatory effects on airway epithelial cells and there is substantial evidence that cigarette smoke weakens airway epithelial cell defenses<sup>211</sup>. Effective respiratory mucociliary clearance relies on proper co-ordinated beating of cilia, along with appropriate levels and composition of airway surface fluid (ASF). Cigarette smoke has been shown to affect mucociliary structure and function by inhibiting ciliogenesis, reducing ciliary beat frequency and altering mucin production<sup>212–216</sup>. Effective epithelial cell defenses also rely on a tightly joined, continuous layer of epithelium as a structural barrier to the underlying tissue. Cigarette smoke has been shown to disrupt this barrier by increasing epithelial cell permeability and causing the disassembly of tight junction components<sup>217–220</sup>. As mentioned previously, cigarette smoke also results in oxidative damage, and the epithelial

cell does not escape this. The lipid-soluble components of cigarette smoke have been shown to induce mitochondrial production of ROS in lung epithelial cells leading to oxidative stress<sup>186</sup>.

## 1.5 Airway Epithelium

### *1.5.1 Structure and Function*

The human respiratory tract is divided into the upper respiratory tract, including the nasal cavity, sinuses, mouth, pharynx (throat) and larynx (voice box), and the lower respiratory tract, including the trachea (wind pipe), primary bronchi and smaller airways (**Figure 1.4**). The lower respiratory tract is further divided into the cartilaginous proximal airway (trachea, bronchi and submucosal glands), the non-cartilaginous distal airway (bronchioles) and the gas exchange region (alveoli)<sup>221</sup>. Starting with the trachea, the airway undergoes a total of up to 23 divisions of the pulmonary tree beginning with a bifurcation into the primary bronchi. The primary bronchi continue to dichotomously bifurcate into several generations of the bronchial airway, followed by the bronchiolar airway, terminal bronchioles, transitional bronchioles, respiratory bronchioles, alveolar ducts and finally ending with the alveolar sacs<sup>221</sup>.

A continuous layer of epithelial cells lines the pulmonary tree and is the interface between the host and the environment<sup>221</sup>. The airway epithelium is composed of a pseudo-stratified morphology in the trachea and major bronchi, a multi-layered morphology with more cuboidal cells in the distal bronchi and terminates in a squamous, single layer morphology in the gas exchange region<sup>131,221</sup>.

There are a variety of unique epithelial cell types including: ciliated, basal, secretory (including goblet, Club and serous cells) and alveolar type I and II cells<sup>131</sup>. The columnar ciliated epithelial cell is the predominant epithelial cell type in the larger human airway and plays a major role in mucociliary clearance<sup>131,222</sup>. Basal cells are responsible for the pseudostratified appearance of the bronchial epithelium and provide a foundation for the attachment of both ciliated and non-ciliated columnar cells to the basement membrane<sup>131</sup>. Basal cells are also the progenitor cell for the majority of epithelial cell types but there is some evidence that secretory cells can also be progenitors<sup>131</sup>. The proximal airway is predominantly lined with ciliated cells and a minority of goblet and basal cells, while the distal airway is lined with Club cells, basal cells and a minority of ciliated cells<sup>131</sup>. Airways less than 2 mm in diameter have a cuboidal epithelial morphology. Large, flat, squamous type I alveolar cells cover 90% of the alveolar surface and are responsible for gas exchange while type II alveolar cells are smaller, cuboidal and only cover 10-15% of the alveolar surface<sup>131,221</sup>. Additionally, Type II cells secrete surfactant and can repopulate type I cells as they are the progenitor cell in the alveolar epithelium<sup>131,221</sup>.

Airway epithelial cells have a multitude of functions. Initially they exhibit a barrier defense function whereby they trap invading foreign substances in epithelial derived surface secretions which with the help of beating cilia propel the inhaled substance out of the lung. Additionally, epithelial cells provide a junctional barrier, including acting as a physical barrier to foreign substances and pathogens, secreting a variety of molecules and regulating water and ion transport<sup>131,222</sup>. Most recently, airway epithelial cells have been identified as key cells involved in immunomodulation in the lung<sup>221</sup>.

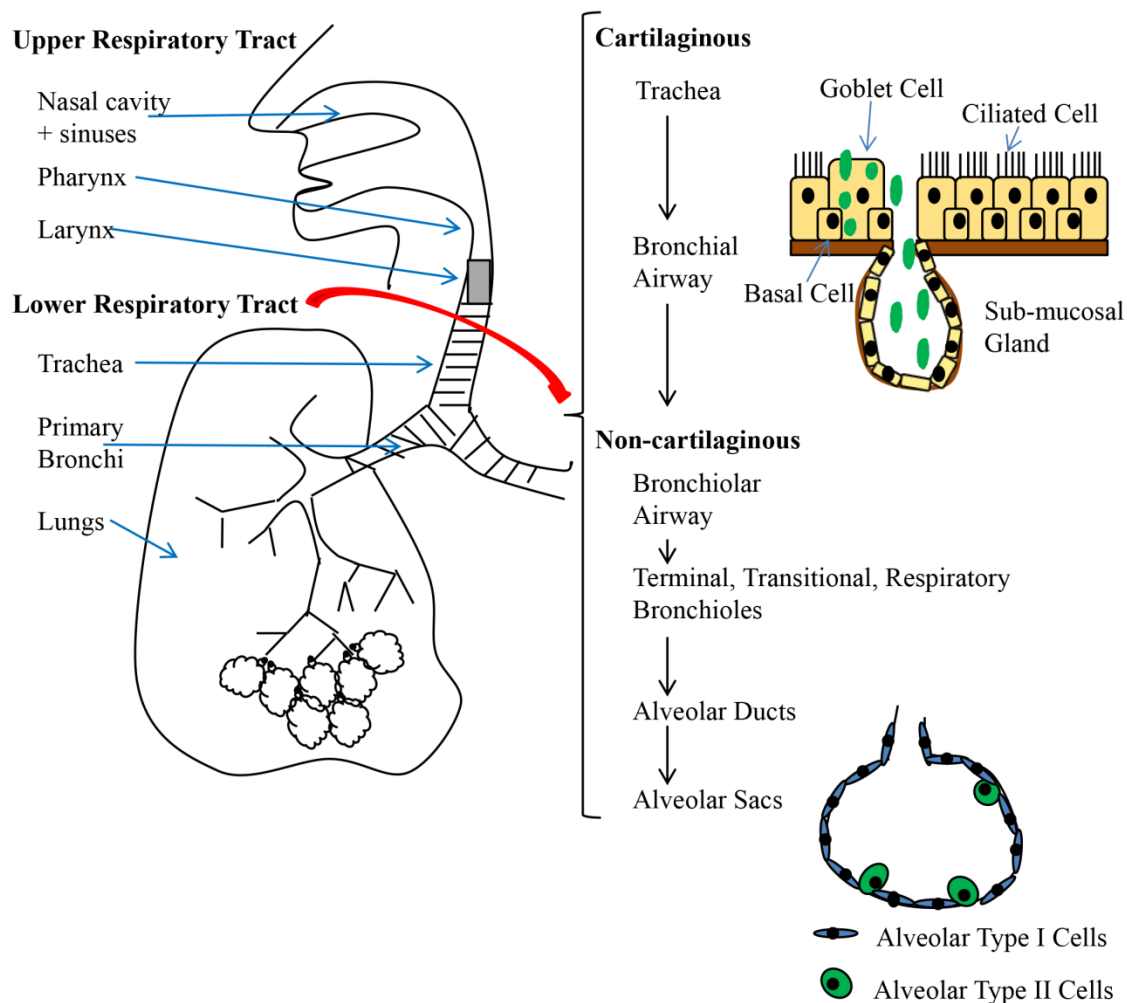


**Figure 1.4: Human airway structure.**

Adapted from<sup>221</sup>.

### 1.5.2 Airway Epithelium in COPD

Alteration in the number and composition of airway epithelial cells in COPD patients contributes to the debilitating physiological effects of this disease. The most striking alteration to the epithelium in COPD patients is decreased numbers of alveolar

epithelial cells due to emphysematous destruction of alveolar walls<sup>223</sup>. In addition, in the upper airways, mucus cell hypertrophy and hyperplasia result in excessive mucus production<sup>223</sup>.

### ***1.5.3 Airway Epithelium in Asthma***

The structure and composition of the airway epithelium in asthmatic patients can vary depending on the severity of the disease. In contrast to healthy individuals, the asthmatic epithelium can have areas of damage where the epithelium is denuded resulting in the presence of creola bodies in sputum<sup>224</sup>. Increased epithelial cell shedding is evidence of a more fragile epithelium suggesting an increased susceptibility to injury<sup>225</sup>. Additionally, a change in airway epithelial cell composition, size and number, including goblet cell metaplasia, hypertrophy and hyperplasia, results in increased mucus production. Underneath the epithelium, asthmatics tend to have thickening of the reticular basement membrane due to increased collagen deposition<sup>223</sup>.

## **1.6 Chemokines**

### ***1.6.1 Classification and Function***

Chemotactic cytokines, or chemokines, comprise the largest family of cytokines with around 50 members known to date<sup>226-229</sup>. They are small (~8-15kDa), positively charged proteins exhibiting 20-70% amino acid sequence homology. Chemokines, in addition to roles in hematopoiesis, angiogenesis and oncogenesis, are responsible for recruitment of leukocytes during inflammation<sup>226</sup>. By formation of a chemotactic gradient,

chemokines regulate the directional movement of leukocytes. They are divided into four subfamilies based on the position of the first two N-terminal cysteine (C) residues; (1) CXC, (2) CC, (3) XC and (4) CX<sub>3</sub>C<sup>230</sup>. The CXC or *alpha* chemokines have a variable amino acid (X) positioned between two cysteines and they are further subdivided into the ELR+ and the ELR- groups. The ELR+ CXC chemokines have a glutamic acid-leucine-arginine (ELR) motif near the N-terminus prior to the first cysteine, which the ELR- CXC chemokines lack. The presence of the ELR motif renders the CXC chemokines angiogenic and chemotactic toward neutrophils<sup>231,232</sup>. In contrast, CXC chemokines lacking the ELR motif are angiostatic and have a preferential activity toward lymphocytes<sup>231,232</sup>. Thus far, 17 CXC chemokines have been identified in humans (CXCL1-CXCL17)<sup>226</sup>. The CC or *beta* chemokines have two terminal cysteines adjacent to each other and comprise the largest group of the chemokines with up to 28 members identified (CCL1-CCL28)<sup>226</sup> which are chemotactic toward a wide variety of cells. The XC or *gamma* chemokine subfamily has one N-terminal cysteine and only has two members: the lymphokines XCL1 and XCL2. The last subfamily of chemokines, CX<sub>3</sub>C or *delta*, includes the sole member fractalkine (CX<sub>3</sub>CL1) which has two N-terminal cysteines separated by three variable amino acids and is tethered to the extracellular surface via a mucin-like stalk<sup>230</sup>.

Chemokine ligands bind with their N-terminus to seven transmembrane (7TM) domain G-protein coupled receptors (GPCRs) that are mainly coupled to the pertussis toxin-sensitive G $\alpha_i$  class of heterotrimeric G-proteins<sup>231,233</sup>. A total of 23 chemokine receptors have been identified including 18 with standard G $\alpha_i$  coupling and 5 atypical chemokine receptors that are non-chemotactic and considered recycling or scavenging

receptors<sup>226</sup>. The CXC subfamily of chemokines binds to the CXC subfamily of receptors (CXCR1-CXCR6), the CC subfamily of chemokines to the CC subfamily of receptors (CCR1-CCR2) and so forth<sup>226</sup>. A large proportion of chemokines and their receptors exhibit promiscuity; a single chemokine can bind to several chemokine receptors and a single chemokine receptor can have multiple chemokine ligands<sup>226</sup>. With the exception of the atypical receptors, such as Duffy antigen receptor for chemokines (DARC) which binds members of both CXC and CC chemokine subfamilies, chemokines bind to their respective family of receptors<sup>226,234</sup>.

Ligand-receptor binding of chemokines triggers activation of signalling cascades and an increase in intracellular calcium, resulting in up-regulation and activation of integrins, actin cytoskeleton rearrangement and cell movement toward the chemokine gradient<sup>235,236</sup>. Without the gradient provided at the sites of inflammation, the presence of chemokines would result in chemokinesis, or random, non-directional movement of leukocytes.

### ***1.6.2 CXCL10***

CXCL10 was first cloned in 1985 from a human monocyte-like cell line<sup>237</sup>. CXCL10 is also commonly referred to as interferon gamma-induced protein of 10 kDa (IP-10) and is also called small-inducible cytokine B10<sup>238</sup>. The murine homolog of CXCL10 (muCXCL10) is also referred to as cytokine responsive gene-2 (crg-2)<sup>239,240</sup>. At the gene level CXCL10 is located on chromosome 4<sup>241</sup> and is composed of 4 exons interrupted by 3 introns, but transcription generates only one known splice variant resulting in a 10kDa

secreted protein<sup>242,243</sup>. It has been reported to be secreted from a variety of cell types including T cells, monocytes, macrophages, fibroblasts, endothelial cells, keratinocytes, eosinophils, neutrophils and epithelial cells in response to diverse pro-inflammatory stimuli<sup>238,244-246</sup>.

CXCL10 is an ELR- CXC chemokine and is predominantly a chemoattractant for activated lymphocytes and NK cells<sup>247-254</sup>. CXCL10 is not constitutively expressed but many stimuli have been shown to induce CXCL10 expression in human cells including IFNs ( $\alpha/\beta/\gamma$ ), IL-1 $\beta$ , IL-2, IL-12, synthetic dsRNA, hypoxia as well as both viral and bacterial infections<sup>238,244,246,255</sup>. CXCL10 is solely recognized by CXCR3, which also recognizes CXCL9, CXCL11 and CCL21<sup>246,251</sup>. CXCL9 and CXCL11 are both structurally and functionally related to CXCL10. CXCR3 is mainly expressed on activated T cells, preferentially of the Th1 phenotype<sup>248,251</sup>, as well as on NK cells, but also shown to be expressed on monocytes, macrophages, dendritic cells (DCs), endothelial cells, mast cells and microglia<sup>238,246,256</sup>. Because CXCL10 predominantly recruits Th1 lymphocytes and NK cells to the sites of infection, it has been linked to antiviral immunity and host defense. In support of this, CXCL10-deficient mice have decreased ability to control viral infections, and impaired T cell recruitment and activation, while CXCL10 transgenic mice show improved control of infection and enhanced NK cell responses<sup>247,257</sup>.

#### 1.6.2.1 CXCL10: Role during HRV infections

CXCL10 has been shown to be expressed by HRV infected human bronchial epithelial cells<sup>245</sup> and is, importantly, one of the most highly induced genes in epithelial

cells following HRV infection *in vitro* and *in vivo*<sup>132,258</sup>. During experimental HRV infections, CXCL10 correlates with viral titres and with lymphocyte recruitment to the airways<sup>259</sup>.

#### 1.6.2.2 CXCL10: Role in smokers, COPD and asthma

Levels of CXCL10 in healthy smokers have not been explicitly investigated but CXCL10 mRNA, as well as total inflammatory cells including neutrophils and lymphocytes, have been shown to be increased in mice following cigarette smoke exposure when compared to control mice<sup>260-262</sup>. In contrast, CSE did not induce CXCL10 in a human bronchial epithelial cell line (16-HBEs), human plasmacytoid DCs or in human monocyte derived macrophages<sup>263-266</sup>.

Levels of CXCL10 are reported to be increased in the airways of patients with severe asthma and in COPD patients<sup>267-269</sup>. Th1 cells expressing CXCR3 have also been reported to be increased in smokers with COPD, which supports a functional link between CXCL10 induction and the recruitment of these cells<sup>270</sup>. Additionally, CXCL10 is induced by allergen challenge and has been shown to contribute to both airway hyperreactivity and airway inflammation in a murine model of allergic airway inflammation<sup>271</sup>. Recently, CXCL10 has been suggested to be a biomarker of both HRV-induced asthma and COPD exacerbations<sup>272,273</sup>.

### 1.6.3 CXCL8

CXCL8 was one of the first chemokines to be characterized. It was concurrently identified from monocytes by several groups<sup>274</sup> and they termed it monocyte-derived neutrophil chemotactic factor (MDNCF)<sup>275</sup>, monocyte-derived neutrophil activating factor (MONAP)<sup>276</sup> and neutrophil-activating factor (NAF)<sup>277</sup>. Subsequently it was proposed that it be referred to as neutrophil activating peptide-1 (NAP-1) or IL-8<sup>274</sup> and this terminology was used until 2000 when chemokines were given a uniform naming system where NAP-1/IL-8 was designated CXCL8<sup>230</sup>. It is now known that, although CXCL8 is produced in large amounts from mononuclear phagocytes, it also is derived from a variety of other cell types including other leukocytes (T cells, eosinophils and neutrophils) and non-leukocytic cells (epithelial cells, endothelial cells, fibroblasts, keratinocytes and hepatocytes)<sup>229,278</sup>. There is no true mouse homolog of CXCL8.

CXCL8 is an 8.5kDa ELR+ CXC chemokine that is one of the most potent chemoattractants for neutrophils. It is rapidly induced by pro-inflammatory cytokines such as tumor necrosis factor-alpha (TNF- $\alpha$ ) and IL-1, cellular stress and bacterial/viral products<sup>278,279</sup>. In solution, CXCL8 is often present as a dimer but is functionally active as both a monomer and a dimer<sup>235,278,280</sup>. CXCL8 is recognized by two receptors CXCR1 (IL-8RA) and CXCR2 (IL-8RB). CXCR2 is the most promiscuous CXC receptor having a high affinity for CXCL8 as well as a number of other chemokines including CXCL1 ,2 ,3, 5, 6, and 7<sup>235</sup>. In contrast, CXCR1 only has a high affinity for CXCL8 but it can also recognize CXCL6 and 7 with lower affinity. In addition to being constitutively expressed on neutrophils, CXCR1 and CXCR2 are also present on monocytes, basophils, eosinophils and

a minority of lymphocytes, although neutrophils generate the strongest response to CXCL8<sup>235,278</sup>. Following CXCL8 triggered neutrophil activation and migration, CXCL8 induces respiratory burst and degranulation in human neutrophils<sup>278</sup>.

At the gene level, CXCL8 is located on chromosome 4 and contains 5 exons separated by 4 introns<sup>281</sup>. Transcription results in 5 possible mRNA products, 4 alternatively spliced and 1 unspliced variant<sup>281,282</sup>. Of the 5 variants, 3 result in functional proteins, 2 of which are secreted. One of the two secreted variants is the 8.5 kDa main splice variant, found in many tissues including the lung.

#### 1.6.3.1 CXCL8: Role during HRV infections

Increased levels of CXCL8 are detected *in vivo* in nasal lavages of individuals following experimental HRV infection<sup>283</sup> and *in vitro* following infection of human bronchial epithelial cells<sup>283</sup>. Coincidentally, increased numbers of neutrophils have also been detected in both mucosa and nasal secretions of patients infected with HRV<sup>284–286</sup>. Importantly, levels of CXCL8 have been shown to correlate with symptom severity during HRV infections<sup>287</sup>.

#### 1.6.3.2 CXCL8: Role in smokers, COPD and asthma

Smokers have an increased number of neutrophils in BAL and generally airway neutrophilia has been shown to associate with a history of smoking<sup>288,289</sup>. Both airway obstruction and an accelerated decline in lung function are associated with increased numbers of neutrophils in sputum of smokers and former smokers<sup>290</sup>. There is also an

increase in CXCL8 in both sputum and bronchial washings of smokers compared to non-smokers<sup>291</sup>.

Increased neutrophil numbers correlate with increased CXCL8 levels in severe asthmatics and during acute exacerbations of both asthma and COPD<sup>292-294</sup>. Additionally, neutrophil numbers correlate with disease severity in patients with COPD and during viral exacerbations of both asthma and COPD<sup>94,292,295</sup>. Both neutrophil degranulation and cell lysis correlate with worse symptoms in asthmatics during virally-induced exacerbations<sup>94</sup>. Increased sputum levels of CXCL8 are also associated with neutrophilic inflammation in asthmatics that smoke<sup>23,289</sup>.

Activated neutrophils can lead to tissue damage, especially when they are present in excess, with the release of mediators including neutrophil elastase, cathepsin G, proteinase-3, MMPs and oxygen radicals<sup>296</sup>. When unchecked, the serine proteases neutrophil elastase, cathepsin G and proteinase-3 are the major factors responsible for the destruction of tissue as well as they are potent mucus secretagogues. Neutrophil elastase in particular has been shown to be responsible for many aspects of COPD, including emphysema, mucus hypersecretion and mucus gland hyperplasia.

### **1.7 Gene Regulation**

Gene expression can be regulated transcriptionally, post-transcriptionally, translationally, post-translationally and even epigenetically. Thus far, CXCL10 and CXCL8 have been shown to be mainly regulated by transcriptional and/or post-transcriptional

mechanisms<sup>259,278,283,297–311</sup>, although cigarette smoke has also been shown to affect gene expression via epigenetic mechanisms<sup>312,313</sup>.

The MAPK signalling pathways are widespread signal transduction pathways involved in eukaryotic cell regulation and have been linked to both transcriptional, post-transcriptional and epigenetic gene regulation<sup>314–316</sup>. They are evolutionarily conserved protein kinase cascades that regulate a variety of cellular events in addition to gene expression including proliferation, differentiation, metabolism, stress response, and apoptosis (**Figure 1.5**)<sup>315–321</sup>. They can be activated by a wide variety of stimuli, including inflammatory cytokines, hormones, growth factors, PAMPS and danger-associated molecular patterns (DAMPS) that activate PRRs, and environmental stresses<sup>314,315</sup>. To date, six mammalian MAPK pathways are known including the well-studied extracellular signal-regulated kinase (ERK)1/2, c-Jun amino terminal kinase (JNK)1/2/3 and p-38 MAPK $\alpha/\beta/\delta/\gamma$  as well as the less studied ERK 3/4, ERK5 and ERK 7/8 pathways<sup>314,318–321</sup>. Each MAPK is phosphorylated by a specific upstream MAPK kinase (MAPKK, MKK or MEK), which is itself phosphorylated by another specific MAPKK kinase (MAPKKK, MKKK or MEKK). It must be noted that this is an oversimplified representation of this signalling cascade, as substantial cross-talk and feed-back loops do exist<sup>317,319–322</sup>. HRV has been shown to activate all 3 of the major MAPK pathways, including ERK 1/2, JNK and p38 MAPK, as well as ERK 5<sup>297,323,324</sup>. Specifically, HRV-induced transcriptional activation of CXCL10 has been shown to be positively regulated via p38 MAPK and negatively regulated via ERK1<sup>297</sup>. Moreover, as evidence of involvement in post-

transcriptional gene regulation, mRNA stability of CXCL8 has been shown to be regulated via the p38 MAPK pathway<sup>325–327</sup>.

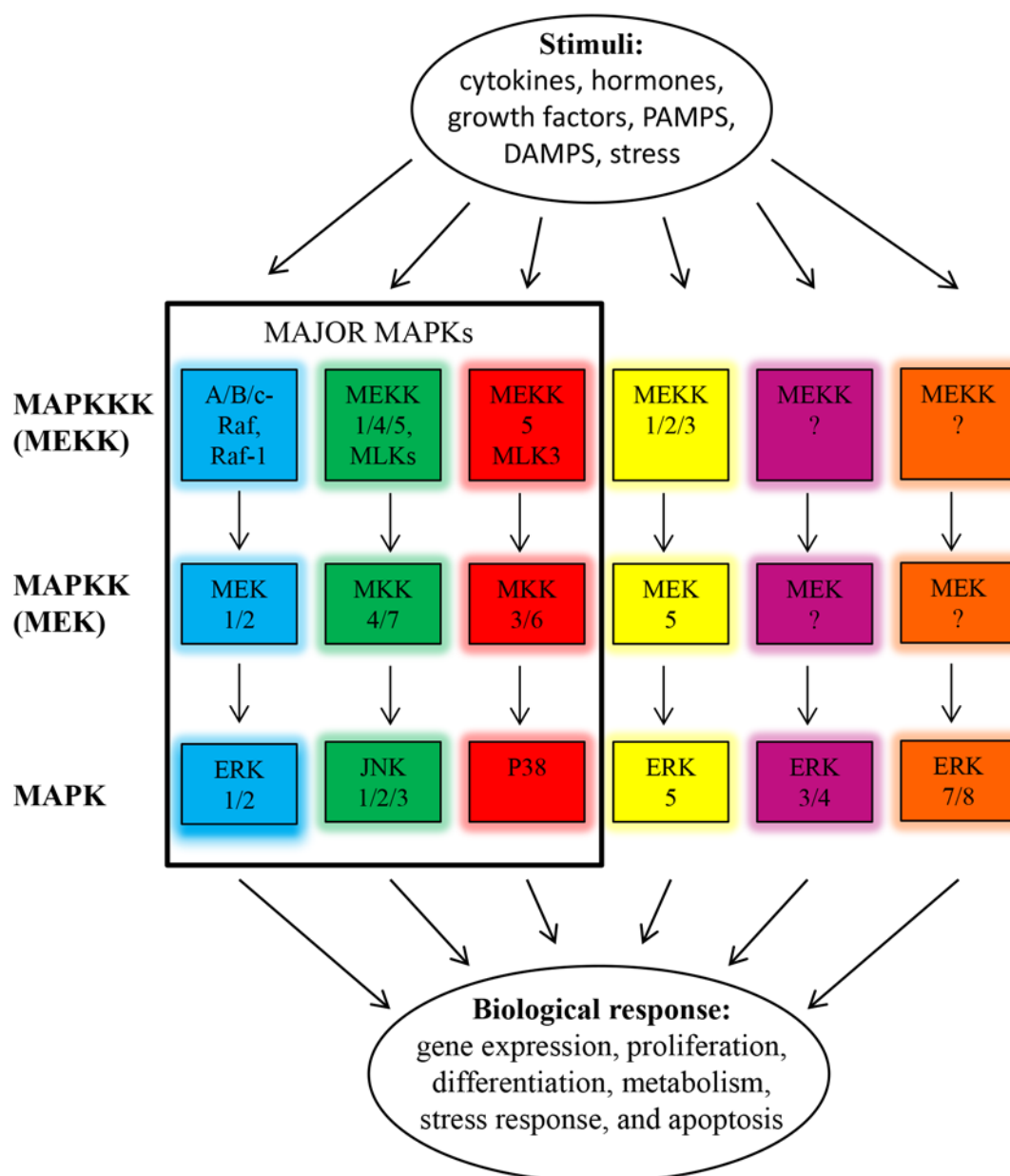


**Figure 1.5: Simplified mammalian MAPK signalling pathway.**

The simplified MAPK signalling pathway shows that each MAPK is phosphorylated by a specific upstream MAPK kinases (MAPKK, MKK or MEK), which is itself phosphorylated by another specific MAPKK kinases (MAPKKK, MKKK or MEKK) but substantial cross-talk and feed-back loops do exist. MLK: mixed-lineage protein kinase.

**1.7.1 Transcriptional Regulation**

Although there are a multitude of transcription factors that can regulate gene expression, only a handful of these have been shown to be involved in regulation of either CXCL10 and/or CXCL8. These include members of the NF- $\kappa$ B, IRF, and signal transducer and activator of transcription (STAT) transcription factor families.

**1.7.1.1 NF- $\kappa$ B**

NF- $\kappa$ B plays a key role in mediating all the classical signs of inflammation<sup>328</sup>. Typically, homo- or heterodimers of the Rel family of proteins including p105/p50 (NF- $\kappa$ B1), p100/p52 (NF- $\kappa$ B2), p65( RelA), RelB or cRel are sequestered and held inactive in the cytoplasm of unstimulated cells by the binding of an inhibitory protein, the inhibitor of NF- $\kappa$ B (I $\kappa$ B)<sup>328-332</sup>. The canonical form of NF- $\kappa$ B is a heterodimer of p65 with either p50 or p52 but the p50/p65 NF- $\kappa$ B heterodimer is ubiquitously expressed and the most widely studied<sup>328,330</sup>. RelB and cRel have limited tissue expression with RelB expression restricted to the thymus, lymph nodes and Peyer's patches, while cRel expression is restricted to hematopoietic cells and lymphocytes<sup>330</sup>. NF- $\kappa$ B family members all contain N-terminal Rel homology domains which are responsible for dimerization, interaction with I $\kappa$ B proteins, nuclear translocation and DNA binding<sup>332,333</sup>. In addition to this, p65 Rel-B and c-Rel also

contain C-terminal transcriptional activation domains (or transactivation domains) (TADs)<sup>330</sup>. There are now eight known members of the I $\kappa$ B family: I $\kappa$ B $\alpha$ , I $\kappa$ B $\beta$ , I $\kappa$ B $\epsilon$ , I $\kappa$ B $\zeta$ , I $\kappa$ BNS, Bcl-3, and the I $\kappa$ B-like p100 and p105 proteins, with I $\kappa$ B $\alpha$  being the prototypical member of this family<sup>328,330</sup>. Although the ‘typical’ members of the I $\kappa$ B family (I $\kappa$ B $\alpha$ ,  $\beta$  and  $\epsilon$ ) are chiefly involved in sequestering NF- $\kappa$ B dimers in the cytoplasm, other members of the I $\kappa$ B family have been suggested to be also involved in stabilizing nuclear and DNA bound dimers as well as positively regulating transcription by acting as transcriptional co-activators<sup>328</sup>.

Activation of the canonical NF- $\kappa$ B pathway utilizes an I $\kappa$ B kinase (IKK) complex composed of IKK $\alpha$ , IKK $\beta$  and IKK $\gamma$  (also known as NF- $\kappa$ B essential modulator (NEMO)) (**Figure 1.6**)<sup>330,331,334,335</sup>. Phosphorylation of I $\kappa$ B $\alpha$  on two serine residues by IKK $\beta$  leads to its poly-ubiquitination and subsequent degradation by the 26S proteasome<sup>336,337</sup>, exposing the nuclear localization sequence on the p50/p65 heterodimer dimer, allowing for translocation to the nucleus, where it may regulate gene transcription by binding to specific recognition sequences located in gene promoter regions of DNA<sup>328,333</sup>.

The canonical NF- $\kappa$ B pathway is activated following HRV infection and is involved in transcriptional activation of both CXCL10 and CXCL8. More specifically, it has been shown that canonical IKK $\beta$ -mediated activation of the p50/p65 NF- $\kappa$ B heterodimer is involved in transcriptional activation of both of these genes<sup>160,297,338</sup>.

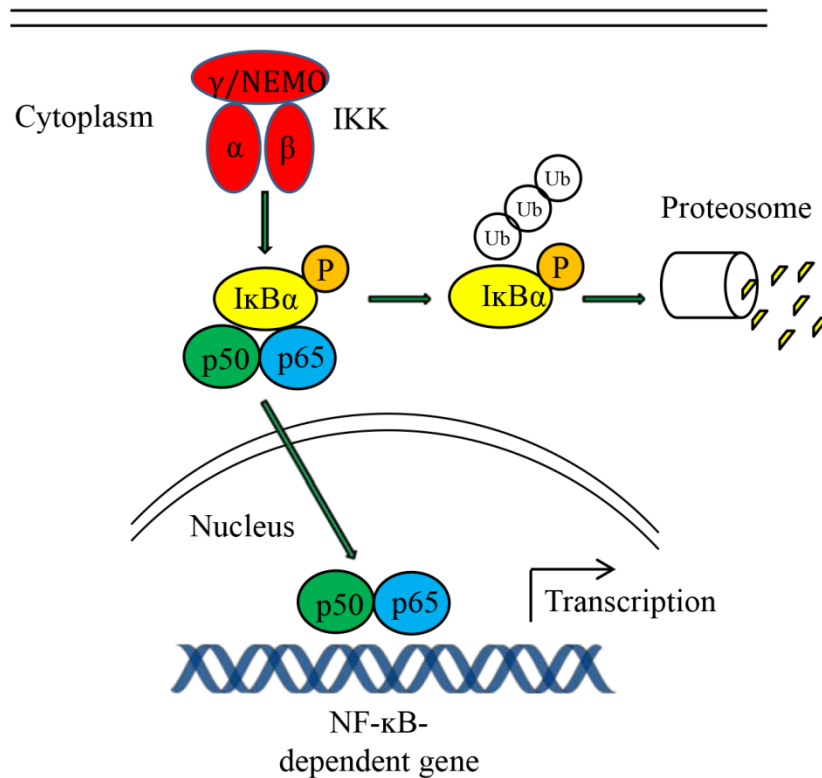


**Figure 1.6: Canonical NF-κB signalling pathway.**

Phosphorylation of IκBα by IKKβ in the IKK complex leads to its poly-ubiquitination (Ub) and degradation by the proteasome. This allows the p50/p65 heterodimer to translocate to the nucleus to regulate gene transcription.

#### 1.7.1.2 IRFs

In humans, the IRF transcription factor family includes 9 members (IRF1-9)<sup>339-341</sup>. IRF-1-3, 7 and 9 (p48) are either constitutively expressed and/or inducible in many cell types, while IRF-4, 5 and 8 expression is limited to immune cells such as B cells, T cells and DCs<sup>342</sup>. IRF-6 appears to be only expressed in skin cells<sup>342</sup>. All IRF family members have a conserved amino (N)-terminal DNA binding domain, which recognizes the consensus interferon-stimulated response element (ISRE) DNA sequence, and a carboxyl

(C)-terminal regulatory domain<sup>341</sup>. They can either interact with each other as homo/heterodimers or with other transcription factors such as NF- $\kappa$ B, STAT and TFIIB<sup>342–344</sup>. Classically, IRF-3 and IRF-7 as homo/heterodimers have been implicated as key regulators of anti-viral gene induction downstream of PRRs, such as the type I IFN response, but this dogma is now being challenged<sup>339</sup>. Previously it has been shown that a minor group HRV induces IRF-3 activation (phosphorylation and homo-dimerization) and that this is required for CXCL10 mRNA expression in airway epithelial cells via TLR3 and MDA5 signalling<sup>154</sup>. More recently, it has been shown that IRF-1, but not IRF-3, is activated following major group HRV infection in airway epithelial cells and is involved in transcriptional activation of CXCL10 via binding to the ISRE binding-site in the CXCL10 promoter and IRF-1 is required for both HRV-induced CXCL10 mRNA and protein expression<sup>298,345</sup>. In support of this, others have also failed to observe IRF-3 activation following HRV infection<sup>346,347</sup>.

### 1.7.1.3 STATs

STAT proteins are latent in the cytoplasm until activated by a cytokine stimulus, such as interleukins, IFNs or growth factors<sup>348</sup>. In the canonical Janus kinase (JAK)-STAT pathway, cytokine binding to its cognate receptor results in receptor dimerization/oligomerization, leading to trans-phosphorylation of associated JAKs on tyrosine residues, subsequent phosphorylation of receptor tails on their src-homology-2 (SH2)-recruitment domains, recruitment of STAT proteins via their SH2 domains and trans-phosphorylation of STAT proteins by JAKs<sup>348</sup>. Phosphorylated STAT proteins

dimerize and translocate to the nucleus to drive transcription<sup>348</sup>. All members in the STAT family have a C-terminal DNA binding and transactivation domain<sup>349</sup>. JAK-STAT signalling has been shown to be negatively regulated by a variety of molecules including the suppressor of cytokine signalling (SOCS) proteins, protein inhibitor of activated STAT (PIAS) family and various protein tyrosine phosphatases (PTPs)<sup>348,349</sup>(**Figure 1.7**).

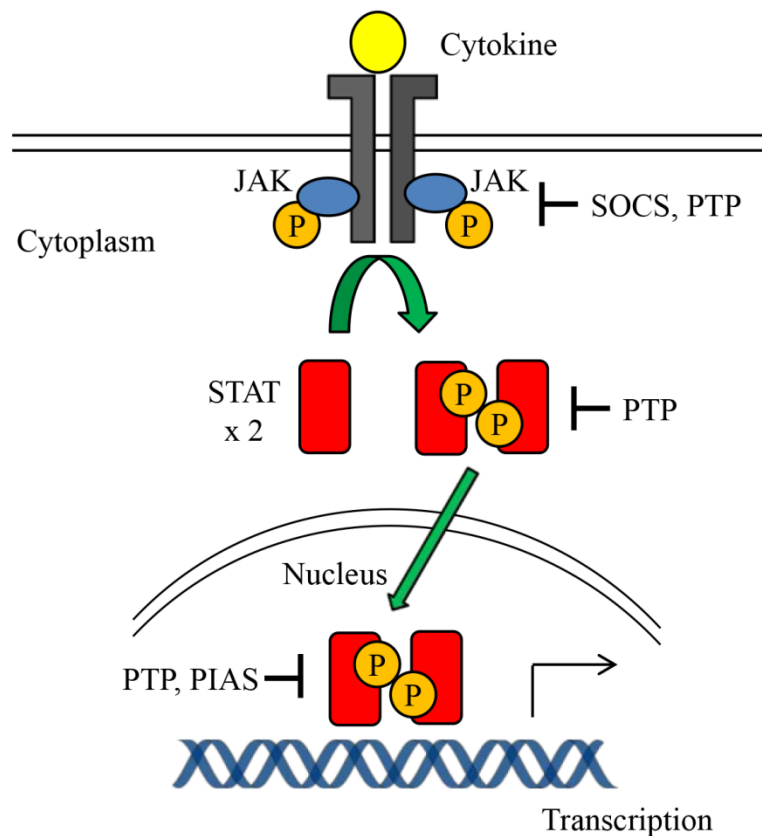


**Figure 1.7: The canonical JAK-STAT pathway and its negative regulation.**

In the canonical JAK-STAT pathway cytokine receptor dimerization or oligomerization leads to trans-phosphorylation of associated JAKs, leading to the recruitment and trans-phosphorylation of STAT proteins by JAKs. Phosphorylated STAT proteins then dimerize and translocate to the nucleus to drive transcription. Targets of negative regulation by SOCS, PIAS and PTPs are shown. Adapted from<sup>349</sup>.

In mammals, there are 7 members in the STAT family, including STAT-1-4, STAT-5A, STAT-5B and STAT-6, and 4 members in the JAK family, including JAK1-3 and tyrosine kinase-2 (TYK2)<sup>349</sup>. STAT-1, 3, 4, 5A, 5B and 6 are able to form homodimers but heterodimers are also formed composed of STAT-1/STAT-2 and STAT-1/STAT-3 depending on the nature of the activating stimulus<sup>348</sup>.

Classically, STAT-1 and STAT-2 are restricted to mediating the effects of IFNs (**Figure 1.8**). Typically, type I IFNs, including IFN- $\alpha$  and IFN- $\beta$ , induce the formation of the IFN-stimulated gene factor 3 (ISGF3) complex, composed of STAT-1 and STAT-2, in conjunction with p48/IRF-9, although a complex composed of a STAT-1 homodimer with p48/IRF-9 is also possible, which then mediates gene transcription via ISRE<sup>350-354</sup>. In contrast, the prototypical type II IFN, IFN- $\gamma$ , induces the formation of a STAT-1 homodimer alone which then mediates gene transcription via the IFN- $\gamma$  activated site (GAS)<sup>350</sup>.

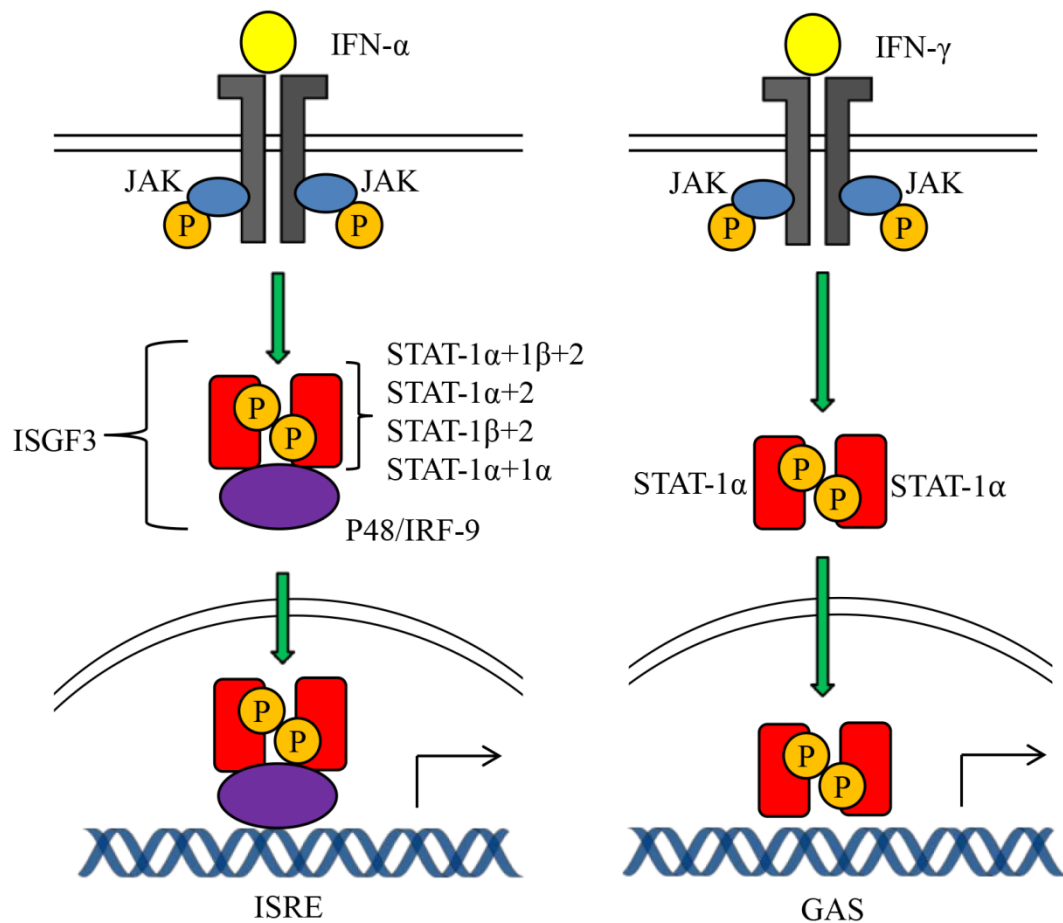


**Figure 1.8: The IFN-mediated JAK/STAT pathways.**

Type I IFNs, including IFN- $\alpha$ , mediate the formation of the ISGF3 complex, which then translocates to the nucleus and activates gene transcription of ISRE-containing genes. The ISGF3 complex is composed of either a trimer of STAT-1 $\alpha$ , STAT-1 $\beta$  and STAT-2, or a heterodimer of STAT-1 $\alpha/\beta$  and STAT-2, or a homodimer of STAT-1 $\alpha$ , in conjunction with p48/IRF-9. Type II IFNs, including IFN- $\gamma$ , mediate the formation of the STAT-1 $\alpha$  homodimer, which then translocates to the nucleus and activates gene transcription of GAS-containing genes.

STAT-1, 2 and 3 are generally ubiquitously expressed and have all been shown to be expressed in airway epithelial cells<sup>159,302,355–358</sup>. Moreover, STAT-1 is activated following HRV infection<sup>159,302,359</sup> and mediates both IFN- $\alpha$  and IFN- $\gamma$ -stimulated

transcription of CXCL10<sup>302,359</sup>. STAT-4 is primarily involved in mediating responses to IL-12 in lymphocytes and regulates differentiation of Th cells<sup>360</sup>. STAT-5 was previously named mammary gland factor (MAF) and has been linked to both development and cancer formation in mammary epithelium<sup>361,362</sup>. Although STAT-5 is also reportedly required for IgE-mediated mast cell function<sup>363,364</sup>, it has not been shown to be expressed in airway epithelium. STAT-6 is primarily involved in downstream IL-4-mediated Th2 differentiation<sup>365</sup> but has also been shown to mediate JAK-independent immune signalling in response to viral infection<sup>366</sup>. Recently, STAT-6 expression has been shown in both normal and asthmatic human bronchial epithelial cells and has been suggested to play a key role in mediating responses to the Th2 cytokines IL-4 and IL-13<sup>367,368</sup> but, to date, STAT-6 expression has not been investigated following HRV infection.

### ***1.7.2 Post-Transcriptional Regulation***

In addition to transcriptional regulation, many genes are also amenable to post transcriptional regulation. This can take many forms, including, but not limited to, alternate splicing, alternate polyadenylation/capping, nuclear export/mRNA localization, microRNA-mediated regulation and regulation of mRNA stability<sup>369</sup>. Interestingly, many inflammatory mediators, including some chemokines, have unstable mRNAs<sup>370</sup>. CXCL8 gene expression in particular is regulated via mRNA stability in many cell types following a variety of stimuli.

### 1.7.2.1 mRNA stability

Typically, mRNA is protected from degradation by exonucleases at the 5' end by the 7-methyl-guanosine cap and at the 3' end by the poly A tail<sup>371</sup>. Decapping enzymes and deadenylases target the removal of these structures, leaving mRNA vulnerable to exonuclease activity<sup>371</sup>. Adenine and uridine (AU)-rich sequences, also called AU-rich elements (AREs), in the 3' untranslated region (UTR) of mRNA are the most common determinants to confer mRNA instability in mammalian cells<sup>371,372</sup>. Although AREs can be present in other areas of mRNA, such as the 5' UTR, their location in the 3' UTR dominates in terms of mRNA stabilization capability<sup>373</sup>. ARE elements can be composed of pentamers of AUUUA segments, nonamers of UUAUUUAUU or other clusters of AU pentamers or nonamers<sup>369</sup>. ARE-binding proteins (ARE-BPs) bind ARE motifs in mRNA via specialized protein domains, including RNA-recognition motifs, zinc-finger domains and K-homology domains<sup>369</sup>. These ARE-BPs can destabilize mRNA by promoting deadenylation, decapping and degradation by exonucleases activity. It is not entirely clear how stabilizing ARE-BPs exert their effects on mRNA but it is suggested that they can do this is by blocking the ARE-binding sites from destabilizing ARE-BPs and/or removing mRNA from sites of decay<sup>374</sup>. Degradation of mRNA in the 5'→3' direction can occur via exonucleases in cytoplasmic foci termed mRNA processing bodies (P-bodies) and in the 3'→5' direction by the exosome<sup>374-376</sup>. The major decay pathway for ARE-containing transcripts in mammalian cells appears to be mediated by the exosome<sup>377-379</sup> but now it is suggested by some that both pathways are involved in the decay of unstable mRNAs<sup>374</sup>. Select ARE-BPs can be regulated by covalent modifications, such as

phosphorylation/dephosphorylation. The p38 MAPK, via its target p38-MAPK-activated kinase 2 (MK2), phosphorylates some ARE-BPs leading to either dissociation from ARE-containing transcripts or the recruitment of 14-3-3 adapter proteins, which block the interaction between ARE-containing mRNA and/or decay machinery<sup>325,376,380</sup>.

CXCL8 is a rapidly degradable gene and it is amenable to mRNA stabilization/destabilization<sup>279</sup>. Activation of the p38 MAPK pathway by a variety of stimuli has been shown to induce CXCL8 mRNA stabilization<sup>325-327</sup>. The 3' UTR of CXCL8 contains four AUUUA motifs, two of which overlap<sup>381</sup>. Several ARE binding proteins have been linked to the regulation of CXCL8 gene stability, including adenine-uridine-rich element RNA-binding factor (AUF)-1<sup>382</sup>, K-homology domain splicing regulatory protein (KHSRP)<sup>383,384</sup>, human antigen R (HuR)<sup>382,384-386</sup> and tristetraproline (TTP)<sup>387-389</sup>.

#### 1.7.2.1.1 AUF-1

AUF-1, also known as heterogeneous nuclear ribonucleoprotein D (hnRNPD), is expressed as 4 functional splice variants (p37, p40, p42 and p45 isoforms) which are involved in either stabilizing or destabilizing mRNAs<sup>371</sup>. The AUF-1 isoforms rank p37 > p42 > p45 > p40 in terms of their binding affinity to ARE-containing transcripts<sup>390</sup>. The p37 isoform reportedly has the greatest destabilizing capability and associates with the exosome<sup>370</sup>. Thus far, there is no known role of the p38-MAPK-MK2 pathway in the regulation of any of the isoforms of AUF-1.

#### 1.7.2.1.2 KHSRP

KHSRP is involved in destabilizing, or mediating the decay, of select mRNAs by recruiting mRNA decay machinery<sup>391–393</sup>. Specifically, KHSRP has been shown to recruit poly (A) ribonuclease (PARN), exosome components and decapping enzymes<sup>393</sup>. KHSRP has been shown to be negatively regulated by the p38-MAPK-MK2 pathway via direct phosphorylation, impairing its ability to bind or causing their dissociation from ARE-containing transcripts, leading to inhibition of KHSRP-mediated mRNA decay<sup>394</sup>.

#### 1.7.2.1.3 HuR

The ubiquitously expressed member of the embryonic lethal, abnormal vision (ELAV) family of RNA-binding proteins HuR stabilizes ARE-containing mRNA transcripts but can also either inhibit or promote translation<sup>369,395–398</sup>. HuR is thought to exert its stabilizing effects by directly competing with destabilizing factors, such as AUF-1, KHSRP and TTP, for ARE binding sites in ARE-containing mRNA transcripts, and in this way blocking the association of destabilizing factors with these transcripts<sup>374,392,396,399</sup>. Alternatively, it has also been shown that HuR may also be involved in relocating transcripts from P-bodies<sup>400</sup>. HuR is mainly localized to the nucleus but does shuttle to the cytoplasm to exert its stabilizing effects<sup>401,402</sup>. It is suggested that it may also bind ARE-containing transcripts in the nucleus and accompany them to the cytoplasm, thereby providing protection from destabilizing factors<sup>397,401</sup>. Interestingly, HuR does not contain

any phosphorylation sites for MAPKs but it is suggested that downstream targets of p38 MAPK may be involved in promoting nuclear-cytoplasmic shuttling of HuR<sup>403,404</sup>.

#### 1.7.2.1.4 TTP

TTP, also known as zinc finger protein 36 (ZFP36), is an early response gene encoding a zinc finger-binding protein, and is the most studied of the ARE binding proteins involved in mediating the decay or destabilization of mRNAs<sup>370,405</sup>. Stimulation of fibroblasts with mitogens has been shown to result in serine phosphorylation of TTP and re-localization from the nucleus to the cytoplasm<sup>406</sup>. TTP binds to AREs via its conserved zinc finger domains, leading to deadenylation and subsequent degradation of the mRNA transcript<sup>370,407</sup>. In addition to mediating degradation via the exosome, TTP has also been shown to associate with protein components in P-bodies<sup>380</sup>. TTP can be negatively regulated by the p38-MAPK-MK2 pathway, inhibiting it from binding AREs and/or modulating its subcellular localization<sup>376,408</sup>. This negative regulation of TTP allows stabilizing factors, such as HuR, to bind ARE-containing mRNAs promoting their stabilization<sup>376</sup>.

### ***1.7.3 Epigenetic Regulation***

Generally speaking, epigenetics is the study of the changes in gene expression based not on the underlying DNA sequence, but rather the changes that occur over/above (epi-) the coded nucleotide sequence (genetic)<sup>409</sup>. These changes encompass post-translational histone modifications, DNA methylation and non-coding RNAs (microRNAs

(miRNAs)<sup>409</sup>. The epigenome is plastic in the sense that it is amenable to changes due to environmental factors, diet, disease and aging<sup>409</sup>. There is now substantial evidence that some of these modifications are heritable<sup>410</sup>.

Regulation of gene expressions ultimately begins at the level of chromatin. Chromatin itself is composed of DNA which is tightly wound around histone proteins, allowing for tight packaging of genomic material inside the nucleus of cells<sup>411</sup>. The most basic unit of chromatin are nucleosomes which are composed of approximately 146 bp of DNA wrapped 1.7 times around a core octamer of histone proteins including two copies of each histone protein (H)2A, H2B, H3 and H4, giving the familiar appearance of ‘beads on a string’,<sup>411,412</sup>. Nucleosomes allow for 5- to 10-fold compaction of DNA<sup>411</sup>. Each nucleosome is separated by up to 80 bp, and then the whole ‘string’ of nucleosomes is then compacted even further to an order of 50-fold or higher using the H1 linker histone proteins<sup>411</sup>.

Gene transcription occurs in areas where chromatin is ‘open’ and DNA is accessible for the binding of transcription factors and RNA polymerase II, whereas a gene is silenced when the chromatin around the promoter region of the gene is ‘closed’<sup>413</sup>. The accessibility, or opening and closing, of chromatin is controlled by DNA methylation and histone modifications. DNA methylation is most common on CpG islands, which are found at or near transcriptional start sites of genes, and hypo-methylation of DNA results in gene transcription while hyper-methylation of DNA results in gene silencing. Generally, but not always, the addition of a moiety to histones results in a decrease of compaction of chromatin due to steric hindrance created by the added moieties, resulting in ‘opening’ or unwinding of DNA and the repositioning/release of histones. Histones can be post-

translationally modified in a variety of ways, including acetylation, methylation, ubiquitination, phosphorylation and SUMOylation, with histone acetylation being the most studied modification<sup>414</sup>.

Histone acetylation is under the control of histone acetyl transferases (HATs) and histone de-acetylases (HDACs), where HATs add acetyl groups to histone tails and ‘open’ chromatin and HDACs remove acetyl groups from histone tails allowing for ‘closing’ of the chromatin<sup>413,414</sup>. To date, there are over 30 known proteins with intrinsic HAT activity, including transcription factors, co-activators and other signalling molecules, with cyclic adenosine monophosphate (AMP)-response element binding protein (CREB)-binding protein (CBP)/p300 being the most widely studied<sup>415</sup>. There are eighteen known HDACs in humans and they are divided into the widely expressed type I HDACs (HDAC1, 2, 3, and 8), the more restricted type II HDACs (HDAC4, 5, 6, 7, 9 and 10), type III HDACs including sirtuins/silent information regulators (SIRT)1-7 and the type IV HDAC11<sup>413</sup>. Of the SIRTs, only SIRT1 has been studied in some detail in humans<sup>416</sup>. Notably, HDACs have the ability to not only de-acetylate histone proteins but also non-histone proteins such as NF-κB.

Cigarette smoke has been shown to have numerous epigenetic effects<sup>409</sup>. It can affect DNA methylation status, modify histones and affect miRNA expression<sup>312,312,417-419</sup>. Cigarette smoke condensate dysregulates DNA methylation status by causing both regional hyper- and hypomethylation of DNA in cultured human bronchial epithelial cells<sup>312</sup>. Moreover, a reduction of HDAC2 has been reported in the airways of smokers, patients with COPD and smoking asthmatics as compared to healthy non-smokers and this

correlated with symptom severity<sup>413,414,420,421</sup>. *In vitro*, CSE also reduced levels/activity of HDAC2 in human airway epithelial cells<sup>313,422</sup> and HDAC1-3 in macrophages<sup>423,424</sup>. Cigarette smoke exposure also increased H3 and H4 acetylation in rat lung, while reducing HDAC2 expression and activity in both rat and mouse lungs<sup>422,425</sup>. A reduction in other HDAC members, including HDAC5 and HDAC8, has also been reported in COPD<sup>420,421</sup>. Additionally, SIRT1 is reduced in the lungs of smokers and COPD patients as compared to healthy non-smokers<sup>415,426</sup>. The reason for the reduction in HDACs in these patients is still not completely understood but it is suggested to be linked to oxidative and nitrative stress induced by cigarette smoke<sup>420,427</sup>. Thus far, there have been no studies examining the role of epigenetic regulation on CXCL10 or CXCL8 gene expression by cigarette smoke.

## 1.8 Objective

The overall objective of this thesis project was to determine if and how cigarette smoke modulates HRV-induced CXCL10 and CXCL8 chemokine responses in human bronchial epithelial cells and subsequently, to delineate the mechanisms involved in this modulation.

## 1.9 Hypothesis

The central hypothesis of this thesis project is that *cigarette smoke alters HRV-induced chemokine responses in a manner that would be expected to result in worse clinical outcomes.* This study not only provides important insight into the inflammatory

state in HRV-infected smokers but particularly during HRV-induced exacerbations in smoking asthmatics and COPD patients.

## **1.10 Thesis Aims**

### ***1.10.1 Aim 1***

The first aim sought to determine if, and how, cigarette smoke alters HRV-induced CXCL10 and CXCL8 chemokine responses in human airway epithelial cells.

### ***1.10.2 Aim 2***

To delineate the mechanisms that lead to modulation of HRV-induced CXCL10 expression by cigarette smoke.

### ***1.10.3 Aim 3***

To delineate the mechanisms that lead to modulation of HRV-induced CXCL8 expression by cigarette smoke.

## Chapter Two: **Materials and Methods**

## 2.1 Materials

The following materials and reagents were purchased from indicated suppliers:

- **AbD Serotec** (Raleigh, NC, USA): glyceraldehyde-3-phosphate-dehydrogenase (GAPDH) antibody (#MCA4739).
- **Affymetrix** (Cleveland, OH, USA): shrimp alkaline phosphatase kit (#78390).
- **Ambion** (Austin, TX, USA): DNA-free DNase I kit (#AM1906).
- **American Type Tissue Collection** (Manassas, VA, USA): HRV-16 (#VR283), HRV-1A, WI-38 human fetal lung fibroblasts (#CCL-75) and H1-HeLa cells (#CRL-1958).
- **Applied Biosystems/Life Technologies** (Carlsbad, CA, USA): 96-well optical reaction plates (#4306737, #4346906), TaqMan universal PCR mastermix (#4304437), RNase inhibitor (#N808-0119) and reverse transcriptase (#4308228).
- **Biorad Laboratories** (Mississauga, ON, Canada): Lowry DC protein assay (#500-0116), 0.45 $\mu$ m nitrocellulose membrane (#162-0115), wet transfer system, protein ladder standard (#161-0373), Bradford protein assay (#500-0006) and EpiQ chromatin analysis kit (#172-5400).
- **Biotium Inc.** (Hayward, CA, USA): firefly luciferase assay kit (#30003-2).
- **BD** (Franklin Lakes, NJ, USA): 5 and 50 cc syringes (#CABD 309603 and 309653).
- **Calbiochem** (Gibbstown, NJ, USA): SB203580 / 4-(4-fluorophenyl)-2-(4-methylsulfinylphenyl)-5-(4-pyridyl)-imidazole (#559389), SB202474 / 4-Ethyl-2(p-methoxyphenyl)-5-(4'-pyridyl)-1H-imidazole (#559387), Nonident-P40 alternative

(#492016) and JAK inhibitor / 2-(1,1-Dimethylethyl)-9-fluoro-3,6-dihydro-7H-benz[h]-imidaz[4,5-f]isoquinolin-7-one (#420099).

- **College of Agriculture Reference Cigarette Program** (University of Kentucky, USA): 3R4F research grade cigarettes.
- **Corning Life Sciences** (Lowell, MA, USA): cell culture plates, dishes and flasks.
- **EMD/Merck Millipore** (Billerica, MA, USA): 0.22  $\mu$ M Steriflip filtration units and xylenes (#XX0060-4).
- **Fisher Scientific** (Ottawa, Ontario, Canada): Superfrost/Plus microscope slides (#12-550-15) and Permount mounting medium (#SP15-100).
- **Fujifilm Medical Systems** (Stamford, CT, USA): SuperRX X-ray film (#4741019238).
- **GE Healthcare Biosciences** (Piscataway, NJ, USA): enhanced chemiluminescent (ECL) substrate reagent (#RPN2209), horseradish peroxidase (HRP)-conjugated anti-rabbit antibody (#NA934V) and illustra MicroSpin G-25 sephadex columns (#27-5325-01).
- **Invitrogen** (Burlington, ON, Canada): Hanks' balanced salt solution (HBSS) (#14175), Ham's F12 medium (#11765), fetal bovine serum (FBS) (#16000), penicillin-streptomycin-amphotericin B (PSF) (#329-100), gentamicin (#15750-060), Dulbecco's modified eagle medium (DMEM) (#11885-084), L-glutamine (#25030), non-essential amino acids (#11140), sodium pyruvate (#11360), TRIzol Reagent (15596-018), GIBCO RNase/DNase-free double distilled water (#10977),

4-(2-hydroxyethyl)-1-piperazineethanesulfonic acid (HEPES) (#15630-080), anti-human mouse monoclonal ICAM-1/CD54 antibody (#MHCD5400), mouse IgG<sub>2A</sub> antibody (#02-6200), R-phycoerythrin goat anti-mouse IgG<sub>2A</sub> antibody (#P-21139), *Escherichia coli* Top10, Oligo (dt) primer (#18418-012), 5X first strand buffer (#Y02321), SuperScript III reverse transcriptase (#18080-044), SYBR greenER qPCR supermix (#11760-500), OptiMEM reduced serum media (#31985), Lipofectamine RNAiMAX transfection reagent (#13778-075) and UltraPure™ phenol:chloroform:isoamyl alcohol 25:24:1 (#15593).

- **Jackson ImmunoResearch Laboratories** (West Grove, PA, USA): HRP-conjugated anti-mouse antibody (#115-035-003).
- **Leica Microsystems** (Concord, Ontario, Canada): eosin and haematoxylin.
- **Lonza** (Walkersville, MD, USA): Bronchial epithelial cell basal growth medium (BEBM) and additives (bovine pituitary extract, epidermal growth factor, epinephrine, gentamicin/amphotericin B, hydrocortisone, insulin, retinoic acid, transferrin and triiodothyronine) (#CC-3170). BEBM was supplemented with additives to make bronchial epithelial cell growth medium (BEGM). AccuGENE 10X tris/borate/ethylenediaminetetraacetic acid (TBE) buffer (#50843).
- **Mirus** (Madison, WI, USA): TransIT-LT1 transfection reagent (#MIR 2300).
- **New England Biolabs** (Ipswich, MA, USA): T4 polynucleotide kinase (#M0201S), T4 polynucleotide kinase buffer (#B0201S), *NheI* restriction enzyme (#R3131S),

*KpnI* restriction enzyme (#R3142S), NEBuffer 1(#B7001S), NEBuffer 2 (B7002S) and 20X bovine serum albumin (BSA).

- **PerkinElmer** (Boston, MA, USA):  $\gamma$ -<sup>32</sup>[P] ATP (#BLU502A250UC).
- **Professional Plastics** (Fullerton, CA, USA): tygon silicon tubing (#ABW00004 and #ABW00022).
- **Promega** (Madison, WI, USA): 5X passive lysis buffer (#E1941), Cyto96™ non-radioactive cytotoxicity assay / lactate dehydrogenase (LDH) assay (#G1780) and pGL4.10 [*luc2*] vector (#E6651).
- **Qiagen** (Mississauga, ON, Canada): QIAquick gel extraction kit (#28704), QIAprep spin mini prep kit (#27104), QIAGEN maxi prep kit (#12663), TE buffer (#1018499) and QIAquick PCR purification kit (#28104).
- **Roche** (Mississauga, ON, Canada): pronase (#53702), anti-protease tablets (#04693116001), 2,2'-azino-bis (3-ethylbenzthiazoline-6-sulphonic acid) (ABTS) (#13846324) and rapid DNA ligation kit (#11635379001).
- **R & D Systems** (Minneapolis, MN, USA): recombinant CXCL10 protein (#266-IP), recombinant CXCL8 protein (#208-IL), CXCL10 capture (#MAB266) and biotinylated detection (#BAF266) antibody for ELISA.
- **Thermo Scientific** (Rochester, NY, USA): Cryogenic vials (#5000-0012), IgG Elution buffer (#21004) and 96-well Immulon 4 ultra-high binding polystyrene microtiter plates (#3855).

- **VWR** (Mississauga, Ontario, Canada): eppendorf tips and tubes, stripettes, Phase Lock Gel-Heavy tubes (#2302830), RNase/DNase free tubes (#20172945), isopropanol (#CAB10224-76) and micro cover glass (coverslips) (#48366067).
- **World Precision Instruments** (Sarasota, FL, USA): 3-way stopcock (#14035-10).

All other materials and reagents, unless specified otherwise, were purchased from **Sigma-Aldrich** (Oakville, ON, Canada).

## 2.2 Human Epithelial Cell Culture

### 2.2.1 *Primary human bronchial epithelial (HBE) cell isolation and culture*

Normal non-transplanted human lungs were obtained from a tissue retrieval service (International Institute for the Advancement of Medicine, Edison, NJ, USA). Ethical approval to receive and utilize lung tissues was obtained from both the Conjoint Health Research Ethics Board of the University of Calgary (Calgary, AB, Canada) and from the Internal Ethics Board of the International Institute for the Advancement of Medicine (Edison, NJ, USA). Lungs were received within 24-36 h after surgical removal; trachea and bronchi were dissected out and incubated in sterile filtered Ham's F12 medium (F12) containing 1  $\mu$ L/mL gentamicin and 1mg/mL pronase for 30-40 h at 4°C. Subsequently, tissue sections were placed in F12 containing 20% FBS (F12/FBS) and cells were forcefully jetted off the luminal surface of the dissected sections using a 5 mL syringe. Cells were then centrifuged in this medium (153 x g, 8 min, room temperature (RT)), re-suspended in 10 mL F12/FBS and non-ciliated epithelial cells were counted using a haemocytometer. For long term storage HBE cells were suspended in a 1:1 solution of

dimethyl sulphoxide (DMSO) and PSF at a density of  $0.5 \times 10^6$  /cryogenic vial and stored in liquid nitrogen. HBE cells were grown in submersion culture in BEGM (supplemented with 5% FBS for the first 72 h of culture) at 37°C in 5% CO<sub>2</sub> until desired confluence. This method of isolation and culture has previously been shown to produce cells of an epithelial cell nature which was confirmed with cytokeratin staining<sup>428</sup>. HBE cells were cultured in 6 well plates unless otherwise specified. Prior to desired treatment, cells were cultured overnight in BEBM or BEGM from which hydrocortisone was removed and then that respective medium was used for subsequent experiments.

### ***2.2.2 Bronchial epithelial cell line (BEAS-2B) culture***

The BEAS-2B bronchial epithelial cell line was a gift from C. Harris (National Cancer Institute, Bethesda, MD, USA). This cell line was generated by viral transformation of normal human bronchial epithelial cells using an Ad12-SV40 hybrid virus and retained their epithelial characteristics as assessed by electron microscopy and cytokeratin staining<sup>429</sup>. BEAS-2B cells were grown in submersion culture in BEGM at 37°C in 5% CO<sub>2</sub> until desired confluence. BEAS-2B cells were cultured in 6 well plates unless otherwise specified. Prior to desired treatment, cells were cultured overnight in BEBM or BEGM from which hydrocortisone was removed and then that respective medium was used for subsequent experiments.

## 2.3 HRV Propagation and Purification

### 2.3.1 HRV-16

HRV-16 was propagated by infection of WI-38 fetal lung fibroblast cells. A vial of WI-38 cells was cultured in WI-38 media (DMEM, 10% FBS, 2 mM L-glutamine, 1% non-essential amino acids, 1% sodium pyruvate and 1X PSF) initially in 1 T-75 cm<sup>2</sup> flask until confluence, then split into 4 T-175 cm<sup>2</sup> flasks until confluence and lastly into 16 T-175 cm<sup>2</sup> flasks. HRV-16 supernatants from previous preparations were diluted with WI-38 media and applied at 8 mL/flask to the confluent WI-38 cells, then incubated for 24-48 h at 34°C in 5% CO<sub>2</sub> until marked rounding of cells, indicating cytotoxicity, was observed. Media was then removed, centrifuged (425 x g, 15 min, 4°C) and stored in 20 mL aliquots at -80°C. Each 20 mL aliquot was used as the viral supernatant for re-infection for subsequent HRV-16 propagations in 16 T-175 cm<sup>2</sup> flasks. 8 mL of fresh WI-38 media was then added to each of 16 T-175 cm<sup>2</sup> flasks and each flask was thoroughly scraped with a cell scraper. The obtained cell lysate was sonicated on ice (Fisher Scientific Sonic Dismembrator Model 500: 15sec at 50% amplitude) and centrifuged (425 x g, 15 min, 4°C). This supernatant (crude cell lysate) was collected and stored at -80°C until purification.

Purification of HRV-16 was conducted via sucrose density centrifugation to remove ribosomes and soluble factors of cell origin. The crude cell lysate was thawed in a 37°C water bath and RNase A was added (80 µL/100 mL of crude cell lysate) to remove any ssRNA (unpackaged virus) and incubated for 30 min at 34°C. Following this incubation, N-laurosarcosine (10 mg/100 mL crude cell lysate) and β-mercaptoethanol (100 µL/100 mL crude cell lysate) was added to break up cellular components and reduce disulphide bonds.

The crude cell lysate was then underlayered with a 30% sucrose solution (30% sucrose, 20 mM Tris-acetate, 0.1 M NaCl) and centrifuged (28,000 rpm, 5 h, 16°C) using the Beckman Coulter Ultracentrifuge Optima XL-100K. Following centrifugation, the WI-38 media supernatant was aspirated until the start of the sucrose layer. The HRV-16-containing sucrose layer, minus the pellet, was combined 1:1 with F12/50 mM HEPES, sterile filtered using a 0.45 µm filter and stored at -80°C. This fraction was termed 'purified HRV-16' and used to infect the BEAS-2B cell line. The pellet was re-suspended in F12/HEPES, sterile filtered using a 0.45 µM filter and stored at -80°C. This fraction was termed 'HRV-16 pellet' and used to infect primary HBE cells.

### **2.3.2 HRV-1A**

HRV-1A was propagated in a similar manner to HRV-16, except H1-HeLa cells were used and these cells were cultured in DMEM media (low glucose, 5% FBS and 1X PSF). HRV-1A and HRV-16 had to be propagated in different cell lines as they display marked differences in their abilities to infect and replicate in WI-38 fibroblasts and H1-HeLas<sup>430</sup>. Purification of HRV-1A was performed in a similar manner to HRV-16.

### **2.3.3 Viral titre**

HRV titres were determined by infection of confluent WI-38 or H1-HeLa cells cultured in 96 well plates. Cells were infected with serial half-log dilutions (purified HRV: 1/300-1/1 x 10<sup>6</sup> and HRV pellet 1/3000-1/1 x 10<sup>9</sup>) and incubated for 5 days at 34°C in 5% CO<sub>2</sub>. Following this incubation cells were fixed with methanol for 1 min and stained with

0.1% crystal violet for 20 min. Plates were washed with distilled water and allowed to dry for a minimum of 48 h. Plates were then analyzed using the Bio-Rad Benchmark microplate reader at 570 nm. Using the values obtained from the spectrophotometric analysis, the 50% tissue culture infectious dose was calculated using the Reed-Muench method<sup>431</sup>.

#### **2.4 HRV Infection of Airway Epithelial Cells**

BEAS-2B cells were infected with HRV-16 at  $10^{4.5}$  50% tissue culture-infective dose (TCID<sub>50</sub>) U/ml (multiplicity of infection (MOI) of ~0.1), while HBE cells were infected with  $10^{5.5}$  TCID<sub>50</sub> U/ml (MOI ~1.0). The higher dose used in HBE cells is needed to ensure robust responses, as it has been shown that, even at high doses of HRV, no more than 10% of HBE cells are infected<sup>118</sup>. Infections were performed in the presence or absence of CSE. Cells were incubated at 34°C and 5% CO<sub>2</sub>.

#### **2.5 Transfection of Cells with Synthetic dsRNA**

Sub-confluent HBE or BEAS-2B cells were transiently transfected with a synthetic dsRNA polyionosinic-polycytodylic acid (poly [I:C]) (0.1 µg/well in BEBM) using TransIT-LT1 transfection reagent as per manufacturers protocol. After 1 h, cells were washed with HBSS and cultured in medium with or without CSE for an additional 24 h at 34°C and 5% CO<sub>2</sub>.

## 2.6 Preparation of CSE

CSE was freshly prepared with minor modifications of previously published methods<sup>432</sup> using 3R4F research grade cigarettes. CSE was generated by bubbling 1 cigarette per 4 mL of media at a rate of 5 min per cigarette using the syringe apparatus illustrated in **Figure 2.1**. The apparatus was constructed using a 50 cc syringe, rubber tubing, 3-way valve, a broken 10 mL stripette and parafilm to seal the connections. Subsequently, the crude CSE was sterile filtered using a 0.22  $\mu\text{m}$  pore filter and 5 dilutions were made using media as the diluent. The absorbance of the crude dilutions of CSE were then determined at 320 nm using a spectrophotometer (Ultrospec 2100 pro UV/visible spectrophotometer) and these values were used to generate a standard curve for each preparation of crude CSE. 320 nm has previously been shown to be the optimal wavelength for CSE and an absorbance of 0.15 at 320 nm has previously been shown not to be cytotoxic to cells<sup>432</sup>. 100% CSE was defined as having an absorbance of 0.15 and generated using the standard curve and the following formulas<sup>263,432,433</sup>:

$$y = mx+c$$

where  $y = 0.15$ ,  $m = \text{slope}$ ,  $x = \text{unknown concentration of CSE (nominally 1/dilution factor)}$  and  $c = \text{y-intercept}$ .

$$100\% \text{ CSE} = 1 \text{ mL crude CSE} + (\text{dilution factor}-1) \text{ mL media}$$

All subsequent dilutions were made from 100% CSE and immediately used to treat cells. For experiments where aged CSE was used the same procedure was followed except 100% CSE was left at 4°C for 24 h prior to further dilution and use.

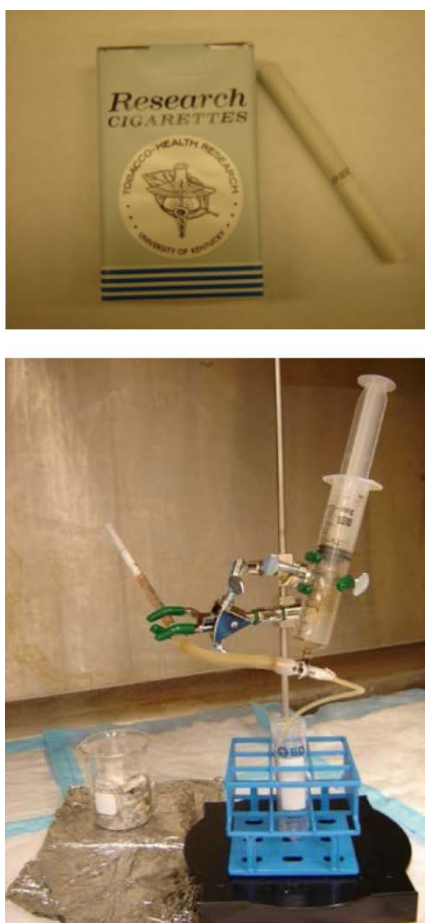


**Figure 2.1: 3R4F research grade cigarettes and syringe apparatus used to generate CSE.**

### **2.7 Treatment of Cells with Nicotine**

Nicotine was supplied as (-)-nicotine hydrogen tartrate salt (Sigma Aldrich # N5260) with a solubility of 50 mg/mL in H<sub>2</sub>O resulting in a final stock concentration of 17.54 mg/mL nicotine. Sub-confluent BEAS-2B cells were treated with serial dilutions (10 µg/mL – 10 ng/mL) of nicotine with or without CSE for 24 h at 34°C and 5% CO<sub>2</sub>.

## 2.8 Measuring Cell Viability

### 2.8.1 3-(4,5-dimethylthiazol-2-yl)-2,5-diphenyltetrazolium bromide (MTT) assay

The viability of cells following various treatments was assessed using the MTT assay which is based on the ability of a mitochondrial dehydrogenase enzyme, succinate dehydrogenase, from viable/proliferating cells to cleave the tetrazolium rings of MTT. MTT is pale yellow in colour but upon cleavage by the mitochondrial dehydrogenase enzyme, dark blue/purple formazan crystals form. The number of surviving cells is directly proportional to the amount of formazan product<sup>434</sup>.

Following the desired treatments of cells the supernatant was aspirated, MTT reagent (1 mg/mL in HBSS) was added (500  $\mu$ L/well of a 6 well plate and 250 $\mu$ L/well of a 24 well plate) and incubated at 37°C for 30 min. The MTT reagent was then aspirated, the formazan crystals were then solubilized by the addition of an organic solvent (DMSO: 1 mL/ well of a 6 well plate and 500  $\mu$ L/well of a 24 well plate), 100  $\mu$ L of each sample was then transferred into a 96 well plate and the colour was quantified by determining the optical density units (ODU) at 570 nm using the Bio-Rad Benchmark microplate reader. Percent viability was calculated compared to medium control using the following formula:

$$\% \text{ viability} = \frac{\text{ODU (sample)}}{\text{ODU (medium control)}} \times 100$$

### 2.8.2 Lactate dehydrogenase (LDH) assay

The viability of cells was also assessed using the Cyto96™ LDH assay which measures the release of a stable cytosolic enzyme that is released upon cell lysis. The

reaction requires the conversion of a tetrazolium salt into a red formazan product and the amount of colour produced is directly proportional to the number of lysed cells<sup>435</sup>.

Following the desired treatment of cells, 60  $\mu$ L of each sample was removed, after which 90  $\mu$ L of 5X passive lysis buffer was added to the control well, incubated for an extra 30 min at 34°C and this was used as the ‘control lysate’. The control lysate was diluted 1:10 with media and this in addition with all other samples were transferred to a 96-well plate. 50  $\mu$ L of tetrazolium salt substrate was added to each well and placed in the dark for 30 min. Following the incubation, 50  $\mu$ L of stop solution was added to each well and the colour was quantified by determining the optical density units (ODU) at 490 nm using the Bio-Rad Benchmark microplate reader. Percent cytotoxicity was calculated compared to medium control using the following formula:

$$\% \text{ cytotoxicity} = \frac{\text{ODU (sample supernatant)}}{\text{ODU (control supernatant) + ODU (control lysate)} \times 10} \times 100$$

## 2.9 Viral Titre Assay

To determine whether CSE had an effect on HRV-16 titre, HBE or BEAS-2B cells were treated with HRV-16 alone or in the combination with CSE for 2 h at 34°C and 5% CO<sub>2</sub>. Cells were then washed with HBSS and control media or CSE was put back for an additional 24 h upon which supernatants were collected. HRV titres were determined by infection of confluent WI-38 cultured in 96 well plates. Cells were infected with various dilutions of HBE or BEAS-2B supernatant (1/500-1/15,000) and incubated for 5 days at 34°C in 5% CO<sub>2</sub>. Following this incubation cells were fixed with methanol for 1 min and

stained with 0.1% crystal violet for 20 min. Plates were washed with distilled water and allowed to dry for a minimum of 48 h. Plates were then analyzed using the Bio-Rad Benchmark microplate reader at 570 nm. Using the values obtained from the spectrophotometric analysis, TCID<sub>50</sub> was calculated using the Reed-Muench method<sup>431</sup>.

## 2.10 Flow Cytometry

BEAS-2B cells were incubated for 24 h with the desired treatment. Following treatment, the cell supernatant was aspirated and cells were washed with 1 mL/well of HBSS. To gently lift cells off the plates, 500 µL/well of non-enzymatic cell dissociation solution (Sigma Aldrich #C5914) was added and plates were placed at 37°C until cells lifted off the bottom of the culture plates (10-30 min). The cell suspensions were then transferred to eppendorf tubes and gently centrifuged (300 x g, 5 min, 4°C). As further analysis required 4 tubes of each treatment (**Table 2.1**) with approximately 1 x 10<sup>6</sup> cells/tube, each sample was re-suspended in 1 mL 1X PBS containing 0.5% BSA and cells were counted using a haemocytometer.

**Table 2.1: Treatment Groups for Flow Cytometry Experiments**

Primary antibody	Secondary antibody	Purpose
1X PBS	1X PBS	Unlabelled control
1X PBS	IgG <sub>2A</sub> -PE	Control
IgG <sub>2A</sub>	IgG <sub>2A</sub> -PE	Negative control
ICAM-1 (CD54)	IgG <sub>2A</sub> -PE	Signal of interest

Following cell counts, the appropriate volume of cells was centrifuged (300 x g, 5 min, 4°C); re-suspended in 50 µL/tube 1X PBS 0.5% BSA and 5 µL/tube of primary antibody (ICAM-1, IgG<sub>2A</sub>) or PBS control was added. Samples were placed on ice for 30 min, then re-suspended in 1 mL/tube 1X PBS and centrifuged (300 x g, 5 min, 4°C). The supernatant was removed by tapping out, the pellet was then re-suspended in 50 µL/tube 1X PBS and 5 µL of secondary antibody (IgG<sub>2A</sub>-PE) was added prior to a 30 min incubation on ice in the dark. Following this incubation, cells were again re-suspended in 1 mL/tube 1X PBS and centrifuged (300 x g, 5 min, 4°C). Supernatant was removed and pellet was re-suspended in 1 mL/tube 1X PBS and immediately delivered to the University of Calgary Flow Cytometry Facility for analysis. Data were expressed as both % ICAM-1 gated events (% of cells expressing ICAM-1) and geometric mean (a measure of ICAM-1 receptors per cell).

### 2.11 Gene Array Analysis

Gene array analysis was performed by Expression Analysis Inc (Durham, NC, USA). Following treatment cellular RNA was isolated and quantified using a Nanodrop spectrophotometer and quality was determined using the Agilent 2100 Lab-on-a-Chip System (Santa Clara, CA, USA). Purified RNA was converted to Gene-Chip target using Affymetrix GeneChip 3' IVT express kit (Affymetrix, Santa Clara, CA, USA). The GeneChip target was then hybridized to Affymetrix U133plus2.0 human GeneChips for analysis of over 47,000 transcripts, washed, stained, and scanned using the protocol described by Affymetrix. Data from all genomics samples underwent rigorous quality

control procedures to detect potential outliers due to processing, instrumentation, or other such reasons.

## **2.12 RNA Isolation, DNase Treatment, cDNA Preparation and Real-Time RT-PCR**

### ***2.12.1 RNA isolation***

RNA was isolated using TRIzol Reagent (mono-phasic solution of phenol and guanidine isothiocyanate) as per manufacturer's instructions based on the single-step method of RNA isolation by acid guanidinium thiocyanate-phenol-chloroform extraction<sup>436,437</sup>. HBE or BEAS-2B cells were cultured and incubated with the desired treatment for the desired length of time upon which supernatant was removed, cells washed with HBSS and 500  $\mu$ L/well of TRIzol was added and pipetted up and down to lyse the cells. Duplicate samples were placed in RNase/DNase free tubes and stored at  $-80^{\circ}\text{C}$  prior to continuation with the following protocol. TRIzol samples were thawed, transferred to Phase Lock Gel-Heavy tubes, chloroform (0.2 mL/1mL TRIzol) was added, mixed vigorously and centrifuged (12,000 x g, 10 min,  $4^{\circ}\text{C}$ ). The RNA-containing aqueous layer was carefully transferred to a fresh RNase/DNase free tube and RNA was precipitated with isopropanol (0.5 mL/1mL TRIzol), inverted several times, incubated at RT for 10 min and then centrifuged (12,000 x g, 10 min,  $4^{\circ}\text{C}$ ). The supernatant was removed, the RNA pellet was washed with 75% ethanol (1 mL/1mL TRIzol), gently vortexed to dislodge the pellet and centrifuged (7,500 x g, 5 min,  $4^{\circ}\text{C}$ ). Following this, the supernatant was again removed and the pellet was allowed to air-dry for 5-10 min. The pellet was then dissolved in 20  $\mu$ L

RNase/DNase-free double distilled (GIBCO) water, then quantified and assessed for purity using the Nanodrop spectrophotometer. RNA was stored at  $-80^{\circ}\text{C}$ .

### ***2.12.2 DNase treatment***

In order to remove genomic DNA contamination from RNA, samples were treated with DNA-*free* DNase I as per manufacturer's instructions. 10  $\mu\text{g}$  of RNA were diluted with GIBCO water to a volume of 10  $\mu\text{L}$ . 1  $\mu\text{L}$  of 10X DNase buffer and 1  $\mu\text{L}$  of DNase I were then added, thoroughly mixed and incubated for 30 min at  $37^{\circ}\text{C}$ . Following the incubation, 5  $\mu\text{L}$  of DNase inactivation reagent was added and samples were incubated at RT for 2 min. The samples were then centrifuged (10,000  $\times g$ , 1 min, RT) and the purified RNA solution contained in the supernatant was carefully collected and transferred to a fresh RNase/DNase free tube. RNA was again quantified spectrophotometrically and stored at  $-80^{\circ}\text{C}$ .

### ***2.12.3 cDNA preparation***

1  $\mu\text{g}$  of input RNA was reverse transcribed to cDNA in a 20  $\mu\text{L}$  reaction mixture containing 1  $\mu\text{L}$  Oligo(dT)20 and 1  $\mu\text{L}$  10 mM dNTP mix. Samples were heated to  $65^{\circ}\text{C}$  for 5 min and then incubated on ice for at least 1 min before the addition of 4  $\mu\text{L}$  5X First strand buffer, 1  $\mu\text{L}$  0.1 M dithiothreitol (DTT) and 1  $\mu\text{L}$  of Superscript 3 reverse transcriptase. Samples were then placed in the Techne Flexigene thermocycler and subject to the following parameters:  $50^{\circ}\text{C}$  for 1 h and  $70^{\circ}\text{C}$  for 15 min. cDNA samples were then stored at  $-80^{\circ}\text{C}$ .

#### **2.12.4 Real-time RT-PCR**

The gene of interest was amplified in a real-time RT-PCR reaction using either the Applied Biosystems Model 7900 or the StepOnePlus sequence detector. The experimental setup consisted of 25  $\mu$ L reaction/well in a 96 well optical plate. Samples were analyzed from either RNA or from cDNA and the primers and probes for each gene are listed in **Table 2.2**. The primers and probes (excluding the 20X gene expression kits) were diluted to 10  $\mu$ M with GIBCO water and stored at  $-80^{\circ}\text{C}$ . When samples were analyzed from RNA the reaction mixture consisted of: 400 ng of RNA sample diluted in GIBCO water to a volume of 3  $\mu$ L, 12.5  $\mu$ L Taqman universal mastermix (1X), 1  $\mu$ L each of forward and reverse primer (400 nM), 0.5  $\mu$ L Taqman probe (200 nM), 0.5  $\mu$ L RNase inhibitor (10 U), 0.375  $\mu$ L Reverse Transcriptase (18.8 U) and GIBCO water to a final volume of 25  $\mu$ L per well. When samples were analyzed following conversion to cDNA, 1  $\mu$ L of cDNA was added per well and the RNase inhibitor and Reverse Transcriptase were omitted. IRF-1 and GAPDH primers and probe were supplied in a 20X gene expression kit and were added accordingly (1.25  $\mu$ L/25  $\mu$ L reaction) to the reaction mixture. The reaction consisted of a reverse transcription step when RNA was used for analysis (30 min at  $48^{\circ}\text{C}$ ) followed by PCR amplification (10 min at  $95^{\circ}\text{C}$ , 40 cycles of 15 sec at  $95^{\circ}\text{C}$  and 1 min at  $60^{\circ}\text{C}$ ). Samples were run in either duplicate or triplicate and a no template control (GIBCO water in place of sample) was run with each gene analyzed to exclude contamination.

**Table 2.2: Real-Time RT-PCR Primers and Probes**

<b>Gene</b>	<b>Primers (F&amp;R) &amp; Probe (P)</b>	<b>Synthesized by</b>
CXCL10	F: GAAATTATTCCTGCAAGCCAATTT R: TCACCCTTCTTTTTCATTGTAGCA P: TCCACGTGTTGAGATCA	Primers: U of C Core DNA Facility Probe: Applied Biosystems
CXCL8	F: CTGGCCGTGGCTCTCTTG R: TTAGCACTCCTTGGCAAACACTG P: CCTTCCTGATTTCTGCAGCTCTGTGTGAA	Primers: U of C Core DNA Facility Probe: Applied Biosystems
IRF-1	F: n/a R: n/a P: n/a	Applied Biosystems 20X IRF-1 Catalog #: Hs00971960
STAT-1	F: GCCCAATGCTTGCTTGGAT R: GCTGCAGACTCTCCGCAACT P: AGCTGCAGAACTGGTT	Primers: U of C Core DNA Facility Probe: Applied Biosystems
RIG-I	F: CAGGATTTGTAAAGCCCTGTTTTT R: CACTGATAATGAGGGCATCATTATATTT P: TACTTTCACATTTGCG	Primers: U of C Core DNA Facility Probe: Applied Biosystems
MDA5	F: TGGTCGAGCCAGAGCTGAT R: ACTCCTGAACCACTGTGAGCAA P: AGAGCACCTACGTCCTG	Primers: U of C Core DNA Facility Probe: Applied Biosystems
GAPDH	F: n/a R: n/a P: n/a	Applied Biosystems 20X GAPDH Catalog #: 4326317E

Data were analyzed using either relative or absolute quantification methods. Using relative quantification data were expressed as fold increase using the comparative  $\Delta\Delta C_T$  method as previously described<sup>438</sup>. In order to permit absolute quantification, a first strand cDNA oligonucleotide was synthesized by the University of Calgary Core DNA Facility (**Table 2.3**) and used as the standard. Each standard was log diluted with GIBCO water (100 fg-0.0001 fg) supplemented with transfer RNA (100 ng/mL) and run with the same reaction mixture and cycling parameters as mentioned above. Data was expressed as either attograms or femtograms calculated from the standard curve after correction for minor variation to the housekeeping gene (GAPDH).

**Table 2.3: Real-Time RT-PCR Standard Sequences**

<b>Gene</b>	<b>Standard Sequence</b>
CXCL10	AAC TTG AAA TTA TTC CTG CAA GCC AAT TTT GTC CAC GTG TTG AGA TCA TTG CTA CAA TGA AAA AGA AGG GTG AGA AGA
CXCL8	CCA AGC TGG CCG TGG CTC TCT TGG CAG CCT TCC TGA TTT CTG CAG CTC TGT GTG AAG GTG CAG TTT TGC CAA GGA GTG CTA AAG AAC
RIG-I	GAG AGC AGG ATT TGT AAA GCC CTG TTT TTA TAC ACT TCA CAT TTG CGG AAA TAT AAT GAT GCC CTC ATT ATC AGT GAG CAT
MDA5	GCC CGT GGT CGA GCC GAG CTG ATG AGA GCA CCT ACG TCC TGG TTG CTC ACA GTG GTT CAG GA

## 2.13 Enzyme Linked Immunosorbent Assay (ELISA)

### 2.13.1 CXCL10

Supernatants from HBE or BEAS-2B cells were collected following various treatments and assayed for CXCL10 protein release using a matched antibody pair CXCL10 sandwich ELISA (R&D Systems). All incubation steps in this procedure were performed at RT and are stated as minimum incubation times. 96-well immulon 4 plates were coated with 100  $\mu$ L/well monoclonal anti-human CXCL10 antibody (3  $\mu$ g/mL) diluted in 1X phosphate buffered saline (PBS) and incubated overnight. Following the primary/capture antibody incubation, wells were washed four times with ELISA wash buffer (0.05% Tween-20 in 1X PBS pH 7.4) then non-specific binding sites were blocked with 300  $\mu$ L/well blocking buffer (1% BSA 5% sucrose in 1X PBS) for 1 h. Following the blocking step, wells were washed as above and 100  $\mu$ L/well of recombinant CXCL10 protein standard in serial dilutions (3000-23.4 pg/mL), as well as samples in three serial dilutions, were applied to duplicate wells and incubated for 2 h. Both the protein standard and the samples were diluted in diluent buffer (0.1% BSA, 0.05% Tween-20 in 1X Tris-buffered saline (TBS)). Wells were washed and 100  $\mu$ L/well biotinylated anti-human CXCL10 detection/secondary antibody (300 ng/mL in diluent buffer) was applied for 2 h. Wells were washed and incubated with 100  $\mu$ L/well streptavidin peroxidase (1  $\mu$ g/mL in diluent buffer) for 30 min. Wells were washed again and developed with the addition of 100  $\mu$ L/well 1:1000 H<sub>2</sub>O<sub>2</sub>/ABTS in citrate phosphate buffer for approximately 30 min in the dark. The reaction was stopped with the addition of 100  $\mu$ L/well 2 mM sodium azide

and the absorbance at 405 nm was read using the Bio-Rad Benchmark microplate reader. Protein concentrations were interpolated from the linear portion of a four-parameter standard curve. The sensitivity of the assay was 30 pg/mL.

### ***2.13.2 CXCL8***

Supernatants from HBE or BEAS-2B cells were collected following various treatments and assayed for CXCL8 protein release using a matched antibody pair CXCL8 sandwich ELISA. All incubation steps in this procedure were performed at RT and are stated as minimum incubation times. 96-well immulon 4 plates were coated with 100  $\mu$ L/well monoclonal anti-human CXCL8 antibody at 1:1200 diluted in carbonate buffer and incubated overnight. Following the primary/capture antibody incubation, wells were washed four times with ELISA wash buffer and then non-specific binding sites were blocked with 100  $\mu$ L/well blocking buffer (1:100 rabbit serum diluted in 1% BSA 0.05% Tween-80 1X PBS) for 30 min. Following the blocking step, wells were washed as above and 100  $\mu$ L/well of recombinant CXCL8 protein standard in serial dilutions (7500-59 pg/mL), as well as samples in three serial dilutions, were applied to duplicate wells and incubated for 90 min. Both the protein standard and the samples were diluted in diluent buffer (1% BSA, 0.05% Tween-80 in 1X PBS). Wells were washed and 100  $\mu$ L/well biotinylated anti-human CXCL8 detection/secondary antibody (1:1200 in diluent buffer) was applied for 90 min. Wells were washed and incubated with 100  $\mu$ L/well streptavidin peroxidase (1  $\mu$ g/mL in diluent buffer) for 30 min. Wells were washed again and developed with the addition of 100  $\mu$ L/well 1:1000 H<sub>2</sub>O<sub>2</sub>/ABTS in citrate phosphate buffer for

approximately 12-13 min at 37°C in the dark. The reaction was stopped with the addition of 100 µL/well 2 mM sodium azide and the absorbance at 405 nm was read using the Bio-Rad Benchmark microplate reader. Protein concentrations were interpolated from the linear portion of a four-parameter standard curve. The sensitivity of the assay was 30 pg/mL.

## 2.14 Western Blotting

### 2.14.1 Whole cell lysate extraction

Following the desired treatment of HBE or BEAS-2B cells, supernatant was removed and cells were lysed with the addition of 500 µL/well ice-cold lysis buffer (1% Triton X-100 in 1X MES buffered saline pH 7.4, anti-protease tablets, 50 nM sodium orthovanadate, 0.4 M sodium pyrophosphate, 1 M sodium fluoride and 100 mM phenylmethanesulfonylfluoride (PMSF)). Cells were scraped off the plate on ice using a cell scraper, transferred to an eppendorf tube and frozen overnight to aid in cell lysis. The following day, samples were defrosted at RT and centrifuged (20,000 x g, 10 min, 4°C). The triton-soluble supernatant was then transferred to fresh tubes and stored at -80°C.

### 2.14.2 Protein assay

Total protein concentration in cell lysates was quantified using the modified Lowry DC protein assay. 5 µL of human serum albumin standard (HSA) (4000-125 pg/mL serial dilutions in 1X PBS) and sample were added in duplicate to a 96-well plate. 25 µL of reagent A' and 200 µL of reagent B were added to each well. The plates were then incubated at RT in the dark for a minimum of 15 min to allow for colour development.

Absorbance was quantified at 705 nm using the Bio-Rad Benchmark microplate reader and protein concentrations of each sample were interpolated from the HSA standard curve.

#### ***2.14.3 Sodium dodecyl sulphate – polyacrylamide gel electrophoresis (SDS-PAGE) and protein transfer***

Equivalent amounts of each sample (10-30 µg total protein diluted in 1X PBS) were separated using the Biorad Mini-PROTEAN gel electrophoresis system. 5X Laemmli sample buffer (50% glycerol, 10% sodium dodecyl sulfate (SDS), 250 mM Tris-HCl pH 6.8, 1 mg/mL bromophenol blue and 0.5 M DTT) was added to each sample and then each sample was boiled for a minimum of 5 min. Samples and a protein ladder standard were then loaded onto a 10% SDS polyacrylamide stacking gel atop a 10% SDS polyacrylamide resolving gel and electrophoresed at 100-150 V in 1X running buffer (192 mM glycine, 0.1% SDS, 25 mM Tris-base pH 8.3). Proteins were then transferred to a 0.45 µm nitrocellulose membrane using a wet transfer system in 1X transfer buffer (20% methanol, 2.5 mM Tris-base, 19.2 mM glycine) for 1-1.5 h at 100 V.

#### ***2.14.4 Immunoblotting***

Non-specific binding sites on nitrocellulose membranes were blocked with 5% skim milk powder in 0.1% Tween-20 1X TBS pH 7.4 (TTBS) at RT for 1 h on an orbital shaker. Membranes were washed 3X with TTBS and incubated with a specific primary antibody (**Table 2.4**) at 4°C overnight with gentle shaking. Membranes were washed a minimum of 3X with TTBS and incubated with the appropriate HRP-conjugated secondary antibody for

1 h at RT on an orbital shaker. Membranes were again washed a minimum of 3X in TTBS and placed in ECL substrate reagent for 1 min. Lastly, membranes were then exposed to film in a dark room for an appropriate length of time and developed using an automated developer.

**Table 2.4: Western Blotting Antibodies**

Target	Epitope	Source & conc.	Supplier & Catalogue #	Dilution & Diluent	MW (kDa)	Secondary Ab dilution
Phosphorylated (p)-I $\kappa$ B $\alpha$	Ser 32/36	Mouse	Cell Signaling 9246	1/2000 in TTBS+ 5% BSA	40	1/1000 in TTBS+ 5% skim milk
IRF-1	C-terminus	Rabbit 200 $\mu$ g/mL	Santa Cruz sc-497	1/4000 in TTBS+ 5% BSA	48	1/10,000 in TTBS+ 5% skim milk
IRF-2	C-terminus	Rabbit 200 $\mu$ g/mL	Santa Cruz sc-498	1/4000 in TTBS+ 5% BSA	50	1/10,000 in TTBS+ 5% skim milk
IRF-9	n/a	Mouse 0.5mg/mL	Abcam Ab56677	2 $\mu$ g/mL in TTBS+ 5% BSA	48	1/2000 in TTBS+ 5% skim milk
p-STAT-1	Tyr701	Rabbit	Cell Signaling 9167	1/1000 in TTBS+ 5% BSA	91,84	1/7500 in TTBS+ 5% skim milk
STAT-1	n/a	Rabbit	Cell Signaling 9172	1/1000 in TTBS+ 5% BSA	91,84	1/7500 in TTBS+ 5% skim milk

p-STAT-2	Tyr690	Rabbit	Cell Signaling 4441	1/1000 in TTBS+ 5% BSA	113	1/5000 in TTBS+ 5% skim milk
p-STAT-2	Tyr690	Rabbit	Santa Cruz sc-21689-R	1/1000 in TTBS+ 5% BSA	113	1/5000 in TTBS+ 5% skim milk
STAT-2	C-terminus	Rabbit	Santa Cruz sc-476	1/1000 in TTBS+ 5% BSA	113	1/5000 in TTBS+ 5% skim milk
p-STAT-3	Tyr705	Rabbit	Cell Signaling 9131	1/1000 in TTBS+ 5% BSA	86,79	1/5000 in TTBS+ 5% skim milk
p-STAT-3	Ser727	Rabbit	Cell Signaling 9134	1/1000 in TTBS+ 5% BSA	86	1/5000 in TTBS+ 5% skim milk
RIG-I	C-terminus	Rabbit	Cell Signaling 4520	1/1000 in TTBS+ 5% BSA	102	1/7500 in TTBS+ 5% skim milk
MDA-5	n/a	Rabbit 1mg/mL	Alexis Biochemicals 210-935-C100	1/1000 in TTBS+ 5% BSA	117	1/7500 in TTBS+ 5% skim milk
p-p38 MAPK	Thr180/ Tyr182	Rabbit	Cell Signaling 9211	1/1000 in TTBS+ 5% BSA	43	1/2000 in TTBS+ 5% skim milk
p38 MAPK	n/a	Rabbit	Cell Signaling 9212	1/1000 in TTBS+ 5% BSA	43	1/2000 in TTBS+ 5% skim milk
AUF-1	n/a	Rabbit	Upstate	1/1000 in	37,40,	1/1000 in

		.72mg/mL	07-260	TTBS+ 5% skim milk	42, 45	TTBS+ 5% skim milk
HuR	N-terminus	Mouse 100µg/mL	Molecular Probes A-21277	1µg/mL in TTBS + 5% skim milk	36	1/2000 in TTBS+ 5% skim milk
KHSRP	Internal sequence of amino acids 648-697	Rabbit 1mg/mL	Abcam Ab83291	1µg/mL in TTBS + 5% skim milk	73	1/10,000 in TTBS+ 5% skim milk
TTP	n/a	Rabbit n/a	Gift courtesy of Perry Blackshear	1/10,000 in TTBS + 5% BSA	36	1/25,000 in TTBS + 5% skim milk
TTP	region between amino acids 78-127	Rabbit 1mg/mL	Abcam Ab33058	1µg/mL in TTBS + 5% BSA	36	1/10,000 in TTBS + 5% skim milk
TTP	C-terminus Amino acids 166- 285	Rabbit 200µg/mL	Santa Cruz Sc-14030	1/1000 in TTBS + 5% BSA	36	1/7,500 in TTBS + 5% skim milk
GAPDH	C-terminus	Mouse 1mg/mL	AbD Serotec MCA-4739	1/40,000 TTBS	37	1/10,000 in TTBS

#### ***2.14.5 Assessment of equal protein loading***

Equal loading of protein was determined by stripping each membrane and re-probing with an antibody to the housekeeping gene GAPDH, which is a gene that is often stably and constitutively expressed at high levels in most tissues and cells. GAPDH expression was initially determined not to be affected with the treatments used in further experiments. Membranes were either gently stripped with IgG elution buffer for 30 min or with a harsher stripping solution for 5 min (70 mM Tris-HCl, 2% SDS, pH 6.8 heated to 80°C + 0.7%  $\beta$ -mercaptoethanol) on an orbital shaker. Membranes were washed a minimum of 3X and blocked in 5% skim milk in TTBS for 30 min. Subsequently, membranes were washed 3X and incubated with GAPDH antibody for 20 min. Again, membranes were washed 3X and incubated with the appropriate HRP-conjugated secondary antibody for 20 min at RT on an orbital shaker. Membranes were then developed as described above.

#### ***2.14.6 Densitometry***

Densitometric analysis was performed using ImageJ software (version 1.41, National Institute of Health, Bethesda, MD, USA). Percent expression of the protein of interest was assessed by comparison to the appropriate control and normalized for minor protein loading variation to GAPDH levels.

## 2.15 Luciferase Reporter Assay

### 2.15.1 CXCL10 promoter constructs

The 972 bp human full length CXCL10 promoter corresponding to the sequence from -875 to +97 (relative to the transcriptional start site) of the 5'-flanking region of the human CXCL10 gene was amplified from human genomic DNA using specifically designed primers:

- Forward = 5' – GCGTAGGTACCTAGAACCCCATCGTAAATC – 3'
- Reverse = 5' – GCGTAGCTAGCTAGCAGCAAATCAGAATGG – 3'.

These primers incorporated the restriction sites for *KpnI* (forward primer) and *NheI* (reverse primer) to allow for proper orientation upstream of a firefly luciferase reporter. The amplicon was resolved using agarose gel electrophoresis and the excised band was gel purified with the QIAquick gel extraction kit according to the manufacturer's instructions. The purified CXCL10 promoter amplicon (18  $\mu$ L) and the pGL4.10 [*luc2*] vector (0.5  $\mu$ g) containing an inducible firefly luciferase reporter gene and an ampicillin resistance gene were separately incubated with the restriction enzymes *KpnI* (1  $\mu$ L/20 units) and *NheI* (1  $\mu$ L/20 units) along with NEBuffer 1 (2.5  $\mu$ L) and 10X BSA (from NEB, 2.5  $\mu$ L) for 2-3 h at 37°C. The resulting double-cut pGL4.10 [*luc2*] vector was then alkaline phosphatase treated at 37°C for 1 h followed by 65°C for 15 min using a shrimp alkaline phosphatase kit according to the manufacturer's instructions in order to prevent re-annealing of the vector upon itself. The double-cut alkaline phosphatase-treated pGL4.10 [*luc2*] vector and the CXCL10 promoter amplicon were resolved on a 1% agarose gel and gel purified as described previously. The amplicon was then cloned into the vector using the Rapid DNA

ligation kit. Competent DH5 $\alpha$  *Escherichia coli* Top10 were transformed with the resulting CXCL10 promoter – luciferase construct via heat shock (30 min on ice, 42°C for 30 sec and 2 min on ice) and grown on Luria-Bertani (LB) agar plates using LB broth (both supplemented with ampicillin (50  $\mu$ g/mL)) overnight at 37°C. Individual colonies were grown in LB broth supplemented with ampicillin (100  $\mu$ g/mL) overnight at 37°C with vigorous shaking. CXCL10 promoter luciferase plasmids were purified using the plasmid QIAprep spin miniprep kit according to the manufacturer’s instructions, double cut with the aforementioned restriction enzymes to ensure the presence of the correct product and the CXCL10 promoter fragment was confirmed by sequencing (University of Calgary Core DNA Services). Large quantities of the CXCL10 promoter luciferase plasmids to be used for future experiments were prepared using the QIAGEN plasmid maxi prep kit according to the manufacturer’s instructions.

The 376 bp human truncated CXCL10 promoter corresponding to the sequence from -279 to +97 (relative to the transcriptional start site) was generated using the full length CXCL10 promoter as a template using specifically designed primers:

- Forward = 5’ – GCGTAGGTACCTAGAGAATGGATTGCAACC – 3’
- Reverse = 5’ – GCGTAGCTAGCTAGCAGCAAATCAGAATGG – 3’ (same as full length CXCL10 promoter reverse primer).

The resulting amplicon was then cloned according to the same protocol as described above. Putative transcription factor binding sites were determined using the Genomatix MatInspector program and supported by previous publications<sup>259,297,298,338,345</sup>. Point mutations within various transcription factor binding sites were then generated using site-

directed mutagenesis techniques within the full length CXCL10 promoter construct. Primer sequences with mutated residues are listed in **Table 2.5**. The resulting amplicons were then cloned according to the same protocol as described above.

**Table 2.5: CXCL10 Promoter Point Mutation Primer Sequences**

<b>Transcription Factor Binding Site</b>	<b>Forward Primer Sequence (5' → 3')</b>
ISRE	GTTTTGGAcAGT <u>GAc</u> ACCTAATTC
NF-κB (κB1)	GCAACATG <u>tGACTT</u> CaCCAGG
NF-κB (κB2)	GCAGAG <u>tGAAAT</u> TaCGTAACTTGG
AP-1	CCAGCAGGTTTTGCTAAG <u>Gat</u> AACTGTAATGC
STAT (STAT #1)	GCTTTTAAATTCATT <u>gCCTCA</u> tAAAGC
STAT (STAT #2)	TGTTT <u>taCCCTCA</u> tAATAGTTATGTTGGAGG

\*Mutated residues in bold lowercase letters. Core sequence underlined.

Tandem repeat constructs containing 5X repeats of either the CXCL10-specific κB1 (5' – TGGGACTTCCCCA – 3') or κB2 (5' – GGGAAATTCCGTC – 3') were synthesized incorporating *KpnI* and *NheI* restriction sites and cloned in a similar manner as described above.

### **2.15.2 CXCL8 promoter constructs**

The 720 bp human full length CXCL8 promoter corresponding to the sequence from -712 to +8 (relative to the transcriptional start site) of the 5'-flanking region of the human CXCL8 gene was amplified from human genomic DNA using specifically designed primers:

- Forward = 5' – CGGGGTACCTATAGTCAGTCCTTACATTGC – 3'
- Reverse = 5' – CCCAAGCTTCTTATGGAGTGCTCCGGTGGC – 3'.

These primers incorporated the restriction sites for *KpnI* (forward primer) and *HindIII* (reverse primer) to allow for proper orientation upstream of a firefly luciferase reporter. The resulting amplicon was cloned in a similar manner to that described for the CXCL10 promoter except NEBuffer 2 in place of NEBuffer 1 was used.

### ***2.15.3 Transient transfection and luciferase assay***

Subconfluent (40-50%) BEAS-2B cells were transiently transfected with the various promoter luciferase constructs using TransIT-LT1 lipid transfection reagent in a 3:1 ratio of lipid:DNA. Briefly, 0.1 µg/well of the promoter construct, TransIT-LT1 transfection reagent and 100 µL/well of BEBM was incubated for 20 min at RT in a separate tube. BEAS-2B cells were washed with HBSS and 600 µL of BEBM and 100 µL of the promoter/transfection lipid mixture was added per well and the cells were then incubated for 5 h at 37°C and 5% CO<sub>2</sub>. Following this incubation the supernatant was aspirated and cells were recovered overnight in BEGM without hydrocortisone containing 5% FBS. The next day, cells were treated with the relevant stimulus and incubated for a further 24 h (CXCL10) or 5 h (CXCL8) at 34°C and 5% CO<sub>2</sub>. Following treatment, supernatant was aspirated, cells were washed with HBSS and 500 µL/well of 1X Passive Lysis Buffer was added. Plates were placed on an orbital shaker for 20 min at RT, and then cells were scraped on ice using a cell scraper and lysates transferred to eppendorf tubes. Samples were then frozen at -80°C overnight to ensure maximal cell lysis. Lysates were then assayed

using the firefly luciferase assay kit and a luminometer (Monolight 3012, BD Biosciences). Each treatment was averaged from triplicate wells and expressed as relative light units (RLU) and/or fold over control.

### 2.16 Actinomycin D Chase Assay

BEAS-2B cells were exposed to medium control, CSE, HRV-16 or the combination for 2 h. Cell supernatants were aspirated and cells were washed with HBSS. Actinomycin D (Sigma Aldrich, catalog # A9415) was initially dissolved in DMSO and then diluted in cell culture media or CSE and added at a final concentration of 10  $\mu\text{g}/\text{mL}$ . Cellular RNA was then isolated at various times for analysis of CXCL8 mRNA levels using real-time RT-PCR.

### 2.17 Inhibitors and siRNA

#### 2.17.1 IKK $\beta$ inhibitor

Pharmacological inhibition of NF- $\kappa$ B was used to confirm the involvement of this pathway in HRV-16-induced CXCL10 induction. For this, the IKK $\beta$  inhibitor, PS1145 / N-(6-chloro-9H- $\beta$ -carbolin-8-yl) (Sigma Aldrich, catalog # P6624) was used to confirm the involvement of the canonical NF- $\kappa$ B pathway. PS1145 was solubilized in DMSO as per manufacturer's instructions and DMSO alone was used as vehicle control. BEAS-2B cells were pre-incubated with PS1145 or an equal volume of vehicle control for 1.5 h at 37°C and 5% CO<sub>2</sub> to ensure maximal inhibition before treatment with medium control, CSE, HRV-16 or the combination for 24 h. The pre-treatment consisted of 500  $\mu\text{L}/\text{well}$  of media

alone or media plus PS1145/DMSO and was left on for the subsequent treatment where 500  $\mu$ L/well was added of the appropriate stimulus. The final concentration of PS1145 was 10  $\mu$ M.

### ***2.17.2 JAK inhibitor***

To determine the involvement of the JAK/STAT pathway in the induction of CXCL10 by HRV-16 and CSE, the JAK inhibitor I was used. JAK inhibitor I is a potent, reversible, cell-permeable and ATP-competitive inhibitor against JAK1, JAK2, JAK3 and Tyk2. This compound was solubilized in DMSO as per manufacturer's instructions and DMSO alone was used as vehicle control. BEAS-2B cells were incubated with various concentrations of the JAK inhibitor together with CSE, HRV-16 or the combination for 24 h at 34°C and 5% CO<sub>2</sub> prior to collection of supernatants for analysis of CXCL10 protein release.

### ***2.17.3 p38 MAPK inhibitor***

Pharmacological inhibition of the p38 MAPK was used to determine the involvement of this pathway in the stabilization of CXCL8 mRNA. The specific inhibitor of the p38 MAPK pathway used was SB203580<sup>439</sup>. SB202474 is as an inactive analog of SB203580 and was used as a negative control for p38 MAPK inhibition studies. Both compounds were solubilized in DMSO as per manufacturer's instructions and DMSO alone was used as vehicle control. BEAS-2B cells were pre-incubated with SB203580 / SB202474 or an equal volume of vehicle control for 1 h at 37°C and 5% CO<sub>2</sub> to ensure

maximal inhibition before treatment with medium control, CSE, HRV-16 or the combination for 24 h at 34°C and 5% CO<sub>2</sub>. The pre-treatment consisted of 500 µL/well of media alone or media plus SB203580/ SB202474/ DMSO and was left on for the subsequent treatment where 500 µL/well was added of the appropriate stimulus. The final concentration of SB203580 and SB202474 was 3 µM.

#### **2.17.4 siRNA**

Sub-confluent HBE cells (70-80%) were used for transient siRNA transfections. Individual siRNAs (**Table 2.6**) were diluted to the appropriate concentrations in 125 µL/well of serum-free OptiMEM media. Lipofectamine RNAiMAX reagent was diluted 1:50 in OptiMEM for a total volume of 125 µL/well. These two dilutions were then combined and incubated at RT for 20 min. A lipid only control was included to ensure that the transfection reagent was not having an effect. A non-targeting siRNA control was also included using either a universal control siRNA with either a low GC or a medium GC content according to the siRNA of interest used. HBE cells were washed with HBSS and 750 µL/well of BEGM without antibiotics (no PSF, gentamicin or amphotericin) was added along with 250 µL/well of the siRNA-transfection lipid mixture and incubated for 24 h at 37°C and 5% CO<sub>2</sub>. The supernatant was then aspirated; cells washed with HBSS and recovered for 24 h at 37°C and 5% CO<sub>2</sub> in BEGM without hydrocortisone. Following recovery, cells were subject to the desired treatment for an additional 24 h at 34°C and 5% CO<sub>2</sub>.

**Table 2.6: siRNA Information**

Target	Sequence (5' → 3')	Supplier and Catalog #
RIG-I	AAGCTTTACAACCAGAATTTA	Qiagen S103019646
RIG-I	TTCTACAGATTTGCTCTACTA	Qiagen S104208673
MDA5	CAGAACTGACATAAGAATCAA	Qiagen S103648981
MDA5	CAGGTGTAAGAGAGCTACTAA	Qiagen S103649037
STAT-1	CAGAAAGAGCTTGACAGTAAA	Qiagen S102662324
STAT-1	CCAGATGTCTATGATCATTTA	Qiagen S102662884
AUF-1	AACAGCCAAGGTTACGGTGGT	Qiagen S100300454
AUF-1	CACAATGTTGGTCTTAGTAAA	Qiagen S102653665
KHSRP	AAGATGATGCTGGATGACATT	Qiagen S100300587
KHSRP	CTGGAGTGAAGATGATCTTAA	Qiagen S100054691
HuR	AAGTAGCAGGACACAGCTTGG	Qiagen S100300139
HuR	ACCAGTTTCAATGGTCATAAA	Qiagen S103246551
Low GC negative	Sequence not available	Invitrogen

control siRNA (non-targeting)		12935-200
Medium GC negative control siRNA (non-targeting)	Sequence not available	Invitrogen 12935-300

## 2.18 Electrophoretic Mobility Shift Assay (EMSA)

### 2.18.1 Nuclear extraction and protein quantification

HBE cells were treated for the desired length of time prior to nuclear protein extraction. Cells were scraped in their medium on ice, the cell lysates were then placed in pre-chilled eppendorf tubes and centrifuged (5000 x g, 5 min, 4°C). The supernatant was aspirated, the pellet was re-suspended in 50 µL Gough Buffer (10 mM Tris-HCl pH 7.5, 150 mM NaCl, 1.5 mM MgCl<sub>2</sub>, 0.65% Nonident P-40, 0.5 mM PMSF and 10 mM DTT), cell lysates were then vortexed for 15 sec, left on ice for 10 min and centrifuged (12000 x g, 2 min, 4°C). The supernatant containing the cytoplasmic fraction was transferred to fresh tubes and stored at -80°C. The pellet, containing the nuclear fraction, was re-suspended in 15 µL of Lysis Buffer C (20 mM HEPES pH 7.9, 25% glycerol, 400 mM NaCl, 1.5 mM MgCl<sub>2</sub>, 0.2 mM ethylenediaminetetraacetic acid (EDTA) pH 8.0, 0.5 mM PMSF and 10 mM DTT) and samples were then immediately agitated by running along an eppendorf tube rack for 5 strokes in one direction and 5 strokes in the opposite direction. Samples were placed on ice for 2 h with agitation as described every 15 min. Following the 2 h incubation, samples were centrifuged (12000 x g, 10 min, 4°C) and the supernatant containing the nuclear fraction was transferred to fresh eppendorf tubes containing 35 µL

Buffer D (20 mM HEPES pH 7.9, 20% glycerol, 50 mM KCl, 0.2 mM EDTA pH 8.0, 0.5 mM PMSF and 10 mM DTT). The nuclear extracts were stored at -80°.

Nuclear protein concentration was quantified using the Bradford protein assay. 2 µL on nuclear extract or HSA standard diluted in Buffer D (4000 pg/mL-125 pg/mL) were applied to duplicate wells of a 96-well plate containing 200 µL/well 1X Bradford reagent and incubated at RT for a minimum of 10 min. Spectrophotometric analysis at 570 nm using the Bio-Rad Benchmark microplate reader was used to determine protein concentration via interpolation from the HSA standard curve.

### ***2.18.2 Oligonucleotide generation, annealing and end-labelling***

CXCL10-specific oligonucleotides corresponding to specific transcription factor binding sites (**Table 2.7**) were synthesized by the University of Calgary DNA services and annealed.

**Table 2.7: EMSA Oligonucleotide Sequences**

<b>Transcription Factor</b>	<b>Sequence</b>
NF-κB1	5' – TGCAACAT <u>GGGACTT</u> CCCCAGGAAC – 3'
NF-κB2	5' – GGAGCAGAG <u>GGAA</u> ATTCCGTAACCT – 3'
ISRE	5' – TGTTTTGGAAAGT <u>GAAAC</u> CTAATTC – 3'
STAT #1	5' – TAAATTCAT <u>TTCC</u> TCAAAAAGCACC – 3'
STAT #2	5' – AGCAATGTTTT <u>CCCT</u> CAAAATAGTT – 3'

\*Core of the putative transcription factor binding site is underlined.

The annealing reaction consisted of: 25  $\mu\text{L}$  each of sense and anti-sense oligonucleotides (100  $\mu\text{M}$  each), 10  $\mu\text{L}$  10X Oligo Annealing Buffer (100 mM Tris-HCl pH 7.5, 1 M NaCl and 10 mM EDTA pH 7.4) and 40  $\mu\text{L}$  of GIBCO water. Annealing was carried out in the Techne Flexigene thermocycler with the following parameters: 95°C for 2 min, X (melting temperature ( $T_m$ ) of the oligonucleotide + 5°C) for 5 min, decrease X to 37°C by 1°C/cycle for 90 min and 37°C for 2 min. Annealed oligonucleotides were stored at -80°C.

Annealed oligonucleotides were 5' end-labelled with T4 polynucleotide kinase and  $\gamma$ -<sup>32</sup>[P] ATP. In a 20  $\mu\text{L}$  reaction, 2  $\mu\text{L}$  of 1.75  $\mu\text{M}$  CXCL10-specific oligonucleotide was incubated for 30 min at 37°C with 1  $\mu\text{L}$  (10 units) of T4 polynucleotide kinase, 2  $\mu\text{L}$  of 10X T4 polynucleotide kinase buffer, 2  $\mu\text{L}$  (40 $\mu\text{Ci}$ )  $\gamma$ -<sup>32</sup>[P] ATP, topped off with GIBCO water. Following this incubation 180  $\mu\text{L}$  of TE buffer (10 mM Tris-HCl pH 7.4, 1 mM EDTA) was added to the radiolabelled oligonucleotide mixture and excess  $\gamma$ -<sup>32</sup>[P] ATP was removed by centrifugation (3000 rpm, 2 min) using G-25 Sephadex spin columns. To ensure end-labelling was successful, 1  $\mu\text{L}$  of radiolabelled oligonucleotide mixture was placed in a scintillation vial containing scintillation fluid and counts per million (cpm) of radioactivity were measured using a scintillation counter.

### ***2.18.3 EMSA binding reaction and non-denaturing PAGE***

The binding reaction consisted of 2  $\mu\text{g}$  nuclear extract incubated with 4  $\mu\text{L}$  of 5X EMSA binding buffer (20% glycerol, 2.5 mM EDTA, 5 mM  $\text{MgCl}_2$ , 250 mM NaCl, 1  $\mu\text{g}$  poly (dI:dC), 50 mM Tris-HCl and 10 mM DTT) and Buffer D up to 14  $\mu\text{L}$  for 20 min on

ice. After the initial 20 min incubation, 2  $\mu\text{L}$  of  $\gamma\text{-}^{32}\text{[P]}$  ATP end-labelled probe was added and samples were incubated for 1 h on ice. As a non-specific binding control, 2  $\mu\text{L}$  of 100X fold excess of the corresponding unlabelled CXCL10-specific oligonucleotide probe was added to a separate binding reaction and treated in the same manner as mentioned above and for the remainder of the protocol. Following the binding reaction, 3  $\mu\text{L}$  of EMSA loading buffer (50% glycerol, 0.05% bromophenol blue) was added to each sample followed by separation on a 6% non-denaturing polyacrylamide gel. Samples were electrophoresed at 200 V for 1.5-2 h in 0.25X TBE buffer. Gels were then dried using a vacuum drier (80°C for 1-1.5 h), exposed to film at -80°C and developed with autoradiography.

#### ***2.18.4 Supershift assays***

Supershift assays were conducted with the same protocol as above except 2  $\mu\text{L}$  of the appropriate purified IgG antibody was added to the binding reaction and incubated for 2 h on ice prior to the addition of the radiolabelled oligonucleotide probe. Antibodies used in supershift assays are listed in **Table 2.8**.

**Table 2.8: Supershift Assay Antibodies**

<b>Target</b>	<b>Epitope</b>	<b>Supplier</b>
p50	Nuclear localization sequence	Santa Cruz Biotechnology, sc-114X
p65	N-terminus	Santa Cruz Biotechnology, sc-109X
cRel	N-terminus	Santa Cruz Biotechnology, sc-848X
IRF-1	C-terminus	Santa Cruz Biotechnology, sc-497X
IRF-2	C-terminus	Santa Cruz Biotechnology, sc-498X
IRF-3	Amino acids 1-425	Santa Cruz Biotechnology, sc-9082X
IRF-7	Amino acids 1-246 at the N-terminus	Santa Cruz Biotechnology, sc-9083X
ISFG3	C-terminus of ISGF-3 $\gamma$ p48	Santa Cruz Biotechnology, sc-496X
STAT-1 $\alpha$	Amino acids 713-750 at the C-terminus of Stat1 $\alpha$ p91	Santa Cruz Biotechnology, sc-345X
STAT-2	C-terminus	Santa Cruz Biotechnology, sc-476X
STAT-3	C-terminus	Santa Cruz Biotechnology, sc-482X

### 2.19 Chromatin Accessibility Assay

To quantitatively assess the chromatin structure and nuclease accessibility of the CXCL10 promoter region the EpiQ Chromatin analysis kit was used according to the manufacturer's instructions with minor modifications. This assay combines in situ chromatin digestion, genomic DNA purification and real-time PCR to assess the chromatin state for the gene promoter of interest.

### ***2.19.1 In situ chromatin digestion***

Sub-confluent (70-80%) BEAS-2B cells cultured in 24-well plates were pre-treated in BEGM without hydrocortisone overnight prior to treatment. 4 wells were designated for each treatment condition (medium control, CSE, HRV-16, HRV-16+CSE) and cells were treated for 12 h or 24 h at 34°C and 5% CO<sub>2</sub>. EpiQ chromatin buffer was divided into two tubes (100 µL/sample) labelled U (undigested) and D (digested) and then incubated at 37°C for 10 min prior to the addition of EpiQ nuclease (2 µL/100µL EpiQ chromatin buffer) to the D tube only. Media was aspirated off the cell culture plates and 100 µL/well of U tube mixture was added to two out of the four wells of each treatment. The same was done with the D tube mixture, so that two wells from each treatment were subject to chromatin digestion and two wells were not. Plates were incubated at 37°C for 1 h. Following incubation, 25 µL of EpiQ stop buffer was added to each well and plates were incubated at 37°C for an additional 10 min. Plates were then tilted and the cell lysate from each well was transferred to a 1.5 mL eppendorf tube containing 375 µL EpiQ DNA lysis solution. Samples were inverted several times and pulse spun in a microcentrifuge for 5 sec. 250 µL of 100% ethanol was added to each sample, then samples were inverted several times and pulse spun in a microcentrifuge for 5 sec. Samples were then stored for up to 2 h at RT prior to isolation of genomic DNA.

### ***2.19.2 Genomic DNA isolation***

Cell lysate samples were transferred to a 2 mL EpiQ mini column in a 2 mL uncapped tube and centrifuged (13,400 x g, 1 min). The flow-through was discarded and 650

$\mu\text{L}$  of EpiQ DNA low-stringency wash solution was applied to each column and centrifuged ( $13,400 \times g$ , 1 min, RT). The flow-through was discarded and  $650 \mu\text{L}$  of EpiQ DNA high-stringency wash solution was applied to each column and centrifuged ( $13,400 \times g$ , 1 min, RT). The flow-through was again discarded and  $650 \mu\text{L}$  of EpiQ DNA high-stringency wash solution was applied to each column and centrifuged ( $13,400 \times g$ , 1 min, RT). The previous step was repeated one more time, the flow-through was discarded and the spin columns were centrifuged once more to dry the columns ( $13,400 \times g$ , 3 min, RT). Each spin column was transferred to a 2 mL capped tube and  $52 \mu\text{L}$  of EpiQ DNA elution solution was added to the center of each column and incubated for 2 min. Samples were capped, centrifuged ( $13,400 \times g$ , 2 min, RT) and the flow-through was retained. The elution step was repeated one more time for a total volume of  $104 \mu\text{L}$  of retained flow-through for each sample. Duplicate samples were then combined and genomic DNA was quantified in each sample using the Nanodrop spectrophotometer. Samples were stored at  $-80^{\circ}\text{C}$  until further analysis by real-time PCR.

### ***2.19.3 Primer design and real-time PCR analysis***

CXCL10 primers were designed and the PCR reaction was optimized according to the EpiQ Chromatin Analysis Kit Primer Design and qPCR Optimization Guide<sup>440</sup>.

CXCL10 primers used for EpiQ chromatin analysis are as follows:

Forward CXCL10 primer: 5' – GAAACAGTTCATGTTTTGGAAAGTGAAACC – 3'

Reverse CXCL10 primer: 5' – GCTGAGACTGGAGGTTTCCTCTGCTG – 3'

5  $\mu\text{L}$  of each genomic DNA sample diluted to 1 ng/mL in TE buffer was added in triplicate to a 96 well optical plate. 15  $\mu\text{L}$  of mastermix (10  $\mu\text{L}$  SYBR greenER, 0.1  $\mu\text{L}$  each forward and reverse CXCL10 primer from a stock of 10  $\mu\text{M}$  and 4.8  $\mu\text{L}$  GIBCO water) was then added to each well. In addition to each sample being analyzed for CXCL10 expression, it was also analyzed in triplicate using EpiQ primers to an epigenetically silenced (reference) and constitutively expressed (control) gene promoter. The EpiQ reference and control primers were supplied with the forward and reverse primer in one tube and were added at 0.2  $\mu\text{L}$ /well to the mastermix. The identity of these genes was not specified by the manufacturer but the control gene was implied to be GAPDH. A no template control (GIBCO water in place of sample) was run with each gene analyzed to exclude contamination. The PCR amplification consisted of: 96°C for 5 min, 40 cycles of 96°C for 15 sec - 63°C for 1 min - 80°C for 30 sec and a melt analysis (70-96°C, 0.2°C/step, 5 sec hold). The data were analyzed using the EpiQ chromatin kit data analysis tool ([www.bio-rad.com/epiq](http://www.bio-rad.com/epiq)) which took into account the expression profiles of the reference and control genes in addition to CXCL10. The data were expressed as % chromatin accessibility where:

- 0-20% = highly inaccessible / completely silenced
- 20-65% = low accessibility / moderately silenced
- 65-95% = mostly accessible / low level of silencing
- 95-100% = fully accessible / not silenced.

## 2.20 Chromatin Immunoprecipitation (ChIP) Assay

To study the interaction between transcription factors binding to specific CXCL10 promoter sites (protein/DNA interaction) following differential cell treatment the ChIP-IT Express kit was used following the manufacturer's instructions with minor modifications.

### 2.20.1 Cell fixation

Following desired treatment of HBE or BEAS-2B cells (3 x 6 well plates/treatment), the cells were subject to fixation in order to cross-link and preserve protein/DNA interactions. The ChIP-IT Express kit includes all buffers (excluding formaldehyde) for fixation. Cellular supernatants were aspirated and 1 mL/well of RT fixation solution (1% formaldehyde: 0.54 mL 37% formaldehyde + 20 mL BEBM) was added and cells were incubated for 5 min at RT with gentle rocking on an orbital shaker. The fixation solution was poured off and cells were washed with 1 mL/well ice-cold 1X PBS for 5 sec. The fixation reaction was stopped via the addition of 1 mL/well RT glycine stop-fix solution (1X glycine buffer and 1X PBS in double-distilled water) and cells were incubated for 5 min at RT with gentle rocking on an orbital shaker. The stop-fix solution was poured off, cells washed with 1 mL/well ice-cold 1X PBS for 5 sec and 500  $\mu$ L/well of ice-cold cell scraping solution (1X PBS, 0.5 nM PMSF) was added. Cells were forcefully scraped off the plates and each treatment was combined in a single tube. The cells were then pelleted by centrifugation (720 x g, 10 min, 4°C) and the supernatant was discarded. The cellular pellet was either stored at -80°C (with the addition of 1  $\mu$ L 100 mM PMSF and 1  $\mu$ L protease inhibitor cocktail (PIC)) or the protocol was continued.

### ***2.20.2 Chromatin shearing by sonication***

According to the manufacturer of the ChIP-IT Express kit, chromatin sheared to a size of 200-1500 bp is ideally used for ChIP experiments. Reagents for this step were not supplied with the ChIP-IT express kit. Cellular pellets were re-suspended in 1 mL ice-cold lysis buffer (5 mM piperazine-N,N-bis (2-ethanesulfonic acid) (PIPES) pH 8, 85 mM KCl, 0.5% Triton X-100) supplemented with 5  $\mu$ L PMSF/mL and 5  $\mu$ L PIC/mL and then incubated on ice for 1 h. Following incubation samples were transferred to an ice-cold dounce homogenizer (Kimble-Kontes #885300-0002 with the tight pestle) and samples were homogenized with a minimum of 40 strokes to aid in the release of cellular nuclei. Nuclei release was confirmed with haematoxylin and eosin (H & E) staining. Samples were aliquoted into microcentrifuge tubes (1 mL/tube) and centrifuged to pellet the nuclei (3000 x g, 10 min, 4°C). The supernatant was discarded by pipetting out; the nuclei were re-suspended in 1 mL/tube shearing buffer (50 mM Tris, 10 mM EDTA, 0.1% SDS, 0.5% sodium deoxycholate, pH 8) and incubated on ice for 10 min. Each sample was then aliquoted into fresh microcentrifuge tubes at no more than 350  $\mu$ L/tube and sonicated 5 times for 10 sec at 15% amplitude with a 30 sec rest on ice between each pulse using the Fisher Scientific Sonic Dismembrator model 500. Samples were then centrifuged (20,000 x g, 10 min, 4°C) and supernatants of the same treatment were combined into one fresh tube. Samples were stored at -80°C.

### ***2.20.3 DNA clean-up and concentration determination***

In order to confirm shearing efficiency and determine DNA concentration, 50  $\mu$ L of each sample were subject to DNA clean-up and run on a 1% agarose gel. Reagents that were supplied with the ChIP-IT express kit include 5 M NaCl, RNaseA and Proteinase K whereas all other reagents were from other suppliers. 150  $\mu$ L of GIBCO water and 10  $\mu$ L of 5 M NaCl was added to each 50  $\mu$ L sample of sheared chromatin and heated on a heat block for 15 min at 95°C in order to reverse the cross-links. To degrade ssRNA, 1  $\mu$ L of RNaseA/sample was added and incubated for 15 min in a 37°C water bath. In order to digest protein, 1  $\mu$ L Proteinase K/sample was added and incubated for 15 min at 67°C in a heat block. Following this, 200  $\mu$ L of phenol/chloroform (phenol: chloroform: isoamyl alcohol 25:24:1 pH 8.05-8.35) was added to each sample and then each sample was vortexed and centrifuged (max speed, 5 min, RT). The supernatant was transferred to a fresh tube, then 20  $\mu$ L of 3 M sodium acetate pH 5.2 and 500  $\mu$ L of 100% ethanol was added. The samples were vortexed and placed at -80°C for at least 1 h. Samples were then defrosted at RT and centrifuged (max speed, 10 min, 4°C). The supernatant was then removed and 500  $\mu$ L of 70% ethanol was added to the pellet and the samples were again centrifuged (max speed, 5 min, 4°C). The supernatant was removed and the pellet was allowed to air dry. Samples were then re-suspended in 30  $\mu$ L GIBCO water and DNA concentration was determined at 260 nm using a spectrophotometer. 4  $\mu$ L of 6X loading buffer was added to 16  $\mu$ L of each sample. Samples and a DNA standard were run on a 1% agarose gel for 45 min-1 h at 100 V. Sizes of sheared DNA fragments were visualized using a gel imager.

#### 2.20.4 ChIP

After the samples had been subject to shearing by sonication, the immunoprecipitation reaction was set up. First, 10  $\mu\text{L}$  of the control chromatin (treated with only medium) was set aside to be used as the input DNA control for the PCR step later in the procedure. With the exception of the sheared chromatin, GIBCO water and antibodies, all reagents were supplied with the ChIP-IT Express kit. The ChIP reactions were carried out in the ChIP-IT express kit-provided siliconized tubes and the reaction components are listed in **Table 2.9**.

The specific antibodies used are listed in **Table 2.10**.

**Table 2.9: ChIP Reaction Components**

Reagent	<60 $\mu\text{L}$ chromatin	>60 $\mu\text{L}$ chromatin
Protein G magnetic beads	25 $\mu\text{L}$	25 $\mu\text{L}$
ChIP Buffer 1	10 $\mu\text{L}$	20 $\mu\text{L}$
Sheared chromatin (~7 $\mu\text{g}$ )	20-60 $\mu\text{L}$	61-100 $\mu\text{L}$
PIC	1 $\mu\text{L}$	1 $\mu\text{L}$
GIBCO water	Up to 100 $\mu\text{L}$	Up to 200 $\mu\text{L}$
Antibody (added last)	2-10 $\mu\text{L}$	2-10 $\mu\text{L}$

**Table 2.10: Antibodies Used in the ChIP Reaction**

<b>Target</b>	<b>Concentration</b>	<b>Volume used per ChIP reaction</b>	<b>Supplier and catalogue #</b>
RNA pol II (positive control)	0.2 $\mu\text{g}/\mu\text{L}$	10 $\mu\text{L}$	Active Motif #39097 or #530100 (ChIP-IT control kit)
IgG (negative control)	0.2 $\mu\text{g}/\mu\text{L}$	10 $\mu\text{L}$	Active Motif #53010 (ChIP-IT control kit)
IRF-1	2 $\mu\text{g}/\mu\text{L}$	2 $\mu\text{L}$	Santa Cruz #sc-497
p65	2 $\mu\text{g}/\mu\text{L}$	2 $\mu\text{L}$	Santa Cruz #sc-109

Only chromatin that was derived from samples that were treated with medium control was subject to ChIP with the control antibodies (RNA pol II or control IgG). ChIP with IRF-1 and p65 was performed on all chromatin samples with the desired treatment. Samples were then vortexed and incubated on an end-to-end rotator overnight at 4°C. Following the overnight incubation, the samples were briefly spun to collect the liquid from the inside of the cap and the tubes were immediately placed on the magnetic stand (assembled according to the manufacturer's instructions) to pellet the magnetic beads. For the following wash steps the magnetic beads were not allowed to dry out (no more than 1 min between removing one wash and adding the next). The supernatant was removed by pipetting and discarded. The beads were then washed one time with ChIP Buffer 1 (800  $\mu\text{L}/\text{tube}$ ). The magnetic beads were pelleted as before, the supernatant removed and the beads were washed two times in the same manner with ChIP Buffer 2 (800  $\mu\text{L}/\text{tube}$ ). The washed

magnetic beads were then re-suspended with 50  $\mu$ L/tube Elution Buffer AM2 and incubated on an end-to-end rotator for 15 min at RT. The siliconized tubes were spun briefly to collect the liquid from caps and 50  $\mu$ L/tube of Reverse Cross-Linking Buffer was added to the eluted chromatin and tubes were immediately placed on the magnetic stand to pellet the magnetic beads. The supernatant, which contained the chromatin, was transferred to fresh PCR tubes. 88  $\mu$ L of ChIP Buffer 2 and 2  $\mu$ L 5 M NaCl was added to the previously set aside 10  $\mu$ L of input DNA to be used as the control. The input DNA and ChIP samples were then incubated for 15 min at 95°C in a thermocycler. The samples were returned to RT and 2  $\mu$ L/tube of Proteinase K was added to degrade protein in the samples. Samples were incubated for 1 h at 37°C. Following this incubation, samples were returned to RT, and 2  $\mu$ L/tube Proteinase K Stop Solution was added to end the reaction. Samples were stored at -20°C and were now ready to be used for PCR analysis.

### ***2.20.5 PCR analysis***

#### **2.20.5.1 Conventional PCR**

Chromatin that was derived from samples treated with medium control and subject to ChIP with the positive control RNA polymerase II and the negative control IgG antibodies was analyzed with conventional PCR using the ChIP-IT Control kit. This step was performed to demonstrate that the positive and negative control antibodies were effective in performing ChIP using the chromatin that was prepared using the above protocol. A positive result using the ChIP-IT control kit would help support that the prepared chromatin is of adequate quality to be used for further analysis. With the

exception of the platinum Taq polymerase all reagents were supplied with the ChIP-IT control kit. First the input DNA control was diluted 1:10 with GIBCO water. Four PCR reactions were then set-up in PCR tubes containing: 5  $\mu$ L of either (1) ChIP DNA with RNA pol II antibody, (2) ChIP DNA with negative control IgG antibody, (3) diluted input DNA or (4) GIBCO water alone with 20  $\mu$ L of PCR master mix (12.5  $\mu$ L 10X PCR loading buffer, 12.5  $\mu$ L PCR loading dye, 5  $\mu$ L 5 mM dNTP mix, 20  $\mu$ L GAPDH control primer mix, 1  $\mu$ L platinum Taq polymerase and 49  $\mu$ L GIBCO water). The PCR amplification reaction consisted of 40 cycles with the following steps per cycle: 20 sec at 94°C, 30 sec at 59°C and 30 sec at 72°C. The PCR products were then resolved on a 3% agarose gel.

#### 2.20.5.2 Real-Time PCR

Chromatin that was derived from samples treated with the desired stimulus and subject to ChIP with the IRF-1 and p65 antibody was then purified using the QIAquick PCR purification kit according to the manufacturer's protocol, concentration was determined using a spectrophotometer and DNA was analyzed using real-time PCR primers and probe encompassing the ISRE and both NF- $\kappa$ B binding regions in the CXCL10 promoter. The primers mapping to the region between -224 and -90 of the CXCL10 promoter have been previously described<sup>441</sup> and were generated by the University of Calgary Core DNA Facility. The sequences of the primers are as follows:

- Forward primer: 5' – TTTGGAAAGTGAAACCTAATTCA – 3'
- Reverse primer: 5' – AAAACCTGCTGGCTGTTTCCTG – 3'

The Primer Express 3 program was used to design a specific probe to this region which was generated by the Applied Biosystems custom oligonucleotide synthesis service and the sequence is as follows:

- Probe: 5' – TGGAGGCTACAATAAA – 3'

This region of CXCL10 was amplified in a real-time PCR reaction using the StepOnePlus sequence detector. The experimental setup consisted of 25  $\mu$ L reaction/well in a 96 well optical plate. The primers and probes were diluted to 10  $\mu$ M with GIBCO water and stored at -80°C. The PCR reaction mixture consisted of: 2  $\mu$ L DNA, 12.5  $\mu$ L Taqman universal mastermix (1X), 1  $\mu$ L each of forward and reverse primer (400 nM), 0.5  $\mu$ L Taqman probe (200 nM) and GIBCO water to a final volume of 25  $\mu$ L per well. The reaction consisted of PCR amplification (10 min at 95°C, 40 cycles of 15 sec at 95°C and 1 min at 57°C). Samples were run in either duplicate or triplicate and a no template control (GIBCO water in place of sample) was run to exclude contamination.

## 2.21 H & E

Cells that needed to be visualized during chromatin preparation for ChIP were stained using H & E. 70  $\mu$ L of cellular suspensions were aliquoted into cytospin funnels and spun onto positively charged microscope slides at 450 rpm for 6 min (Thermo Electron Corporation Cytospin 4). Following the cytospin, slides were placed in 95% ethanol for 10 min. Slides were then rinsed in distilled water and placed in haematoxylin for 5 min. Slides were again rinsed in distilled water and then run under warm tap water for 1 min. A colour change from purple to blue was observed. Slides were rinsed in 75% ethanol and dipped

20-30 times in eosin before being placed in 95% ethanol. Slides were then thoroughly rinsed twice in 100% ethanol and twice in xylene. A cover slip was mounted using permount and mounted slides were allowed to air dry for 5 min before being visualized under a microscope.

## 2.22 Statistical Analyses

All data are presented as mean  $\pm$  standard error of the mean (SEM). An “n” is defined as either a distinct set of HBE cell derived from a lung donor or a distinct passage of BEAS-2B cells. Statistical analysis was performed using the GraphPad Prism 5 software. Normally distributed data were analyzed using either paired t tests or one-way repeated measures analysis of variance (ANOVA) with student Newman-Keuls post hoc analysis. Data that were not normally distributed were analyzed using either Wilcoxon matched pairs signed-rank test or Friedman’s test with Dunn’s post hoc analysis. To determine whether there was synergy between HRV-16 and CSE, the sum of HRV-16 alone and CSE alone was compared with HRV-16+CSE. Paired t tests or Wilcoxon matched-pairs signed-rank tests were used to determine differences. Data that had two independent variables were analyzed using two-way repeated measures ANOVA with Bonferroni’s multiple comparison post hoc analysis. Values of  $p \leq 0.05$  were considered significant.

## Chapter Three: **CSE Differentially Modulates HRV-Induced Chemokine Responses in Airway Epithelial Cells**

Portions of data presented in this Chapter have been published:

Hudy MH, Traves SL, Wiehler S, Proud D. Cigarette smoke modulates rhinovirus-induced airway epithelial cell chemokine production. *Eur. Respir. J.* 2010;35(6):1256–1263.

Copyright © European Respiratory Society.

Proud D, Hudy MH, Wiehler S, et al. Cigarette smoke modulates expression of human rhinovirus-induced airway epithelial host defense genes. *PLoS ONE.* 2012;7(7):e40762.

This work was reprinted with permission based on the PLoS open-access license: Creative Commons Attribution 2.5 Generic License (<http://creativecommons.org/licenses/by/2.5/legalcode>).

### 3.1 Background

As previously mentioned, the airway epithelial cell is the only cell type that has been shown, thus far, to be infected with HRV *in vivo*<sup>30</sup>. The airway epithelium is also the primary target of inhaled cigarette smoke. Based on previous literature presented in the introduction of this thesis, it is reasonable to assume that cigarette smoke alters the immune response to HRV in a manner that results in worse clinical outcomes in HRV-infected smokers and particularly, during HRV-induced exacerbations of COPD and asthma in individuals who smoke. To date, only a limited number of studies have examined how cigarette smoke affects HRV-induced responses in the lung<sup>442,443</sup>, specifically in airway epithelial cells<sup>132,355,444,445</sup>. Two of the four published studies in airway epithelial cells are a result of data generated from this thesis project, while another was published concurrently by others.

Although many components of the immune response induced by HRV could potentially be altered by CSE, a complete examination of this would be an enormous undertaking. Thus, this thesis focuses on two particularly important chemokines involved in HRV-induced inflammation, namely CXCL10 and CXCL8. The chemokines CXCL10 and CXCL8 are readily and robustly induced in airway epithelial cells following HRV infection<sup>258,259,446,447</sup>. Each of these chemokines significantly contributes to the immune response following infection with HRV. CXCL10 is a chemoattractant for type 1 lymphocytes and NK cells and has been linked to host defence<sup>247,257,448</sup>. CXCL8 is one of

the most potent chemoattractants for neutrophils and is intimately involved in the pro-inflammatory response following infection<sup>235,278</sup>.

### ***3.1.1 Effects of cigarette smoke on HRV-induced CXCL10***

Prior to publications based on studies from this thesis project<sup>132,445</sup> and one concurrent study from another research group<sup>355</sup>, there had been no previous literature on the effects of cigarette smoke on HRV-induced CXCL10.

### ***3.1.2 Effects of cigarette smoke on HRV-induced CXCL8***

Prior to a publication based on findings from this thesis project<sup>445</sup>, there has only been one report on the effects of the combined exposure of HRV and cigarette smoke on airway epithelial CXCL8 production<sup>444</sup>. In this study by Wang *et al*, A549 cells were treated with CSE alone or HRV-16+CSE for 3 days. They showed an increase in CXCL8 mRNA and protein induced by the combined stimulus of HRV-16+CSE compared to CSE alone using a variety of CSE concentrations. Unfortunately, it was not clear from this study whether CSE alone induced significant levels of CXCL8, since the authors did not compare levels to medium control. Additionally, this study did not look at the effect on CXCL8 mRNA and protein induction by HRV alone; therefore, this study was inconclusive as to whether the combined treatment of HRV-16+CSE modulated CXCL8 expression compared to HRV-16 treatment alone.

## 3.2 Hypothesis

Cigarette smoke modulates HRV-induced CXCL10 and CXCL8 expression in airway epithelial cells in a manner that would be expected to lead to worse clinical outcomes.

## 3.3 Results

### *3.3.1 CSE alone or in combination with HRV-16 is not overtly cytotoxic to airway epithelial cells*

In order to establish a concentration of CSE to use for further studies, either alone or in combination with HRV-16, it was necessary to evaluate cell viability post treatment in both cell types that would be utilized for future experiments. A concentration of HRV-16 that did not cause overt cell death but caused a biological response has previously been established in both HBE and BEAS-2B cells (unpublished laboratory data). Based on previous literature, in which CSE was prepared in a similar fashion to that done in these studies, which evaluated CSE cytotoxicity on rat alveolar type II cells, a top concentration of CSE was chosen that had an optical density of 0.15 at 320 nm (100% CSE). A 24 h time-point was chosen to evaluate cell viability because further studies aimed at evaluating alteration of HRV-16-induced chemokine responses, which have previously been shown to be robust at this time-point<sup>132,259,297,298,323</sup>.

In the current study, viability of HBE and BEAS-2B cells was evaluated using both MTT and LDH viability assays following treatment with 2-fold serial dilutions of CSE alone or in combination with HRV-16 (**Figure 3.1**). A concentration of 50% CSE either

alone or in combination with HRV-16 did not overtly affect cell viability of either HBE (**Figure 3.1 A and C**) or BEAS-2B (**Figure 3.1 B and D**) cells. Concentrations of CSE above 50% had minor effects on cell viability, particularly in BEAS-2B cells; hence a concentration of 50% CSE was chosen for use in further studies. All subsequent studies were conducted using 50% CSE unless stated otherwise.

**Figure 3.1 A and B** containing viability results as assayed by MTT were removed due to copyright restrictions. Data contained in these figures can be found in Supplementary figure A in:

Hudy MH, Traves SL, Wiehler S, Proud D. Cigarette smoke modulates rhinovirus-induced airway epithelial cell chemokine production. *Eur. Respir. J.* 2010;35(6):1256–1263.

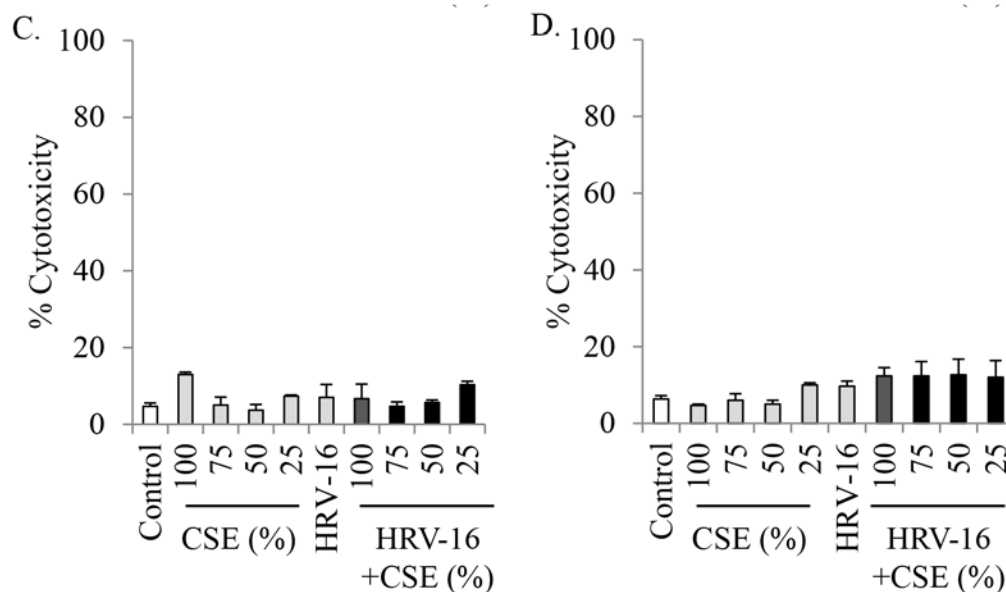


**Figure 3.1: CSE alone or in combination with HRV-16 does not overtly affect cell viability of airway epithelial cells at concentrations of  $\leq 50\%$  CSE.**

HBE (A&C) and BEAS-2B (B&D) cell viability was assessed by MTT and LDH viability assays 24 h post-treatment with medium control, 2-fold serial dilutions of CSE, HRV-16, or HRV-16 in combination with 2-fold serial dilutions of CSE. Data are presented as mean  $\pm$  SEM (n=3). Asterisks denote significant difference compared to control medium (\*  $p \leq 0.05$ , \*\*  $p < 0.01$  and \*\*\*  $p < 0.001$ ). Data presented in A & B have been published<sup>445</sup>.

### ***3.3.2 CSE inhibits HRV-16-induced CXCL10 in airway epithelial cells***

A time-course of HRV-16-induced CXCL10 was previously determined in primary epithelial cells<sup>259</sup>. Spurrell *et al.* reported that CXCL10 mRNA and protein were significantly induced by HRV-16 at 24 h post-infection of epithelial cells. A limited time course in both HBE cells and BEAS-2B cells confirmed these observations (**Figure 3.2**).

CSE alone did not induce CXCL10 mRNA or protein at various time-points examined (data not shown). Although Spurrell *et al.* showed that CXCL10 protein continued to increase with time at 48 and 72 h post HRV-16 infection<sup>259</sup>, prolonged exposure to CSE could have adverse effects on epithelial cell viability, therefore, the 24 h time-point was chosen for subsequent experiments to evaluate if and how CSE modulated HRV-16-induced CXCL10.

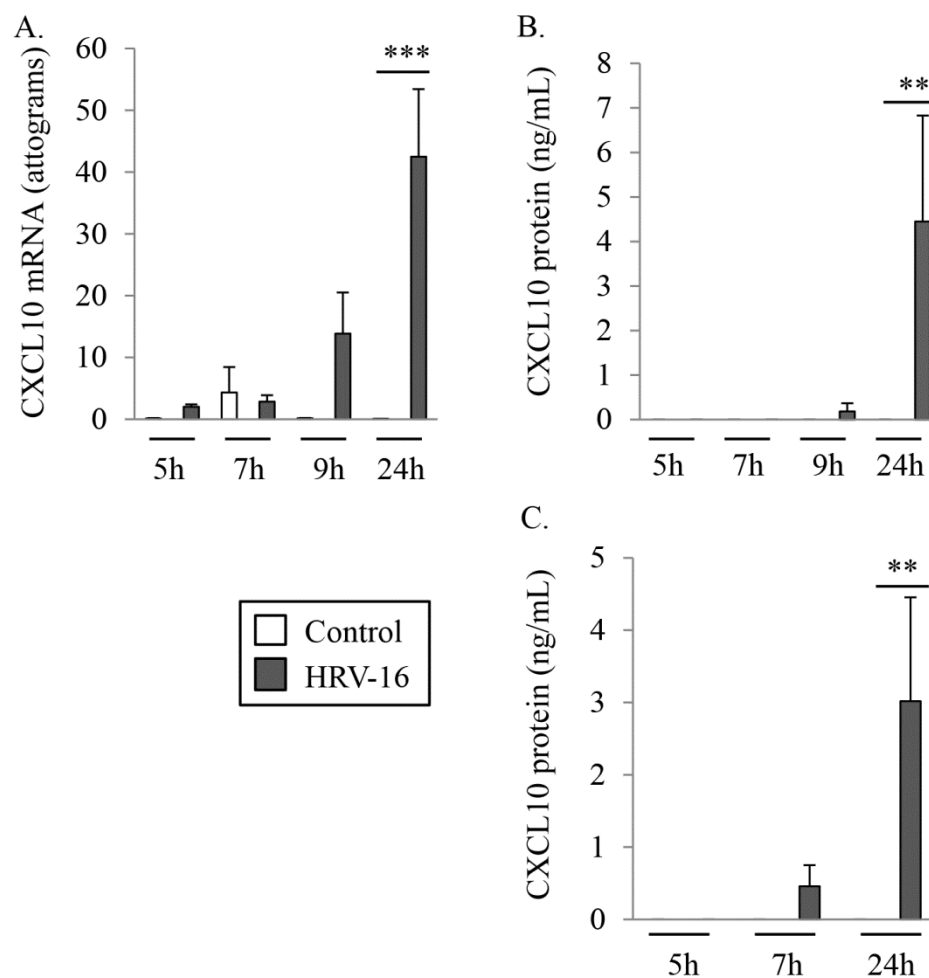


**Figure 3.2: Time-course of HRV-16-induced CXCL10 in airway epithelial cells.**

CXCL10 mRNA (A; n=3) and protein (B; n=3 & C; n=4) were determined at various times post treatment with medium control or HRV-16 in HBE (A & B) and BEAS-2B (C) cells. Data are presented as mean  $\pm$  SEM. Asterisks denote significant induction of CXCL10 with HRV-16 compared to medium control for that respective time-point (\*\*  $p < 0.01$  and \*\*\*  $p < 0.001$ ).

A gene microarray study was conducted as a joint effort of the Proud and Leigh labs utilizing HBE cells derived from four distinct donors. HBE cells were then treated with medium control, CSE, HRV-16 or the combination for HRV-16 plus CSE for 24 h<sup>132</sup>. In

this gene microarray, the most highly up-regulated gene following treatment with HRV-16 for 24 h was CXCL10, being enhanced 540 fold compared to medium control (**Figure 3.3 A**). CSE alone did not enhance the expression of CXCL10 but significantly decreased HRV-16-induced CXCL10 expression to 65 fold compared to medium control (**Figure 3.3 A**). The same HBE-derived mRNA samples that were used for the gene microarray were verified for CXCL10 expression using real time RT-PCR (**Figure 3.3 B**). The trend assessed by real time RT-PCR was the same compared to the gene microarray results: CXCL10 mRNA was enhanced by HRV-16 and HRV-16-induced CXCL10 was significantly inhibited by CSE. Matched supernatant samples were also analyzed for CXCL10 protein release (**Figure 3.3 C**). HRV-16 treatment induced CXCL10 protein release from HBE cells and HRV-16-induced CXCL10 was significantly inhibited by CSE.

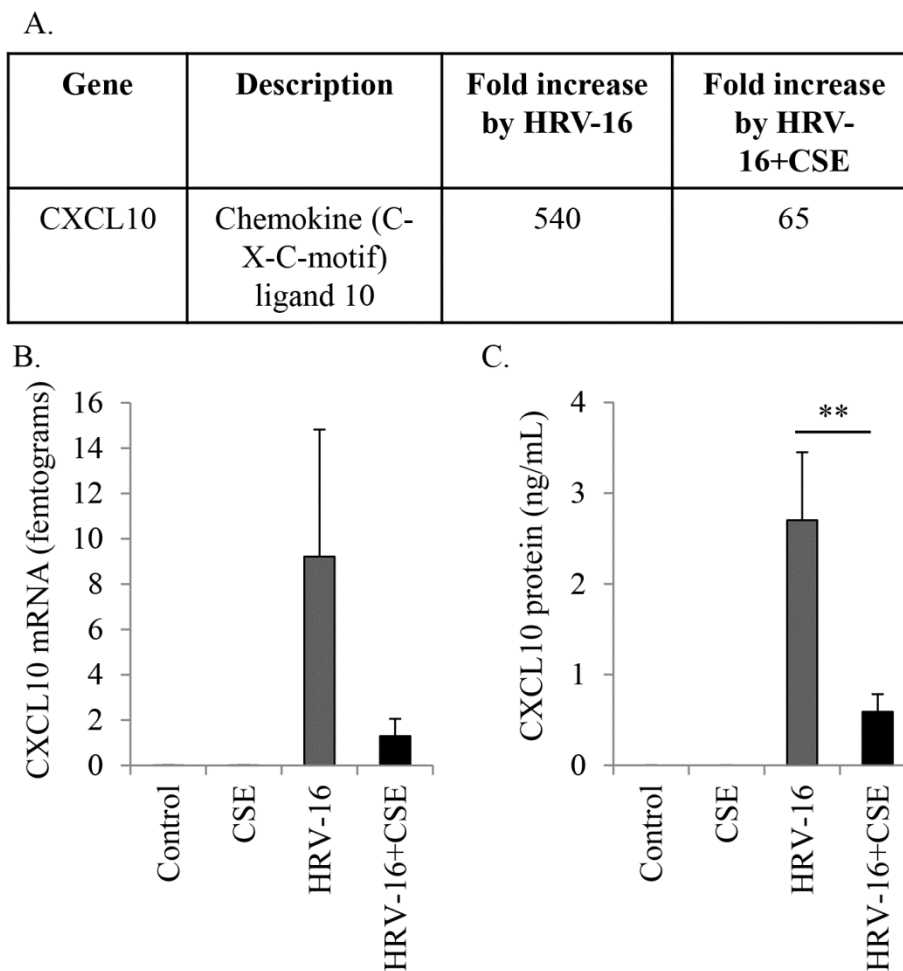


**Figure 3.3: CSE inhibits HRV-16-induced CXCL10 in airway epithelial cells as assessed by gene microarray.**

HBE cells were treated for 24 h with either medium control, CSE, HRV-16 or HRV-16+CSE. Cellular RNA was harvested and analyzed via gene microarray (A) and verified with real time RT-PCR (B) while CXCL10 protein levels in matched supernatants were measured by ELISA (C). Data are presented as mean  $\pm$  SEM from 4 HBE cell donors. Asterisks denote significant inhibition with HRV-16+CSE compared to HRV-16 alone (\*\*  $p < 0.01$ ). Data presented in this figure have been published<sup>132</sup>.

The aforementioned studies were extended to a larger number of HBE cell donors as well as to the BEAS-2B bronchial epithelial cell line (**Figure 3.4**). Ten HBE cell donors

were analyzed for CXCL10 following treatment with medium control, CSE, HRV-16 or the combination of HRV-16 and CSE for 24 h. In agreement with the previous experiments, HRV-16 induced CXCL10 mRNA and protein, as well as HRV-16-induced CXCL10 mRNA and protein was significantly inhibited in the presence of CSE (**Figure 3.4 A and B**). The magnitude of HRV-16-induced CXCL10 induction differed in these sets of experiments, most likely due to the variability seen between individual HBE cell donors. As HBE cells are from distinct individuals, variability in magnitude of gene expression is expected. It should be noted that the trends remained the same between HBE cell donors and the degree of HRV-16-induced CXCL10 inhibition by CSE also remained very similar.

As some planned future experiments, such as promoter transfection experiments or experiments requiring a large number of cells, would be technically difficult to conduct using primary HBE cells, BEAS-2B cells were also analyzed for CXCL10 following the same treatments for 24 h (**Figure 3.4 C and D**). HRV-16 induced CXCL10 mRNA and protein from BEAS-2B cells and this induction was inhibited by CSE. Although there was a trend in each passage of BEAS-2B cells for inhibition of HRV-16-induced CXCL10 mRNA, only inhibition of CXCL10 protein was significant. A larger number of experiments could have been performed to try and achieve significance for CXCL10 mRNA but was deemed unnecessary since protein levels, which are more relevant, were significantly inhibited. Since the general trend was the same between BEAS-2B cells compared to HBE cells in terms of HRV-16-induced CXCL10 and its inhibition by CSE, BEAS-2B cells were deemed an appropriate surrogate to use for subsequent experiments that would be difficult to perform using HBE cells.

**Figures 3.4 A-D** were removed due to copyright restrictions. Data contained in these figures can be found in Figure 2 in:

Hudy MH, Traves SL, Wiehler S, Proud D. Cigarette smoke modulates rhinovirus-induced airway epithelial cell chemokine production. *Eur. Respir. J.* 2010;35(6):1256–1263.

**Figure 3.4: CSE inhibits HRV-16-induced CXCL10 in airway epithelial cells.**

CXCL10 mRNA (A; n=10) and protein (B; n=10) levels were determined at 24 h post-treatment in HBE cells. CXCL10 mRNA (C; n=9) and protein (D; n=10) levels were determined at 24 h post-treatment in BEAS-2B cells. Data are presented as mean  $\pm$  SEM. Asterisks denote significant inhibition with HRV-16+CSE compared to HRV-16 alone (\*\*  $p < 0.01$  and \*\*\*  $p < 0.001$ ). The data presented in this figure have been published<sup>445</sup>.

In order to establish whether there was a concentration-dependent effect of HRV-16-induced CXCL10 inhibition by CSE, studies using serial fold-dilutions of CSE were performed. HBE cells were treated with medium control, 2-fold dilutions of CSE, HRV-16, or the combination of HRV-16 with 2-fold dilutions of CSE. HRV-16-induced CXCL10 mRNA and protein was significantly inhibited by all 3 serial 2-fold dilutions of CSE (Figure 3.5 A and B).

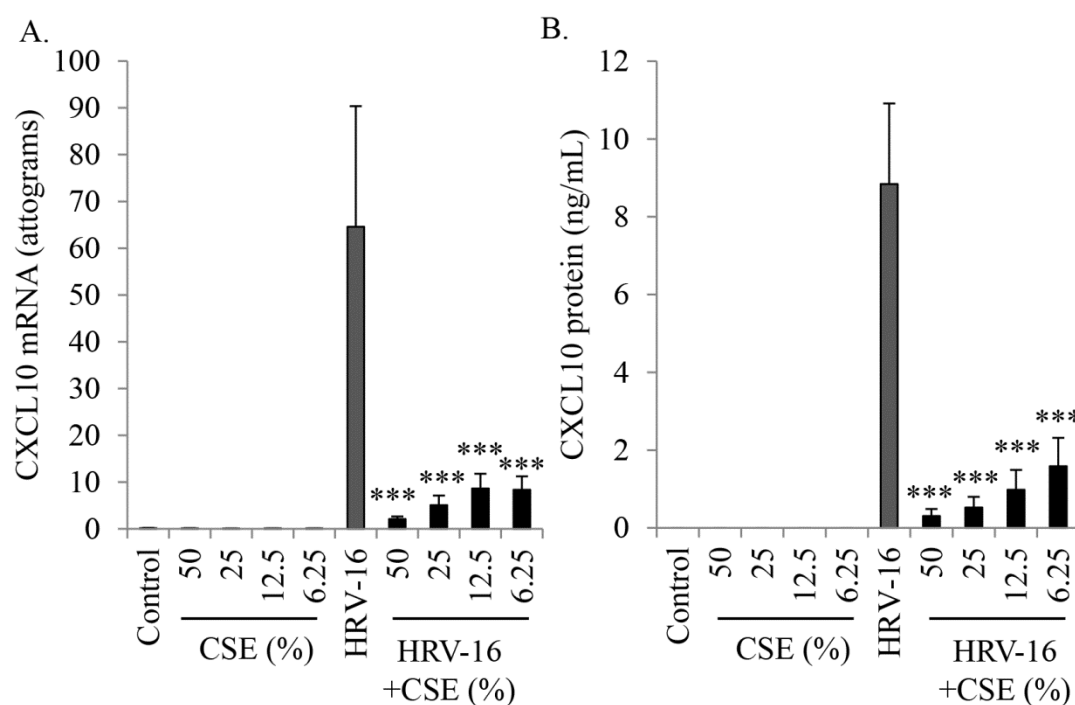


**Figure 3.5: At a variety of concentrations CSE inhibits HRV-16-induced CXCL10 in airway epithelial cells.**

CXCL10 mRNA (A) and protein (B) levels were determined at 24 h post-treatment with varying concentrations of CSE alone or in combination with HRV-16 in HBE cells. Data are presented as mean  $\pm$  SEM (n=4). Asterisks denote significant inhibition with HRV-16+CSE compared to HRV-16 alone (\*\*\* p<0.001).

These studies were extended to BEAS-2B cells and the same phenomenon was observed: 3 serial 2-fold dilutions of CSE potently inhibited HRV-16-induced CXCL10 (**Figure 3.6 A**). This inhibition was examined further with 10 fold-dilutions of CSE and resulted in a concentration-dependent inhibition of HRV-16-induced CXCL10 (**Figure 3.6 B**). Thus, even very low concentrations of CSE were still capable of significantly inhibiting HRV-16-induced CXCL10.

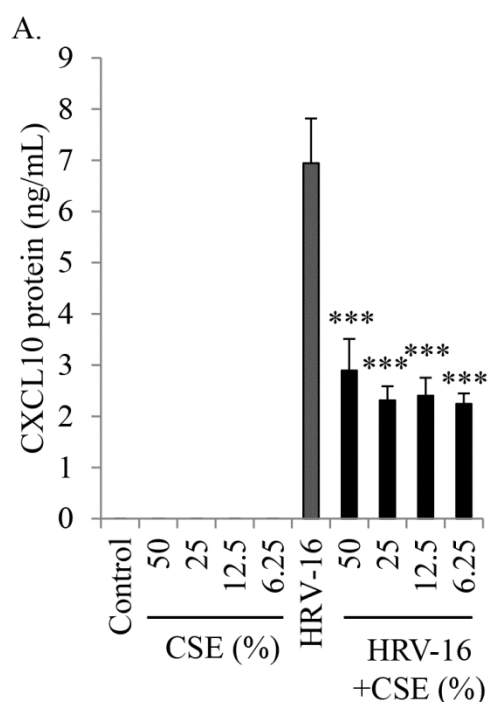


**Figure 3.6 B** was removed due to copyright restrictions. Data contained in this figure can be found in Supplementary figure E in: Hudy MH, Traves SL, Wiehler S, Proud D. Cigarette smoke modulates rhinovirus-induced airway epithelial cell chemokine production. *Eur. Respir. J.* 2010;35(6):1256–1263.

**Figure 3.6: Even at low concentrations, CSE inhibits HRV-16-induced CXCL10 in airway epithelial cells.**

CXCL10 protein levels were determined at 24 h post-treatment with 2-fold (A) and 10 fold (B) dilutions of CSE alone or in combination with HRV-16 in BEAS-2B cells. Data are presented as mean  $\pm$  SEM (n=3). Asterisks denote significant inhibition with HRV-16+CSE compared to HRV-16 alone (\*  $p \leq 0.05$ , \*\*  $p < 0.01$  and \*\*\*  $p < 0.001$ ). Data presented in B have been published<sup>445</sup>.

### ***3.3.3 CSE and HRV-16 each induce CXCL8 alone and at least additively increase CXCL8 in combination in airway epithelial cells***

A time-course of HRV-16-induced CXCL8 has previously been determined by members of our laboratory<sup>323</sup>. HRV-16 induced significant levels of CXCL8 mRNA as early as 3 h post-infection and significant levels of protein were seen between 6 and 24 h<sup>323</sup>. Based on additional time-course studies of CXCL8 mRNA and protein induced with CSE (**Figure 3.7 A & B**), CXCL8 mRNA levels following treatment with CSE, HRV-16 or HRV-16+CSE were measured at 5 h post stimulation, while protein levels were assessed at 24 h after stimulation.

HRV-16 alone and CSE each induced CXCL8 mRNA and protein from both HBE (**Figure 3.8 A & B**) and BEAS-2B cells (**Figure 3.8 C & D**). The combination of HRV-16 and CSE induced levels of CXCL8 mRNA and protein that were significantly greater than those induced by either stimulus alone. CXCL8 mRNA and protein induced by the combination of CSE and HRV-16 in BEAS-2B cells was synergistic compared to the two stimuli individually (**Figure 3.8 C & D**). Synergistic induction of CXCL8 mRNA by HRV-16+CSE was also observed in HBE cells (**Figure 3.8 A**). By contrast, CXCL8 protein production from HBE cells by HRV-16+CSE was not significantly greater than the sum of responses to each stimulus individually (**Figure 3.8 B**). Collectively, these data show that CXCL8 is induced by each of CSE and HRV-16 and then at least additively induced by the combined treatment of HRV-16+CSE.

**Figures 3.7 A and B** were removed due to copyright restrictions. Data contained in these figures can be found in Supplementary figure C in:  
Hudy MH, Traves SL, Wiehler S, Proud D. Cigarette smoke modulates rhinovirus-induced airway epithelial cell chemokine production. *Eur. Respir. J.* 2010;35(6):1256–1263.

**Figure 3.7: Time-course of CSE-induced CXCL8 in airway epithelial cells.**

CXCL8 mRNA (A) peaked at 5 h post CSE treatment and CXCL8 protein (B) continuously increased post CSE treatment up to 24 h in BEAS-2B cells. Data are presented as mean  $\pm$  SEM (n=4). Asterisks denote a significant difference between CSE and medium control within each time-point (\*\*\*p<0.001). Data presented in this figure have been published<sup>445</sup>.

**Figures 3.8 A-D** were removed due to copyright restrictions. Data contained in these figures can be found in Figure 1 in:

Hudy MH, Traves SL, Wiehler S, Proud D. Cigarette smoke modulates rhinovirus-induced airway epithelial cell chemokine production. *Eur. Respir. J.* 2010;35(6):1256–1263.

**Figure 3.8: CSE and HRV-16 each induce CXCL8 alone and at least additively increase CXCL8 in combination in airway epithelial cells.**

CXCL8 mRNA (A; n=10) levels were determined at 5 h and protein (B; n=9) levels were determined at 24 h post treatment in HBE cells. CXCL8 mRNA (C; n=6) levels were determined at 5 h and protein (D; n=10) levels were determined at 24 h post-treatment in BEAS-2B cells. Data are presented as mean  $\pm$  SEM. Asterisks denote significant difference between HRV-16+CSE compared to HRV-16 or CSE alone (\* $p \leq 0.05$ , \*\*  $p < 0.01$  and \*\*\*  $p < 0.001$ ). Hash marks denote a significant difference between HRV-16+CSE and the sum of the values from CSE and HRV-16 treatments alone. The data presented in this figure have been published<sup>445</sup>.

In order to determine whether enhancement of CXCL8 by HRV-16+CSE occurred at earlier time-points, a limited time-course study was conducted. Additive induction of CXCL8 protein was only apparent at 24 h following treatment with HRV-16+CSE at the time-points assessed in HBE cells (**Figure 3.9**). The time-course was not continued past 24 h as viability of cells exposed to CSE for longer periods of time was a concern.

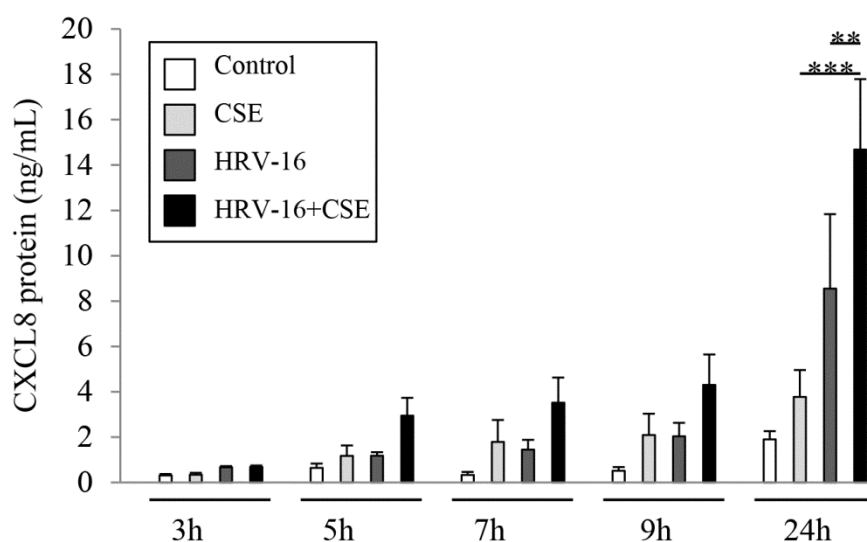


**Figure 3.9: Time-course of CSE-induced and HRV-16-induced CXCL8 protein release from airway epithelial cells.**

CXCL8 protein levels were determined at various times post treatment with medium control, CSE, HRV-16 or HRV-16+CSE in HBE cells. Data are presented as mean  $\pm$  SEM (n=3). Asterisks denote a significant difference between HRV-16+CSE compared with HRV-16 or CSE alone (\*\* p<0.01 and \*\*\* p<0.001).

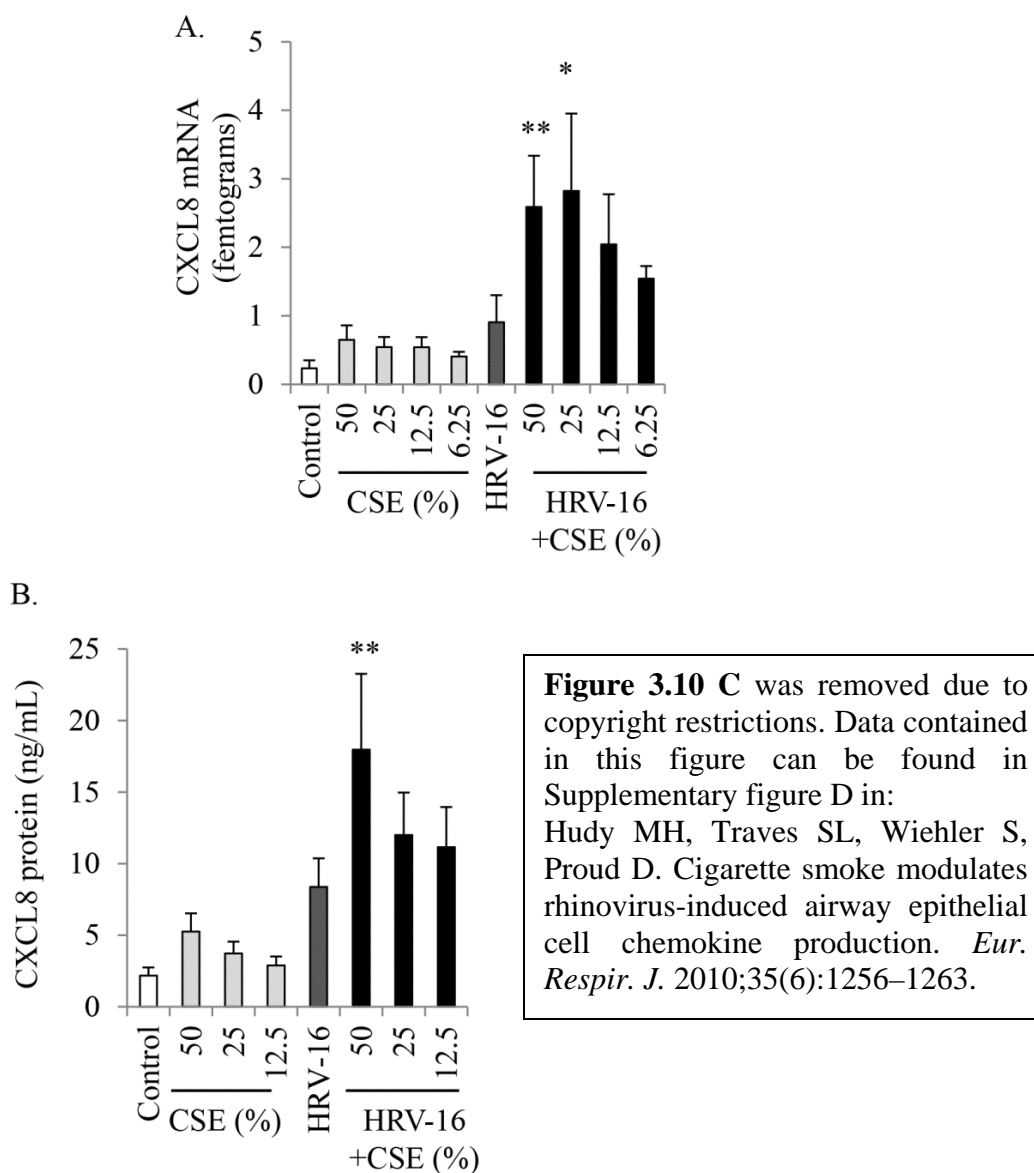


**Figure 3.10: CSE concentration-dependently induces CXCL8 alone and in combination with HRV-16 in airway epithelial cells.**

CXCL8 mRNA levels were determined at 5 h post-treatment with varying concentrations of CSE alone or in combination with HRV-16 in HBE cells (A; n=4). CXCL8 protein levels were determined at 24 h post-treatment with varying concentrations of CSE alone or in combination with HRV-16 in HBE (B; n=8) and BEAS-2B (C: n=3) cells. Data are presented as mean  $\pm$  SEM. Asterisks denote a significant difference between HRV-16+CSE compared with HRV-16 alone (\* $p \leq 0.05$  and \*\*  $p < 0.01$ ). Data presented in C have been published<sup>445</sup>.

The effects of CSE alone or in combination with HRV-16 on CXCL8 protein production was concentration-dependent (**Figure 3.10**). Synergistic induction of CXCL8 mRNA was only observed at 50% and 25% CSE in HBE cells (**Figure 3.10 A**) and synergistic induction of CXCL8 protein was only observed at 50% CSE in both HBE and BEAS-2B cells (**Figure 3.10 B & C**).

#### ***3.3.4 CSE modulates HRV-1A-induced CXCL10 and CXCL8 from airway epithelial cells***

To determine if the effects of CSE on viral production of the epithelial chemokines CXCL10 and CXCL8 was unique for HRV-16, a minor group rhinovirus serotype (HRV-1A), was used as a stimulus in BEAS-2B cells. As was the case with HRV-16, CSE inhibited HRV-1A-induced production of CXCL10 (**Figure 3.11 A**). Only a small volume of HRV-1A was available for use, thus only 3 experiments were permitted and HRV-1A-induced CXCL10 inhibition by CSE was not significant but the trend was the same for each individual passage. CSE in combination with HRV-1A significantly induced additive induction of CXCL8 (**Figure 3.11 B**).

**Figures 3.11 A and B** were removed due to copyright restrictions. Data contained in these figures can be found in Supplementary figure F in:  
Hudy MH, Traves SL, Wiehler S, Proud D. Cigarette smoke modulates rhinovirus-induced airway epithelial cell chemokine production. *Eur. Respir. J.* 2010;35(6):1256–1263.

**Figure 3.11: CSE modulates HRV-1A-induced CXCL10 and CXCL8 from airway epithelial cells.**

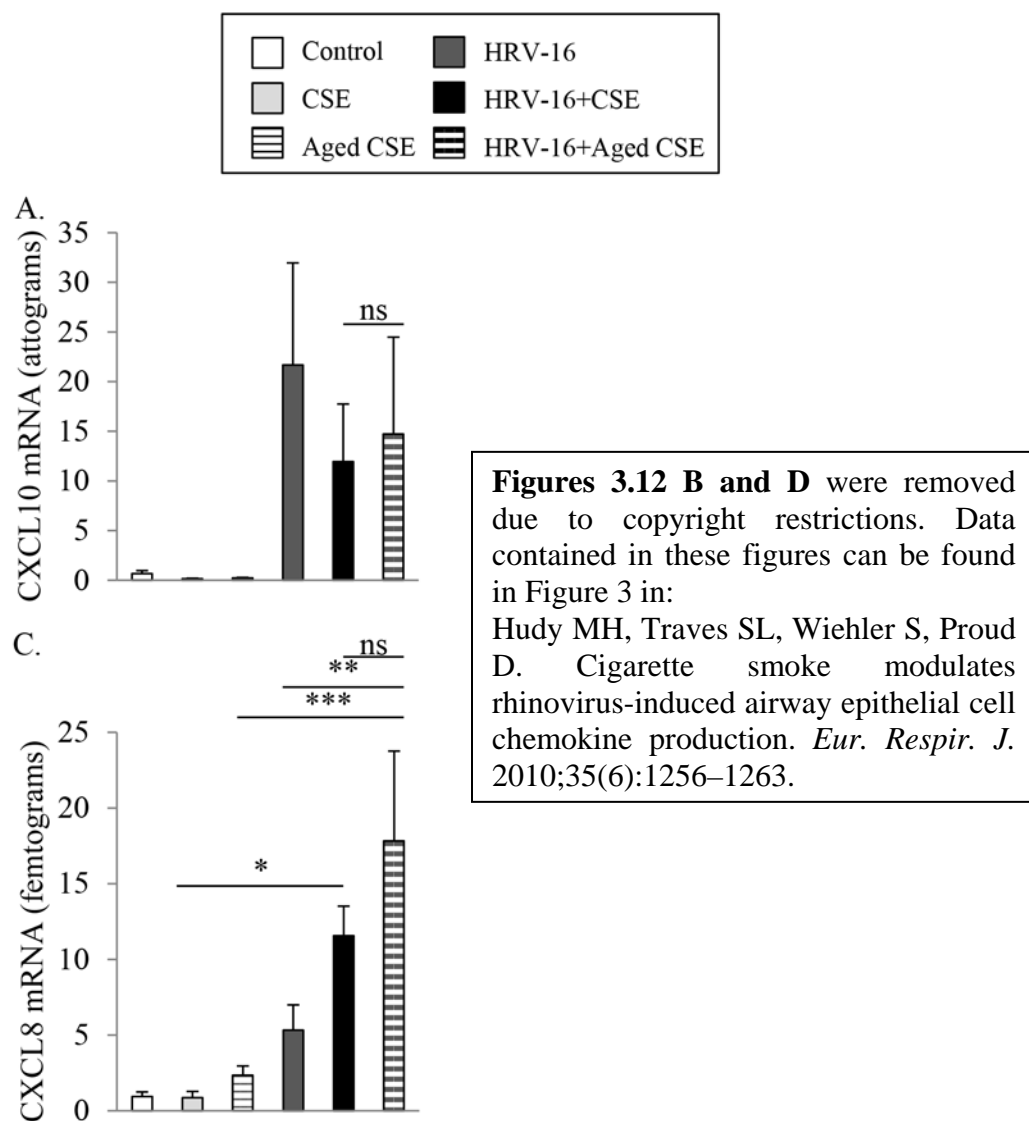
CXCL10 (A) and CXCL8 (B) protein levels were determined 24 h post-treatment in BEAS-2B cells. Data are presented as mean  $\pm$  SEM (n=3). Asterisks denote a significant difference between HRV-16+CSE compared with HRV-16 or CSE alone (\*\*\* p<0.001). Data presented in this figure have been published<sup>445</sup>.

**3.3.5 Inhibition of CXCL10 and induction of CXCL8 is unaffected by “aging” of CSE**

In order to determine whether the ability of CSE to modulate HRV-16-induced CXCL10 or CXCL8 was mediated by unstable, short-lived or volatile components in the extract, CSE was incubated for 24 h at 4°C prior to use. Fresh CSE was prepared immediately before the start of the experiment to compare the effects of fresh versus aged CSE.

Although inhibition of HRV-16-induced CXCL10 mRNA by CSE (fresh and “aged”) was not statistically significant, there was no significant difference between the two preparations of CSE (**Figure 3.12 A**). The magnitude of CXCL10 was markedly

variable between experiments and explains why statistical significance was not reached. Evaluation of protein levels, which are more relevant, show that both freshly prepared and “aged” CSE significantly inhibited HRV-16-induced CXCL10, and they did this to a comparable extent (**Figure 3.12 B**). Additionally, both freshly prepared and “aged” CSE induced comparable levels of CXCL8 mRNA (**Figure 3.12 C**) and protein (**Figure 3.12 D**), either alone or in combination with HRV-16. Interestingly, both freshly prepared and “aged” CSE in combination with HRV-16 synergistically induced CXCL8 protein levels (**Figure 3.12 D**).



**Figures 3.12 B and D** were removed due to copyright restrictions. Data contained in these figures can be found in Figure 3 in: Hudy MH, Traves SL, Wiehler S, Proud D. Cigarette smoke modulates rhinovirus-induced airway epithelial cell chemokine production. *Eur. Respir. J.* 2010;35(6):1256–1263.

**Figure 3.12:** The effects of freshly prepared versus “aged” CSE alone or in combination with HRV-16 on CXCL10 and CXCL8 production in airway epithelial cells.

CXCL10 mRNA (A; n=6) and protein (B; n=8) levels were determined 24 h post treatment in BEAS-2B cells. CXCL8 mRNA (C; n=6) and protein (D; n=8) levels were determined 5 h and 24 h respectively post-treatment in BEAS-2B cells. Data are presented as mean  $\pm$  SEM. Asterisks denote a significant difference between the specified groups (\*  $p \leq 0.05$ , \*\*  $p < 0.01$  and \*\*\*  $p < 0.001$ ). Hash marks denote a significant difference between HRV-16+CSE and the sum of the values from CSE and HRV-16 treatments alone. ns = not significant. Data presented in B & D have been published<sup>445</sup>.

### ***3.3.6 Nicotine does not mimic the modulating effects of CSE on HRV-16-induced CXCL10 and CXCL8***

Nicotine is the key addictive component in cigarette smoke<sup>449,450</sup> and many claim that it is one of the key components responsible for many physiological effects in the body. In order to determine whether nicotine was responsible for mediating HRV-16-induced effects on CXCL10 and CXCL8, various dilutions of nicotine were used both alone and in combination with HRV-16 prior to determination of CXCL10 and CXCL8 protein levels.

Human plasma nicotine concentration in smokers has been reported to be around 1-50 ng/mL<sup>451</sup>. The solubilized concentration of nicotine in the ASF is unknown. It is logical to speculate that the concentration of nicotine would be higher than in the plasma, since this would be the first point of contact for cigarette smoke, although it must be acknowledged that there could be substantial variations depending on how many cigarettes an individual smokes per day. The nicotine concentration of the 3R4F research grade cigarettes is reported to be 0.73 mg/cigarette<sup>452</sup>. After dilution of CSE following the standard protocol used for this project, and assuming complete solubility of nicotine, the concentration of nicotine in the final CSE preparation applied to cells would be around 10-20 µg/mL. Therefore, various nicotine dilutions covering this range were used for further experiments.

Chosen concentrations of nicotine alone or in combination with HRV-16 did not affect BEAS-2B cell viability as assessed by the MTT viability assay (**Figure 3.13 A**). Nicotine alone did not have any effect on CXCL10 or CXCL8 protein production at any of the concentrations of nicotine that were used (**Figure 3.13 A & B**). Additionally, nicotine did not modulate HRV-16-induced CXCL10 (**Figure 3.13 B**) or CXCL8 (**Figure 3.13 C**).

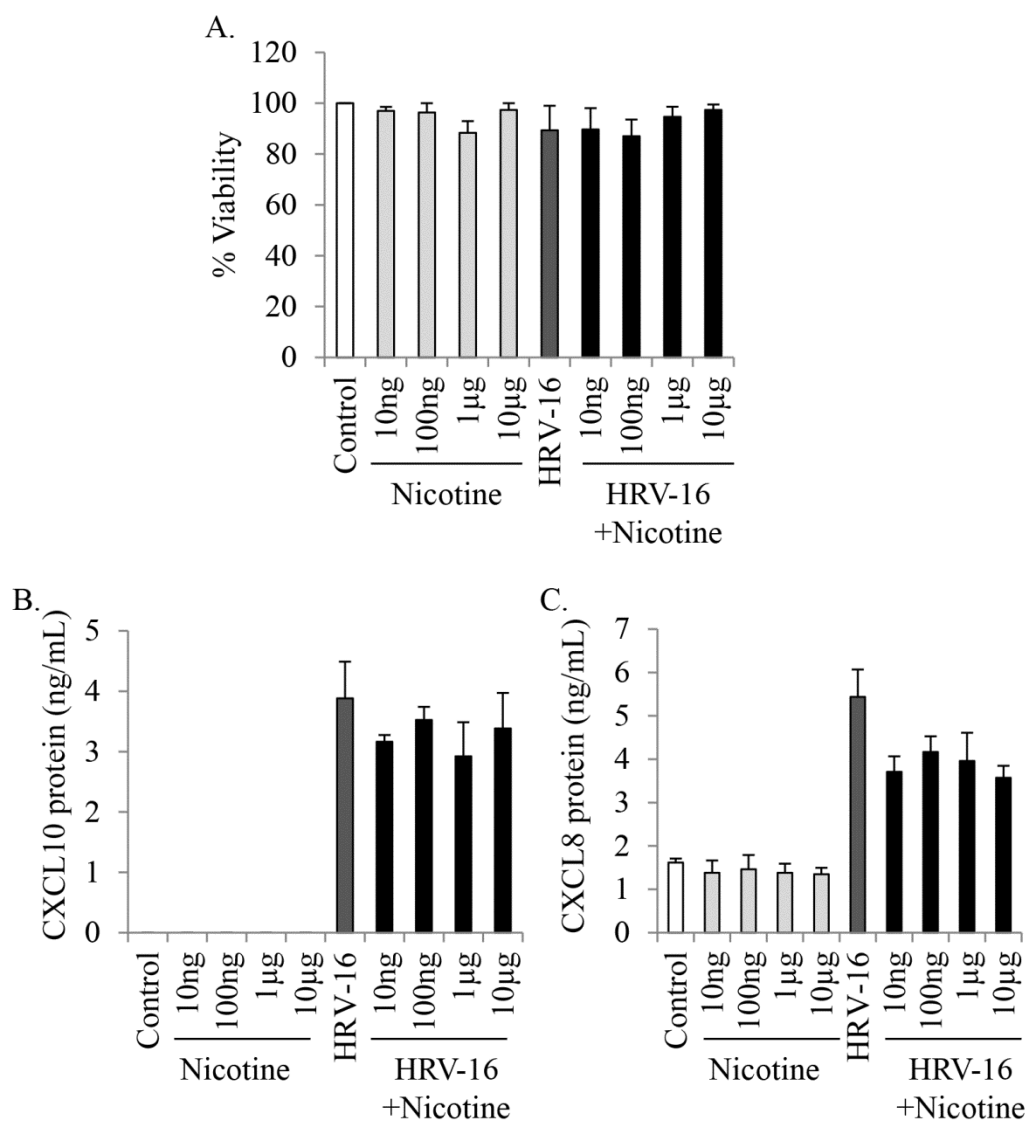


**Figure 3.13: The effects of nicotine alone or in combination with HRV-16 on airway epithelial cell viability and chemokine production.**

Cell viability was determined using the MTT viability assay in BEAS-2B cells that were treated with varying concentrations of nicotine in the presence or absence of CSE for 24 h (A). CXCL10 (B) and CXCL8 (C) protein levels were determined 24 h post-treatment in BEAS-2B cells. Data are presented as mean  $\pm$  SEM (n=3).

### 3.4 Discussion

The data presented in this chapter clearly show that HRV-induced pro-inflammatory responses are differentially regulated by CSE. HRV infection results in the induction of both CXCL10 and CXCL8 from airway epithelial cells. HRV-induced CXCL10 is significantly and potently inhibited by CSE, while, in contrast, HRV-induced CXCL8 is further, at least additively, enhanced by CSE.

To determine whether there was a concentration-dependent effect of HRV-induced CXCL10 inhibition by CSE and CXCL8 enhancement by the combination of HRV+CSE, studies using serial fold-dilutions of CSE were performed. Interestingly, CSE was markedly more potent in suppressing HRV-induced CXCL10 than in enhancing CXCL8 production. HRV-induced CXCL10 was inhibited by CSE at even low concentrations, while CXCL8 enhancement was only significant when a high dose of CSE was used in conjunction with HRV. This suggests that a different mechanism may be involved in the modulation of these two chemokines.

The modulation of chemokine responses did not appear to be unique for HRV-16, as a minor group HRV (HRV-1A) had a similar trend in the modulation of CXCL10 and CXCL8. Moreover, the ability of CSE to modulate HRV-induced epithelial CXCL10 and CXCL8 production did not appear to be regulated by unstable, short-lived volatile components in soluble CSE, as comparable results were observed using CSE prepared 24 h prior to use. This does not eliminate the possibility that unstable and volatile components that are present in cigarette smoke are unable to affect chemokine responses, for instance the components that were too short lived to even be present in the 'freshly prepared' CSE.

However, short-lived, volatile components of soluble CSE are not playing a role modulating the chemokine responses observed in this study.

Nicotine, the major addictive component in cigarette smoke was not, at least on its own, responsible for the modulation of HRV-induced chemokine responses, as nicotine alone did not inhibit HRV-induced CXCL10 or enhance HRV-induced CXCL8. There are over 4000 components in cigarette smoke and a thorough examination of which component is responsible for these effects is beyond the scope of this thesis. It is also possible that a combination of many components in cigarette smoke are responsible for these effects, making delineation of the components responsible for these effects that much more difficult.

In summary, it has been shown here that CSE differentially modulates HRV-induced CXCL8 and CXCL10 responses in airway epithelial cells. This study has shown for the first time that HRV-induced CXCL10 is inhibited in the presence of CSE and the combined treatment of HRV and CSE enhances the production of CXCL8 at least additively above either treatment alone. Thus, these results warranted a further examination of the mechanisms involved in the regulation of HRV-induced CXCL10 and CXCL8 by CSE.

## **Chapter Four: Modulation of HRV-Induced Chemokine Production by CSE is Independent of Effects on Receptor Expression and Viral Replication**

Portions of data presented in this Chapter have been published:

Hudy MH, Traves SL, Wiehler S, Proud D. Cigarette smoke modulates rhinovirus-induced airway epithelial cell chemokine production. *Eur. Respir. J.* 2010;35(6):1256–1263.

Copyright © European Respiratory Society.

## 4.1 Background

As discussed in detail in **Chapter 1**, major group HRVs, such as HRV-16, are recognized by ICAM-1 on airway epithelial cells resulting in internalization and downstream signaling events. Following internalization, HRVs undergo replication via a dsRNA intermediate in the cytoplasm, ultimately resulting in the release of new virion particles. The results presented in **Chapter 3** show that CSE differentially affects HRV-induced chemokine responses. HRV-induced CXCL10 was inhibited by CSE, while HRV-induced CXCL8 was further enhanced by CSE. Thus, it is unlikely that a common mechanism, such as effects on HRV receptor expression or HRV replication, are, at least, solely responsible for such disparate chemokine results.

## 4.2 Hypothesis

CSE does not modulate HRV-induced CXCL10 and CXCL8 chemokine expression by altering HRV receptor expression or replication of HRV in airway epithelial cells.

## 4.3 Results

### ***4.3.1 CSE alone or in combination with HRV-16 does not alter the number of airway epithelial cells expressing the HRV-16 receptor, ICAM-1.***

In order to assess whether the major group HRV receptor, namely ICAM-1, was modulated by CSE, flow cytometry analysis was performed for ICAM-1 expression on BEAS-2B cells following treatment with control medium alone, CSE alone, HRV-16 alone or the combined stimulus. The number of BEAS-2B cells expressing the ICAM-1 receptor

did not change regardless of treatment (**Figure 4.1 A**), as 100% of cells expressed ICAM-1 and continued to express this receptor following all of the treatments. The number of receptors being expressed per cell can be relatively compared using the geometric mean calculated from the histogram plot. HRV-16 alone increased the number of ICAM-1 receptors per cell compared to the medium control (**Figure 4.1 B**). Interestingly, the number of receptors per cells was not decreased, but rather, increased following stimulus with HRV-16+CSE compared to medium control and CSE alone (**Figure 4.1 B**).

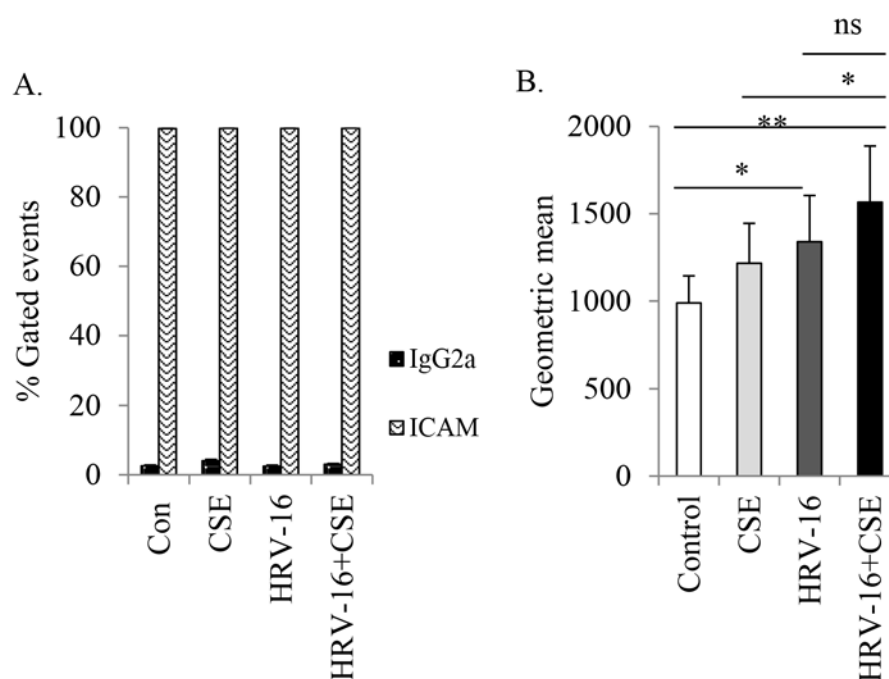


**Figure 4.1: CSE alone, HRV-16 alone or the combination of HRV-16+CSE do not alter the number of airway epithelial cells expressing ICAM-1 but both HRV-16 alone and HRV-16+CSE increase the number of ICAM-1 receptors per cell.**

ICAM-1 receptor levels were determined by flow cytometry 24 h post-treatment in BEAS-2B cells and indicate % of airway epithelial cells expressing ICAM-1 (A) and the relative number of ICAM-1 receptors per cell (B). Data are presented as mean  $\pm$  SEM (n=4). Asterisks denote a significant difference between the specified groups (\*  $p \leq 0.05$  and \*\*  $p < 0.01$ ). ns = not significant.

### 4.3.2 CSE does not affect HRV-16 titre in airway epithelial cells

In order to determine the effects of CSE on HRV-16 replication, HBE or BEAS-2B cells were exposed for 1 h to HRV-16 alone or HRV-16+CSE. Cells were then washed with HBSS to remove excess HRV-16, and fresh control medium or CSE was applied accordingly. Viral titres obtained in supernatants from HBE (**Figure 4.2 A**) and BEAS-2B (**Figure 4.2 B**) cells after 24 h, expressed as Log TCID<sub>50</sub>, were not different between cells exposed to HRV-16 alone or HRV-16 in combination with CSE. Control medium and CSE were then further re-applied to BEAS-2B cells for an additional 24 h to assess whether CSE had an effect on HRV-16 viral titre at later time-points (24 to 48 h). Again, viral titres were not different between cells exposed to HRV-16 alone and HRV-16+CSE (**Figure 4.2 B**).

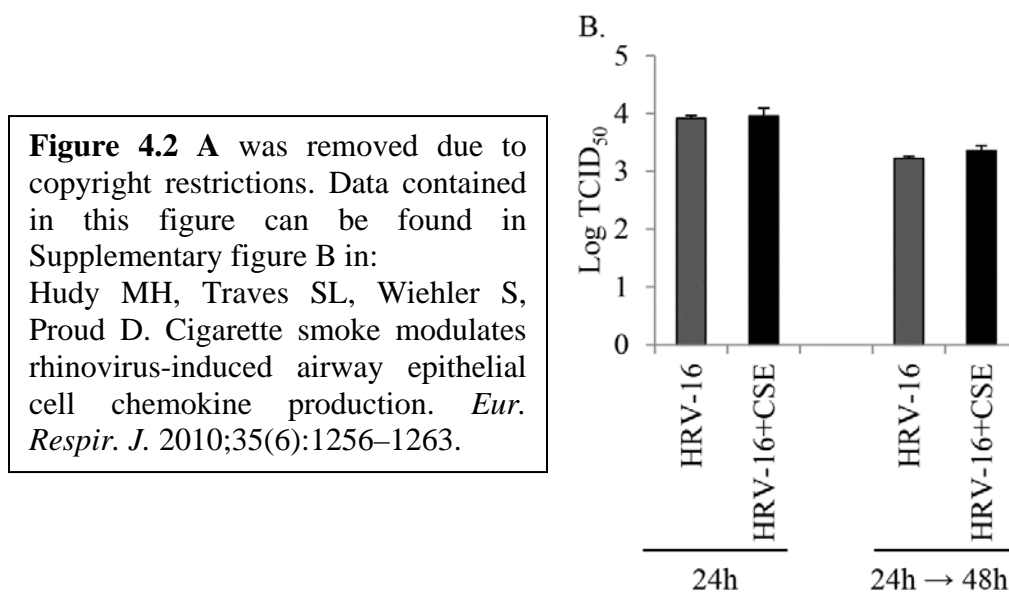


### Figure 4.2: CSE does not affect HRV-16 titre in airway epithelial cells.

Viral titres were determined in supernatants from HBE (A) and BEAS-2B (B) cells that were infected with HRV-16 in the presence or absence of CSE for 24 h (A&B) and additionally from 24 h to 48 h (B). Data are presented as mean  $\pm$  SEM (n=3). Data presented in A have been published<sup>445</sup>.

### ***4.3.3 CSE inhibits poly [I:C]-induced CXCL10 and poly [I:C]+CSE enhance CXCL8 above either stimulus alone in airway epithelial cells.***

Poly [I:C] can be used as a synthetic analog of the dsRNA intermediate formed during HRV replication and it has previously been demonstrated that poly [I:C] robustly induces both CXCL10 and CXCL8 production from airway epithelial cells<sup>158,259,355,453</sup>. This tool was used in order to determine whether the chemokine responses observed with poly [I:C] and CSE would correlate with those seen with HRV-16 and CSE. Prior to analysis of chemokine responses, viability of cells transfected with a standard concentration of poly [I:C] alone or subsequently treated with CSE was assayed using both the MTT and LDH viability assays in both HBE and BEAS-2B cells (**Figure 4.3**). There were no overt effects on cell viability observed with poly [I:C] alone or in combination with CSE in either cell type.

As previously reported, poly [I:C] induced robust production of CXCL10 mRNA and protein (**Figure 4.4**). As seen with HRV-16-induced CXCL10, Poly [I:C]-induced CXCL10 protein production was potently inhibited by CSE in HBE cells (**Figure 4.4 A**). This inhibition was also seen in BEAS-2B cells at both the mRNA (**Figure 4.4 B**) and protein level (**Figure 4.4 C**). Furthermore, poly [I:C]-induced CXCL8 protein production and this was further enhanced with the combination of poly [I:C]+CSE (**Figure 4.5**).

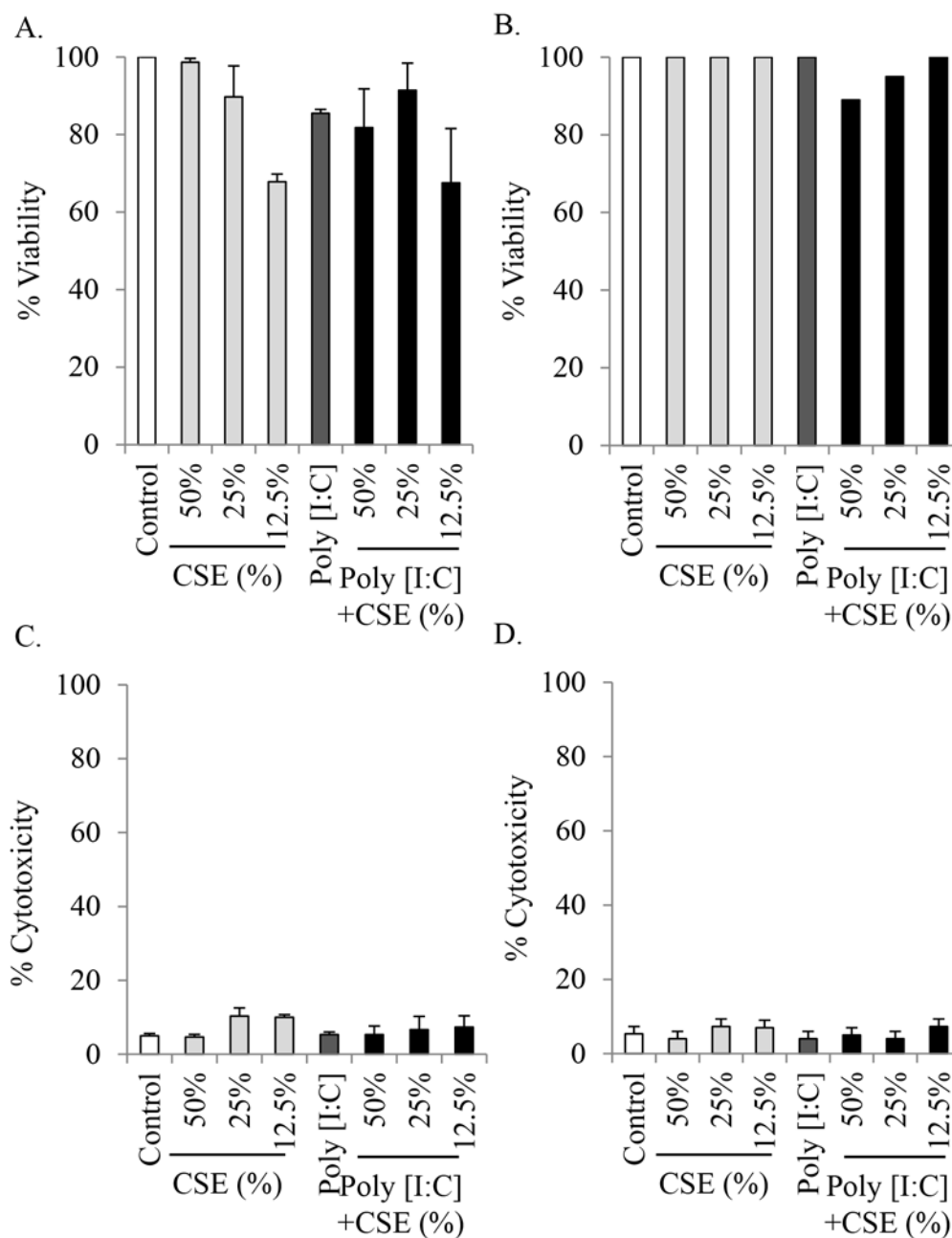


**Figure 4.3: CSE alone or in combination with poly [I:C] does not overtly affect airway epithelial cell viability.**

HBE (A&C) and BEAS-2B (B&D) cell viability was assessed by MTT and LDH viability assays 24 h post-treatment with medium control, 2-fold serial dilutions of CSE, poly [I:C], or poly [I:C] in combination with 2-fold serial dilutions of CSE. Data are presented as mean  $\pm$  SEM (A&C&D: n=3, B: n=1).

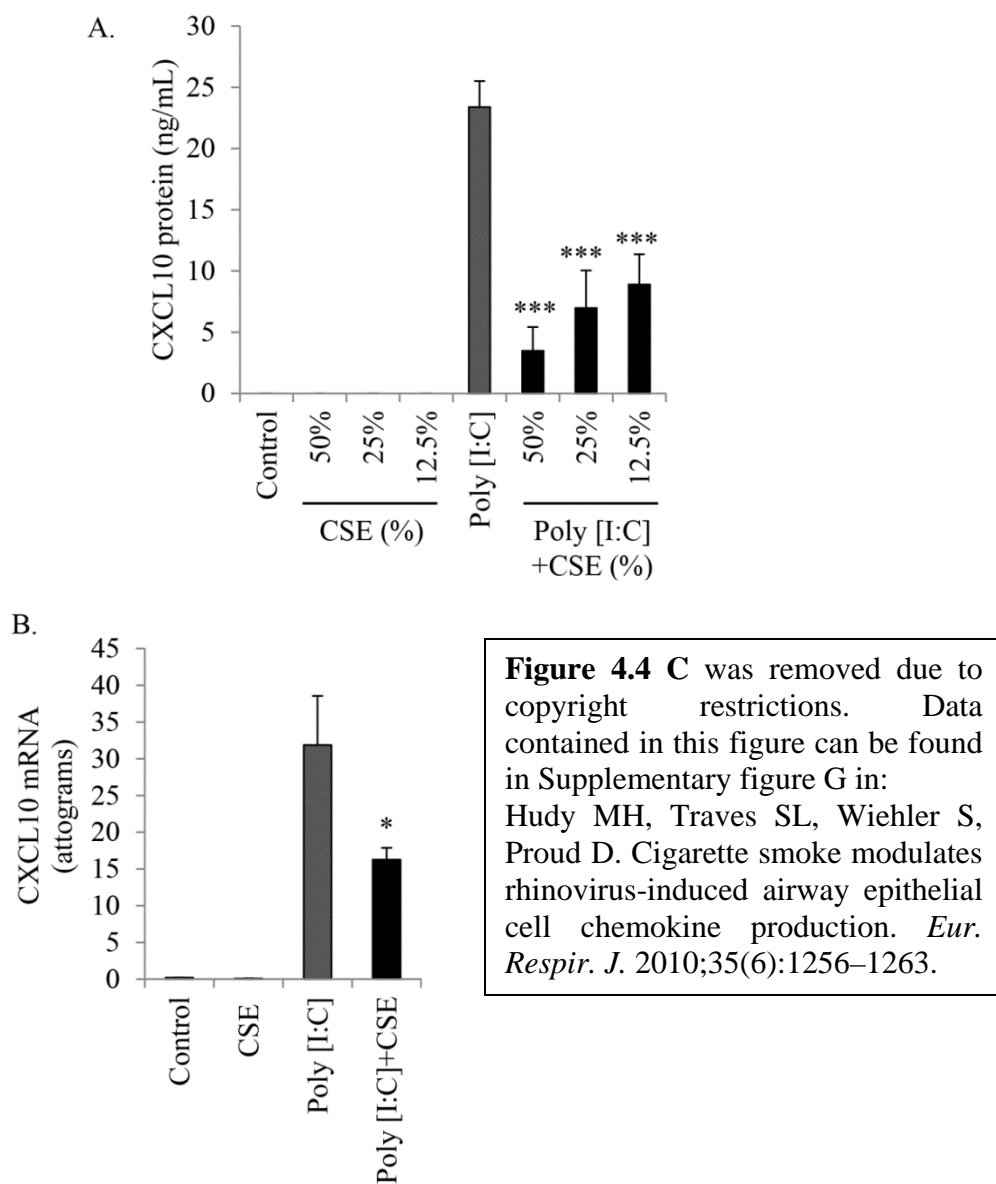


**Figure 4.4: CSE inhibits poly [I:C]-induced CXCL10 in airway epithelial cells.**

CXCL10 protein levels were determined at 24 h post-treatment with control medium, varying concentrations of CSE alone or in the presence of poly [I:C] in HBE cells (A; n=4). CXCL10 mRNA (B; n=3) and protein (C; n=3) levels were determined at 24 h post-treatment in BEAS-2B cells. Data are presented as mean  $\pm$  SEM. Asterisks denote a significant difference between poly [I:C]+CSE and poly [I:C] alone (\*  $p \leq 0.05$  and \*\*\*  $p < 0.001$ ). Data presented in A & C have been published<sup>445</sup>.

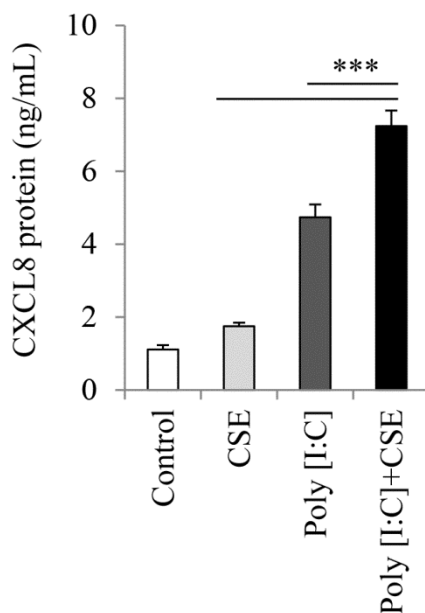


**Figure 4.5: CSE and poly [I:C] each induce CXCL8 alone and further increase CXCL8 in combination in airway epithelial cells.**

CXCL8 protein levels were determined at 24 h post treatment in BEAS-2B cells. Data are presented as mean  $\pm$  SEM (n=3). Asterisks denote significant difference between poly [I:C]+CSE compared to poly [I:C] or CSE alone (\*\*\* p<0.001).

#### 4.4 Discussion

The data presented in this chapter show that CSE does not significantly affect HRV receptor expression, at least of major group HRVs, and does not alter HRV-16 replication in a relevant time frame to have an effect on CXCL10 and CXCL8 chemokine expression.

Initial examination using flow cytometry revealed that ICAM-1 was basally expressed on all BEAS-2B cells. The number of cells expressing ICAM-1 did not change following treatment with CSE, HRV or the combination of HRV+CSE for 24 h. The number of receptors per cell was also examined and showed that CSE alone did not alter

the number of receptor per cell while HRV alone or in combination with CSE significantly enhanced the number of ICAM-1 receptors per cell. Indeed, it has been previously shown that HRV induces the expression of its cognate receptor ICAM-1<sup>454</sup>. Unfortunately, these data could not be confirmed in primary HBE cells due to technical difficulties involved with lifting these cells off culture plates. HBE cells could only be successfully lifted following very lengthy incubation with a variety of cell lifting solutions (upwards of an hour), after which no expression of ICAM-1 could be detected, most likely due to enzyme-related receptor cleavage. Based on very similar responses shown in **Chapter 3** between the BEAS-2B cell line and primary HBE cells, it can be speculated that relative ICAM-1 expression following the treatments of interest would be comparable.

Next, using viral titre assays it was determined that CSE did not alter HRV replication following a 24 h exposure. In support of this, a previous study, performed in A549 alveolar cells, using CSE, HRV-16 and a viral titre assay, showed that CSE did not alter HRV replication<sup>444</sup>. Additionally, a recent publication has also shown that although CSE does increase HRV RNA levels in BEAS-2Bs after a 48 h exposure, this effect is not seen at 24 h<sup>355</sup>. This data suggests that early effects on HRV-induced CXCL10 and CXCL8 expression following CSE exposure are not due effects on viral replication. How CSE modulates HRV-induced CXCL10 and CXCL8 at later time-points was not explored in this study, but it is possible that CSE may have an effect on viral replication at later time-points and this could subsequently affect chemokine expression levels.

CXCL10 production is dependent on HRV replication, as it has been shown that ultraviolet (UV) inactivated virus that is replication deficient, does not induce the

production of CXCL10<sup>259</sup>. Conversely, although initial CXCL8 production is not dependent on viral replication, as UV-inactivated HRV is still able to generate CXCL8 production, it is thought that replication-dependent signalling contributes to subsequent CXCL8 generation<sup>323</sup>. Here it was found that the synthetic analog of the dsRNA stage formed during HRV replication, namely poly [I:C], induced robust production of both CXCL10 and CXCL8 at 24 h after treatment. Moreover, CSE modulated these poly [I:C]-induced responses in an analogous manner to its modulation of HRV-induced CXCL10 and CXCL8. These results further support the notion that CSE is not inhibiting HRV-16 replication, particularly through impacting the formation of the dsRNA replication intermediate, since similar effects regarding the modulation of CXCL10 are observed with poly [I:C].

In summary, the data presented in this chapter have shown that CSE does not alter major group HRV receptor expression or HRV replication in a relevant time frame to account for alterations in HRV-induced CXCL10 and CXCL8 expression. Additionally, poly [I:C], a synthetic mimic for the dsRNA stage formed during HRV replication, revealed that similar modulatory effects by CSE on poly [I:C]-induced CXCL10 and CXCL8 were seen. This implies that the modulatory effects that CSE has on these HRV-induced chemokines must take place further downstream from the HRV replication stage or in an altogether different manner. Thus, a further examination of the mechanisms involved in the differential modulation of HRV-induced CXCL10 and CXCL8 by CSE were warranted.

#### **4.5 Future Studies**

Future studies could include an investigation into the expression levels of the minor group HRV receptor, namely the LDL receptor, and as to whether it is altered by CSE. Additionally, similar viral titre experiments could be conducted using a member of the minor group HRVs. If the results were similar to the ones presented in this chapter, this would further validate that CSE has non-selective effects on HRV-induced airway epithelial cell chemokine responses.

## Chapter Five: **Mechanisms of HRV-induced CXCL10 inhibition by CSE**

Portions of data presented in this Chapter have been published:

Hudy MH, Traves SL, Wiehler S, Proud D. Cigarette smoke modulates rhinovirus-induced airway epithelial cell chemokine production. *Eur. Respir. J.* 2010;35(6):1256–1263.

Copyright © European Respiratory Society.

Proud D, Hudy MH, Wiehler S, et al. Cigarette smoke modulates expression of human rhinovirus-induced airway epithelial host defense genes. *PLoS ONE.* 2012;7(7):e40762.

This work was reprinted with permission based on the PLoS open-access license: Creative Commons Attribution 2.5 Generic License (<http://creativecommons.org/licenses/by/2.5/legalcode>).

## 5.1 Background

CXCL10 expression is regulated mainly at the transcriptional level. Two proximal NF- $\kappa$ B and one ISRE site in the CXCL10 promoter region have been shown to be important for transcriptional control of human CXCL10 following a variety of stimuli<sup>299–304</sup>.

### 5.1.1 Regulation of CXCL10 expression by HRV

CXCL10 has been shown to be enhanced by HRV in human bronchial epithelial cells via transcriptional mechanisms, involving two NF- $\kappa$ B and one ISRE transcription factor binding sites in the CXCL10 promoter region<sup>259,297,298,338,345</sup> (**Figure 5.1**). Specifically, the p50/p65 NF- $\kappa$ B heterodimer and IRF-1 have been implicated to be the transcription factors involved in binding to the NF- $\kappa$ B and ISRE sites respectively<sup>297,298</sup>. Although, specific sites involved have not been delineated, regions upstream of the ISRE binding site have also been suggested to be important in HRV-induced CXCL10 promoter activation in airway epithelial cells<sup>259</sup>.

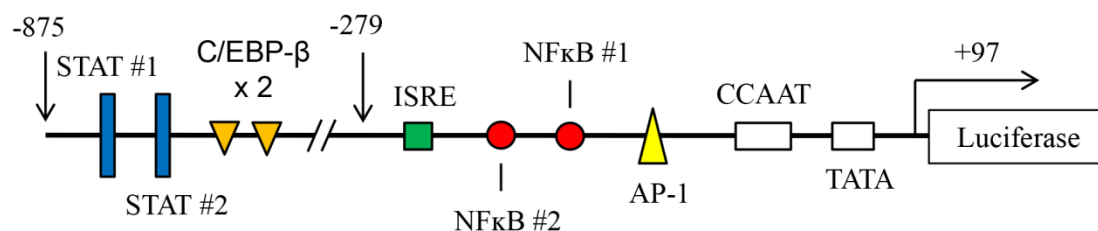


**Figure 5.1: Schematic diagram of the putative CXCL10 promoter.**

A schematic diagram of the putative 972 bp CXCL10 promoter construct inserted upstream of a firefly luciferase gene. Diagram is not to scale.

### **5.1.2 Regulation of CXCL10 expression by cigarette smoke**

Although the effects of cigarette smoke on CXCL10 have not been examined, cigarette smoke has been shown to have modulatory effects on transcription factors which have putative binding sites in the CXCL10 promoter<sup>203,210,263,433,455–461</sup>. Furthermore, cigarette smoke has also been shown to epigenetically affect gene expression in the airways<sup>312,313</sup>.

## **5.2 Hypothesis**

The inhibition of HRV-16-induced CXCL10 expression by CSE occurs at the level of transcription, involving inhibition of one or more transcription factors such as NF-κB, IRF-1, and/or involves aspects of epigenetic regulation.

## **5.3 Results**

### **5.3.1 CSE suppresses HRV-induced and poly [I:C]-induced CXCL10 promoter activation**

In order to determine whether the inhibition of HRV-16-induced CXCL10 by CSE was being mediated at the transcriptional level, the BEAS-2B bronchial epithelial cell line was transiently transfected with a full-length CXCL10 promoter-luciferase construct (**Figure 5.1**) and assayed for firefly luciferase activity following a 24 h treatment with medium control, CSE, HRV-16 or HRV-16+CSE (**Figure 5.2 A & B**). Since poly [I:C], a mimic for viral dsRNA generated during the replication cycle, was also shown to induce CXCL10 production which was inhibited in the presence of CSE (**Chapter 3**), it was used

to perform analogous experiments (**Figure 5.2 C & D**). BEAS-2B cells were used for these experiments as primary HBE cells are difficult to transfect with large promoter constructs. The use of BEAS-2B cells for these experiments was justified based on similar results seen with primary HBE and BEAS-2B cells regarding CXCL10 expression (**Chapter 3**). Data are displayed as both raw RLU (**Figure 5.2 A & C**) and fold increase compared to medium control (**Figure 5.2 B & D**) to show that the trend in the data remained the same regardless of how the data were expressed.

CSE alone did not induce CXCL10 promoter activation and, indeed, slightly suppressed basal promoter activation (**Figure 5.2 A-D**). As previously reported, both HRV-16 (**Figure 5.2 A & B**) and poly [I:C] (**Figure 5.2 C & D**) induced robust activation of the CXCL10 promoter alone<sup>259,338</sup>. Interestingly, CSE significantly inhibited both HRV-16-induced and poly [I:C]-induced CXCL10 promoter activation (**Figure 5.2 A-D**).

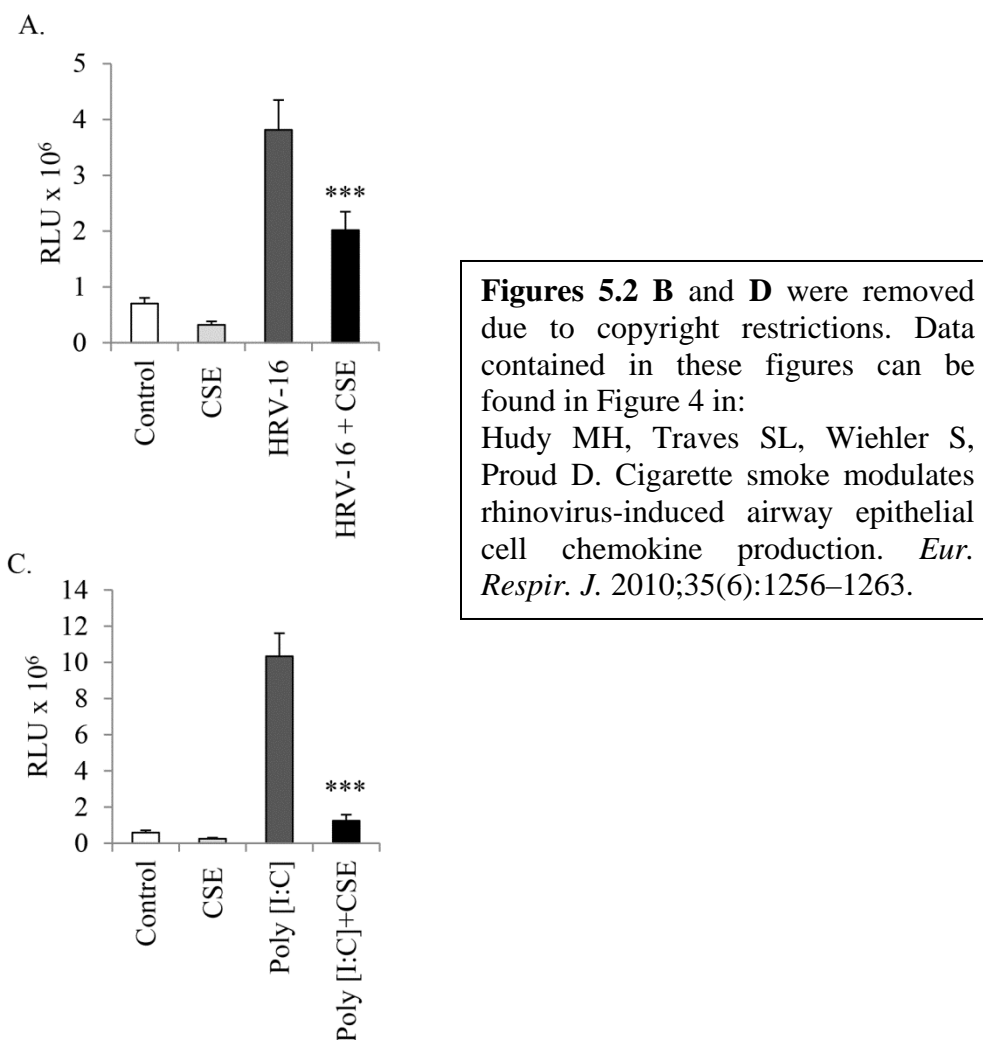


**Figure 5.2: CSE inhibits both HRV-16-induced and poly [I:C]-induced CXCL10 promoter activation in airway epithelial cells.**

BEAS-2B cells that were transiently transfected with the full length (972bp) CXCL10 promoter were then treated with control medium, CSE alone, HRV-16 alone or the combination for 24 h (A&B; n=14). BEAS-2B cells that were transiently transfected with the full length (972 bp) CXCL10 promoter were then treated with control medium, CSE alone, or transfected with poly [I:C] alone or in combination with CSE for 24 h (C&D; n=6). Cell lysates were assessed for firefly luciferase activity and data are presented as both relative light units (RLU; A&C) and fold induction as compared to cells treated with only medium control (B&D). Data are presented as mean  $\pm$  SEM. Asterisks denote a significant difference between HRV-16+CSE compared to HRV-16 alone or between poly [I:C]+CSE compared to poly [I:C] alone (\*\*\* p<0.001). B & D have been published<sup>445</sup>.

### ***5.3.2 HRV-16-induced CXCL10 promoter activation is suppressed by CSE but not dependent on activator protein 1 (AP-1)***

It has previously been shown that HRV-16-induced CXCL10 expression is dependent both on binding of NF- $\kappa$ B to each of the two NF- $\kappa$ B recognition sequences and on binding of IRF-1 to the ISRE sequence in the CXCL10 promoter<sup>259,298</sup>. To investigate which putative binding sites play a role in CSE-mediated inhibition of HRV-16-induced promoter activation, BEAS-2B cells were transiently transfected with either the wild type CXCL10 promoter or the CXCL10 promoter with mutations in the ISRE, each of two NF- $\kappa$ B, or the AP-1 transcription factor binding sites and then treated with control medium, CSE alone, HRV-16 alone or the combination (**Figure 5.3 A (RLU) & B (fold induction)**). Mutation of the AP-1 recognition sequence did not lead to any significant differences in HRV-16-induced CXCL10 promoter activation or its inhibition by CSE compared to the wild type promoter. CSE alone did not induce activation of the  $\Delta$ AP-1 CXCL10 promoter either. As previously reported, however, mutation of the ISRE or either of the NF- $\kappa$ B recognition sequences reduced HRV-16-induced CXCL10 promoter activation essentially to baseline levels<sup>259,297</sup>. It was not possible to evaluate if CSE inhibition is affected in the absence of viral drive, but it seemed feasible that the same sites involved in HRV-induced CXCL10 promoter activation may also be involved in CSE-mediated inhibition. Therefore, alternative approaches were used to evaluate this.

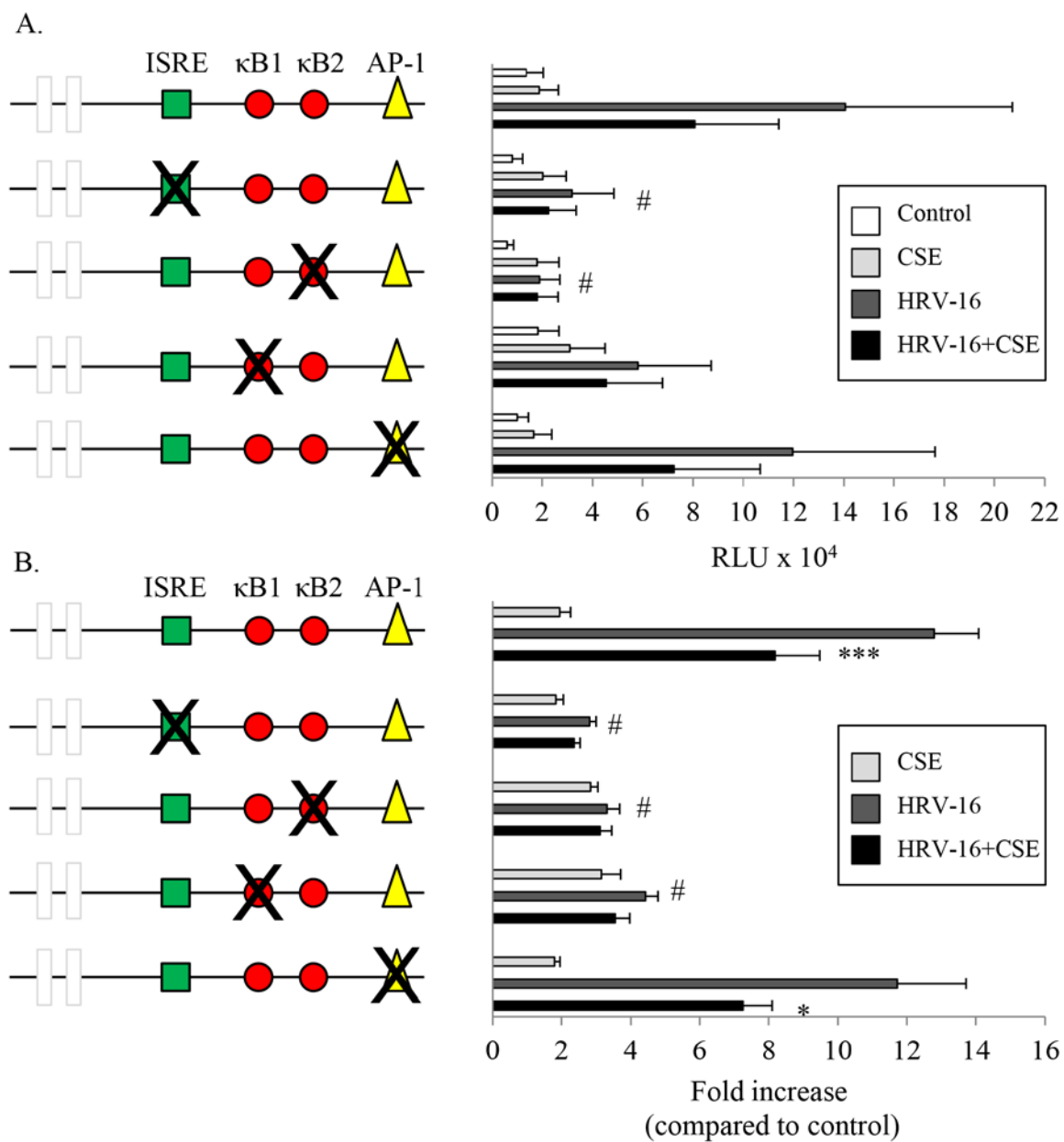


**Figure 5.3: Effects of point mutations on CXCL10 promoter activation in airway epithelial cells.**

BEAS-2B cells that were transiently transfected with the wild type CXCL10 promoter or the CXCL10 promoter with various point mutations in putative transcription factor binding sites were then treated with control medium, CSE alone, HRV-16 alone or the combination

for 24 h. Cell lysates were assessed for firefly luciferase activity and data are presented as both relative light units (RLU; A) and fold induction as compared to cells treated with only medium control for each respective promoter variant (B). Data are expressed as mean  $\pm$  SEM (n=8). Asterisks denote a significant difference between cells treated with HRV-16+CSE and cells treated with HRV-16 that were transfected with the corresponding CXCL10 promoter variant (\*  $p \leq 0.05$  and \*\*\*  $p < 0.001$ ). Hash marks denote a significant difference between the specified treatment and HRV-16 treatment in the wild type CXCL10 promoter.

### ***5.3.3 Inhibition of HRV-16-induced CXCL10 by CSE is partially dependent on inhibition of NF- $\kappa$ B***

Involvement of NF- $\kappa$ B in transcriptional activation of HRV-16-induced CXCL10 was confirmed using the selective IKK $\beta$  inhibitor, PS1145 (**Figure 5.4**). As a first step to delineate the role of NF- $\kappa$ B in HRV-16-induced CXCL10 inhibition by CSE, BEAS-2B cells were transfected with promoter-luciferase constructs containing tandem repeats of 5 copies of either the CXCL10-specific NF- $\kappa$ B #1 or the NF- $\kappa$ B #2 recognition sequences prior to stimulation with either medium, CSE alone, HRV-16 alone or the combination. HRV-16 infection induced activation of both 5X NF- $\kappa$ B #1 and 5X NF- $\kappa$ B #2 and, in each case, activation was significantly, if modestly, inhibited in the presence of CSE (**Figure 5.5 A (RLU) & B (fold induction)**).

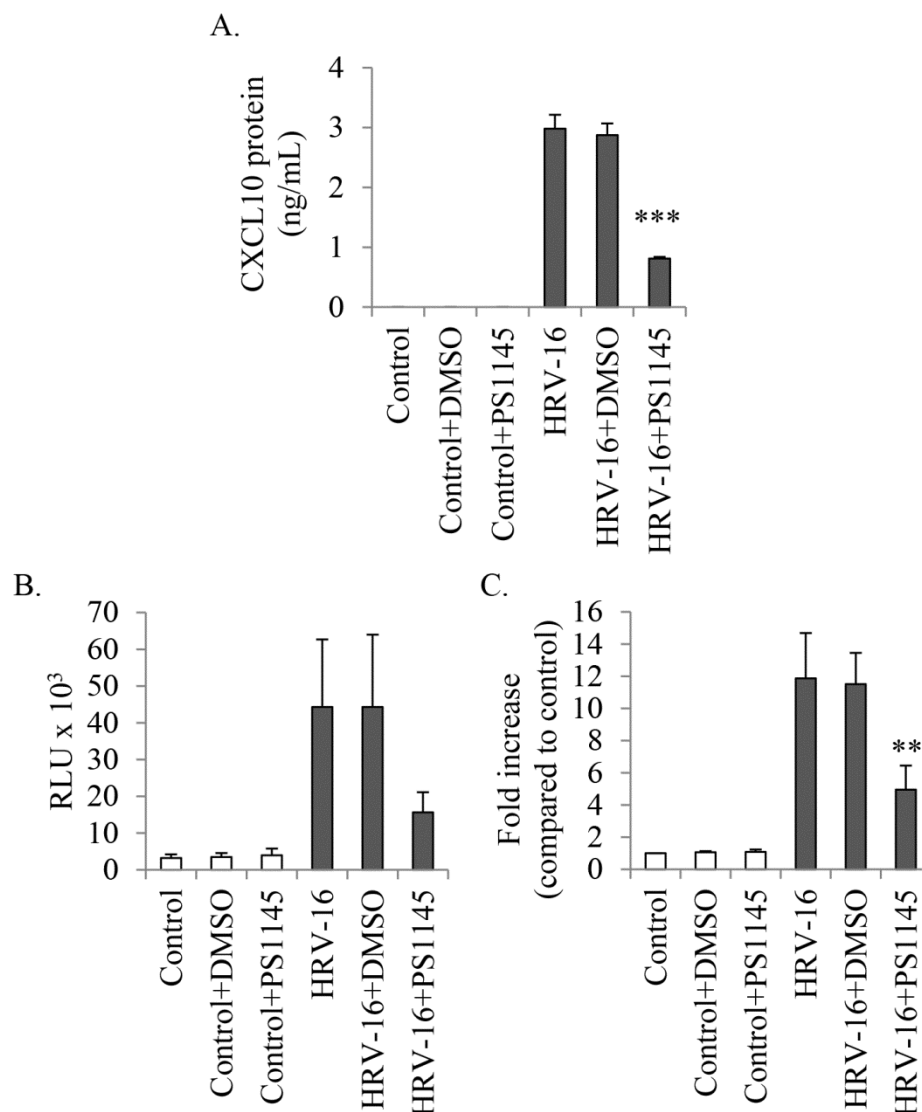


**Figure 5.4: Induction of CXCL10 protein by HRV-16 is partially dependent on transcriptional activation by NF- $\kappa$ B.**

BEAS-2B cells were treated with control medium alone or in combination with DMSO or PS1145 and HRV-16 alone or in combination with DMSO or PS1145 for 24 h, were then assessed for CXCL10 protein levels via ELISA (A; n=3). BEAS-2B cells were transiently transfected with the wild type CXCL10 and were then treated with the same stimuli for 24 h and cell lysates were then assessed for firefly luciferase activity and data are presented as both relative light units (RLU; B; n=6) and fold induction as compared to cells treated with only medium control (C; n=6). Data are expressed as mean  $\pm$  SEM. Asterisks denote a significant difference between cells treated with HRV-16+PS1145 and cells treated with HRV-16 alone (\*\* p<0.01 and \*\*\* p<0.001).

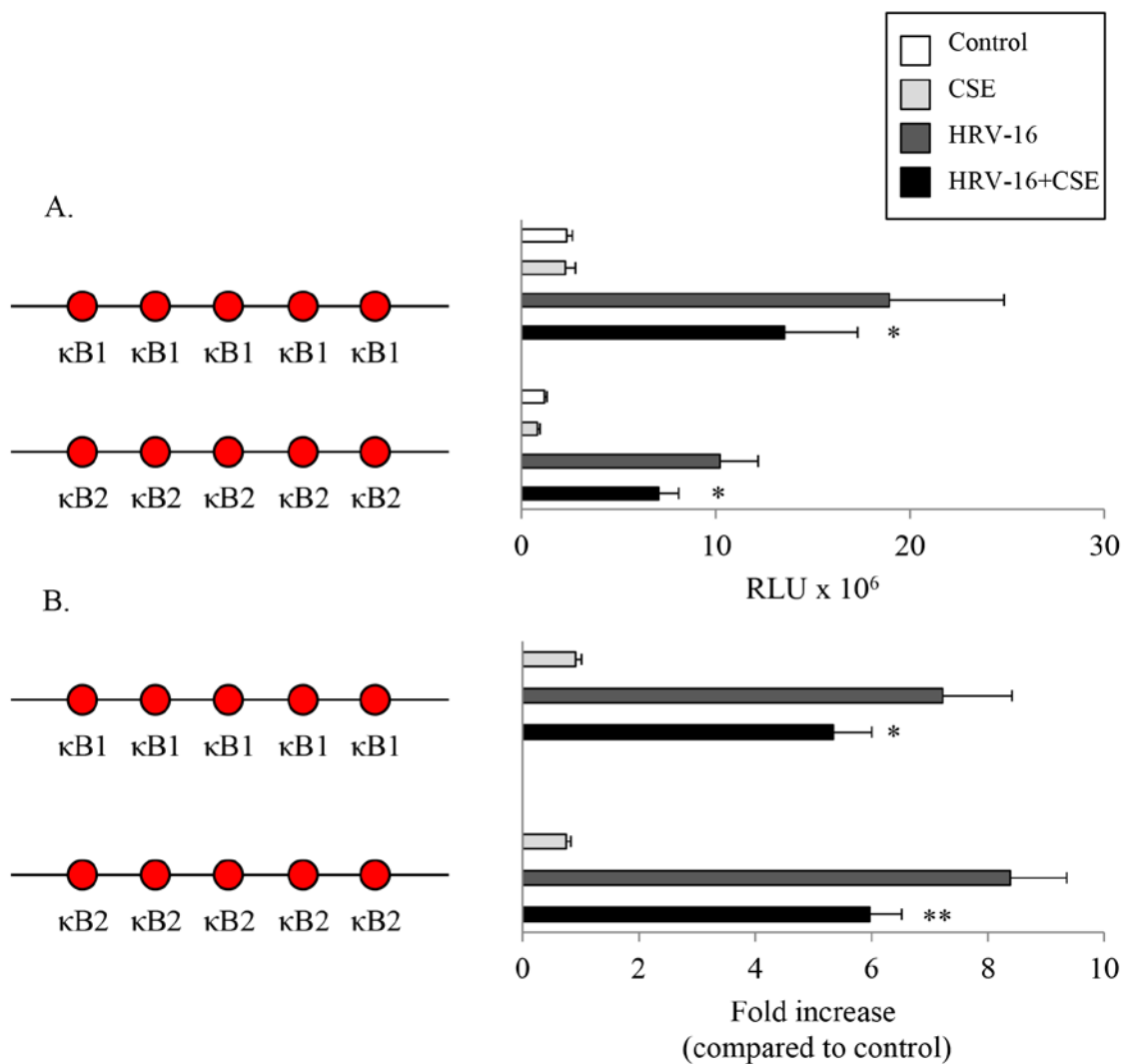


**Figure 5.5: CSE inhibits HRV-16-induced promoter activation of two CXCL10-specific NF- $\kappa$ B recognition sequences.**

BEAS-2B cells transiently transfected with two different CXCL10-specific 5x NF- $\kappa$ B promoter constructs representing sites in the CXCL10 promoter (NF- $\kappa$ B #1 and NF- $\kappa$ B #2) were then treated with control medium, CSE alone, HRV-16 alone or the combination for 24 h. Cell lysates were assessed for firefly luciferase activity and data are presented as both relative light units (RLU; A) and fold induction as compared to cells treated with only medium control for each respective promoter variant (B). Data are expressed as mean  $\pm$  SEM (n=8). Asterisks denote a significant difference between cells treated with HRV-16+CSE and cells treated with HRV-16 that were transfected with the corresponding promoter variant, (\* $p \leq 0.05$  and \*\*  $p < 0.01$ ).

To determine if CSE had an effect on HRV-16 induced nuclear translocation and/or binding of NF- $\kappa$ B to recognition sequences in the CXCL10 promoter, EMSA analysis was used. As it has previously been reported in airway epithelial cells<sup>297</sup>, two oligonucleotide-protein complexes were formed by 3 h post HRV-16 infection (**Figure 5.6 A & B**), and these complexes persisted through 6 and 9 h post HRV-16 infection<sup>297</sup>. The same publication has also reported that the upper complex is a heterodimer of the p50 and p65 subunits of NF- $\kappa$ B, while the lower band comprises p50 homodimers<sup>297</sup>. This was confirmed using antibodies to the p50 and p65 NF- $\kappa$ B subunits (**Figure 5.6 A & B (right panels)**). As, the cRel NF- $\kappa$ B subunit has previously been shown not to be involved<sup>297</sup>, an antibody to cRel was used as a negative control. When primary HBE cells were treated with HRV-16 in combination with CSE, the intensity of both bands was reduced (**Figure 5.6 A & B (left panels)**), suggesting that CSE inhibited HRV-16-induced nuclear translocation and/or binding of NF- $\kappa$ B subunits to both NF- $\kappa$ B transcription factor binding sites in the CXCL10 promoter.

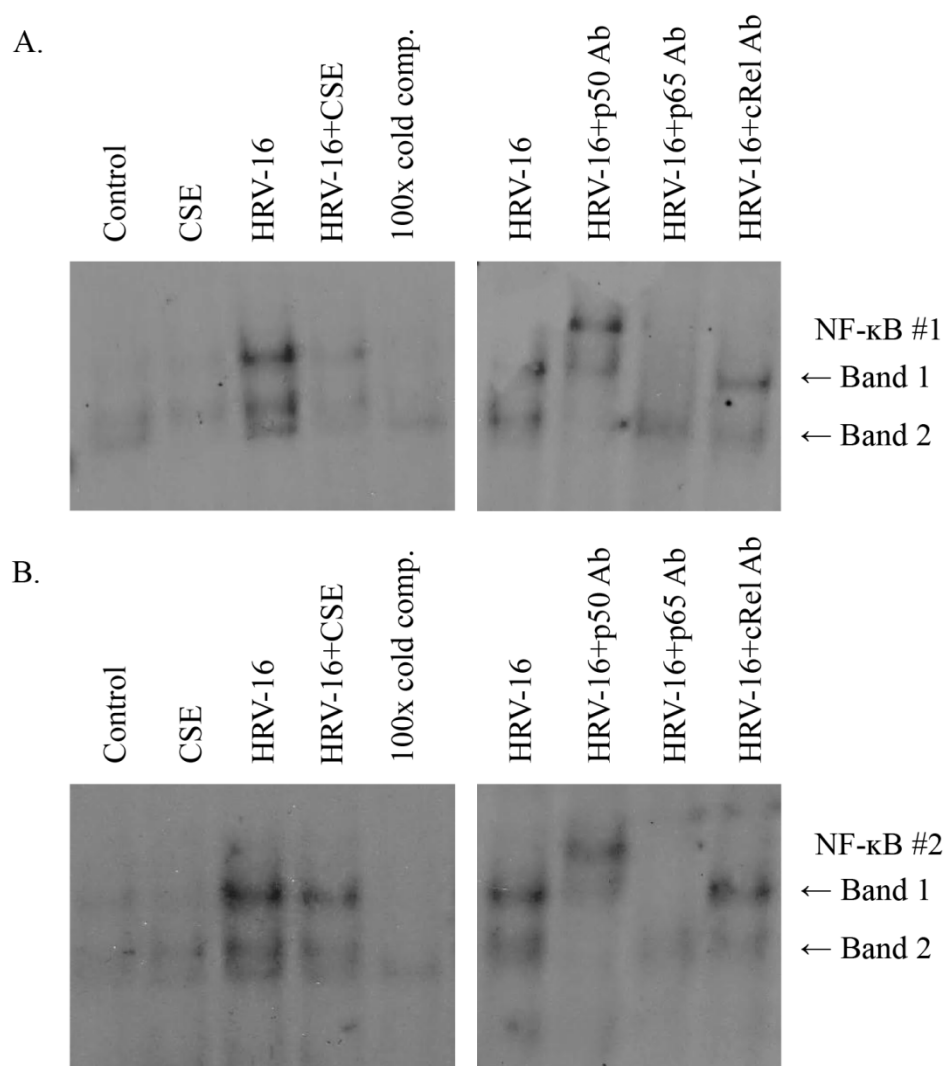


**Figure 5.6: CSE inhibits HRV-16-induced NF- $\kappa$ B translocation/binding to the CXCL10-specific NF- $\kappa$ B recognition sequences.**

HBE cells were treated with control medium, CSE alone, HRV-16 alone or the combination for 3 h prior to nuclear protein extracts being prepared. EMSA (left) and supershift (right) results are presented for nuclear protein extracts incubated with either radiolabelled CXCL10-specific  $\kappa$ B1 (A) or  $\kappa$ B2 (B) oligonucleotide probes. For supershifts, nuclear extracts were incubated for 2 h with antibodies to p50, p65 or cRel NF- $\kappa$ B subunits. 100x cold comp. indicates the presence of 100 fold excess un-radiolabelled oligonucleotide probe. Data are representative of 2 or 3 separate experiments.

Activation of NF- $\kappa$ B requires phosphorylation, ubiquitination and subsequent degradation of I $\kappa$ B $\alpha$ <sup>330</sup>. This occurs via the inhibitory actions of IKK $\beta$  which phosphorylates I $\kappa$ B $\alpha$  leading to its dissociation from the NF- $\kappa$ B complex, ubiquitination of I $\kappa$ B $\alpha$  and degradation by the 26S proteasome. HRV-16-infection resulted in induction of p-I $\kappa$ B $\alpha$  at various early and late time-points (3, 6, and 24 h). This induction was inhibited in the presence of CSE at all time-points studied in HBE cells (**Figure 5.7 A**). An extended time-course in BEAS-2B cells showed similar results (**Figure 5.7 B**).

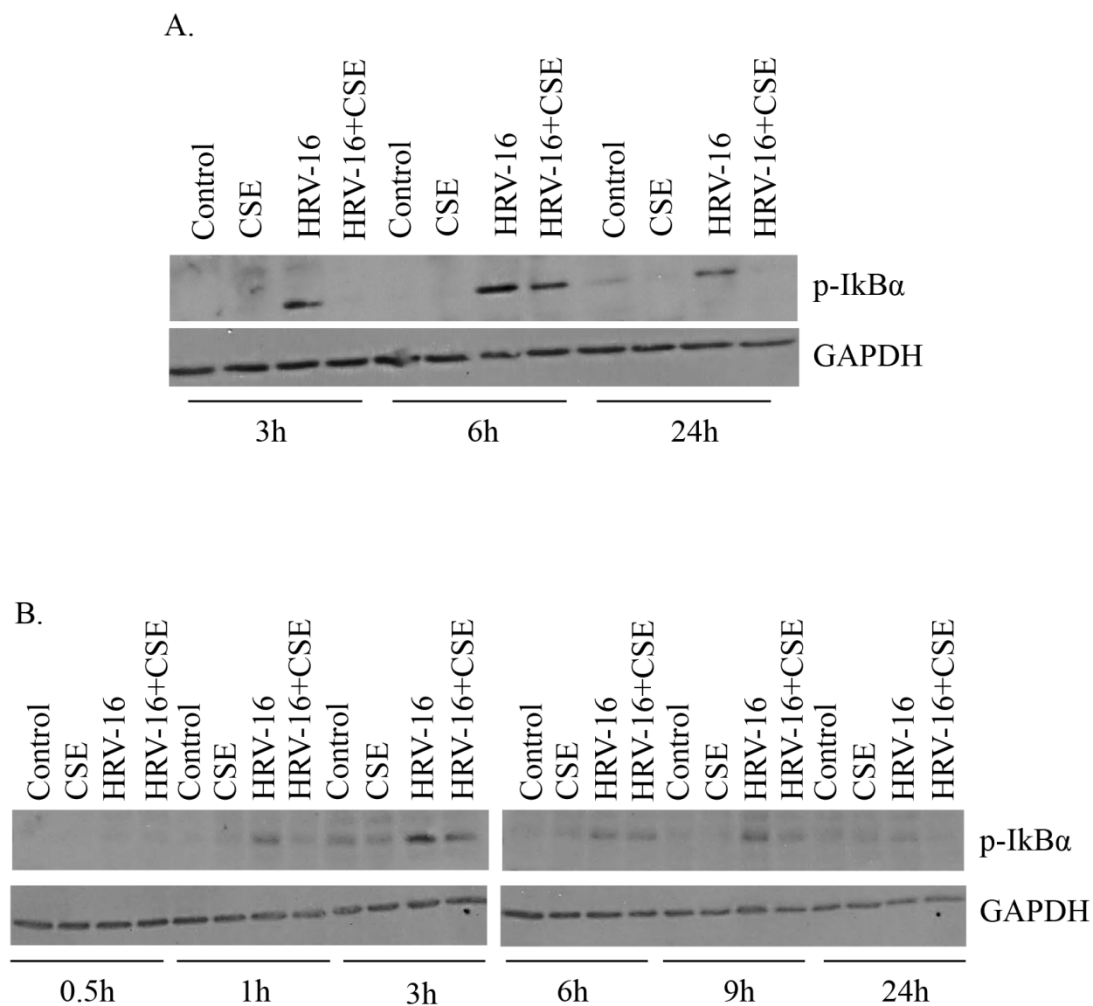


**Figure 5.7: HRV-16-induced phosphorylation of I $\kappa$ B $\alpha$  is inhibited by CSE in airway epithelial cells.**

Whole cell lysates were harvested from HBE (A) and BEAS-2B (B) cells treated with control medium, CSE alone, HRV-16 alone or the combination at various time-points and analyzed via immunoblotting. Membranes were probed with a specific p-I $\kappa$ B $\alpha$  antibody, then were stripped and re-probed with antibody to GAPDH to ensure equal protein loading. Data are representative of 3 separate experiments.

#### ***5.3.4 Inhibition of HRV-16-induced CXCL10 by CSE is partially dependent on inhibition of IRF-1***

As previously reported in airway epithelial cells<sup>297</sup>, EMSA analysis utilizing a radiolabelled oligonucleotide corresponding to the ISRE recognition sequence in the CXCL10 promoter showed that HRV-16-induced formation of three complexes, represented by two strong bands (band 1 and 3) and one weaker band (band 2) at 6 h post treatment (**Figure 5.8**). As has also been previously reported, antibodies to IRF-1 shift the upper band, which was confirmed (**Figure 5.8 (right panel)**), while siRNA targeted to IRF-1 prevents formation of all 3 bands<sup>297,298</sup>. When HBE cells were treated with HRV-16 in combination with CSE, the intensity of all three bands was considerably reduced (**Figure 5.8**).

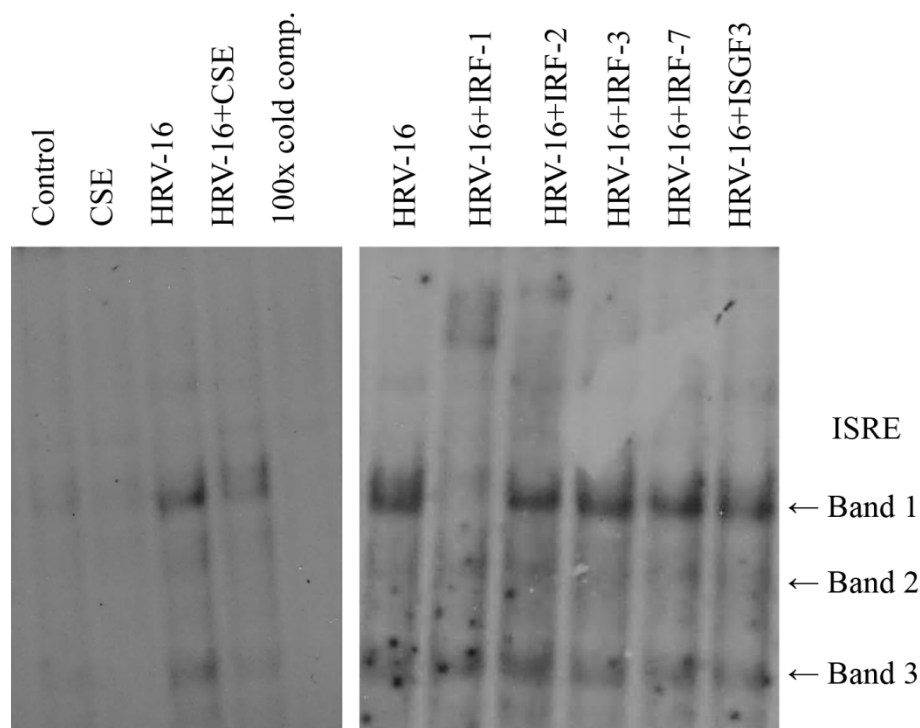


**Figure 5.8: CSE inhibits HRV-induced IRF-1 translocation/binding to the CXCL10-specific ISRE recognition sequence.**

HBE cells were treated with control medium, CSE alone, HRV-16 alone or the combination for 6 h prior to nuclear protein extracts being prepared. EMSA (left) and supershift (right) results are presented for nuclear protein extracts incubated with radiolabelled CXCL10-specific ISRE oligonucleotide probe. For supershifts, nuclear extracts were first incubated for 2 h hours with antibodies to IRF-1, IRF-2, IRF-3, IRF-7 or ISGF3. 100x cold comp. indicates the presence of 100 fold excess un-radiolabelled oligonucleotide probe. Data are representative of 3 separate experiments.

The gene microarray study previously mentioned in **Chapter 3** showed that IRF-1 gene was significantly induced by HRV-16 alone (**Figure 5.9 A**). CSE alone did not enhance the expression of IRF-1 but significantly decreased HRV-16-induced IRF-1 expression to 2.6 fold compared to medium control (**Figure 5.9 A**). The gene microarray results were verified using an additional 7 individual HBE donors for IRF-1 expression using real time RT-PCR (**Figure 5.9 B**). The trend assessed by real time RT-PCR was the

same compared to the gene microarray results: CXCL10 mRNA was enhanced by HRV-16 and HRV-16-induced CXCL10 was significantly inhibited by CSE. HRV-16-infection resulted in induction of IRF-1 protein at 6 and 24 h post infection in HBE cells and this was also inhibited in the presence of CSE (**Figure 5.9 C**).

It has been reported that IRF-2 can inhibit transcriptional activation of genes caused by IRF-1 via competition for binding sites<sup>341</sup>, so it was examined whether CSE alters IRF-2 expression. Although there was a low basal expression level of IRF-2 protein in HBE cells, this was not noticeably altered in the presence of CSE alone, HRV-16 alone, or the combination of these two stimuli at the time-points that were studied (**Figure 5.10**).

A.

Gene	Description	Fold increase by HRV-16	Fold increase by HRV-16+CSE
IRF-1	Interferon regulatory factor-1	4.5	2.6

B.

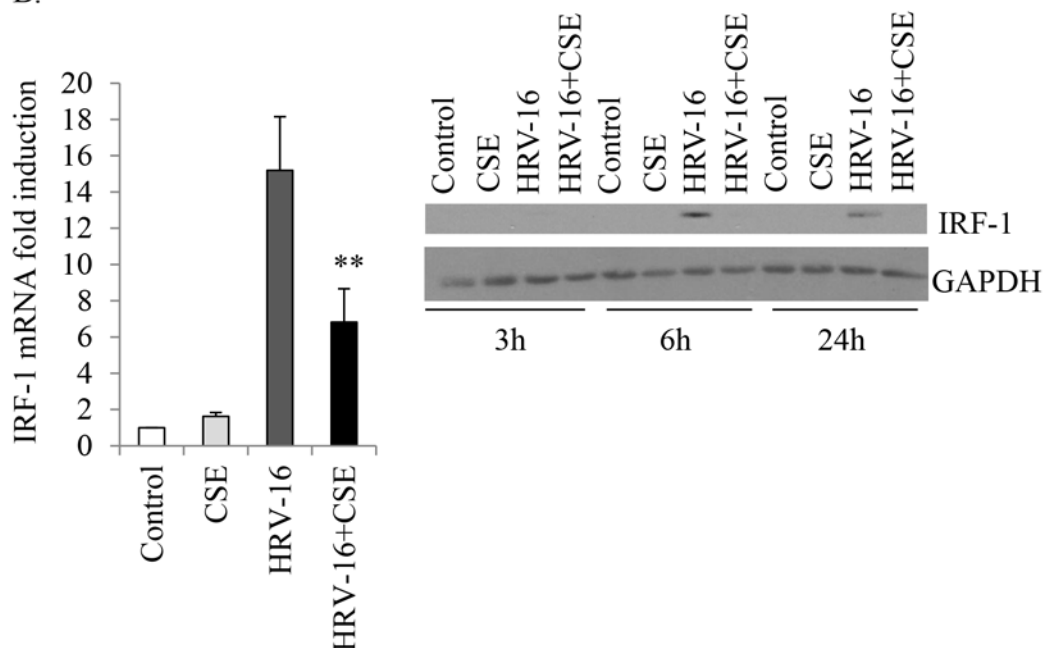


**Figure 5.9: CSE inhibits HRV-16-induced IRF-1 expression in airway epithelial cells.**

HBE cells were treated with either control medium, CSE, HRV-16 or HRV-16+CSE. Cellular RNA was harvested at 24 h and analyzed via gene microarray (A; n=4) or real time RT-PCR (B; n=7). Data are presented as mean  $\pm$  SEM. Asterisks denote significant inhibition with HRV-16+CSE compared to HRV-16 alone where \*\* p<0.01. Whole cells lysates from cells treated with the same stimuli were harvested at various time-points and analyzed via immunoblotting (C; representative of 3 separate experiments). Membranes were probed with a specific IRF-1 antibody, then were subsequently stripped and re-probed with an antibody to GAPDH to ensure equal protein loading.

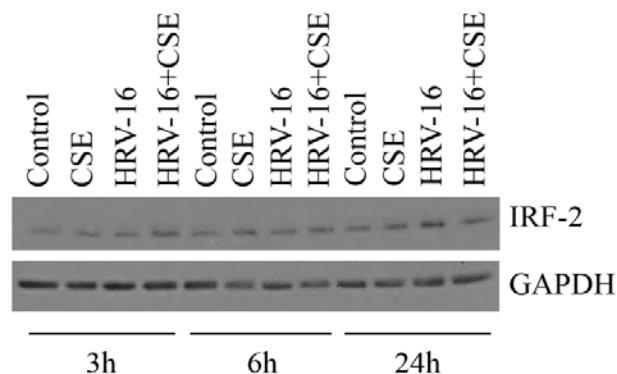


**Figure 5.10: IRF-2 expression is not altered by CSE, HRV-16 or the combination in airway epithelial cells.**

HBE cells were treated with either control medium, CSE, HRV-16 or HRV-16+CSE. Whole cells lysates were harvested at various time-points and analyzed via immunoblotting. Membranes were probed with a specific IRF-2 antibody, then were subsequently stripped and re-probed with an antibody to GAPDH to ensure equal protein loading. Data are representative of 3 separate experiments.

### ***5.3.5 Induction of HRV-16-induced CXCL10 and its inhibition by CSE is partially dependent on STAT-1***

It has previously been reported that truncation of the 972 bp full length CXCL10 promoter to 376 bp results in partial loss of HRV-16-induced activation<sup>259</sup>. This implies that transcription factor recognition sequences between 279 and 875 bp upstream of the transcriptional start site may play a role in HRV-16-induced promoter activation, but these sites were not identified. Here it was confirmed that HRV-16-induced activation the truncated 376 bp CXCL10 promoter was significantly decreased compared to the 972 bp CXCL10 promoter (**Figure 5.11**). HRV-induced activation of the truncated CXCL10 promoter by HRV-16 was still reduced by CSE, although this did not reach statistical significance.

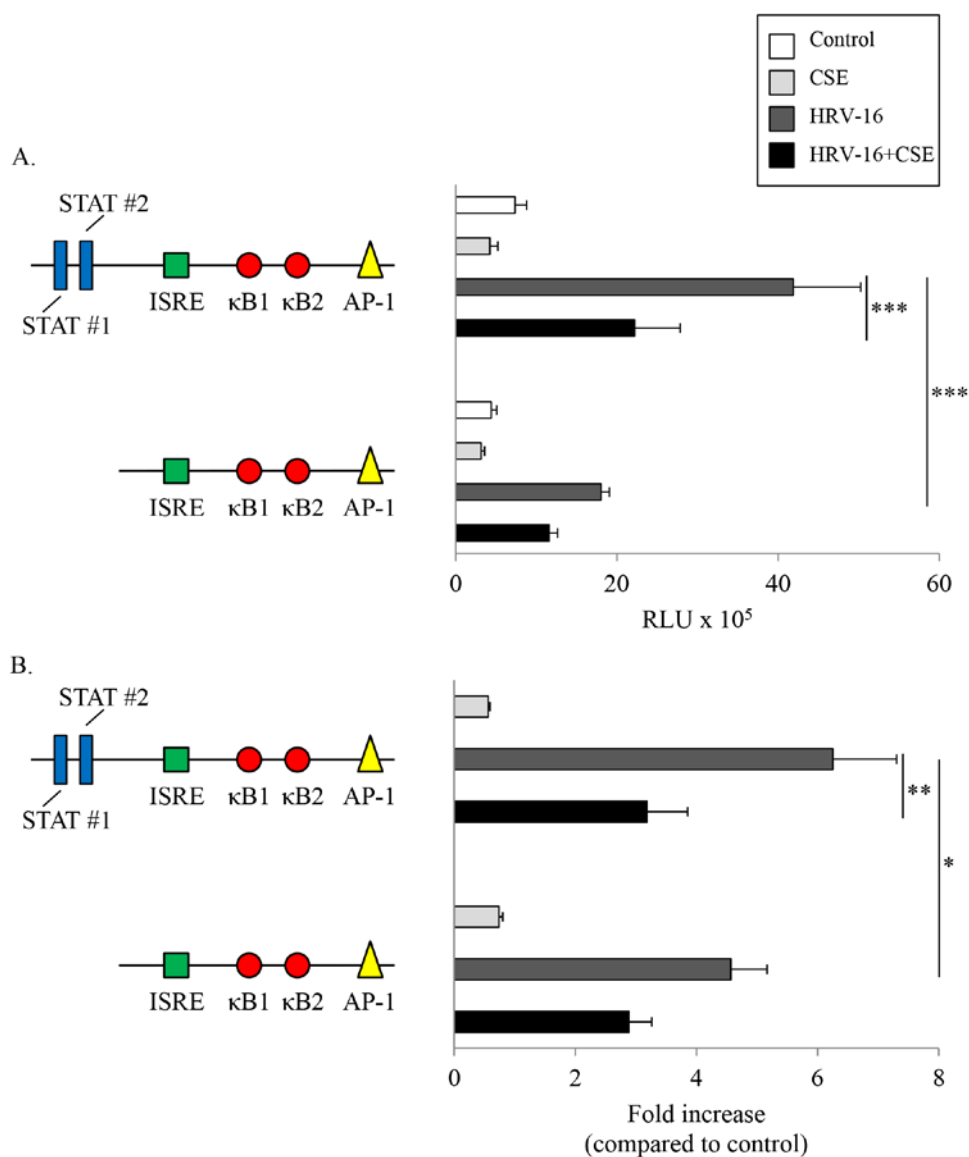


**Figure 5.11: Effects of CXCL10 promoter truncation on activation by HRV-16 in airway epithelial cells.**

BEAS-2B cells that were transiently transfected with the full-length (972 bp) or truncated (392 bp) CXCL10 promoter were then treated with control medium, CSE alone, HRV-16 alone or the combination for 24 h. Cell lysates were assessed for firefly luciferase activity and data are presented as both relative light units (RLU; A) and fold induction as compared to cells treated with only control medium for each respective promoter variant (B). Data are expressed as mean  $\pm$  SEM (n=7). Asterisks denote a significant difference as indicated (\* $p \leq 0.05$ , \*\*  $p < 0.01$  and \*\*\*  $p < 0.001$ ).

Individual mutations in either of the putative CCAAT/enhancer-binding protein (C/EBP)- $\beta$  recognition sequences did not decrease either HRV-16-induced activation of the 972 bp promoter, or alter the inhibition of this response by CSE (data not shown). Mutation of either of the two putative STAT recognition sequences did appear to affect CXCL10 promoter activation when the data was expressed in terms of fold induction. When the data were expressed as raw RLU (**Figure 5.12 A**), rather than fold induction (**Figure 5.12 B**), in contrast to all of the other mutations performed, mutations in the STAT sites affected basal promoter drive (Wild type;  $58,684 \pm 21,158$ ,  $\Delta$ STAT #1;  $11,674 \pm 4,964$ ,  $\Delta$ STAT #2;  $9,049 \pm 1,675$ ). In terms of absolute RLU, mutation of either STAT site led to a marked, significantly reduced level of HRV-16-induced activation of the CXCL10 promoter, with no further inhibition in the presence of CSE.

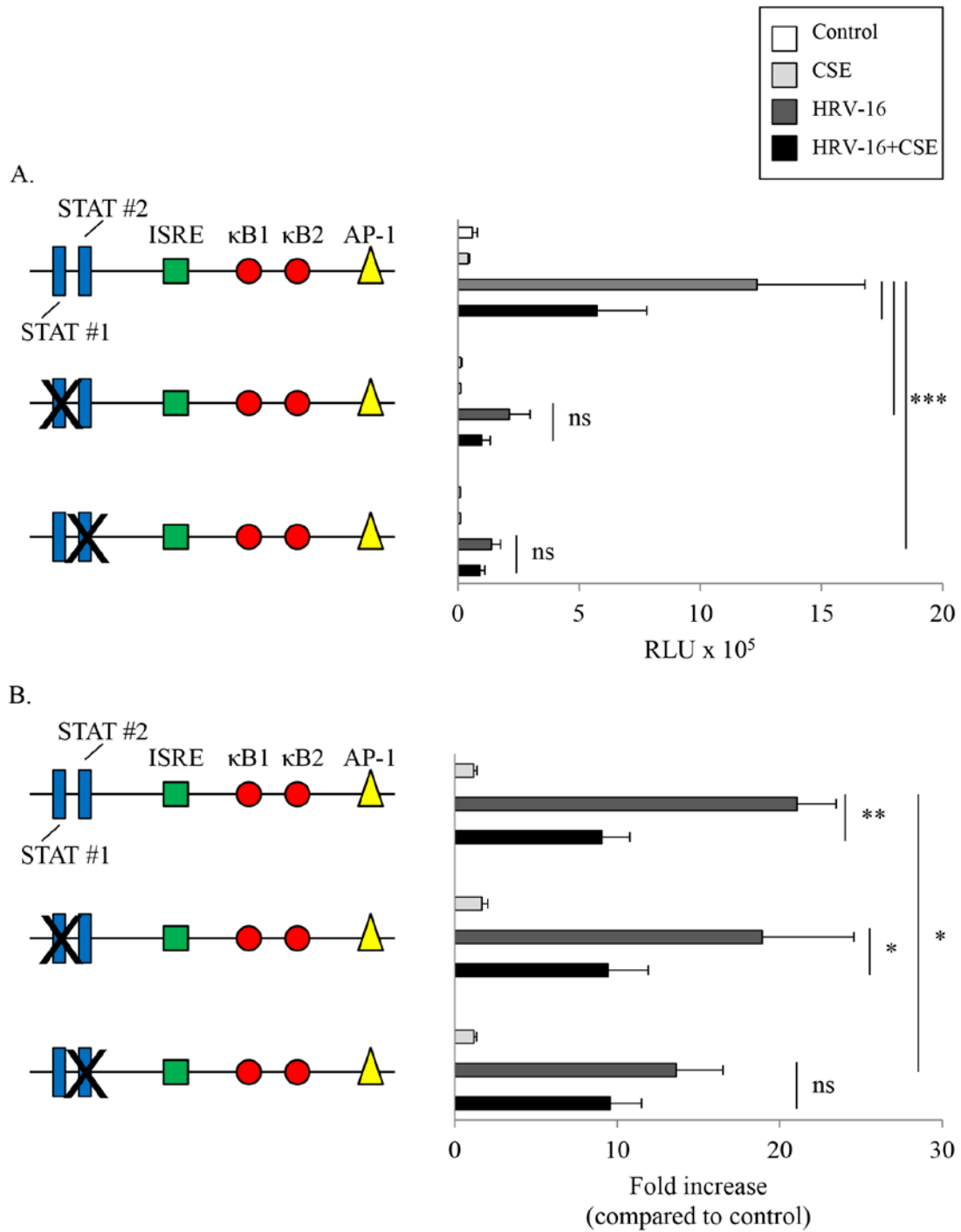


**Figure 5.12: Effects of STAT site point mutations on CXCL10 promoter activation in airway epithelial cells.**

BEAS-2B cells transiently transfected with the wild type CXCL10 promoter or the CXCL10 promoter with point mutations in either of two putative STAT transcription factor binding sites were then treated with control medium, CSE alone, HRV-16 alone or the combination for 24 h. Cell lysates were assessed for firefly luciferase activity and data are presented as both relative light units (RLU; A) and fold induction as compared to cells treated with only medium control for each respective promoter variant (B). Data are expressed as mean  $\pm$  SEM (n=8). Asterisks denote a significant difference as indicated (\* $p \leq 0.05$ , \*\*  $p < 0.01$  and \*\*\*  $p < 0.001$ ).

Because the core sequences of the two STAT transcription factor binding sites in the CXCL10 promoter were identical, EMSA was performed using a single radiolabelled oligonucleotide corresponding to these sequences. Initial time course studies in HBE cells showed HRV-16-induced formation of a single binding complex beginning to form as early as 3 or 6 h and persisting to 9 h in nuclear extracts from HBE cell donors, although some variability between donors in terms of timing of complex formation was observed. Further analysis at the 6 h time-point showed HRV induction of a single band that was completely abrogated in the presence of CSE (**Figure 5.13 A (left panel)**). Using antibodies to various STAT proteins, complex formation was inhibited by antibodies to STAT-1 and STAT-2, with supershifted complexes retained in the loading well (**Figure 5.13 A (right panel)**). An antibody to STAT-3 had no effect. Supershift antibodies were verified to pick up each respective STAT protein at the appropriate molecular weight using immunoblotting (**Figure 5.13 B**).

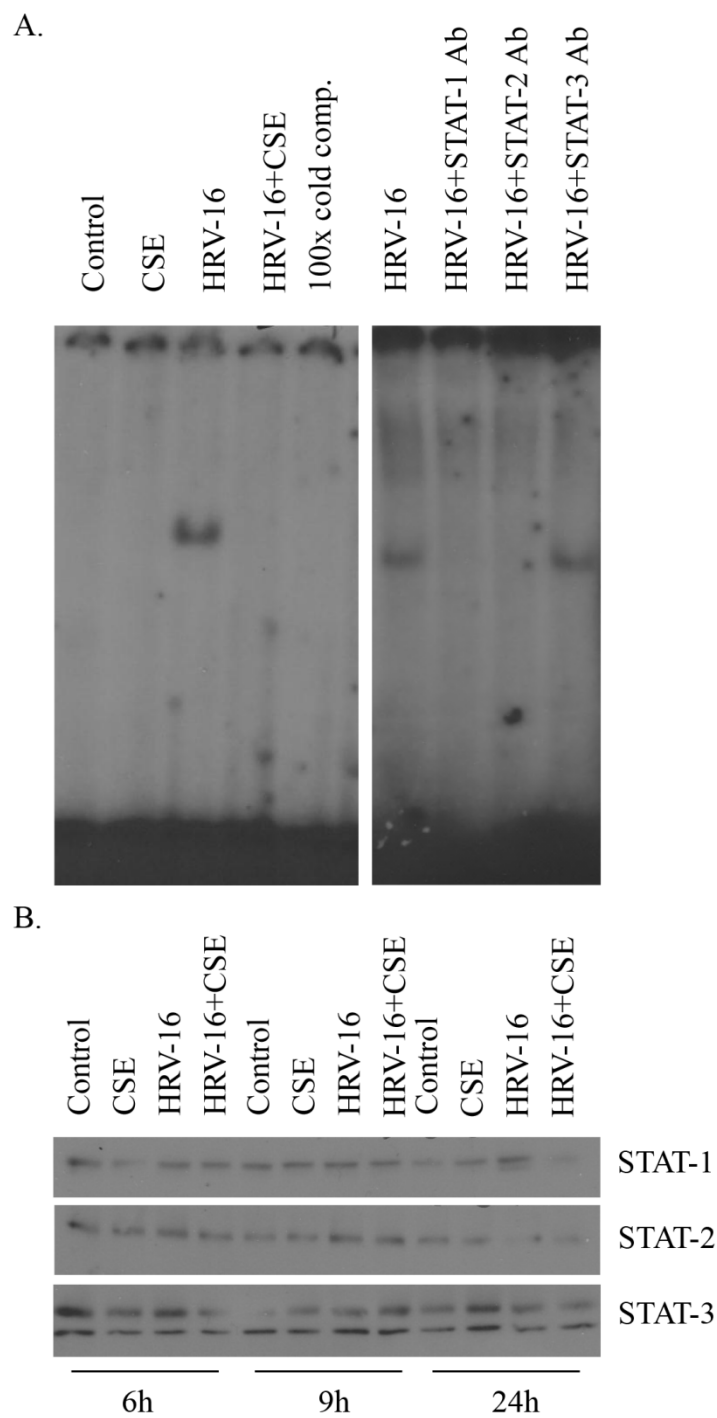


**Figure 5.13: CSE inhibits HRV-induced transcription factor translocation/binding to the CXCL10-specific STAT recognition sequence.**

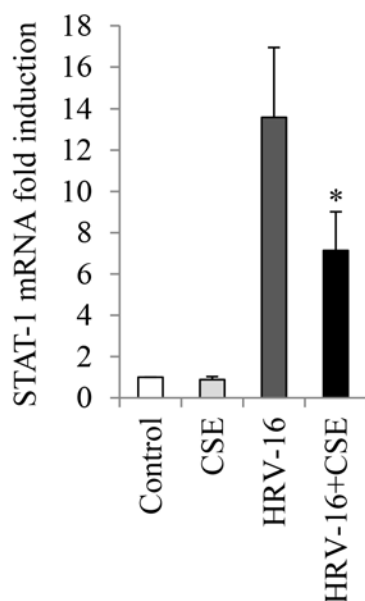
A: HBE cells were treated with medium control, CSE alone, HRV-16 alone, or the combination for 6 h prior to nuclear protein extracts being prepared. EMSA (left) and supershift (right) results are presented for nuclear protein extracts incubated with a radiolabelled CXCL10-specific STAT oligonucleotide probe. For supershift assays, nuclear extracts were first incubated for 2 h with antibodies to STAT-1, STAT-2 or STAT-3 prior to EMSA. The lane labelled 100x cold comp. contained 100 fold excess un-radiolabelled oligonucleotide probe. EMSA and supershift data are representative of 2 or 3 separate experiments. B: EMSA supershift antibodies were verified via immunoblotting using HBE cell lysates treated with medium control, CSE alone, HRV-16 alone, or the combination for 6, 9 and 24h.

Further analyses by western blotting were unable to detect activated STAT-2 (p-STAT-2) in HRV-16-infected HBE cells using two different antibodies, while total STAT-2 was constitutively expressed and unchanged, regardless of treatment (**Figure 5.13 B** and data not shown). Additionally, STAT-2 gene expression was not significantly induced by HRV-16 in the gene array study. By contrast, STAT-1 gene expression was readily induced by HRV-16 in the gene array study (**Figure 5.14 A**) and this was confirmed by real-time RT-PCR with an additional 6 individual HBE donors (**Figure 5.14 B**). In both cases, HRV-16-induced gene expression of STAT-1 was significantly suppressed in the presence of CSE. Moreover, HRV-16-induced phosphorylation of STAT-1 as early as 9 h post-treatment, and activation at both 9 and 24 h post infection was inhibited in the presence of CSE (**Figure 5.15 C**). Additionally, both basal expression and HRV-16-induced expression of total STAT-1 was reduced by CSE at 24 h (**Figure 5.15 C**).

A.

Gene	Description	Fold increase by HRV-16	Fold increase by HRV-16+CSE
STAT-1	Signal Transducer and Activator of Transcription-1	16	8.3

B.



C.

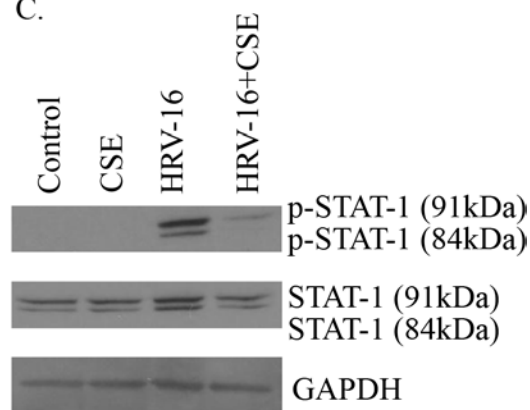


**Figure 5.14: CSE inhibits HRV-16-induced p-STAT-1 in airway epithelial cells.**

HBE cells were treated with either control medium, CSE, HRV-16 or HRV-16+CSE. Cellular RNA was harvested at 24 h and analyzed via gene microarray (A; n=4) or real time RT-PCR (B; n=6). Data are presented as mean  $\pm$  SEM. Asterisks denote significant inhibition with HRV-16+CSE compared to HRV-16 alone where \*\*  $p < 0.01$ . Whole cells lysates were harvested at 24 h post-treatment and analyzed via immunoblotting (C; representative of 3 separate experiments). Membranes were probed with a specific p-STAT-1 antibody, then were subsequently stripped and re-probed with an antibody to total STAT-1, stripped again and re-probed with an antibody to GAPDH to ensure equal protein loading. Data presented in this figure have been published<sup>132</sup>.

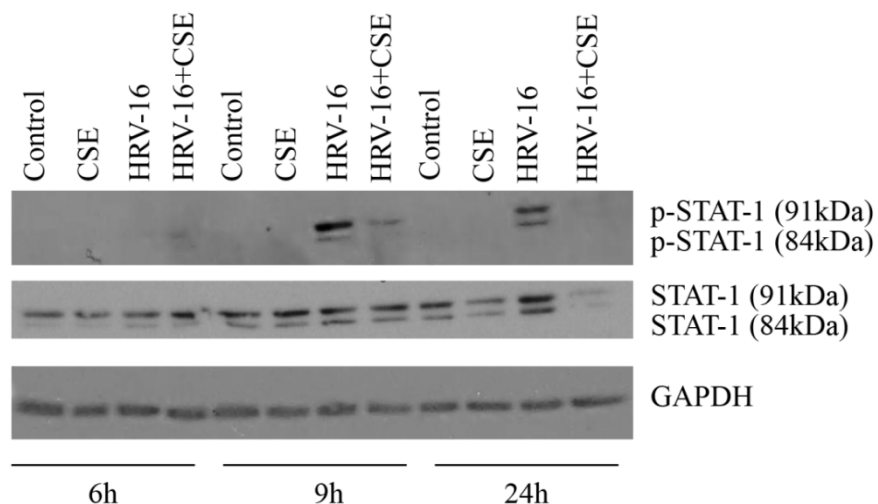


**Figure 5.15: HRV-16 induces p-STAT-1 as early as 9 h post-treatment and this induction is inhibited in the presence of CSE in airway epithelial cells.**

HBE cells were treated with either control medium, CSE, HRV-16 or HRV-16+CSE and whole cells lysates were harvested at various time-points post-treatment and analyzed via immunoblotting. Membranes were probed with a specific p-STAT-1 antibody, then were subsequently stripped and re-probed with an antibody to total STAT-1, stripped again and re-probed with an antibody to GAPDH to ensure equal protein loading. Data are representative of 3 separate experiments.

Evidence that activation of the STAT pathway plays a functional role in HRV-16-induced CXCL10 expression was obtained by showing that a selective JAK inhibitor caused a concentration-dependent inhibition of HRV-16-induced CXCL10 protein release (**Figure 5.16**). Ten-fold dilutions in the range of 1000-0.1 nM were chosen because this particular JAK inhibitor displays potent inhibitory activity against members of the JAK family at between 1-15 nM and inhibits other kinases only at much higher concentrations.

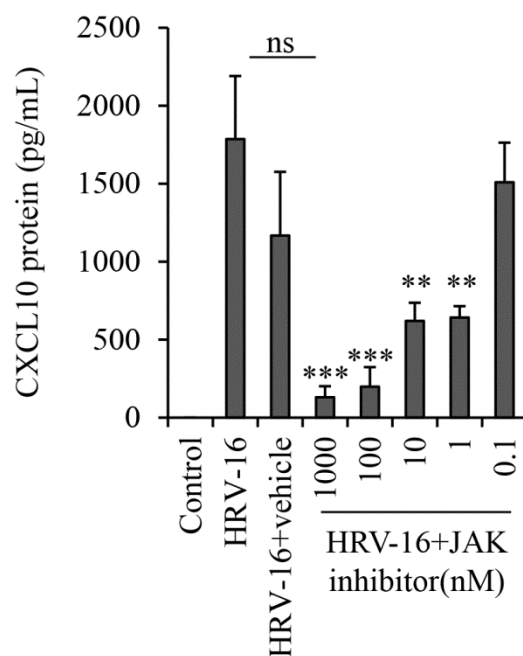
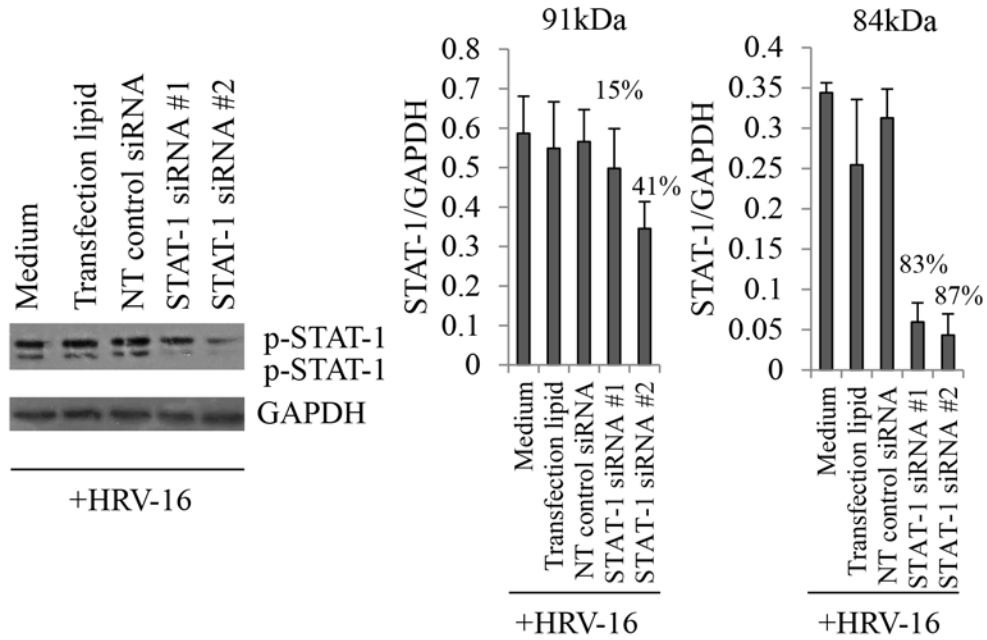


**Figure 5.16: HRV-16-induced CXCL10 is concentration-dependently inhibited in the presence of a specific JAK inhibitor.**

HBE cells were treated with control medium, HRV-16 or HRV-16+various concentrations of the JAK inhibitor (10 fold dilutions). Supernatants were harvested at 24 h post-treatment and analyzed via ELISA. Data are presented as mean  $\pm$  SEM (n=3). Asterisks denote a significant difference compared to HRV-16 alone (\*\* p<0.01 and \*\*\* p<0.001). Vehicle denotes the presence of the JAK inhibitor diluent alone (DMSO).

As another approach to evaluating the role of STAT-1 in the induction of HRV-16-induced CXCL10, siRNA studies using duplexes targeting STAT-1 were performed. Unfortunately, although the siRNAs targeting STAT-1 did significantly knock-down the 84 kDa isoform of STAT-1 they did not effectively knock-down the 91 kDa isoform (**Figure 5.17 A**). With only sufficient knock-down of the 84 kDa isoform there was no significant impact on the expression of HRV-16-induced CXCL10 (**Figure 5.17 B**).

A.



B.

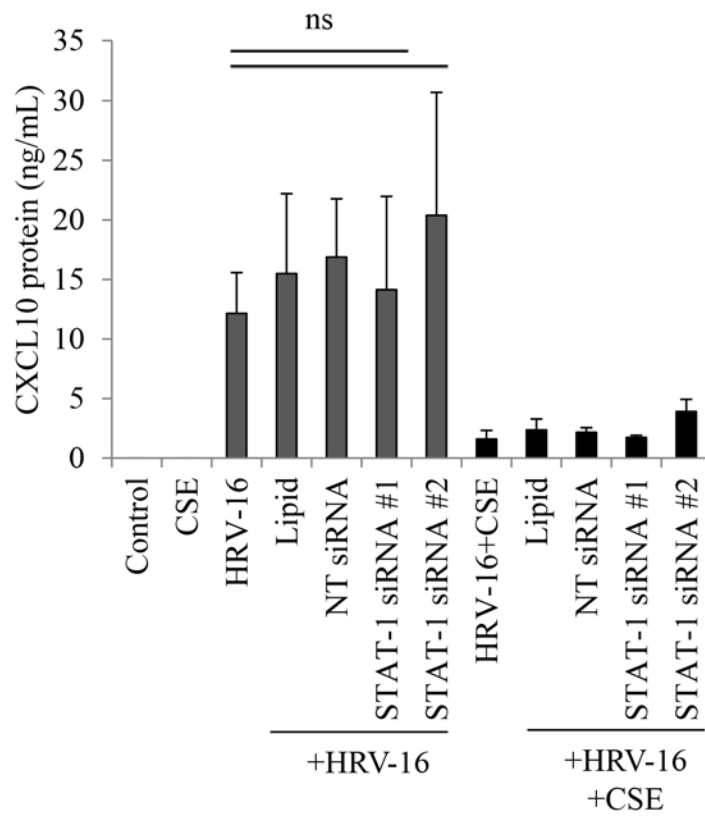


**Figure 5.17: Effects of STAT-1-targeting siRNA on p-STAT-1 knock-down and CXCL10 protein expression in airway epithelial cells.**

HBE cells were treated for 24 h prior to harvesting cell supernatants for analysis with ELISA and whole cell lysates for analysis with immunoblotting. To determine the level of p-STAT-1 protein knock-down membranes were probed with a specific p-STAT-1 antibody, then were subsequently stripped and re-probed with an antibody to GAPDH to ensure equal protein loading (A, left panel; representative of 3 separate experiments). Densitometry analysis with % knock-down relative to HRV-16 alone is shown on the right panel (A; n=3). Matching supernatants were analyzed for CXCL10 protein (B; n=3). Data are presented as mean  $\pm$  SEM. ns = not significant. NT denotes non-targeting control siRNA.

**5.3.6 ChIP of HRV-induced CXCL10 with NF- $\kappa$ B and IRF-1**

In order to determine whether CSE decreased *in vitro* endogenous association of HRV-induced NF- $\kappa$ B and IRF-1 to their respective transcription factor binding sites in the CXCL10 promoter, ChIP was performed using p65 and IRF-1 antibodies following stimulation of cells with either control medium, HRV-16 alone, CSE alone or HRV-16+CSE for 6 h. The 6 h time-point was used to correlate these data with previously generated EMSA data. Initial experiments focused on optimizing fixing of protein-DNA complexes in cells, extracting nuclei and shearing of chromatin to optimally sized fragments (200-1500 bp) (**Figure 5.18 A**). In order to establish whether the protocol was effective, initial ChIP experiments were performed using a RNA polymerase II antibody and GAPDH conventional PCR primers, which would provide a robust signal if the technique was working successfully. Preliminary results indicated that the optimized ChIP procedure was working using both BEAS-2B and HBE cells (**Figure 5.18 B**). Following ChIP with p65 and IRF-1, specifically designed CXCL10 primers, corresponding to relevant areas where each transcription factor would bind in the CXCL10 promoter, were

used to determine if there was a difference in binding association of HRV-induced p65 and IRF-1 following treatment with CSE. Unfortunately, the CXCL10 signal was either too low to be detected by real-time PCR or the antibodies used in ChIP were inadequate.

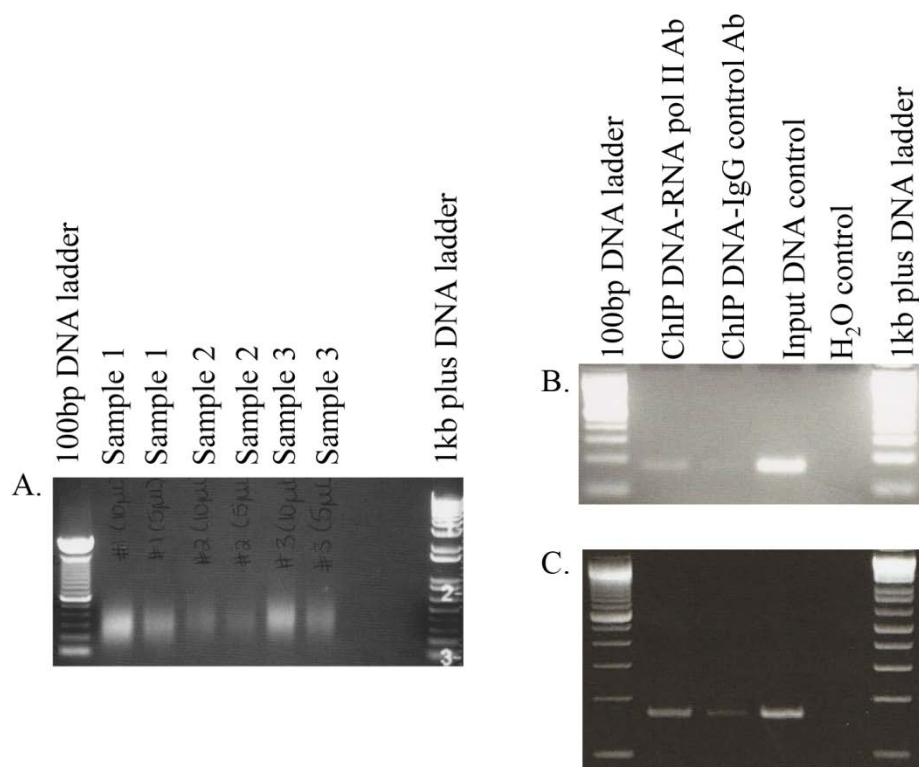


**Figure 5.18: ChIP Optimization.**

Agarose gel of sheared BEAS-2B cell DNA to be used for ChIP (A). Sheared DNA from BEAS-2B (B) and HBE (C) was subject to ChIP with either an RNA polymerase II antibody or an IgG control antibody and analyzed for GAPDH expression using specific primers in conjunction with conventional PCR. Input DNA that was not subject to ChIP and water alone was used as positive and negative controls respectively.

### ***5.3.7 Induction of HRV-16-induced CXCL10 and its inhibition by CSE is partially dependent on MDA5***

Up to this point, factors regulating transcriptional activation directly upstream of the CXCL10 promoter were examined. It is possible that other factors further upstream from NF- $\kappa$ B, IRF-1 and STAT-1 could be influencing the induction of CXCL10 by HRV-16 and the inhibition of HRV-16-induced CXCL10 by CSE. As the signalling pathways are complex directly upstream from each of these transcription factors, and not necessarily overlapping or fully defined, an analysis using the ‘top-down’ (starting with the initiating stimulus and working down the signalling pathway) as opposed to the ‘bottom-up’ (starting from the transcription factor and working up the signalling pathway) approach was used. HRV-16 binds to its cognate receptor, is internalized and begins replication. In **Chapter 4** it was shown that CSE did not markedly affect ICAM-1 expression and, more importantly, CSE did not inhibit ICAM-1 expression. Additionally, it was demonstrated that CSE did not alter HRV-16 titre in the relevant time frame to correlate with the reduction of downstream HRV-16-induced signalling.

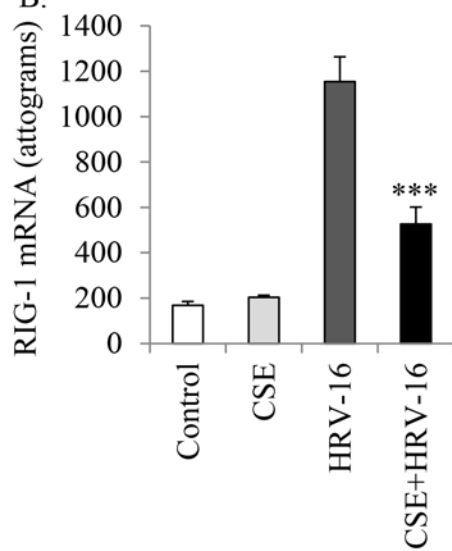
The HRV replication stage utilizes a dsRNA intermediate that can be recognized by the immune system via the PRR viral sensors TLR3, RIG-I and MDA5. Therefore, an analysis of the effects of CSE on HRV-16-induced PRR was performed. Members of the Proud/Leigh laboratory have been unable to detect either constitutive or HRV-16-induced protein expression of TLR3 in primary human bronchial epithelial cells using an antibody that readily detects recombinant TLR3 (unpublished data). Both RIG-I and MDA5 gene expression were significantly induced by HRV-16 in the gene array study (**Figure 5.19 A**)

and suppressed in the presence of CSE. These data were confirmed by real-time RT-PCR (**Figure 5.19 B & D**). RIG-I and MDA5 protein expression were also induced by HRV-16 at 24 h and this was inhibited in the presence of CSE (**Figure 5.19 C & E**). A limited time-course revealed that induction of both of these helicases occurred as early as 9 h post HRV-16 treatment was also inhibited in the presence of CSE (**Figure 5.20 A & B**).

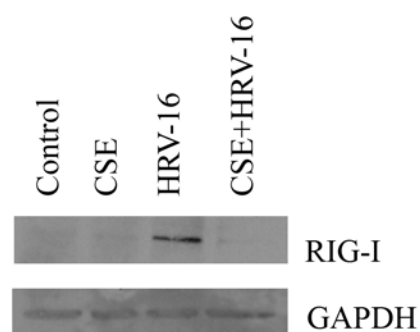
A.

Gene	Fold increase by HRV-16	Fold increase by HRV-16+CSE
RIG-I	32	15.7
MDA5	18	10

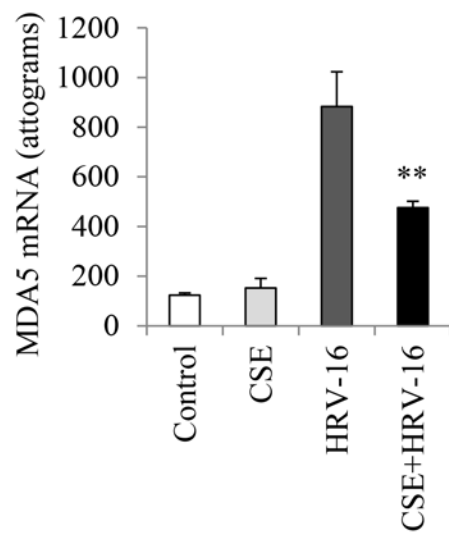
B.



C.



D.



E.

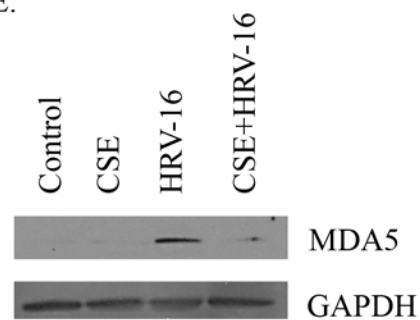


**Figure 5.19: CSE inhibits HRV-16-induced RIG-I and MDA5 in airway epithelial cells.**

HBE cells were treated with either control medium, CSE, HRV-16 or HRV-16+CSE. Cellular RNA was harvested at 24 h and analyzed via gene microarray (A; n=4) or real time RT-PCR (B & D; n=4). Data are presented as mean  $\pm$  SEM. Asterisks denote significant inhibition with HRV-16+CSE compared to HRV-16 alone where \*\*  $p < 0.01$  and \*\*\*  $p < 0.001$ . Whole cells lysates were harvested at 24 h post-treatment and analyzed via immunoblotting (C & E; representative of 4 separate experiments). Membranes were probed with a specific RIG-I or MDA5 antibody, then were subsequently stripped and re-probed with an antibody to GAPDH to ensure equal protein loading. Data presented in this figure have been published<sup>132</sup>.

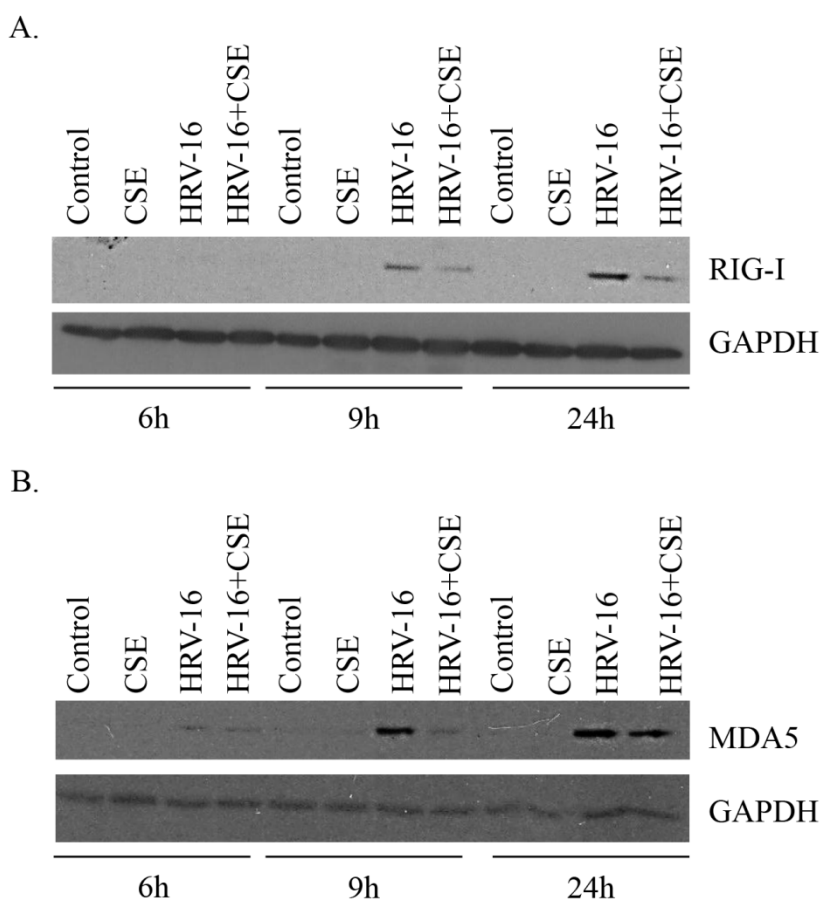


**Figure 5.20: Time-course of RIG-I and MDA5 induction by HRV-16 and inhibition in the presence of CSE in airway epithelial cells.**

BEAS-2B cells were treated with either control medium, CSE, HRV-16 or HRV-16+CSE. Whole cells lysates were harvested at various time-points and analyzed via immunoblotting. Membranes were probed with a specific RIG-I (A) and MDA5 (B) antibody, then were subsequently stripped and re-probed with an antibody to GAPDH to ensure equal protein loading. Data are representative of 3 separate experiments.

In order to determine whether RIG-I and/or MDA5 had a direct role in the expression of HRV-16-induced CXCL10, siRNA studies utilizing duplexes targeting both of these helicases were conducted. Although both RIG-I siRNA duplexes were able to knock-down protein expression of RIG-I, duplex #2 was more effective than duplex #1 (93% knock-down versus 55% knock-down) (**Figure 5.21 A**). CXCL10 protein level determination in matched supernatants following knock-down of RIG-I revealed that HRV-16-induced CXCL10 was not affected following this knock-down even with the more effective siRNA duplex (**Figure 5.21 B**).

Both MDA5 siRNA duplexes were extremely potent in knocking down protein expression of HRV-16-induced MDA5, resulting in almost a complete knock out of the protein (**Figure 5.22 A**). When CXCL10 protein levels were analyzed in matched supernatants, knock-down of HRV-16-induced MDA5 significantly reduced HRV-16-induced CXCL10 protein expression (**Figure 5.22 B**). Collectively, these data suggest that HRV-16-induced MDA5, but not RIG-I, are involved in regulating HRV-16-induced CXCL10 expression and suppression of HRV-16-induced MDA5 by CSE is one of the mechanisms contributing to the inhibition of HRV-16-induced CXCL10 by CSE.

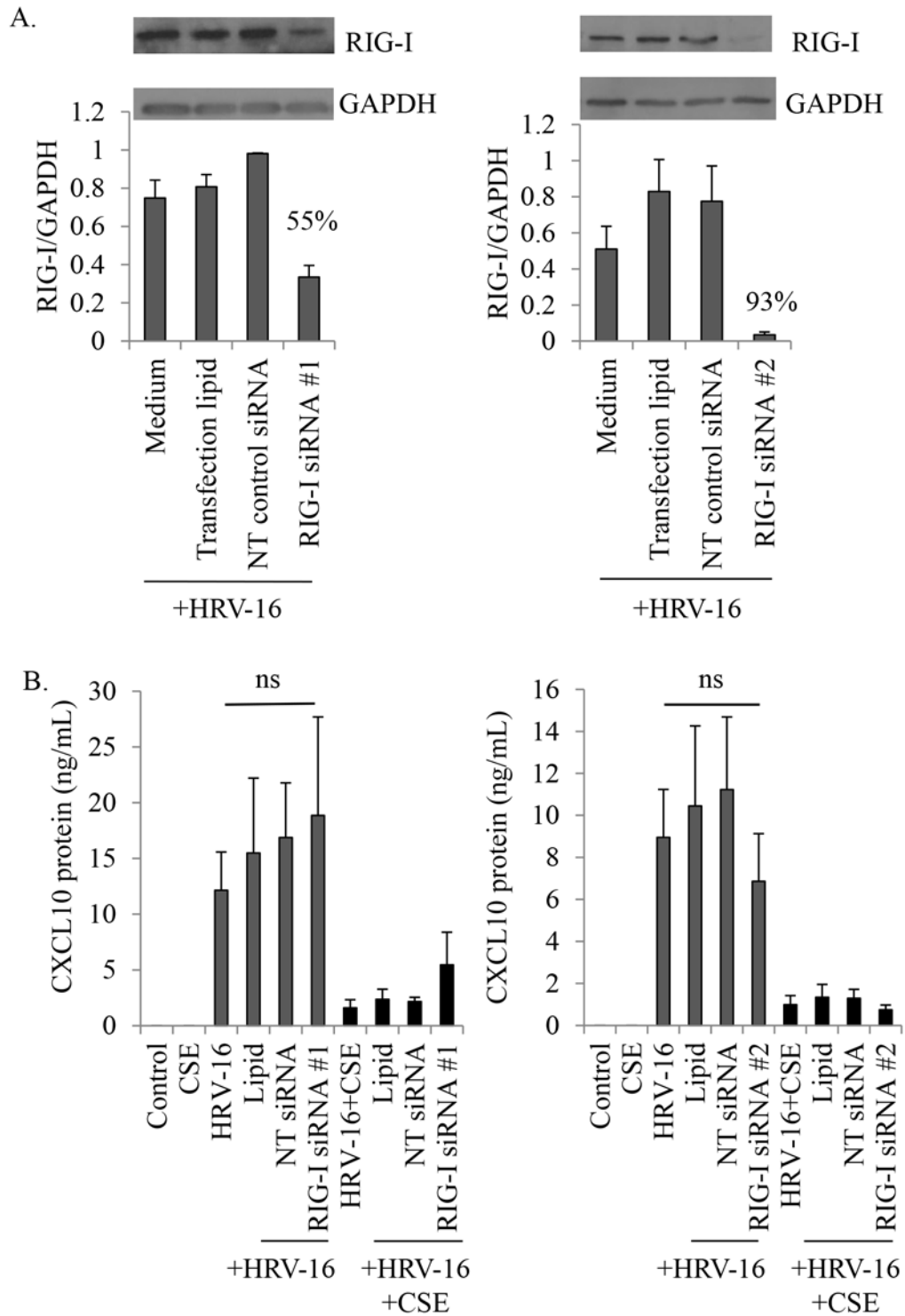


**Figure 5.21: Knock-down of HRV-16-induced RIG-I does not affect CXCL10 protein expression in airway epithelial cells.**

HBE cells were treated for 24 h prior to harvesting cell supernatants for analysis with ELISA and whole cell lysates for analysis with immunoblotting. To determine the level of RIG-I protein knock-down membranes were probed with a specific RIG-I antibody, then were subsequently stripped and re-probed with an antibody to GAPDH to ensure equal protein loading and analyzed by densitometry with % knock-down relative to HRV-16 shown (A; representative of 3 separate experiments and n=3 for densitometry). Matching supernatants were analyzed for CXCL10 protein (B; n=3). Data are presented as mean  $\pm$  SEM. NT denotes non-targeting control siRNA.

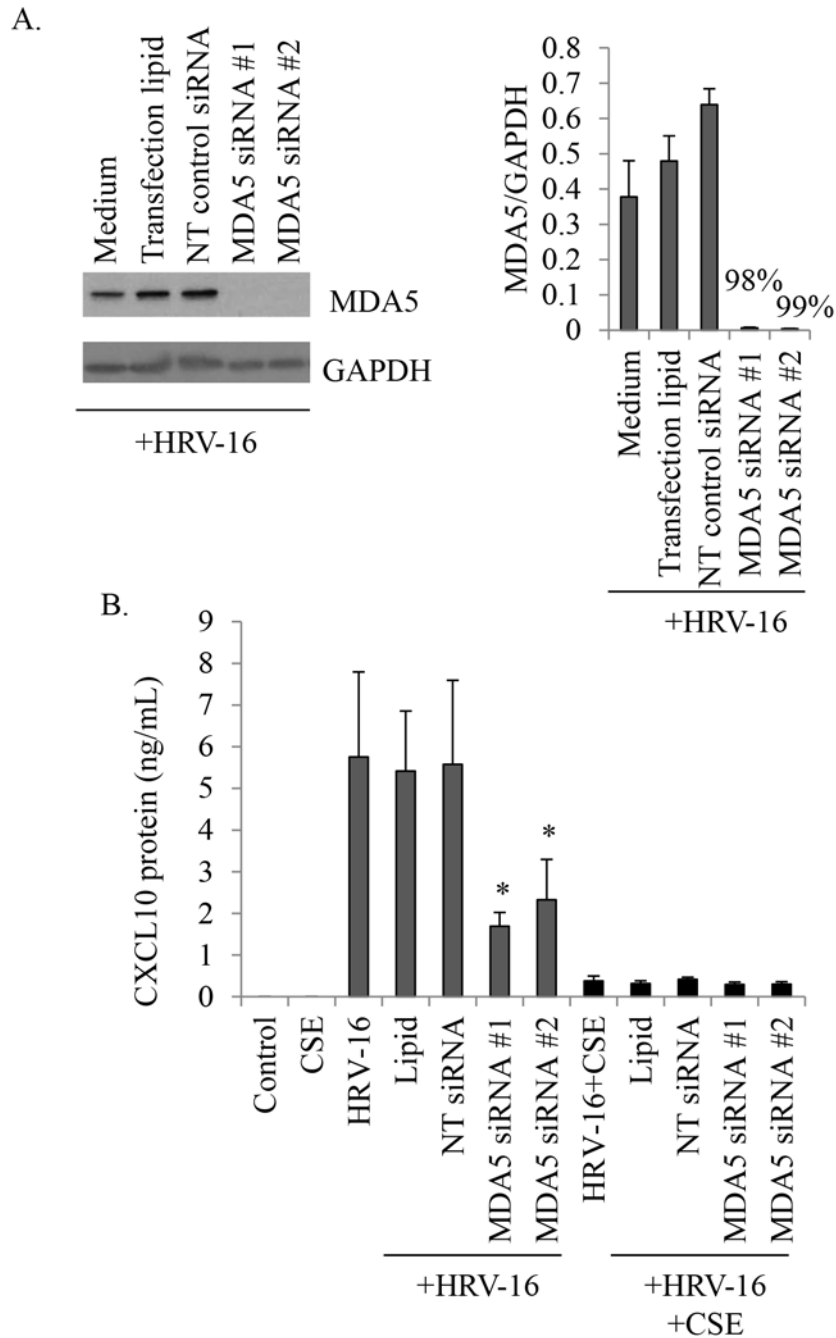


**Figure 5.22: Knock-down of HRV-16-induced MDA5 results in suppression of CXCL10 protein expression in airway epithelial cells.**

HBE cells were treated for 24 h prior to harvesting cell supernatants for analysis with ELISA and whole cell lysates for analysis with immunoblotting. To determine the level of

MDA5 protein knock-down membranes were probed with a specific MDA5 antibody, then were subsequently stripped and re-probed with an antibody to GAPDH to ensure equal protein loading and analyzed by densitometry with % knock-down relative to HRV-16 shown (A; representative of 3 separate experiments and n=3 for densitometry). Matching supernatants were analyzed for CXCL10 protein (B; n=3). Data are presented as mean  $\pm$  SEM. Asterisks denote significant inhibition MDA5 siRNA compared to HRV-16 alone (\*p $\leq$ 0.05). NT denotes non-targeting control siRNA.

### ***5.3.8 Inhibition of HRV-16-induced CXCL10 by CSE is, in part, regulated epigenetically***

To determine if CSE also inhibits HRV-16-induced CXCL10 expression by modifying DNA accessibility around the transcriptional start site of the CXCL10 promoter, the EpiQ™ chromatin analysis kit was used in conjunction with specific primers targeting the region around the TATA box in the CXCL10 promoter. At both 12 h and 24 h after infection of BEAS-2B cells with HRV-16, the chromatin accessibility around the transcriptional start site of the CXCL10 gene was  $58.3 \pm 4\%$  and  $37 \pm 3.9\%$  respectively. An earlier time-point (6 h) was also analyzed but failed to provide a detectable signal following real-time PCR analysis (data not shown). When cells were treated with HRV-16 in combination with CSE, the chromatin accessibility in this region was significantly reduced to  $33.3 \pm 11.6$  and  $23 \pm 6.9\%$  respectively (**Figure 5.23**), suggesting that, in addition to direct inhibition of HRV-16-induced activation of transcription factors, CSE also inhibits HRV-16-induced CXCL10 expression via epigenetic regulation of this gene.

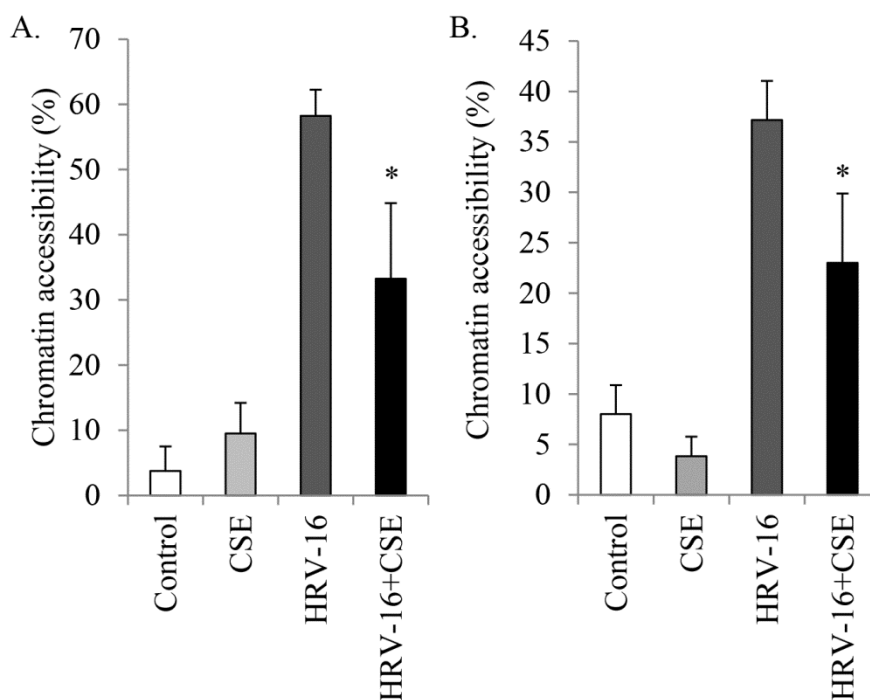


**Figure 5.23: HRV-induced chromatin accessibility of the CXCL10 promoter region is partially suppressed by CSE.**

BEAS-2B cells were treated for 12 h (A; n=4) or 24 h (B; n=6) with medium control, CSE, HRV-16 or the combination. Whole cells were then incubated for an additional hour with EpiQ™ chromatin buffer in the presence or absence of EpiQ™ nuclease. Cellular genomic DNA was then isolated and analyzed with real time PCR using specific primers designed to amplify the CXCL10 promoter region near the transcriptional start site along with reference and control genes provided with the EpiQ™ kit. Data analysis was then performed using the EpiQ™ Chromatin Kit Data Analysis Tool and presented here as % chromatin accessibility. Data are presented as mean ± SEM. Asterisks denote significant inhibition with HRV-16+CSE compared to HRV-16 alone (\*p≤0.05).

#### 5.4 Discussion

The data presented in this chapter investigated the mechanism behind the novel observation first reported in **Chapter 3**, that HRV-induced CXCL10 is inhibited by CSE. The inhibition of HRV-induced CXCL10 by CSE appears to be regulated by multiple mechanisms, as it is demonstrated that CSE-mediated inhibition of HRV-induced CXCL10

expression occurs both via inhibition of HRV-induced activation of multiple transcription factors/signaling pathways and by regulation of chromatin accessibility.

Initially, a CXCL10 promoter-luciferase reporter plasmid was used to determine if CXCL10 induction was being regulated transcriptionally. In agreement with previous literature, HRV treatment alone induced CXCL10 promoter activation<sup>259,297,338</sup>. A novel observation was then subsequently made, that HRV-induced CXCL10 promoter activation was partially inhibited by CSE. It has previously been shown that HRV-induced production of CXCL10 in airway epithelial cells is dependent on viral replication, and that a synthetic dsRNA mimic (poly [I:C]) of the dsRNA stage that is generated during HRV replication, also induces CXCL10 production<sup>259,338</sup>. Here it was also shown that poly [I:C]-induced CXCL10 promoter activation was partially inhibited by CSE. Collectively, these data suggest that CSE inhibits HRV-induced CXCL10, at least in part, through transcriptional mechanisms.

Various approaches were then used in order to determine which transcription factors were playing a role in this inhibition. First, promoter luciferase constructs were generated with mutations in proximal putative transcription factor binding sites shown to be important in HRV-induced CXCL10 promoter activation, including ISRE and two NF- $\kappa$ B binding sites, along with a mutation in the AP-1 binding site which has previously been shown not to be important in HRV-induced CXCL10 promoter activation<sup>259,297</sup>. As previously reported, mutation of the AP-1 site did not alter HRV-induced CXCL10 promoter activation but it also did not alter inhibition by CSE. This suggests that, despite evidence in other systems that cigarette smoke can modulate activation of the AP-1 pathway<sup>455-458</sup>,

CSE-mediated inhibition of HRV-induced CXCL10 expression does not involve such a mechanism. Consistent with earlier studies, mutation of the ISRE site or either of the NF- $\kappa$ B sites completely abrogated HRV-induced activation of the CXCL10 promoter. Thus, it was not possible using standard promoter studies to evaluate if CSE exerts inhibitory effects at these sites, but it seemed feasible that the same sites involved in HRV-induced CXCL10 promoter activation may also be involved in CSE-mediated inhibition. Alternative approaches were used to evaluate this.

Using a combination of tandem repeat reporter constructs, EMSA and western blotting, it was demonstrated that CSE alone did not activate the NF- $\kappa$ B pathway. Rather, CSE clearly inhibited HRV-induced activation of NF- $\kappa$ B, as shown by inhibition of HRV-induced activation of CXCL10-specific tandem repeat NF- $\kappa$ B constructs, inhibition of the phosphorylation of I $\kappa$ B $\alpha$ , and inhibition of HRV-16-induced nuclear translocation and/or binding of NF- $\kappa$ B subunits to both NF- $\kappa$ B transcription factor binding sites in the CXCL10 promoter. In a broader context, these data suggest that the inhibition of HRV-induced NF- $\kappa$ B signalling by CSE may contribute to the down-regulation of numerous HRV-induced genes in airway epithelial cells.

The data here add to a conflicting body of literature regarding activation of the NF- $\kappa$ B pathway in airway epithelial cells following cigarette smoke exposure. Although several studies show that cigarette smoke alone increases the activation of NF- $\kappa$ B in airway epithelial cells<sup>263,433,459-461</sup>, others have reported that NF- $\kappa$ B activation/ translocation/ binding is not affected by cigarette smoke exposure<sup>203,210,455</sup>. Studies have also examined the effects of CSE on NF- $\kappa$ B activation in response to several inflammatory stimuli. In

contrast to the data presented here, cigarette smoke condensate modestly enhanced respiratory syncytial virus nuclear abundance of p65 in A549 cells<sup>210</sup>. Also in contrast, LPS-induced activation of NF- $\kappa$ B in BEAS-2B cells was not affected by CSE<sup>455</sup>. Consistent with the current study, however, cigarette smoke conditioned medium inhibited nuclear translocation of the p65 subunit of NF- $\kappa$ B in BEAS-2B cells exposed to poly [I:C]<sup>203</sup>. Overall, the varying results obtained in these studies could imply that the effects of cigarette smoke on NF- $\kappa$ B activation may be dependent on the initiating stimulus or on the varying methods of cigarette smoke preparation (extract/condensate/conditioned medium), although the use of various airway epithelial cell populations and variable time frames may also contribute to these variations in responses.

In addition to NF- $\kappa$ B, HRV-induced CXCL10 expression is dependent upon activation of IRF-1<sup>298</sup>. Here it was demonstrated, for the first time, that HRV-induced IRF-1 mRNA and protein expression were suppressed in the presence of CSE. Additionally, EMSA results suggest that CSE inhibits HRV-induced nuclear translocation and/or binding of IRF-1 to the ISRE recognition sequence in the CXCL10 promoter. Because IRF-2 has been shown to be a negative regulator of IRF-1<sup>341</sup>, it was determined whether CSE altered IRF-2 expression. Neither HRV nor CSE, either alone or in combination, altered constitutive expression of IRF-2, suggesting that effects of CSE on IRF-1 expression are not mediated via alterations of IRF-2. The demonstration that CSE inhibits HRV-induced IRF-1 expression is consistent with the observation that IFN- $\gamma$ -induced IRF-1 protein expression is reduced in macrophages from smokers as compared to non-smokers<sup>462</sup>.

Although only the proximal ISRE and two NF- $\kappa$ B recognition sequences in the CXCL10 promoter have been directly linked to HRV-induced CXCL10 promoter activation, truncation of the promoter to 376 bp, preserving these proximal recognition sequences, led to a significant drop in HRV-induced promoter activation<sup>259</sup>. Indeed, here it was confirmed that HRV-induced activation the truncated promoter was significantly reduced compared to the wild type. Although HRV-induced activation of the truncated CXCL10 promoter by HRV was still reduced by CSE, this did not reach statistical significance. These data suggested that transcription factor recognition sequence(s) between 279 and 875 bp upstream of the transcriptional start site were contributing to HRV-induced CXCL10 promoter activation and, potentially, to the inhibition by CSE.

Mutations to either of the C/EBP- $\beta$  sites did not result in a reduction in HRV-induced CXCL10 promoter activation or alter CSE-mediated inhibition. Mutations to either of two distal STAT sites resulted in inconclusive results. Unfortunately, in contrast to previous promoter-luciferase studies, when the data with individual STAT site mutations were expressed as RLU and fold induction, the trend was not the same. Based on raw RLU numbers, mutation of either of the STAT sites caused a significant reduction in both basal and HRV-induced CXCL10 promoter activation. The cause of this reduction is unclear. It is difficult to clearly interpret these data due to the effects on basal activation but they potentially implicate both STAT sites as important in HRV-induced CXCL10 promoter activation and do not rule out that they may be important in HRV-induced CXCL10 inhibition by CSE. Although promoter-luciferase studies are useful tools for analyzing transcriptional regulation are they are also inherently artificial non-physiological systems

and may not mimic the regulation of the endogenous gene. Alternate approaches are often used to validate promoter-luciferase data. Moreover, due to the inconclusive nature of this data set, alternative approaches were used to further evaluate the role of STAT transcription factors in the regulation of HRV-induced CXCL10 expression and its inhibition by CSE.

EMSA analysis showed that HRV induced a DNA/protein complex with the CXCL10-specific STAT oligonucleotide. Furthermore, HRV-induced complex formation was inhibited in the presence of CSE. The binding complex formed was shifted using antibodies to both STAT-1 and STAT-2, but not STAT-3. Activation of STAT-2 with the stimuli of interest was undetectable in HBE cells using two different p-STAT-2 antibodies specifically designed for immunoblotting. Although the specificity of EMSA supershift antibodies (STAT-1, STAT-2 and STAT-3) were verified by immunoblotting, this raises the possibility that the antibody to total STAT-2 used in supershift experiments was not entirely selective, despite only the proteins of interest being visualized on the immunoblot at those particular exposure times. Nonetheless, the discrepancy between EMSA and immunoblotting data regarding the involvement of STAT-2 is not entirely clear. In accordance with the EMSA data, activated STAT-3 (p-STAT-3) detection by immunoblotting showed constitutive expression without noticeable alteration, regardless of the treatment used (data not shown). By contrast, and consistent with earlier reports<sup>132,159</sup>, STAT-1 was detected in HBE cells and HRV infection induced phosphorylation of this protein. Moreover, CSE inhibited HRV induced STAT-1 phosphorylation.

In other cell types, CXCL10 expression is reported to be regulated by JAK/STAT signalling by stimuli including IFN- $\gamma$  and HRV exposure<sup>359,302</sup>. Initially, evidence that

activation of the STAT pathway played a functional role in HRV-16-induced CXCL10 expression in airway epithelial cells was obtained by showing that a selective JAK inhibitor resulted in inhibition of HRV-induced CXCL10 protein release. Others have concurrently reported that HRV-induced p-STAT-1 is inhibited by CSE<sup>355</sup>, but this is the first demonstration that inhibition of the JAK/STAT signalling pathway can modulate HRV-induced epithelial CXCL10 production. In support of this, inhibition of the JAK/STAT signalling pathway has been shown to modulate HRV-induced CXCL10 production in human monocytic cells, albeit via replication-independent mechanisms<sup>359</sup>.

The specific involvement of STAT-1 was evaluated using siRNA knock-down of STAT-1, but unfortunately the results were inconclusive. STAT-1 is expressed as two isoforms, or functional splice variants, including STAT-1 $\alpha$  (91kDa) and STAT-1 $\beta$  (84kDa). Two different siRNAs targeting STAT-1 were purchased, but they were only able to effectively knock-down one of the two isoforms of this protein, namely STAT-1 $\beta$ . Knock-down of STAT-1 $\beta$  did not have an effect on HRV-induced CXCL10 expression indicating that this isoform of STAT-1 is most likely not playing a significant role in viral induction of this gene. This data does not rule out the involvement of STAT-1 $\alpha$ , and in fact, the limited information available on STAT-1 regulation of CXCL10 expression generally focuses on the 91kDa splice variant, suggesting that this may be the dominant isoform<sup>302,304,463</sup>. Specific knock-down of STAT-1 $\alpha$  would have made these results more conclusive.

The difference between the STAT-1 $\alpha$  (750 amino acids) and the STAT-1 $\beta$  (712 amino acids) isoforms is that STAT-1 $\beta$  lack 38 C-terminal amino acids (amino acids 713-

750). Contained within these 38 amino acids is a critical serine residue (Ser727), the phosphorylation of which is required for maximal transcription induced by IFN- $\gamma$ <sup>464</sup>. Furthermore, the STAT-1 antibody used for supershift experiments targeted the C-terminal sequence of this protein, and specifically the portion that is not present in the STAT-1 $\beta$  isoform. Thus, collectively, these data suggest that STAT-1 $\alpha$ , but not STAT-1 $\beta$ , is involved in HRV-induced CXCL10.

Although it has been reported that IFN- $\gamma$  stimulation can induce STAT-1 $\alpha$  to bind to the ISRE region of the CXCL10 promoter as part of an ISGF3 complex composed of a STAT-1 $\alpha$  homodimer in conjunction with p48/IRF-9<sup>302,465</sup>, this does not occur upon exposure of epithelial cells to HRV. It has previously been shown that antibodies recognizing ISGF3 complex components did not alter complex formation with the ISRE region of the CXCL10 promoter<sup>297,338</sup> but that this is regulated by antibodies to IRF-1<sup>298</sup>. Thus, these data further suggest that STAT-1, and specifically STAT-1 $\alpha$ , regulates CXCL10 expression through the distal STAT transcription factor binding sites, rather than the ISRE binding site, in the CXCL10 promoter.

Classically, the ISGF3 complex consists of tyrosine phosphorylated -STAT-1 $\alpha$ , and/or -STAT-1 $\beta$  and -STAT-2 proteins, in conjunction with a 48 kDa (p48) DNA-binding protein that has been reported to specifically binds to ISRE<sup>354,466</sup>. Although the STAT-2 antibody caused a supershift of the STAT-protein complex, activated STAT-2 (p-STAT-2) could not be detected. Additionally, no alteration in constitutive IRF-9 was detected following any of the stimuli of interest (data not shown). Thus, the data here suggest that it is unlikely that an ISGF3 complex is involved in binding/activation of the distal CXCL10-

specific STAT sites, although an ISGF3 complex used in supershift experiments would have helped to make this speculation more conclusive. Similar to that which occurs during IFN- $\gamma$  stimulation in cells resulting in phosphorylation of STAT-1 $\alpha$  but not of STAT-2 and subsequent binding to the GAS sequence in other genes, it is feasible that phosphorylation of STAT-1 triggers homodimerization and migration to the nucleus where it can bind to the distal CXCL10 STAT sites in the CXCL10 promoter. Additionally, it is feasible that these sites are alternate binding sites for a STAT-1 $\alpha$  homodimer since CXCL10 does not contain a conserved GAS element in its promoter region<sup>239</sup>.

Next, the ChIP technique was used in an attempt to determine whether the protein-DNA interactions that are observed with the EMSA analysis are also observable in a more endogenous environment. ChIP allows for analysis of endogenous DNA-protein interactions in the cell rather than just using a nuclear extract containing translocated protein in conjunction with a synthetic oligonucleotide which corresponds to the region of interest. Unfortunately, ChIP also has its limitations. In this case, although ChIP with a readily expressed protein (RNA polymerase II) and PCR analysis with a constitutively expressed gene (GAPDH) was successful, ChIP with p65 NF- $\kappa$ B subunit or IRF-1 followed by the more sensitive real-time PCR analysis using specific primers was unsuccessful. Reasons for this are not entirely clear, but it is possible that since CXCL10 is expressed at much lower levels than GAPDH, that this technique is just not sensitive enough to detect these lower levels. It is also possible that the timeframe that was analyzed (6 h post HRV infection of cells), although in correspondence with the time-frame utilized for EMSA analysis, was too early in the process of transcriptional activation of CXCL10 by HRV to

detect any significant changes. Indeed, chromatin structure analysis using the EpiQ kit revealed that opening of CXCL10 around the transcriptional start site was detectable at 12 h but not at 6 h. But this again could also be due to sensitivity of this technique and does not rule out that chromatin opening and association of p65 and IRF-1 with the CXCL10 promoter doesn't occur at earlier time-points.

Although CSE appears to affect multiple signalling pathways to regulate HRV-induced CXCL10 expression, and this could just be a result of CSE inhibiting HRV-induced upstream events, it was determined in **Chapter 4** that CSE did not inhibit HRV-induced ICAM-1 expression nor alter HRV titre in the relevant time frame (24 h) required for HRV-induced signalling. A dsRNA intermediate formed during viral replication of RNA viruses such as HRV can be detected via PRRs including TLR3, RIG-I and/or MDA-5 resulting in a variety of signalling events. To date, there is controversy in the literature about the relative role of these PRRs in HRV-induced signalling<sup>154,155,157</sup>. Here it is demonstrated that HRV induces both RIG-I and MDA5, but not TLR3 (unpublished laboratory data) in primary human bronchial epithelial cells and this induction is significantly inhibited in the presence of CSE. HRV-induced expression of RIG-I and MDA5 is seen as early as 9 h post infection, suggesting that both of these proteins could readily affect CXCL10 gene expression at 24 h. siRNA knock-down studies showed that MDA-5, but not RIG-I, was involved in regulating HRV-induced CXCL10 expression and these results imply that suppression of HRV-induced MDA5 by CSE is one of the mechanisms contributing to the inhibition of HRV-induced CXCL10 by CSE. These data are consistent with a report that showed that knock-down of MDA5, but not RIG-I, lead to

the decreased expression of CXCL10 induced by HRV1B, a minor group rhinovirus<sup>154</sup>. Additionally, while RIG-I preferentially recognizes RNA from a variety of RNA viruses, MDA5 has been shown to preferentially bind picornavirus RNA<sup>165</sup>. Moreover, RIG-I has been shown to favour uncapped 5' triphosphate ssRNA and short dsRNA, while MDA5 favours longer dsRNA<sup>467-469</sup>. Since HRV has a longer RNA genome, this is consistent with MDA5 being important for HRV-induced CXCL10 expression, while RIG-I does not appear to be. While it is possible that MDA5 is more suitable for the detection of the HRV dsRNA replication intermediate, it is also possible that MDA5 may just have a higher affinity for dsRNA than RIG-I. These possibilities have not yet been explored and provide future avenues to explore.

Although one of general results of MDA5 signalling is the production of antiviral type I IFNs<sup>149,166</sup>, HRV-induced CXCL10 has been shown to be type I IFN-independent<sup>259</sup>. In conjunction with the data shown here, this suggests that MDA5 could directly induce CXCL10 production without the need for initial up-regulation of type I IFNs. In support of this it has been shown that long dsRNA, such as that produced during HRV replication, can induce anti-viral responses independent of IFN<sup>470</sup>. Moreover, virus-induced ISG induction has been shown to be independent of Type I and Type III IFN receptors<sup>471</sup>.

Recently it has been shown that other PRRs may also be involved in the recognition of HRV infection and the subsequent innate immune antiviral response<sup>157</sup>. Triantafilou *et al* demonstrated that in addition to MDA5, but not RIG-I, TLR2, TLR7 and TLR8 expression are induced following HRV infection of primary airway epithelial cells and that this successively triggers innate immune antiviral response including production of IL-6 and

IFN- $\beta$ . In agreement with this study, cell surface expression of TLR2 has been shown to be involved in recognition of viral proteins<sup>166</sup>. Thus, it is possible that during HRV infection, in addition to MDA5, TLR2, TLR7 and/or TLR8 may be playing a role in the subsequent expression of CXCL10. Since HRV-induced CXCL10 generation is dependent on viral replication<sup>259</sup>, it is possible that only following initial replication and enhancement of TLR expression that these receptors are contributing to CXCL10 generation. On the other hand, since TLR2 expression, but not TLR7 and TLR8, has been shown to be up-regulated following exposure to UV-inactivated HRV and still able to induce innate immune antiviral responses<sup>157</sup>, it is more likely that this PRR is not contributing to CXCL10 generation unless there is differential signalling via this receptor depending on the replication competency of HRV.

Transcriptional control of gene activation also involves epigenetic mechanisms regulating accessibility of DNA to both the basal transcriptional complex and specific transcription factors via chromatin remodelling. It is evident that cigarette smoke can exert effects on chromatin remodelling<sup>312,313</sup>. However, while it is known that CXCL10 is amenable to epigenetic control<sup>441,472</sup>, there are no prior reports of cigarette smoke modulating DNA accessibility in the area of the CXCL10 promoter. Since little CXCL10 mRNA is expressed under basal conditions, CSE alone had no effect the degree of constitutive accessibility. By contrast, HRV alone caused significant chromatin unwinding, leading to enhanced DNA susceptibility to nuclease digestion. When cells were treated with HRV+CSE, CXCL10 DNA accessibility was significantly suppressed compared to cells treated with virus alone, demonstrating that CSE inhibits HRV-induced CXCL10

expression via epigenetic regulation of accessibility of DNA around the CXCL10 transcriptional start site. HRV-induced chromatin accessibility was higher at 12 h than 24 h, which correlates with HRV-induced CXCL10 mRNA first becoming detectable by real-time RT-PCR at 9 h. Moreover, the suppression of HRV-induced chromatin accessibility occurs early in CXCL10 gene transcription at 12 h and it is further sustained up to 24 h when HRV-induced CXCL10 protein is robust and also significantly inhibited by CSE.

In summary, the data presented in this chapter report the novel observation that HRV-induced CXCL10 inhibition is a result of a combination of multiple mechanisms. Partial suppression of transcription factors involved in HRV-induced CXCL10 generation, namely NF- $\kappa$ B, IRF-1 and STAT-1, partial suppression of upstream signalling via the viral sensor MDA5, and partial suppression of HRV-induced CXCL10 chromatin accessibility all contribute to the collective, potent inhibition of HRV-induced CXCL10 at the protein level.

## 5.5 Future Studies

A number of potential future studies could enhance and/or strengthen the conclusions drawn from the data presented in this chapter. A selection of these are discussed below.

Using custom designed siRNA to specifically knock-down the STAT-1 $\alpha$  isoform would help to more conclusively decipher the involvement of this isoform in the generation of HRV-induced CXCL10. This siRNA could be designed in such a manner as to target the 38 amino acid sequence in the C-terminal portion of STAT-1 that is present in the STAT-

1 $\alpha$  isoform but not the STAT-1 $\beta$  isoform. Additionally, the lack of a role for STAT-1 $\beta$  in HRV-induced CXCL10 could be further examined by using supershift antibodies targeting only this isoform. If an antibody to STAT-1 $\beta$  did not cause a shift in the protein-DNA complex formed using CXCL10-specific STAT oligonucleotides, while the STAT-1 $\alpha$  did, then this would more conclusively implicate the specific involvement of the STAT-1 $\alpha$  isoform. A supershift antibody to the ISGF3 complex could be used to help eliminate the involvement of STAT-2 and IRF-9.

Although the EpiQ chromatin accessibility studies showed that HRV-induced CXCL10 chromatin accessibility was reduced by CSE, the manner of how this occurred was not addressed. Studies investigating whether histone modifications and/or DNA methylation are altered by CSE in the CXCL10 promoter area could provide more insight into this, although, admittedly, this could be difficult to do. ChIP techniques would have to be utilized in conjunction with antibodies to modified histones and methylated DNA and then real-time analysis would have to be performed using CXCL10-specific primers. The same problems already encountered with the ChIP technique could therefore arise with this investigation as well.

Lastly, since there is suggestion that TLR2, TLR7 and/or TLR8 may be involved in the recognition of HRV, analysis of the expression of these PRRs and whether they are affected by CSE may be useful. If either and/or all of these were to be shown to be induced by HRV and/or altered by CSE in this *in vitro* model, then a further investigation to determine whether signalling through these PRRs is linked to HRV-induced CXCL10 generation could be useful.

## Chapter Six: **Mechanisms of CXCL8 Enhancement by the Combination of HRV and CSE**

Portions of data presented in this Chapter have been published:

Hudy MH, Traves SL, Wiehler S, Proud D. Cigarette smoke modulates rhinovirus-induced airway epithelial cell chemokine production. *Eur. Respir. J.* 2010;35(6):1256–1263.

Copyright © European Respiratory Society.

## 6.1 Background

In response to a variety of stimuli, CXCL8 mRNA expression is rapidly induced and can be detected as early as 1 h post stimulus, although it can persist for up to 72 h<sup>305,306</sup>. It is now well known that CXCL8 gene expression is regulated both transcriptionally and post-transcriptionally<sup>278,305</sup>. Reported mechanisms of CXCL8 gene regulation will be discussed in detail below.

### 6.1.1 Transcriptional regulation of CXCL8

CXCL8 has been shown to be regulated via transcription factors binding to the AP-1, C/EBP- $\beta$  (NF-IL-6) and NF- $\kappa$ B binding sites in the CXCL8 promoter<sup>306-311,473</sup>. The region between -1 and -133 in the 5' flanking region of the CXCL8 gene has been shown to be sufficient for the transcriptional regulation of this gene<sup>279</sup>, including when induced by HRV-16<sup>323</sup>. A representative diagram of the CXCL8 promoter is depicted in **Figure 6.1 A**. The distal AP-1 site is located between -120 and -126 in the gene promoter has been shown to interact with protein dimers of the Jun and Fos family<sup>306</sup>. The proximal C/EBP- $\beta$  site located between -81 and -92 and the NF- $\kappa$ B site located between -70 and -80 have been shown to interact with protein dimers of the C/EBP basic-leucine zipper and Rel/NF- $\kappa$ B family respectively<sup>306</sup>. The extent to which each transcription factor contributes to CXCL8 induction seems to be dependent not only on the stimulus but also on the cell type studied.

#### 6.1.1.1 Transcriptional Regulation of CXCL8 by HRV

There is some controversy in terms of the mechanisms behind HRV-induced transcriptional regulation of CXCL8 gene expression. It has been reported, using the A549 alveolar carcinoma cell line infected with HRV type 14, that HRV-induced stimulation of CXCL8 is NF- $\kappa$ B dependent involving an increase in p50/p65 heterodimer binding to the NF- $\kappa$ B consensus sequence in the CXCL8 promoter<sup>283</sup>. Additionally, this study used CXCL8 promoter-luciferase constructs to show that HRV-14-induced CXCL8 promoter activation is decreased when the NF- $\kappa$ B sequence is mutated. Interestingly, using similar methods, this study also shows that C/EBP- $\beta$  is only partially required for CXCL8 gene expression. In support of these findings, another study, using transiently transfected CXCL8 promoter-luciferase constructs in the BEAS-2B bronchial epithelial cell line, demonstrated that HRV-16-induced activation of the CXCL8 promoter is dependent on NF- $\kappa$ B, partially dependent on C/EBP- $\beta$  but not dependent on AP-1<sup>323</sup>. In contrast to these two reports, Kim and colleagues have reported that although HRV activates NF- $\kappa$ B, HRV stimulates CXCL8 gene expression independent of NF- $\kappa$ B activation<sup>474</sup>. In this aforementioned study, the BEAS-2B bronchial epithelial cell line and HRV type 16 were used in conjunction with inhibitors of NF- $\kappa$ B to show that HRV-16 still induced CXCL8 even when NF- $\kappa$ B signalling was inhibited. The discrepancy between these studies could in part be attributed to different cell types, culture conditions, and serotypes of HRV; and in part to different techniques used to investigate the involvement of NF- $\kappa$ B in CXCL8 gene regulation.

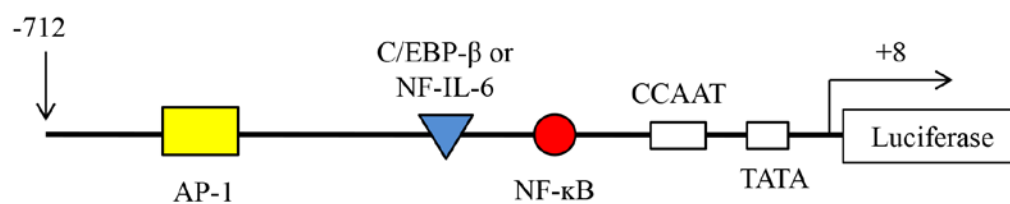
### 6.1.1.2 Transcriptional Regulation of CXCL8 by Cigarette Smoke

As discussed in **Chapter 3**, cigarette smoke has been shown to induce the expression of CXCL8 in a variety of cell types. The mechanism behind this induction has not been rigorously studied as only a handful of studies have been reported. Cigarette smoke has been shown to activate NF- $\kappa$ B<sup>263,433,459,461</sup>, have no effect on NF- $\kappa$ B<sup>203,210,455</sup> and to modulate stimulus-induced NF- $\kappa$ B signalling in airway epithelial cells<sup>203,210</sup>. One study reports that cigarette smoke-induced CXCL8 expression is dependent on the NF- $\kappa$ B pathway in macrophages but does not show a direct link in transcriptional regulation<sup>423</sup>. In **Chapter 5**, the current study shows that CSE does not alter NF- $\kappa$ B signalling alone, but inhibits HRV-16-induced NF- $\kappa$ B signalling. It is therefore unlikely, and contradictory to previous results presented in this thesis, that the enhancement of CXCL8 following treatment with HRV-16+CSE is regulated by transcriptional activation via NF- $\kappa$ B. Cigarette smoke has also been reported to modulate C/EBP- $\beta$ <sup>475,476</sup> and AP-1<sup>456,458,477-480</sup>. Furthermore, cigarette smoke conditioned medium up-regulates C/EBP- $\beta$  and coincides with increased CXCL8 levels in human fibroblasts<sup>476</sup>. Also notable, cigarette smoke induces CXCL8 expression and c-jun binding to the AP-1 site in the CXCL8 promoter in THP-1 monocytic cells<sup>480</sup>. It is therefore plausible that the enhancement of CXCL8 by HRV-16+CSE compared to either treatment alone is mediated via transcriptional mechanisms specifically involving C/EBP- $\beta$  and/or AP-1.

### 6.1.2 Post-transcriptional regulation of CXCL8

CXCL8 has very unstable mRNA susceptible to rapid degradation<sup>279</sup>. Located within the proximal portion of the 3' UTR of CXCL8 mRNA are AREs containing four AUUUA motifs, two of which overlap (**Figure 6.1 B**)<sup>381</sup>. As discussed in **Chapter 1**, AREs are hallmarks of mRNAs that are amenable to stabilization/destabilization and are shown to be involved in docking of mRNA stabilizing/destabilizing proteins.

A.



B.

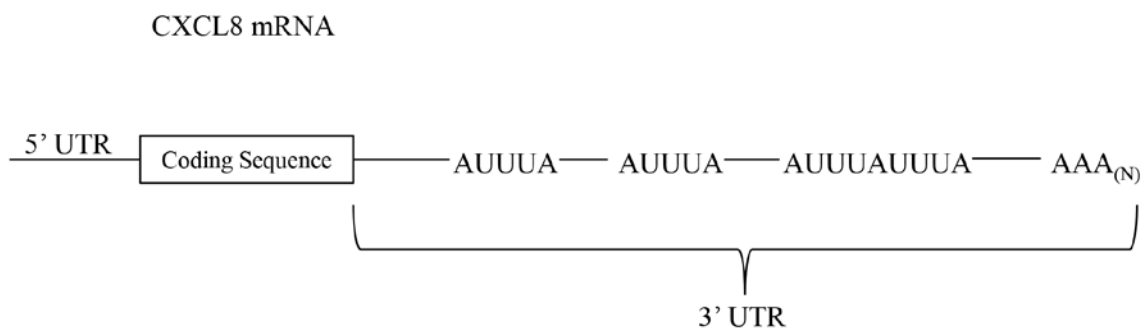


**Figure 6.1: Schematic diagrams of the putative CXCL8 promoter and mRNA transcript.**

A: A schematic diagram of the putative 720 bp CXCL8 promoter construct inserted upstream of a firefly luciferase gene. B: A schematic diagram of the CXCL8 promoter highlighting the AREs in the 3' UTR. Diagrams are not to scale.

Activation of the p38 MAPK pathway following a variety of stimuli has been shown to induce CXCL8 mRNA stabilization<sup>325–327</sup>. More specifically, activation of the MAPKK6-p38 MAPK-MK2 signalling pathway is linked to stabilization of the CXCL8 transcript<sup>325</sup>. As evidence of this, inhibition of the p38 MAPK pathway using pharmacological inhibitors, including SB203580 and SB202190, has been shown to suppress CXCL8 in some cells<sup>279</sup>. Although p38 MAPK can significantly contribute, it is not necessarily essential for CXCL8 expression<sup>279</sup>.

Thus far, there is no general consensus of which ARE binding protein(s) is/are most important in the regulation of CXCL8 gene stability. At least four ARE binding proteins have linked to the regulation of CXCL8 gene stability, including HuR<sup>382,384–386</sup>, which stabilizes mRNA, KHSRP<sup>383,384</sup> and TTP<sup>387–389</sup>, which both destabilize mRNA, and AUF-1<sup>382</sup>, which has four isoforms and has been shown to both stabilize and destabilize mRNA transcripts. To date none of these proteins have specifically been linked to CSE-induced stabilization of CXCL8.

Palanisamy *et al* have shown using uv-crosslinking and immunoprecipitation experiments that both AUF-1 and HuR associate with CXCL8 mRNA in human saliva<sup>382</sup>. Wang *et al* have shown using supershift-EMSA, immunoprecipitation and uv-crosslinking experiments that following stimulus with nitric oxide, HuR associated with CXCL8 mRNA in monocytic THP-1 cells<sup>385</sup>. Although Winzen and colleagues also have shown that CXCL8 mRNA is stabilized through the 3' UTR via HuR, in their hands, HuR does not associate with the AUUUA core elements but rather with the auxiliary domain in the CXCL8 3'UTR<sup>386</sup>. Additionally, Winzen and colleagues have shown that KHSRP

associates with the 3' UTR of CXCL8 and is essential for rapid degradation of this transcript<sup>383</sup>. It has also been demonstrated that both HuR and KHSRP associate with the 3' UTR of CXCL8 but, at least in breast cancer cells following IL-1 $\beta$  treatment, there was a much greater association of the stabilizing factor HuR than the destabilizing factor KHSRP<sup>384</sup>. Additionally, while TTP is expressed at very low levels in cystic fibrosis lung epithelial cells at rest, upon stimulation it has been shown to regulate CXCL8 mRNA expression in these cells<sup>387,388</sup>.

#### 6.1.2.1 Post-Transcriptional Regulation of CXCL8 by HRV

HRV has not been shown to directly up-regulate CXCL8 via mRNA stabilization but HRV has been shown to induce rapid phosphorylation of p38 MAPK in the BEAS-2B bronchial epithelial cell line<sup>323,324,481,482</sup>. Moreover, this pathway has also been linked to HRV-induced CXCL8 expression<sup>482</sup>. Only one publication had reported that HRV induces one of the stabilizing/destabilizing proteins that are linked to CXCL8 induction, and that is AUF-1, but it was only induced at late time-points including 24 and 48 h which would not be relevant for the early induction of CXCL8 being investigated here<sup>259</sup>.

#### 6.1.2.2 Post-Transcriptional Regulation of CXCL8 by Cigarette Smoke

CSE has been shown to induce rapid phosphorylation of p38 MAPK in human airway smooth muscle<sup>483</sup>, lung fibroblasts<sup>484</sup>, small airway epithelial<sup>485</sup> and bronchial epithelial cell cultures<sup>458,485,486</sup>. Moreover, using a pharmacological inhibitor of p38 MAPK, Moretto *et al.* have shown that there is a link between CSE-induced CXCL8 and p38

MAPK activation in human lung fibroblasts<sup>484</sup>. Recently, this group has also demonstrated that p38 MAPK-MK2 pathway is directly responsible for CSE-induced CXCL8 expression by mRNA stabilization in human bronchial smooth muscle cells<sup>485</sup>.

To date, there is no literature whether cigarette smoke modulates the expression/activation of AUF-1, KHSRP, HuR or TTP.

## 6.2 Hypothesis

CXCL8 enhancement by the combination of HRV and CSE above either treatment alone is regulated either transcriptionally, but not involving NF- $\kappa$ B, or post-transcriptionally by stabilizing CXCL8 mRNA.

## 6.3 Results

### *6.3.1 HRV-16-induced CXCL8 enhancement by CSE is not regulated transcriptionally*

Data presented in **Chapter 3** showed that CSE-induced CXCL8 mRNA was beginning to accumulate at 5 h post treatment and HRV-16-induced CXCL8 mRNA was further enhanced with CSE starting at 5 h post-treatment. In order to determine whether the enhancement of HRV-16-induced CXCL8 by CSE was being regulated on the transcriptional level, the BEAS-2B bronchial epithelial cell line was transiently transfected with a full-length CXCL8 promoter-luciferase construct (**Figure 6.1 A**) and assayed for firefly luciferase activity following a 5 h treatment with medium control, CSE, HRV-16 or HRV-16+CSE (**Figure 6.2**). BEAS-2B cells were used for these experiments as primary cells are difficult to transfect with large promoter constructs. The use of BEAS-2B cells for

these experiments was justified based on similar results seen with primary HBE and BEAS-2B cells regarding CXCL8 expression in **Chapter 3**.

What was found was that CSE alone did not induce the activation of the CXCL8 promoter. In contrast, HRV-16 alone significantly induced CXCL8 promoter activation. Surprisingly, HRV-16-induced CXCL8 promoter activation was not enhanced in combination with CSE. Interestingly, HRV-16-induced CXCL8 promoter activation was significantly inhibited in the presence of CSE. Data are displayed as both raw RLU (**Figure 6.2 A**) and fold increase compared to medium control (**Figure 6.2 B**) to show that the trend in the data remained the same regardless of how the data was expressed. Thus, these data suggest that HRV-16-induced CXCL8 protein enhancement by CSE is not regulated on the transcriptional level.

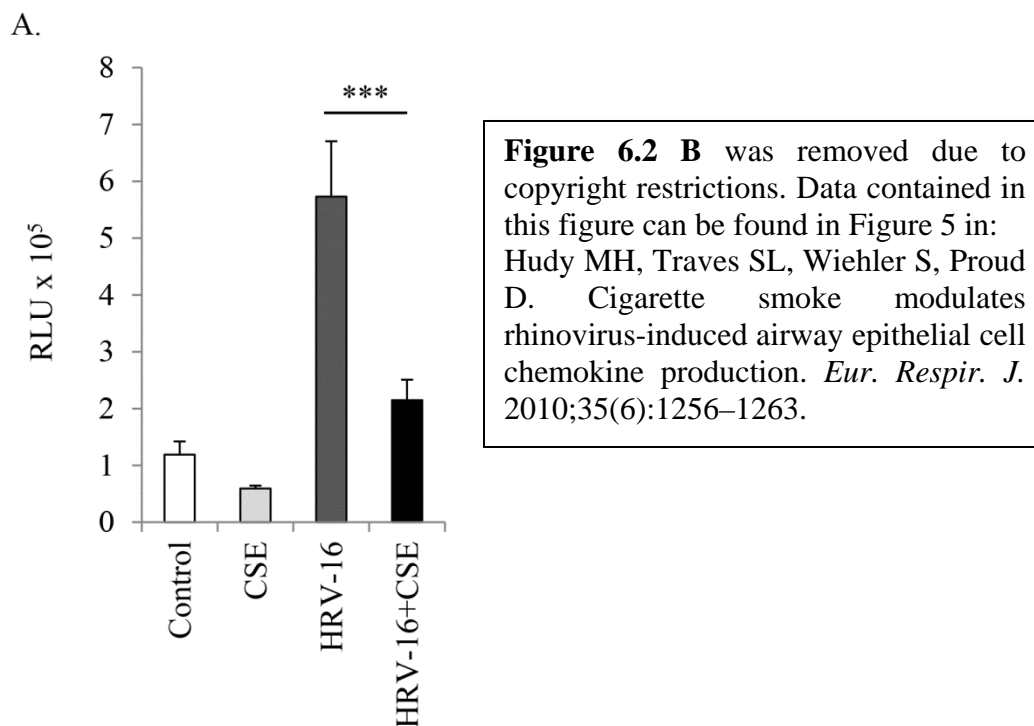


**Figure 6.2: HRV-16-induced CXCL8 enhancement by CSE is not regulated transcriptionally in airway epithelial cells.**

BEAS-2B cells that were transiently transfected with the full length CXCL8 promoter were then treated with medium, CSE alone, HRV-16 alone or the combination for 5 h. Cell lysates were assessed for firefly luciferase activity and data are presented as both relative light units (RLU; A) and fold induction as compared to cells treated with only medium control (B). Data are presented as mean  $\pm$  SEM (n=6). Asterisks denote a significant difference between HRV-16+CSE and HRV-16 alone (\*\*\*) p<0.001). Data presented in B have been published<sup>445</sup>.

**6.3.2 The combination of HRV-16 and CSE stabilizes CXCL8 mRNA**

As previously mentioned, CXCL8 can be regulated post-transcriptionally through mRNA stabilization. In order to determine whether the combination of HRV-16 and CSE was stabilizing CXCL8 mRNA, studies using the actinomycin D chase assay were conducted. Actinomycin D is an inhibitor of transcription and the actinomycin D chase

assay is used to monitor the decay rate of mRNA of a given gene over time following a particular treatment<sup>487</sup>.

Preliminary data demonstrated that induction of CXCL8 steady state mRNA was first observed at 2 h after stimulation with HRV-16 in HBE and BEAS-2B cells (unpublished laboratory results). Additive induction of CXCL8 protein following treatment with HRV-16+CSE compared to either treatment alone was observed as early as 5 h post-treatment (**Chapter 3, Figure 3.9**). Thus, a 2 h exposure before addition of actinomycin D was used with 3 h post actinomycin D exposure as the last time-point collected. As actinomycin D can be quite toxic to cells, limiting the time of exposure is essential. Primary HBE cells were not used for this experiment due to the large volume of cells that would be required per cell donor. In BEAS-2B cells treated with either CSE alone or HRV-16 alone, CXCL8 mRNA decayed, with 50% loss occurring between 2 and 3 h in each case (**Figure 6.3**). In cells exposed to the combination of HRV-16 and CSE, however, a significant stabilization of CXCL8 mRNA was observed, such that there was no significant degradation of CXCL8 mRNA over the 3 h time period studied (**Figure 6.3**). The half-life of CXCL8 mRNA has been reported to be  $\sim 4.6$  h<sup>305</sup> but due to toxicity effects of actinomycin D at a longer duration of exposure (unpublished laboratory results), the actinomycin D chase experiment was not continued on past 3 h.

**Figure 6.3** was removed due to copyright restrictions. Data contained in this figure can be found in Figure 6 in: Hudy MH, Traves SL, Wiehler S, Proud D. Cigarette smoke modulates rhinovirus-induced airway epithelial cell chemokine production. *Eur. Respir. J.* 2010;35(6):1256–1263.

**Figure 6.3: The combination of HRV-16 and CSE stabilizes CXCL8 mRNA in airway epithelial cells.**

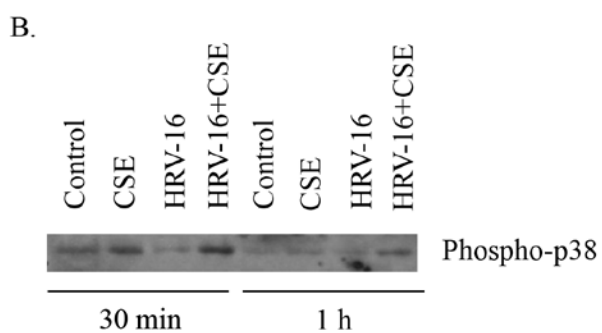
BEAS-2B cells were treated for 2 h with medium control, CSE, HRV-16 or the combination and then actinomycin D (10 µg/mL) was added to inhibit further transcription. Total cellular RNA was extracted at 30, 60 (1 h), 120 (2 h) and 180 (3 h) min and CXCL8 mRNA levels were assessed with real time RT-PCR. Data are expressed as a percentage of CXCL8 mRNA at time 0 for each treatment. Data are presented as mean ± SEM (n=4). Asterisks denote a significant difference between HRV-16+CSE and HRV-16 alone for the respective time-point (\* p≤0.05). Data presented in this figure have been published<sup>445</sup>.

**6.3.3 The p38 MAPK pathway is involved in CSE-induced and HRV-16+CSE-induced CXCL8**

As previously mentioned, stability of CXCL8 mRNA<sup>279</sup> and the induction of CXCL8 by cigarette smoke has been linked to the p38 MAPK pathway<sup>484–486</sup>. Additionally, inhibition of the p38 MAPK pathway reduces HRV-16 induced CXCL8 production from airway epithelial cells<sup>323</sup>. In agreement with this earlier study<sup>323</sup>, HRV-16 induced rapid phosphorylation of p38 (**Figure 6.4 A**). Also consistent with earlier reports<sup>484–486</sup>, CSE

also modestly induced phosphorylation of p38 MAPK in BEAS-2B cells. The combination of HRV-16 and CSE induced additive phosphorylation of p38 MAPK at 30 minutes (as assessed by densitometry), but the response to the combination was less than additive at later time-points (**Figure 6.4 A**). Similar results were obtained in HBE cells (**Figure 6.4 B**).

In order to link the involvement of the p38 MAPK pathway to CXCL8 production following treatment, this pathway was inhibited using the selective p38 MAPK inhibitor SB203580 prior to measuring CXCL8 protein levels. A concentration of 3  $\mu$ M was used because this has been shown to effectively inhibit p38 MAPK and have no substantial inhibitory effects on other kinases<sup>488</sup>. SB203580 significantly inhibited CSE-induced CXCL8 protein production as well as CXCL8 production in response to the combination of HRV-16 and CSE (**Figure 6.4 C**). The vehicle control (DMSO) or the negative control for SB203580 (SB202474) did not significantly alter CXCL8 protein production following CSE, HRV-16 or HRV-16+CSE treatment. Together, these data suggest that enhanced p38 MAPK activation by HRV-16+CSE could contribute to enhanced CXCL8 protein production.



**Figures 6.4 A and C** were removed due to copyright restrictions. Data contained in these figures can be found in Figure 7 in:

Hudy MH, Traves SL, Wiehler S, Proud D. Cigarette smoke modulates rhinovirus-induced airway epithelial cell chemokine production. *Eur. Respir. J.* 2010;35(6):1256–1263.

**Figure 6.4: The p38 MAPK pathway is involved in CSE-induced and HRV-16+CSE-induced CXCL8 production in airway epithelial cells.**

A: BEAS-2B cells were treated with medium control, CSE, HRV-16 or the combination for the times indicated and probed using a specific antibody to phosphorylated-p38 MAPK, then were subsequently stripped and re-probed using an antibody to total p38 MAPK to ensure equal protein loading (representative of 3 separate experiments). B: HBE cells were treated with medium control, CSE, HRV-16 or the combination for the times indicated and probed using a specific antibody to p38 MAPK (representative of 2 separate experiments). C: BEAS-2B cells were incubated with media alone or in the presence of DMSO, SB202474 or SB203580 for 1h before treatment with CSE, HRV-16 or the combination for 24h. Data are presented as mean  $\pm$  SEM (n=3). Asterisks denote a significant difference with treatment + SB203580 versus treatment alone or treatment + DMSO/SB202474 (\* $p \leq 0.05$  and \*\*\* $p < 0.001$ ). Data presented in A & C have been published<sup>445</sup>.

**6.3.4 CSE, HRV-16 and HRV-16+CSE all fail to alter the expression of AUF-1, KHSRP or HuR**

Stability of CXCL8 mRNA has been reported to be regulated, in various systems, by the stabilizing/destabilizing proteins AUF-1, TTP, KHSRP and HuR, but to date none of these proteins have specifically been linked to CSE-induced enhancement by stabilization of HRV-induced CXCL8. To investigate the roles of these specific mRNA stabilizing/destabilizing proteins it was first determined whether the expression of these proteins was altered with CSE alone, HRV-16 alone or HRV-16+CSE. Using the actinomycin D chase assay, mRNA stabilization of CXCL8 by HRV-16+CSE was observed within 3 h post-treatment, therefore, expression levels of these stabilizing/destabilizing proteins were examined at early time-points, as this would be most relevant to the time-frame for stabilization of CXCL8 mRNA following treatment with CSE, HRV-16 and HRV-16+CSE. Although there was constitutive expression of AUF-1, KHSRP and HuR at 30 min, 1 h and

3 h, neither treatment markedly affected the expression level of these proteins in HBE cells at the time-points studied (**Figure 6.5**).

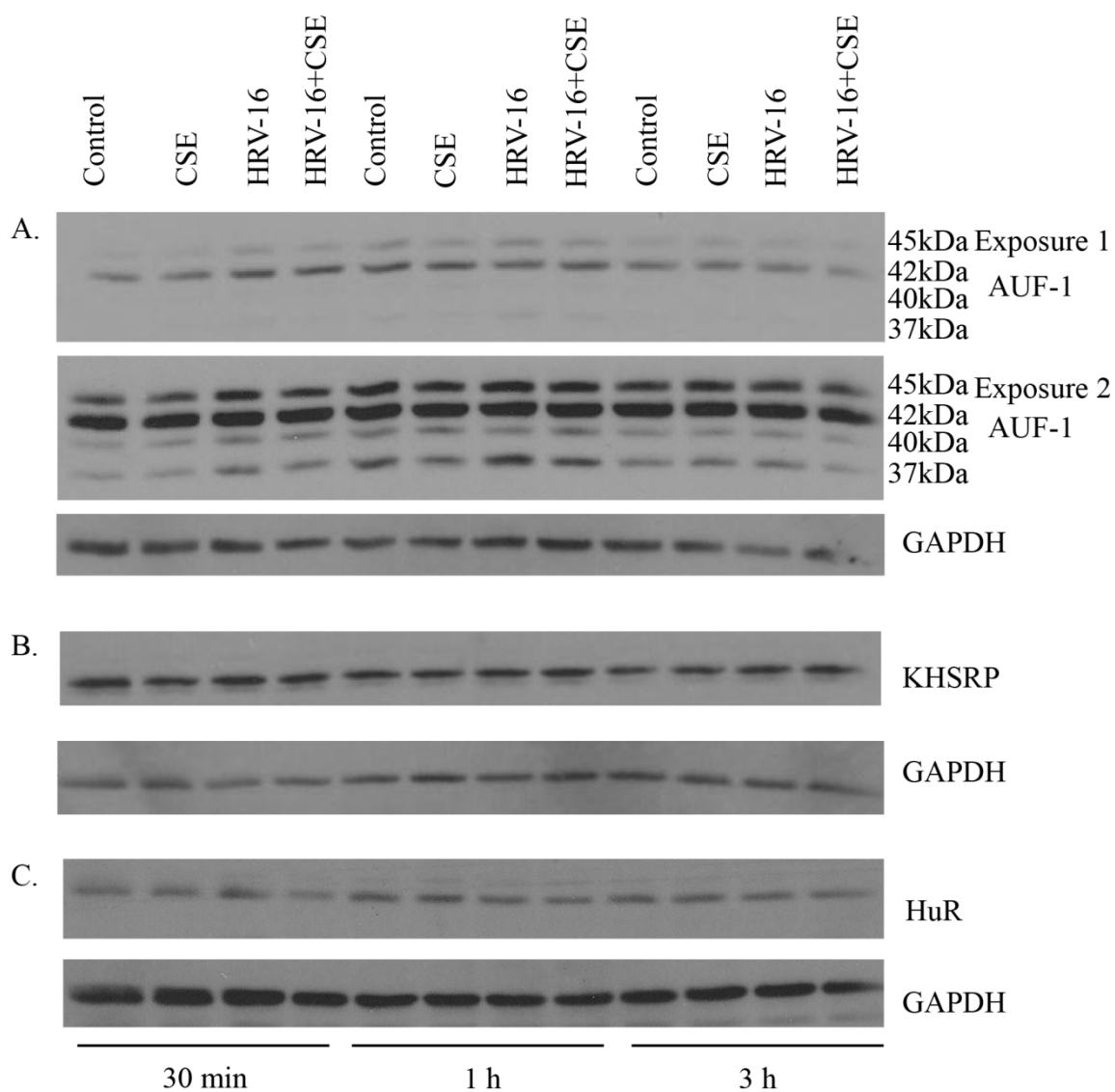


**Figure 6.5: CSE alone, HRV-16 alone or the combination of the two stimuli does not alter the expression of ARE-binding proteins AUF-1, KHSRP and HuR at early time-points in airway epithelial cells.**

HBE cells were treated with medium control, CSE, HRV-16 or HRV-16+CSE for the times indicated. Total cell lysates were harvested and analyzed via immunoblotting. Membranes were probed with specific AUF-1 (A), KHSRP (B) or HuR (C) antibodies, then were subsequently stripped and re-probed with an antibody to GAPDH to ensure equal protein loading. Data are representative of 3 separate experiments.

Examination of AUF-1 and HuR expression at later time-points, including 6 and 9 h post treatment with CSE, HRV-16 or HRV-16+CSE resulted in similar observations, with no marked difference in expression levels of these proteins following treatment (**Figure 6.6**). Using three different antibodies, TTP protein detection was unsuccessful in both the HBE and BEAS-2B cells, either constitutively or following any of the treatments.

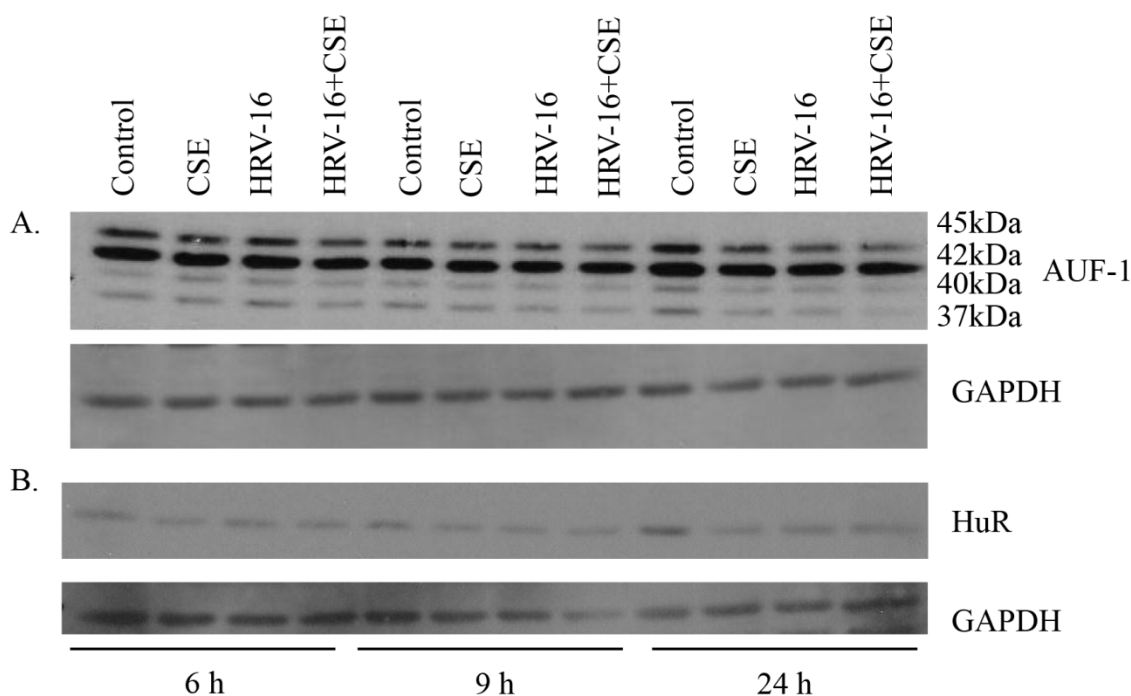


**Figure 6.6: CSE alone, HRV-16 alone or the combination of the two stimuli does not alter the expression of ARE-binding proteins AUF-1 and HuR at later time-points in airway epithelial cells.**

HBE cells were treated with medium control, CSE, HRV-16 or HRV-16+CSE for the times indicated. Total cell lysates were harvested and analyzed via immunoblotting. Membranes were probed with specific AUF-1 (A) or HuR (B) antibodies, then were subsequently stripped and re-probed with an antibody to GAPDH to ensure equal protein loading. Data are representative of 3 separate experiments.

### ***6.3.5 HuR is involved in enhancement of CXCL8 by the combination of HRV-16+CSE***

The function of mRNA stabilizing/destabilizing proteins can also be regulated via post-translational modifications, including but not limited to phosphorylation, that affect the activity or localization of these proteins. Unfortunately, there are no currently available commercial antibodies which identify post-translational modifications of AUF-1, KHSRP or HuR. siRNA knock-down of each protein was used as an alternative approach to assess the role of AUF-1, KHSRP or HuR in the regulation of HRV-induced CXCL8 expression by CSE.

As a reference to compare effects of siRNA knock-down on levels of CXCL8, protein levels from a collection of 6 HBE cell donors that were used for subsequent siRNA experiments are shown in **Figure 6.7**. Although the pattern in CXCL8 protein expression was similar to that reported in **Chapter 3**, the magnitude was different from other HBE cell donors used earlier in the project. Since primary cells are derived from different individuals, donor-to-donor variation is expected.

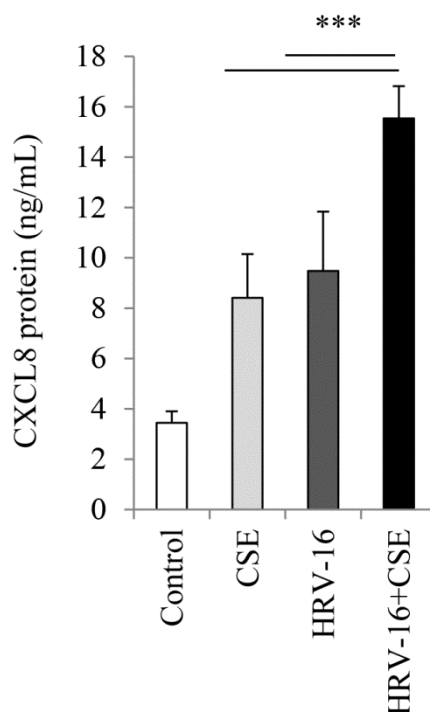


**Figure 6.7: CXCL8 protein production is enhanced by HRV-16+CSE compared to CSE or HRV-16 alone in airway epithelial cells.**

HBE cells from 6 HBE cell donors to be used for siRNA experiments were treated with medium control, CSE, HRV-16 or HRV-16+CSE for 24 h and cell supernatants were assessed for CXCL8 protein release. Data are presented as mean  $\pm$  SEM (n=6). Asterisks denote a significant difference between the specified treatments (\*\*\*) p<0.001).

HBE cells were transfected with two different siRNA duplexes targeting AUF-1 (**Figure 6.8**), KHSRP (**Figure 6.9**) or HuR (**Figure 6.10**). Appropriate controls were performed in parallel including, treatment with medium alone, mock transfection with the transfection reagent (lipid) alone, as well as transfection with the appropriate concentration of a universal control non-targeting siRNA. Cells were recovered for 24 h prior to an additional 24 h treatment with HRV-16+CSE. Initial studies focused on validation of respective protein knock-down. Although there was basal expression of AUF-1, KHSRP

and HuR in HBE cells (**Figure 6.5**), siRNA knock-down was confirmed following the treatment of interest (HRV-16+CSE) in order to ensure that this treatment was not limiting the ability of the siRNAs to successfully produce knock-down. For all siRNA validation experiments (**Figure 6.8A, 6.9A and 6.10A**), similar levels of knock-down were observed in cells treated with medium alone, CSE alone or HRV-16 alone (data not shown).

AUF-1 is expressed as four alternatively spliced products with differing molecular weights, including 37, 40, 42 and 45 kDa isoforms. Neither the transfection reagent alone nor the control non-targeting siRNA (30 nM) had a significant effect on protein expression of any AUF-1 isoform (**Figure 6.8 A**). Each of the two siRNAs targeting AUF-1 was only able to significantly knock-down the expression of the 45 kDa isoform of AUF-1. Densitometry calculations showed that the knock-down of the 45 kDa isoform was substantial, with around 90% knock-down with each of the two siRNAs (**Figure 6.8 A**). A higher concentration (100 nM) of AUF-1 siRNA was tried but, at this concentration, effects on cell viability were apparent. Next, CXCL8 protein levels were measured from supernatants collected from HBE cells treated with these siRNAs. No significant differences were observed between HRV+CSE treated cells after pre-treatment with medium alone, transfection reagent alone or either of the two AUF-1 siRNA duplexes (**Figure 6.8 B**).

Transfection reagent alone, or the control non-targeting siRNA (10 nM), did not have a significant effect on protein expression of KHSRP (**Figure 6.9 A**). Each of the two siRNAs targeting KHSRP were significantly able to knock-down the expression of KHSRP protein as assessed by densitometry, with a 61% and 78% knock-down compared to HRV-

16+CSE alone (**Figure 6.9 A**). CXCL8 protein level measurements revealed that KHSRP knock-down did not reverse the enhancement of HRV-16-induced CXCL8 by CSE (**Figure 6.9 B**). One of the two siRNA duplexes had a slight, but significant, effect on enhancing CXCL8 protein levels in cells treated with HRV-16+CSE.

Transfection reagent alone, or the control non-targeting siRNA (10 nM), did not have a significant effect on protein expression of HuR (**Figure 6.10 A**). Each of the two siRNAs targeting HuR were significantly able to knock-down the expression of HuR protein as assessed by densitometry, with 68% and 70% knock-down compared to HRV-16+CSE alone (**Figure 6.10 A**). CXCL8 protein level measurements revealed that HuR protein knock-down, using two different HuR-targeting siRNA duplexes, did have a significant effect on CXCL8 protein expression from HBE cells following treatment with HRV-16+CSE (**Figure 6.10 B**). CXCL8 protein expression was reduced to levels observed with treatment of HBE cells with CSE or HRV-16 alone (**Figure 6.7**). Compared to medium alone, CSE alone induced CXCL8 protein levels to  $8.4 \pm 1.7$  ng/mL and HRV-16 alone induced CXCL8 protein levels to  $9.5 \pm 2.4$  ng/mL. The combination of HRV-16+CSE induced CXCL8 protein levels to levels above 15 ng/mL. Levels of CXCL8 protein released from HBE cells following treatment with HRV-16+CSE in conjunction with HuR-targeting siRNA #1 or siRNA #2 were  $8.9 \pm 1.6$  ng/mL and  $9.0 \pm 1.5$  respectively.

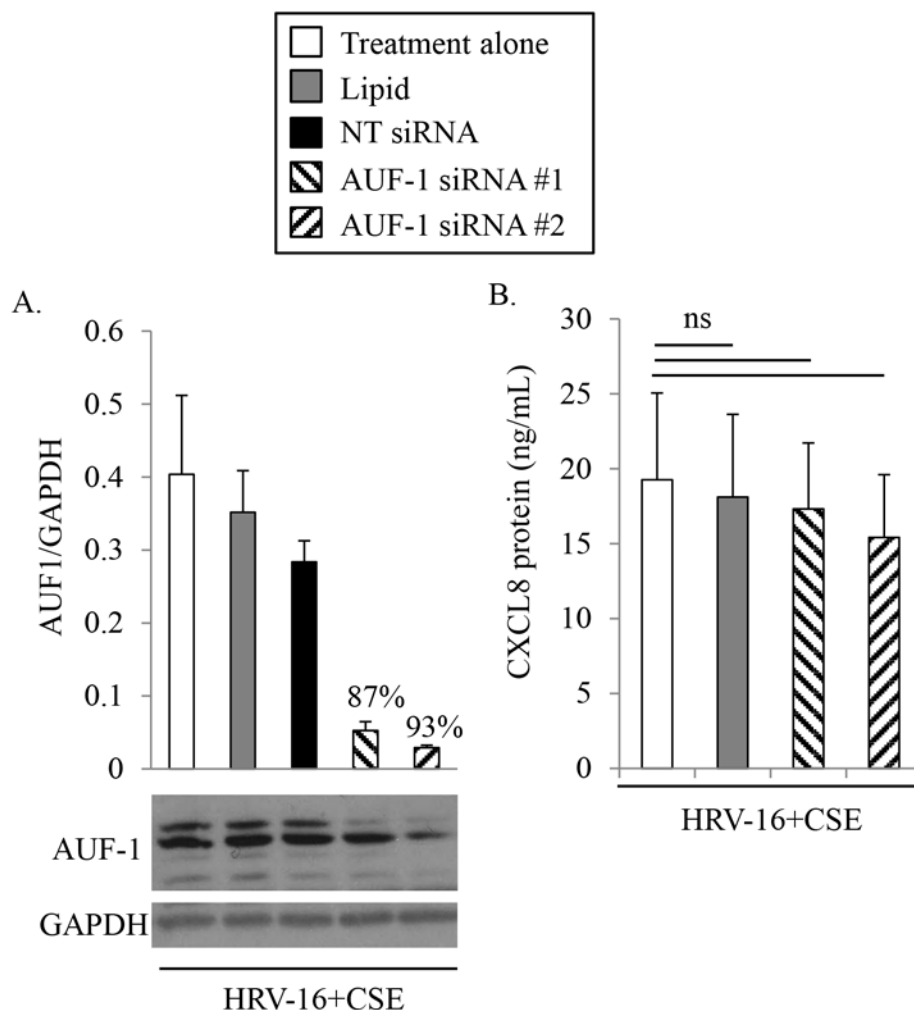


**Figure 6.8: Effects of AUF-1-targeting siRNA on CXCL8 protein expression in airway epithelial cells.**

HBE cells were treated for 24 h prior to harvesting cell supernatants for analysis with ELISA and whole cell lysates for analysis with immunoblotting. To determine the level of AUF-1 protein knock-down membranes were probed with a specific AUF-1 antibody recognizing 4 isoforms of AUF-1, then were subsequently stripped and re-probed with an antibody to GAPDH to ensure equal protein loading (A; representative of 3 separate experiments). Densitometry analysis with % knock-down relative to HRV-16+CSE alone is also shown (A; n=3). Supernatants were analyzed for CXCL8 protein (B; n=3). Data are presented as mean  $\pm$  SEM. Lipid denotes transfection reagent alone. NT denotes non-targeting control siRNA. ns = not significant.

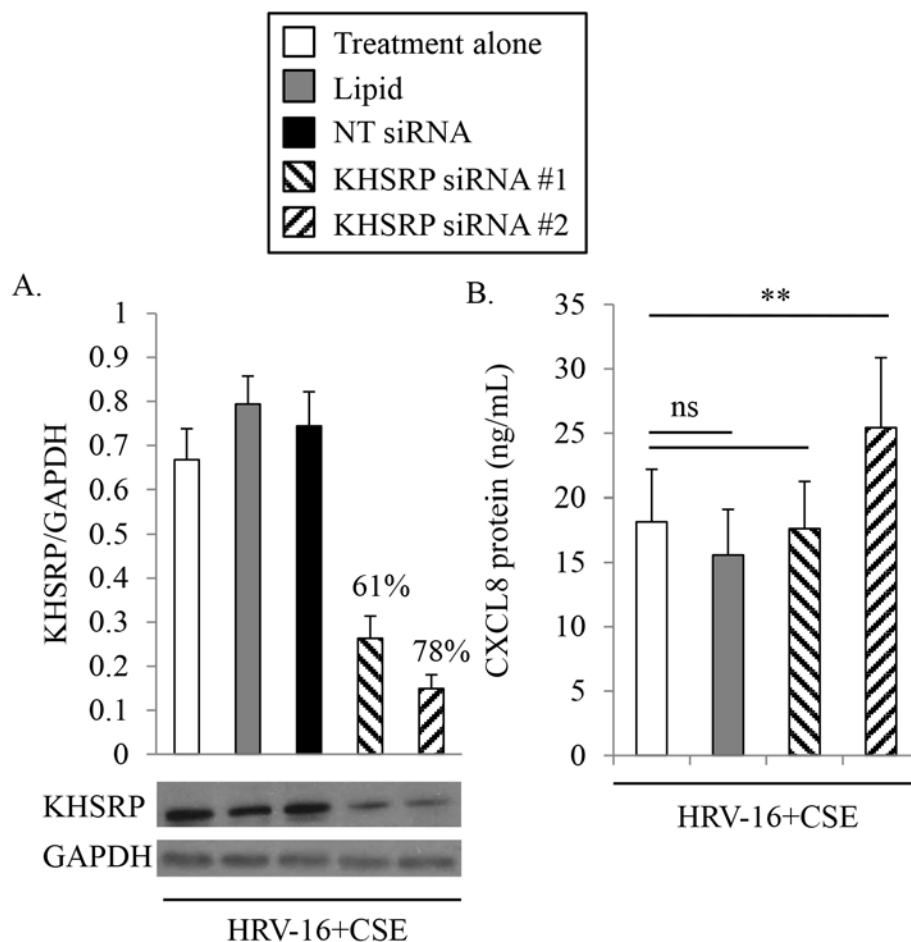


**Figure 6.9: Effects of KHSRP-targeting siRNA on CXCL8 protein expression in airway epithelial cells.**

HBE cells were treated for 24 h prior to harvesting cell supernatants for analysis with ELISA and whole cell lysates for analysis with immunoblotting. To determine the level of KHSRP protein knock-down membranes were probed with a specific KHSRP antibody, then were subsequently stripped and re-probed with an antibody to GAPDH to ensure equal protein loading (A; representative of 3 separate experiments). Densitometry analysis with % knock-down relative to HRV-16+CSE alone is also shown (A; n=3). Cell supernatants were analyzed for CXCL8 protein (B; n=5). Data are presented as mean  $\pm$  SEM. Lipid denotes transfection reagent alone. NT denotes non-targeting control siRNA. Asterisks denote a significant difference between the specified treatments (\*\*p<0.01). ns = not significant.

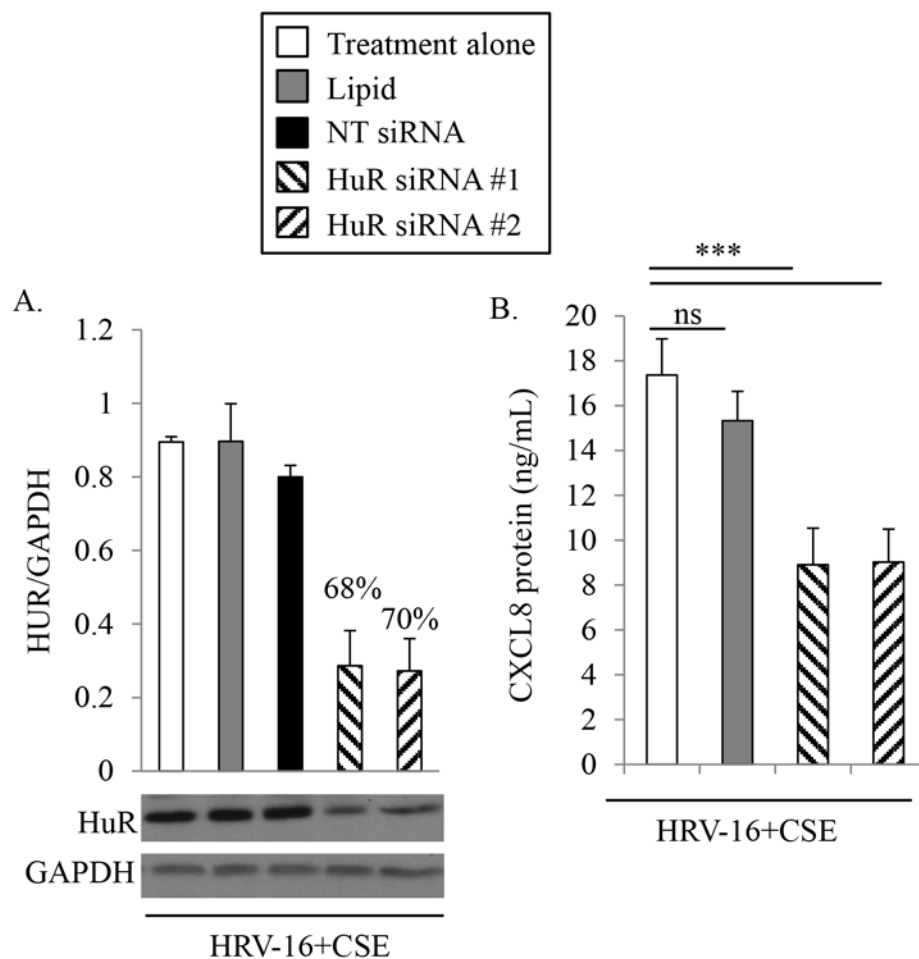


**Figure 6.10: Effects of HuR-targeting siRNA on CXCL8 protein expression in airway epithelial cells.**

HBE cells were treated for 24 h prior to harvesting cell supernatants for analysis with ELISA and whole cell lysates for analysis with immunoblotting. To determine the level of HuR protein knock-down membranes were probed with a specific HuR antibody, then were subsequently stripped and re-probed with an antibody to GAPDH to ensure equal protein loading (A; representative of 3 separate experiments). Densitometry analysis with % knock-down relative to HRV-16+CSE alone is also shown (A; n=3). Cell supernatants were analyzed for CXCL8 protein (B; n=6). Data are presented as mean  $\pm$  SEM. Lipid denotes transfection reagent alone. NT denotes non-targeting control siRNA. Asterisks denote a significant difference between the specified treatments (\*\*\*)  $p < 0.001$ .

## 6.4 Discussion

This chapter investigated the mechanism behind the novel observation first reported in **Chapter 3**, that the combination of HRV-16+CSE enhanced CXCL8 expression, at least additively, above either HRV-16 or CSE treatment alone in airway epithelial cells.

Initially, a CXCL8 promoter-luciferase reporter plasmid was used to determine if CXCL8 induction was being regulated transcriptionally. In agreement with previous literature<sup>323</sup>, HRV-16 treatment alone induced CXCL8 promoter activation. Although CSE enhanced epithelial expression of both CXCL8 mRNA and protein, a novel observation was made that it did not induce CXCL8 promoter activation. Furthermore, this study has shown, for the first time that the combination of HRV-16+CSE did not enhance HRV-16-induced CXCL8 promoter activation, despite the more than additive induction of steady state CXCL8 mRNA, but rather, CSE caused a significant inhibition of this activation. It has been reported here and in prior publications that HRV-induced CXCL10 promoter activation is inhibited in the presence of CSE<sup>355,445</sup>. Evidence provided in **Chapter 5** show that in the case of CXCL10, this reduction is regulated partially via NF- $\kappa$ B. Since CXCL8 has been shown to be, in part, regulated transcriptionally through NF- $\kappa$ B<sup>283,307,308,489</sup>, inhibition of HRV-16-induced CXCL8 promoter activation by CSE is consistent with the regulation of HRV-16-induced CXCL10 by CSE. Although previous literature has shown that CSE can modulate the transcription factors C/EBP- $\beta$  and AP-1<sup>456,458,475-480</sup>, the data here suggest these transcription factors are not contributing to transcriptional activation of CXCL8 by the combined treatment of HRV-16 and CSE. It is, however, possible that their inhibition is contributing to transcriptional repression of HRV-16-induced CXCL8 by CSE.

In summary, the data presented here suggest that HRV-16-induced CXCL8 protein enhancement by CSE is not regulated on the transcriptional level, and other avenues of regulation needed to be examined.

It is widely accepted that CXCL8 gene expression can be regulated via mRNA stabilization. In this study, the enhancement of CXCL8 by HRV-16+CSE did not appear to be regulated on the transcriptional level, but rather via mRNA stabilization as evidenced by the actinomycin D chase assay and the involvement of the p38 MAPK pathway. The actinomycin D data suggest that the increased stability of CXCL8 mRNA with the combined treatment of HRV-16 and CSE compared to either treatment alone could explain the enhancement of CXCL8 protein levels. Both HRV-16 and CSE alone induced phosphorylation of p38 MAPK and, at the earliest time-point this induction by the combination of stimuli was additive. The fact that induction by the combination of HRV-16 and CSE became less than additive at later time-points when mRNA was still stable raises questions about whether the p38 MAPK pathway is the sole mechanism regulating mRNA stability. Nonetheless, selective inhibition of the p38 MAPK pathway reduced CXCL8 production by each stimulus alone, with significant effects on CSE and particularly on CXCL8 production by the combination of HRV-16 and CSE, clearly indicating that this pathway plays a role in the synergistic induction of CXCL8 induction by these stimuli.

Although significant CXCL8 mRNA stabilization was observed using the actinomycin D chase assay with the combined treatment of HRV-16+CSE, CSE alone did not stabilize CXCL8 mRNA despite the induction of CXCL8 protein without increase in promoter drive. The reasons for this are unclear. It is possible that mRNA stabilization of

CXCL8 by CSE is occurring at a later time-point than was assessed using the actinomycin D chase assay. Alternatively, the higher transcription rate induced by HRV-16 is making the mRNA stabilization effect noticeable with the actinomycin D chase assay and basal transcription of CXCL8 is not sufficient to see this mRNA stabilization effect using this assay. In either case, it is also possible that a build-up of mRNA is needed, such as that induced early with HRV-16+CSE, in order to allow mRNA stabilizing factors to have ample product to act on.

At least four ARE binding proteins have linked to the regulation of CXCL8 gene stability, including AUF-1, TTP, KHSRP and HuR. Initial investigation focused on whether CSE, HRV-16 or the combined treatment was having an effect on protein expression levels of AUF-1, TTP, KHSRP or HuR. Although AUF-1, KHSRP and HuR were all constitutively expressed at early time-points in human airway epithelial cells, treatment with CSE alone, HRV-16 alone or HRV-16+CSE did not modulate the expression level of either of these proteins within the time frame in which CXCL8 mRNA stabilization occurs. TTP protein expression was not detected in either HBE or BEAS-2B cells regardless of treatment using two different antibodies; therefore it is unlikely that the expression of TPP would be contributing to CXCL8 gene regulation by HRV+CSE. These data imply that, if AUF-1, KHSRP or HUR are involved the enhancement of HRV-induced CXCL8 by CSE, it is not via modulation of their expression levels.

Although expression levels of AUF-1, KHSRP or HuR were not altered, it remained possible that treatment with CSE, HRV-16 or HRV-16+CSE could affect the activation or the localization of these proteins within the cell. As evidence of this, the activity of TTP,

KHSRP and HuR have been shown to be regulated by phosphorylation<sup>380,394,403</sup>. Unfortunately, antibodies detecting activated forms of these proteins are not readily available. In addition, when activated, HuR translocates from the nucleus to the cytoplasm, where it can exert stabilizing effects on newly synthesized gene transcripts<sup>395,398,401,403,490</sup>. To further assess the role of these stabilizing/destabilizing proteins in enhancement of HRV-16-induced CXCL8 by CSE, siRNA knock-down of each of AUF-1, KHSRP and HuR was performed.

Despite using AUF-1-targeting siRNA duplexes from two different suppliers targeting different regions of the molecules, knock-down all four AUF-1 isoforms was unsuccessful. The reasons for this are unclear but could be better achieved with siRNAs targeting each individual isoform. The siRNA did successfully reduce expression of the largest isoform (45kDa), but this resulted in no significant change in HRV-16+CSE-induced CXCL8 protein expression. These data suggest that the 45 kDa isoform of AUF-1 is not involved in the enhancement of CXCL8 protein following treatment with HRV-16+CSE compared to either treatment alone, but no firm conclusions can be drawn regarding the other isoforms. The 40 and 45 kDa isoforms of AUF-1 are purported to be involved in de-stabilizing mRNA, the 42 kDa isoform in stabilizing mRNA, while the 37 kDa isoform is involved in either stabilizing/destabilizing mRNA<sup>390</sup>. Since there was a very strong basal expression of the 42kDa isoform of AUF-1, it would have been valuable to determine if it was contributing to the stabilization of CXCL8 mRNA. Unfortunately, knock-down of this isoform was not achieved with two separate AUF-1-targeting siRNA duplexes from two different suppliers.

Specific siRNA targeting KHSRP resulted in substantial knock-down of this protein but this has no inhibitory effect on the expression of CXCL8 following treatment with HRV-16+CSE. One of the two siRNA duplexes had a slight, but significant, effect on enhancing CXCL8 protein levels in cells treated with HRV-16+CSE. Accordingly, KHSRP may be involved in dampening the expression of CXCL8, but since only one of the two siRNAs had this effect, this result is inconclusive. The discrepancy between the two siRNA duplexes is unclear, and a third siRNA may have helped to resolve this difference, although this would not have helped to explain how CSE modulates HRV-induced CXCL8 expression. These data suggest that, although KHSRP may be involved in globally dampening CXCL8 protein expression, it is most likely not involved in the enhancement of CXCL8 protein following treatment with HRV-16+CSE compared to either treatment alone.

Knock-down of HuR was also successful using two different siRNA duplexes, and in contrast to AUF-1 and KHSRP, abrogation of HuR resulted in inhibition of the increased CXCL8 production observed upon combined stimulation with HRV-16+CSE. These data suggest that HuR is involved in stabilizing CXCL8 mRNA when HBE cells are treated with HRV-16+CSE, leading to elevated protein levels compared to cells treated with HRV-16 alone.

In summary, the data in this chapter show, for the first time, that the enhancement of HRV-induced CXCL8 in human airway epithelial cells by CSE compared to either treatment alone is regulated post-transcriptionally, via mRNA stabilization and HuR plays a key role in this stabilization.

## 6.5 Future Studies

Using specifically designed siRNA to each isoform of AUF-1 would help to delineate the involvement of this protein in the enhancement of CXCL8 induced by HRV+CSE. Since each isoform can behave in a different manner in terms of stabilizing/destabilizing mRNA, this would help to tease out if there is any involvement of any of the AUF-1 isoforms and in what manner they may affect CXCL8 expression.

Using immunoprecipitation assays, future studies could determine the relative association of HuR with the 3' UTR of CXCL8 following stimulus with CSE, HRV alone or the combination of the two stimuli. This would help to correlate the HuR siRNA CXCL8 protein data findings with the regulation of CXCL8 mRNA. Additionally, it could be evaluated whether HuR siRNA directly alters CXCL8 mRNA levels following CSE, HRV or HRV+CSE treatment. This would help to determine whether HuR is the sole factor responsible for the stabilization of CXCL8 mRNA following treatment with HRV+CSE, or if it is only partially contributing to its stabilization.

It has been shown that following an inflammatory stimulus, HuR associates with the 3'UTR of CXCL8 in the BEAS-2B bronchial epithelial cells line and the AMP-activated protein kinase pathway may be contributing to increased nuclear-cytoplasmic shuttling of HuR<sup>395</sup>. A variety of other pathways have also been shown to contribute to the nuclear-cytoplasmic shuttling of HuR<sup>403</sup>. Future studies could determine how the combination of HRV and CSE alters HuR in human bronchial epithelium; whether it is through activation due to phosphorylation and/or regulation of nuclear-cytoplasmic shuttling of HuR.

**Chapter Seven: General Discussion, Limitations, Future  
Directions and Clinical Relevance**

Although a discussion section has been provided in each individual results chapter, a **general discussion** for the overall doctoral thesis project is provided here, including **limitations, future directions, clinical relevance** and, finally, **general conclusions** derived from this body of work as a whole.

## 7.1 General Discussion

### 7.1.1 Rationale of study

Cigarette smoke has profound effects on the human body and is linked to the development and progression of many diseases<sup>177-179</sup>. HRV is one of the most common viral pathogens infecting humans, and it is known to be a major contributing factor to virus-induced exacerbations of airway diseases such as COPD and asthma<sup>1-6</sup>. Both cigarette smoke and HRV encounter the airway epithelium as one of the first cellular points of contact within the human body, and in fact, the airway epithelial cell is the only cell type shown to be infected by HRV *in vivo*<sup>30</sup>. Although many studies have been conducted analyzing the responses in airway epithelial cells following either HRV infection or cigarette smoke exposure, if and how cigarette smoke modulates HRV-induced responses in these cells has not been thoroughly studied. Since smokers have been shown to have worse outcomes during acute respiratory tract infections compared to non-smokers<sup>24-29</sup>, an investigation into the mechanisms underlying this phenomenon was warranted. Therefore, the goal of this thesis was to determine whether cigarette smoke had an effect on HRV-induced inflammatory responses. If an altered response was to be determined, a further investigation into the underlying mechanisms was to take place. The scope of inflammatory

responses was narrowed down to two chemokines, namely CXCL10 and CXCL8, because these chemokines have been shown to be induced during HRV infections both *in vitro* and *in vivo*, as well as they have also been shown to be important mediators in COPD, and in asthmatics who smoke. This investigation was to take place using an *in vitro* airway epithelial cell culture model, in conjunction with purified HRV and cigarette smoke in the form of CSE.

### ***7.1.2 CSE differentially modulates HRV-induced chemokine expression in airway epithelial cells***

**Chapter 3** reports the novel observation that, indeed, CSE does modulate HRV-induced CXCL10 and CXCL8 chemokine responses. Surprisingly, CSE was demonstrated to divergently modulate HRV-induced production of these two chemokines. CSE alone did not induce CXCL10 production in airway epithelial cells but HRV-induced CXCL10 was shown to be potently inhibited by CSE. In contrast, both CSE alone and HRV alone induced CXCL8 production from airway epithelial cells, and when cells were treated with the combination of HRV and CSE, CXCL8 was induced to levels above what either stimulus was capable of alone. This phenomenon was shown not to be limited to a major group HRV (HRV-16) since a similar effect on CXCL10 and CXCL8 protein levels was observed using a member of the minor group of HRV (HRV-1A).

Although it has previously been published that HRV induces CXCL10 from both HBE and BEAS-2B cells<sup>259,297,298</sup>, this study showed, for the first time, that HRV-induced CXCL10 is inhibited in the presence of CSE<sup>445</sup>. This effect was shown both at the mRNA

level, using gene microarray techniques and quantitative real time RT-PCR, as well as at the protein level. In support and validation of these data, a recent publication has concurrently shown that HRV-induced CXCL10 is inhibited in the presence of CSE at both the mRNA and protein level in BEAS-2B cells and at the mRNA level in normal human bronchial epithelial (NHBE) cells<sup>355</sup>.

CXCL10 mRNA, as well as total inflammatory cells including neutrophils and lymphocytes have been shown to be increased in mice following cigarette smoke exposure when compared to control mice<sup>260-262</sup>. Moreover, CXCR3-deficient mice exposed to cigarette smoke show a reduction of inflammation, with fewer total inflammatory cells, neutrophils and lymphocytes in BAL and lung tissue<sup>260,261</sup>. In contrast to these studies but in agreement to the data presented in this thesis, CSE did not induce CXCL10 in a human bronchial epithelial cell line (16-HBEs), human plasmacytoid DCs or in human monocyte derived macrophages<sup>263-266</sup>. Additionally, LPS-, RSV- and IFN- $\gamma$ -induced CXCL10 was significantly inhibited in the presence of CSE in human cells<sup>263-266</sup>. Furthermore, LPS-induced migration of lymphocytes was ablated in the presence of CSE<sup>263</sup>. This suggests that in an *in vitro* cell culture model, CSE generally attenuates stimulus-induced CXCL10 production. The discrepancies between the studies conducted using mouse models and the studies using human cells suggest that the cigarette smoke-induced inflammatory response may differ between the mouse and the human. It is also possible that the response induced by whole cigarette smoke exposure may be different to that induced by soluble CSE. Additionally, length of time of cigarette smoke exposure may also contribute to these reported divergent results. Nonetheless, the data presented in this thesis are in accordance

to that seen with other human cell culture models, regardless of the initial CXCL10-inducing stimulus.

Although, levels of CXCL10 have been reported to be increased in the airways of asthmatic and COPD patients<sup>267,268,273</sup>, conclusions drawn from these studies must be viewed with caution. Costa *et al* measured an increase of CXCL10 in induced sputum from COPD patients compared to non-smoking control subjects, but this was not significant compared to smokers with normal lung function<sup>268</sup>. In addition, there was no significant difference in CXCL10 expression in induced sputum between normal non-smokers and normal smokers<sup>268</sup>. Along the same lines, although CXCR3 positive Th1 cells in smokers with COPD were increased compared to non-smoking subjects (but not compared to smokers with normal lung function), there was no difference between non-smoking subjects and smokers with normal lung function<sup>270</sup>. This suggests that the induction of CXCL10 and subsequent recruitment of CXCR3 positive Th1 cells in COPD patients is due to factors associated with disease pathogenesis, rather than to cigarette smoking *per se*. Moreover, although Ying *et al* had reported an increase in CXCL10 positive cells in both the bronchial mucosa and BAL fluid of patients with severe asthma, COPD patients, as well as current and ex-smokers, compared to non-smoking control subjects, this was only at the mRNA level, and in fact, CXCL10 protein was not significantly different except in the patients with severe asthma<sup>269</sup>. Taken together, these results do not indicate that cigarette smoke is the driving factor for CXCL10 induction, and thus do not contradict the results generated in this thesis. However, it is possible that the observations regarding the modulation of HRV-induced CXCL10 by CSE may differ in airway epithelial cells derived

from asthmatics and COPD patients who smoke. Further study using epithelial cells derived not only from normal human lungs, but those from otherwise healthy smokers, asthma patients who smoke and COPD patients could help clarify this.

In accordance with a previously published study<sup>444</sup>, CSE alone induced CXCL8 production in airway epithelial cells. Unlike this prior publication, this thesis study has, for the first time, demonstrated that CXCL8 is enhanced, at least additively, with the combination of HRV and CSE compared to either stimulus alone. Although the study by Wang and colleagues examined CXCL8 production following exposure to HRV and CSE in airway epithelial cells, they did not show that the combined treatment enhanced CXCL8 above that induced with HRV alone.

In **Chapter 4** it was established that the effects of CSE on HRV-induced chemokine responses was not due to effects on HRV receptor expression or HRV replication. Analysis using flow cytometry techniques indicated that CSE did not alter the number of airway epithelial cells expressing the major group HRV receptor ICAM-1. Interestingly, the number of ICAM-1 receptors per cell was increased by the combination of HRV and CSE, but since this was also the case following HRV treatment alone, the increase following HRV+CSE treatment could be attributed to HRV. Using the viral titre assay, this chapter also reported that HRV titre was not affected by CSE in a relevant time frame to affect the changes in observed CXCL10 and CXCL8 chemokine responses.

Taken together, the results presented in **Chapter 3** and **Chapter 4** demonstrated that HRV-induced CXCL10 and CXCL8 were differentially regulated by CSE, and that this

observed modulation was not due to alterations in HRV-receptor expression or effects on viral titre.

### ***7.1.3 CSE inhibits HRV-induced CXCL10 via multiple mechanisms***

Multiple mechanisms regulating the inhibition of HRV-induced CXCL10 are reported in **Chapter 5**. Since previous literature has highlighted that HRV-induced CXCL10 is regulated mainly at the level of transcription<sup>259,297,298,338,345</sup>, this was the starting point for mechanistic studies in this chapter.

Promoter-luciferase studies indicated that CSE inhibited HRV-induced transcriptional activation of CXCL10. Interestingly, and in line with data presented in **Chapter 4**, poly [I:C]-induced CXCL10 promoter activation was also significantly inhibited by CSE. The involvement of AP-1 in HRV-induced CXCL10 suppression by CSE was ruled out using point mutation studies. Since point mutations of the ISRE and both NF- $\kappa$ B binding sites were inconclusive, other approaches were used to examine their involvement.

Using tandem repeat luciferase constructs of both NF- $\kappa$ B CXCL10-specific binding sites, it was determined that both of these sites were playing a partial role in HRV-induced CXCL10 inhibition by CSE. In support of this, EMSA studies demonstrated that the binding and/or translocation of the HRV-induced p50 and p65 subunits were reduced following CSE treatment. Moreover, examination of I $\kappa$ B- $\alpha$  showed that HRV-induced phosphorylation of this inhibitor was reduced by CSE in a relevant time frame. Moreover, EMSA analysis also showed that binding and/or translocation of a HRV-induced

transcription factor to the CXCL10-specific ISRE binding site was reduced by CSE. In agreement with previously published studies<sup>298</sup>, the transcription factor binding to this site was confirmed to be IRF-1. In accordance with this, HRV-induced IRF-1 mRNA and protein were inhibited by CSE.

Although regions distal to the ISRE and NF- $\kappa$ B binding sites in the CXCL10 promoter have been suggested to be important in HRV-induced CXCL10 production, this had not been explored in any detail. Initial truncations of the CXCL10 promoter confirmed that these regions were, indeed, important in HRV-induced activation of the CXCL10 promoter. Additionally, the data suggested that this region of the CXCL10 promoter may also be involved in the inhibition of HRV-induced CXCL10 by CSE. Due to technical issues, further investigation using point mutations were inconclusive as to the involvement of two putative STAT sites in the distal portion of the CXCL10 promoter. Alternate approaches, therefore, were again used to examine this. The involvement of the JAK/STAT pathway in the induction of CXCL10 protein was confirmed via inhibition studies. EMSA analysis using a CXCL10-specific STAT oligonucleotide revealed that a DNA-protein complex was formed following HRV infection of airway epithelial cells. Moreover, the formation of this complex was substantially inhibited by CSE. Supershift analysis revealed that STAT-1 and/or STAT-2 were involved in the formation of this complex. Interestingly, STAT-1 mRNA, protein and activation by phosphorylation were all suppressed by CSE, while activated STAT-2 could not be detected in airway epithelial cells. Taken together, these data suggest that STAT-1 is involved in HRV-induced CXCL10, likely via binding to two STAT recognition sequences in the CXCL10 promoter, and this is also suppressed by

CSE. The lack of activation of STAT-2 raised the possibility that the antibody to STAT-2 used for EMSA supershifts was not specific.

Examination of upstream signalling pathways linked to the recognition of the HRV dsRNA replication intermediate, showed that HRV induced both RIG-I and MDA5. Additionally, both of these helicases were suppressed by CSE, and in a relevant time frame to potentially affect HRV-induced CXCL10 generation. Additional experiments using siRNA knock-down indicated that MDA5, but not RIG-I, was directly linked to HRV-induced CXCL10. Whether the induction of the MDA5 pathway by HRV was directly linked to activation of NF- $\kappa$ B, IRF-1 or STAT-1 is unknown, but future studies could focus on deciphering this. It is possible that activation of NF- $\kappa$ B, IRF-1 and STAT-1 could be through MDA5-induced signalling and/or via non-MDA5-dependent signalling.

Although CXCL10 has been shown to be regulated mainly at the transcriptional level, there is some precedent in the literature for this gene to be regulated by post-transcriptional mechanisms, particularly by mRNA stabilization/destabilization<sup>491-495</sup>. Accordingly, analysis of the CXCL10 '3 UTR reveals one short ARE (AUUUA)<sup>259</sup>. Not unlike CXCL8, the p38 MAPK pathway has been linked to CXCL10 mRNA stabilization<sup>493-495</sup>. Although an enhancement of p38 MAPK activation is seen with the combined stimulus of HRV and CSE in this thesis study, this does not accurately correlate with the down-regulation of CXCL10 mRNA at 24 h. The stabilizing/destabilizing protein AUF-1 has been shown to be up-regulated 24 and 48 h post HRV infection of bronchial epithelial cells, and this correlates with a decrease of CXCL10 mRNA after 24 h<sup>259</sup>. It is possible that if isoforms of this protein which are involved in destabilization of mRNA are

enhanced, either in expression or activation, with the combination of HRV+CSE at later time-points, that this may be contributing to decreased expression of CXCL10 mRNA.

In **Chapter 5** it was shown that the suppression of HRV-induced CXCL10 by CSE was also regulated, at least in part, epigenetically. Specifically, using a chromatin accessibility assay, analysis showed that CSE caused a reduction in HRV-induced chromatin accessibility around the transcriptional start site of the CXCL10 promoter. In other words, the induction of CXCL10 by HRV caused an unwinding and ‘opening’ of the chromatin around the CXCL10 transcriptional start site, likely allowing for binding of induced transcription factors, while CSE suppressed the degree of this HRV-induced ‘opening’ of chromatin. This correlates with the reduction in HRV-induced CXCL10 mRNA and protein inhibition by CSE, although not to the same quantitative degree. The reason for this may be that the potent inhibition of HRV-induced CXCL10 by CSE is a cumulative effect of the suppression of many factors. Decreased chromatin accessibility leads to a reduction in CXCL10 and this is then further reduced by the cumulative, modest suppression of multiple transcription factors and signalling pathways that lead to HRV-induced CXCL10 generation.

At first glance, the reduction in chromatin accessibility by CSE may appear to contradict the effects cigarette smoke has been reported to have on epigenetic alterations. It is reported that HDAC levels are suppressed in cigarette smokers, COPD patients and smoking asthmatics, and that this correlates with increased pro-inflammatory gene expression<sup>413-415,420,421,426</sup>. Although the expression of some genes may be enhanced in smokers, others have been shown to be reduced, suggesting that gene suppression may be

regulated via other mechanisms. Indeed, the tight junction protein E-cadherin is reduced following cigarette smoke exposure and this appears to be due to increased recruitment of HDACs, as HDAC inhibitors reversed the effects of cigarette smoke exposure on E-cadherin<sup>496</sup>. Thus, it is possible that cigarette smoke can concurrently reduce global expression/activation of HDACs but it can also alter the recruitment of the remaining expressed/activated HDACs to select gene promoters.

In summary, the data presented in **Chapter 5** demonstrate that the induction of CXCL10 by HRV is regulated transcriptionally, via mechanisms involving NF- $\kappa$ B, IRF-1 and STAT-1, and CSE inhibits HRV-induced CXCL10 by having a suppressive effect on all of these targets. Furthermore, CXCL10 induction is also dependent on HRV-induced MDA5 signalling, likely following recognition of the dsRNA replication intermediate, and this signalling is also suppressed by CSE. Lastly, CSE reduces HRV-induced accessibility around the transcriptional start site of the CXCL10 promoter. Thus, the inhibition of HRV-induced CXCL10 by CSE is mediated by a cumulative effect of multiple mechanisms resulting in substantial suppression of HRV-induced CXCL10 at the protein level.

#### ***7.1.4 CSE enhances HRV-induced CXCL8 via mRNA stabilization***

**Chapter 6** demonstrated that, not unlike CXCL10, HRV-induced CXCL8 promoter activation is suppressed by CSE. Since HRV-induced CXCL8 expression is regulated by NF- $\kappa$ B, and it was shown that NF- $\kappa$ B is inhibited by CSE; this data did not contradict the findings reported in **Chapter 5**. However, this result did not explain how CXCL8 mRNA and protein were enhanced by the combined treatment of HRV and CSE, except that it was

not via transcriptional mechanisms. Therefore, other avenues were explored in order to explain this observation. Since CXCL8 is known to be regulated not only transcriptionally, but also post-transcriptionally via mRNA stabilization, this was an obvious starting point to initiate further investigation.

Using actinomycin D chase studies it was shown that combined treatment with HRV and CSE significantly reduced the rate of CXCL8 mRNA degradation over time. This stabilization occurred at early time-points and correlated with the enhancement of CXCL8 mRNA by HRV+CSE seen as early as 5 h post treatment. The p38 MAPK pathway, which has been linked to mRNA stabilization, was also more activated at early time-points following the combined treatment. A further investigation of ARE-BPs linked to CXCL8 mRNA stability was conducted and revealed that three of the four of these proteins were expressed in airway epithelial cells, but surprisingly, none of these proteins were noticeably affected in expression level by CSE, HRV or the combined stimulus. As an alternate approach, involvement of individual ARE-BPs in HRV+CSE-induced CXCL8 generation was explored using siRNA knock-down studies targeting each of these ARE-BPs. These investigations demonstrated that HuR was playing a significant role in the enhanced production of CXCL8 by HRV and CSE compared to either stimuli alone. Unfortunately, no conclusion could be drawn regarding the involvement of 3 of the 4 isoforms of AUF-1, as the specific siRNAs used only knocked-down protein expression of the 45 kDa isoform of AUF-1. Nonetheless, taken together, the data presented in **Chapter 6** support the novel observation that CXCL8 enhancement by HRV and CSE is mediated, at least in part, via HuR-mediated mRNA stabilization.

## 7.2 Limitations

Although studies for this thesis project were carefully conducted and controlled as much as possible, no study is without limitations. Some of these limitations will be addressed below.

There are a variety ways of exposing cells and tissues to cigarette smoke in the laboratory and, thus far, no standard method has been generally accepted<sup>497</sup>. Two main cigarette smoke exposure systems have been reported, namely, gas phase exposure and aqueous extract exposure<sup>497</sup>. Gas phase exposure utilizes a system whereby a cigarette smoke is ‘puffed’ into the exposure chamber, such as an incubator. This is usually achieved using a commercially engineered, single or multiple port, smoking machine. The cells or tissues are kept in the incubator for a desired length of time with exposure to gaseous cigarette smoke which is funneled into the airspace of the incubator. Cells exposed to the smoke can either remain static, with medium covering the surface, or be gently rocked to directly expose the cells to the gaseous cigarette smoke. An advantage of this approach is that the cells are exposed to the same phase of cigarette smoke as that which would occur *in vivo*, and, moreover, the duration and frequency of exposure can be easily manipulated. The other, more accessible and economically feasible method, involves the use of an aqueous extract prepared from the combustion of cigarettes. This is achieved by ‘smoking’ a cigarette using either a manual or mechanical pump, which allows the captured cigarette smoke to be bubbled directly into a solution that can subsequently be used to treat cells. Variations of this method use either cell culture medium, a buffered saline solution or even

DMSO to collect the aqueous extract. The length of time to combust the cigarette, the number of cigarettes used and the volume of aqueous solution used vary widely throughout published studies. Some, but not all, investigators then filter the extract to remove any larger particulate matter that may have collected. This filtered extract is either placed directly on cells, diluted with medium or standardized using a spectrophotometer at 320 nm prior to dilution. Thus, although these are the two main methods of cigarette smoke exposure for *in vitro* tissue culture experimentation, the methods are highly varied and hinder the ability to make general conclusions from different research groups. Therefore, this limitation applies not only to this study but to all other studies that analyze cell responses to cigarette smoke exposure *in vitro*. A rigorously defined, universally accepted protocol for cigarette smoke exposure in the cell/tissue culture model would allow for more justified general conclusions and, likely, more consistent conclusions between research groups.

For this thesis project, an aqueous cigarette smoke extract was prepared with the aim of mimicking the solubilized components of cigarette smoke that one would presumably find in the ASF lining the human airway epithelium of a smoker. Although this was done in order to reflect cigarette smoke exposure *in vivo*, this procedure is not without limitations. As mentioned above, direct exposure to gaseous phase cigarette smoke in a humidified, temperature controlled environment may have provided a more reflective representation of that which is seen *in vivo*.

Another limitation of the CSE exposure system is that the data collected for this thesis project reflect changes that have occurred based on a single, relatively acute exposure

to CSE. One may argue that this is not reflective of the physiological chronic cigarette smoke exposure that is seen in smokers *in vivo*, and multiple exposures could have changed the conclusions that were drawn from this study. Unfortunately, chronic exposure to cigarette smoke in the cell culture system is near impossible since the lifespan of cultured cells is a few weeks at best. In addition, repeated acute exposures can cause cell death. This could, in part, be overcome by using primary epithelial cells cultured from brushings derived from chronic cigarette smokers themselves. Moreover, epithelial cells derived from asthmatic subjects (smokers and non-smokers) and COPD patients could add additional insight into how cigarette smoke modulates HRV-induced responses in a disease model.

CSE exposure to epithelial cells used in this study could have been performed by utilizing epithelial cells that were differentiated at air-liquid-interface (ALI) rather than an undifferentiated, submerged monolayer epithelium. Although this would better reflect the epithelial cell structure and composition of the human airways, the disadvantage of differentiated ALI epithelium is that it takes a substantially longer time to culture prior to utilization for studies, these cells are much harder to infect with HRV, and certain tools, such as transfection of siRNA, become much more difficult to accomplish in this cell culture system.

Another limitation of this study is that culture of airway epithelial cells alone may not completely explain the physiologically relevant responses that are occurring *in vivo*. Undoubtedly, the interaction of cells in the airways contributes to inflammatory responses observed following HRV infection. Although, thus far, only airway epithelial cells have been shown to be infected by HRV *in vivo*, this does not rule out that other cell types, either

in the lumen of the airways, such as macrophages, or sub-epithelial cells, such as fibroblasts and airway smooth muscle cells, are not responding to HRV, either in a replication dependent or independent manner, and contributing to epithelial responses via paracrine effects. It is feasible to think that in asthmatics where epithelial cell damage occurs, sub-epithelial cells may become more accessible for HRV infection. It has been shown that HRV-induced CXCL10 responses are enhanced when airway epithelial cells are either co-cultured with monocytes or supernatants from HRV-infected monocytes are added to epithelial cells, indicating that monocytic cells can release factors that contribute to an additional increase of CXCL10 by airway epithelial cells<sup>498</sup>. Again, if monocytes can respond to HRV exposure by producing soluble products, then, since HRV infects the lower airways, where monocytic cells tend to be the predominant immune cell, it is feasible that these cells could become infected or stimulated. Studies *in vitro* have shown that HRV enter monocytes and macrophages, but does not replicate inside them<sup>499,500</sup>. Interestingly, it has been shown that CXCL10 is produced from HRV-infected monocytic cells in a replication-independent manner<sup>359</sup>. Moreover, although cigarette smoke has been shown to affect airway epithelial cell responses both in the current thesis and in many other studies, it is not the only cell type in the lung that is subject to this noxious agent. It is possible that inflammatory responses induced by cigarette smoke in other cell types in the lung may be releasing factors that have a paracrine effect on the airway epithelium.

In summary, although significant limitations are acknowledged for this thesis study, the results generated from the current project provide novel insight into cigarette smoke-mediated changes that are occurring in airway epithelial cells infected with HRV. An

extension of this project addressing the limitations above would enhance the data generated here and provide additional insight into how cigarette smoke may alter HRV-induced epithelial responses *in vivo*.

### 7.3 Future Directions

Although possibilities for additional experiments stemming from the ones presented in each chapter have already been discussed, here possibilities to expand the project as a whole will be addressed. In particular, this thesis project concentrated on addressing the main research question using an *in vitro* human cell culture model, but this study could be expanded and enhanced using an appropriate *in vivo* model.

A common starting point for an *in vivo* model is the use of an established animal model, and although numerous options are available, the mouse model is by far the most commonly used for studies of cigarette smoke exposure. There would be several possibilities using a mouse model to expand this project. One, this tool could be used to explore if and how gaseous cigarette smoke exposure alters HRV-induced responses in the otherwise healthy mouse lung. One limitation of this model is that it only allows examination of lung responses as a whole, since isolating airway epithelial responses would not be possible. Moreover, although countless studies have been conducted using mice exposed to gaseous cigarette smoke, either acutely or chronically, there are several hurdles that would have to be overcome. One of these hurdles is the addition of HRV, since murine ICAM-1 does not recognize major group HRV. Rather than using a major group HRV, a minor group member of this virus could be used, which is readily recognized by the mouse

LDL receptor. To date, a handful of studies examining minor group HRV-infection in the mouse have been successfully conducted<sup>155,443,501-504</sup>. In **Chapter 3** it was shown that the seminal observations of this thesis utilizing major group HRV also apply to a minor group HRV, thus, using minor group HRV in the mouse could be an appropriate model for further study. It must be noted, however, that the murine model of HRV infection has several major limitations (discussed below) that distinguish it from human disease. Alternatively, since a transgenic mouse expressing human ICAM-1 has been generated<sup>501</sup>, this could also be a possibility for future investigation, although many of the same limitations apply. Another hurdle with the mouse model is that, although mice express a homolog of human CXCL10<sup>505</sup>, they do not express a homolog of human CXCL8. In order to address this, other CXCR2-specific neutrophil chemoattractants, such as macrophage inflammatory protein-2 (MIP-2) and keratinocyte-derived chemokine (KC) expressed in the mouse<sup>506</sup>, could be measured in the mouse as a surrogate to the human CXCL8 readout.

Another possibility to extend this project using a mouse model would be to use a disease model in conjunction with HRV infection and cigarette smoke exposure. There are a variety of mouse models of ‘asthma’, or more accurately, allergic airway inflammation, that could be utilized for this purpose<sup>507-512</sup>. Additionally, an injury-induced model of COPD (elastase- or LPS-induced) has been used to model emphysematous destruction and ‘chronic’ inflammation, but a more relevant cigarette-exposure model of COPD could be established since, thus far, there is no consistent model of cigarette smoke-induced COPD in the mouse<sup>513</sup>.

Although using a mouse model does provide attractive possibilities for future studies there would be some limitations. Unfortunately, mice do not completely replicate the anatomical or genetic characteristics and physiological and pharmacological responses seen in humans. In addition, infection of mice requires doses of HRV many orders of magnitude greater (10,000 to 100,000 fold) than needed to infect humans, and there is no sustained viral replication in the mouse. Other animal models are also a possibility to extend this project, but they also have either similar or additional obstacles/limitations.

Arguably, the best *in vivo* model to use for the extension of this project is the human. The Proud-Leigh laboratory has recently obtained permission to begin experimental HRV infections in the human. Thus, experimental HRV infections could be conducted in volunteers in order to compare HRV-induced responses and outcomes between healthy subjects, smokers (current and former), as well as asthmatic subjects who smoke and asthmatic subjects who are non-smokers. Ethical issues preclude these kinds of studies in patients with COPD. It would be of interest to see if levels of CXCL10 and CXCL8 are influenced in a similar manner by cigarette smoke in the human lung. Addressing the difference between current and former smokers, and healthy non-smokers, would provide additional information if cigarette smoke induced changes during HRV-infections endure over time or whether they are reversible.

#### **7.4 Clinical Relevance**

The airway epithelial cell is the principal site of HRV infection. Because HRV does not cause overt epithelial cytotoxicity, it is generally believed that HRV-induced alterations

in epithelial biology are responsible for initiating symptoms of the common cold and triggering exacerbations of lower airway diseases. It has been demonstrated that infection of human airway epithelial cells with HRV, either *in vitro* or *in vivo*, induces expression of a large number of genes that could regulate airway inflammatory status. Among these are the chemokines, CXCL10 and CXCL8.

It has previously been shown that CXCL10-deficient mice demonstrate increased viral replication and mortality in response to viral infection<sup>257</sup>. Thus, it is feasible that CSE-induced suppression of CXCL10 could impair host defence against HRV. Indeed, it has been reported that there is deficient induction of CXCL10 in HRV-infected BAL cells from COPD patients compared to non-smoking control subjects<sup>514</sup>. Since experimentally HRV-infected COPD patients have been reported to have worse symptoms of longer duration compared to otherwise healthy smokers<sup>514</sup>, a reduction in CXCL10 may, in part, contribute to these clinical outcomes. Although, based on the results presented in this thesis, it would be expected that CXCL10 would also be decreased in otherwise healthy smokers during HRV infection, the consequence of this outcome may be exaggerated in COPD patients due to other disease-related immune response impairments.

Thus far, it is still unclear whether COPD patients have increased susceptibility to viral infections, and further studies are needed to delineate this. However, there is some evidence that COPD patients experimentally infected with HRV have a higher viral load as compared to otherwise healthy smokers<sup>515</sup>. Interestingly, it has also been shown in mice that are exposed to cigarette smoke and infected with influenza virus, that there is increased viral load in the lung compared to mice which were not exposed to cigarette smoke<sup>207</sup>.

Cigarette smoke-mediated impairment of host defenses may not be limited to viral infections as it has also been shown that LPS-induced CXCL10 is also reduced by CSE<sup>263</sup>. This suggests that cigarette smoke may also impair host defenses against bacteria. Thus, this thesis adds to the body of literature that suggests cigarette smoke generally impairs the host defense against pathogens. This would suggest that some of the same mechanisms may be at play mediating both altered viral and bacterial host responses in smokers compared to non-smokers.

While CXCL10 is involved in the recruitment of activated T lymphocytes and NK cells, CXCL8 is one of the most potent chemoattractants for neutrophils. Excessive neutrophil recruitment and activation has been linked to severity in COPD, and during viral exacerbations of asthma. Therefore, if the dysregulation reported in this thesis regarding HRV-induced CXCL10 and CXCL8 chemokine expression by cigarette smoke is also seen *in vivo*, it may help to explain why smokers have longer and more severe HRV respiratory tract infections. A reduction of HRV-induced CXCL10 by cigarette smoke would presumably result in decreased recruitment of cells involved in clearing viral infection, namely T lymphocytes and NK cells. In contrast, enhancement of CXCL8 by the combination of HRV infection and cigarette smoke would likely lead to an increase in neutrophilic inflammation, resulting in over exuberant neutrophil-mediated inflammatory events. In other words, the consequence of cigarette smoke induced chemokine dysregulation would lead to a suppressed host defence response, while, at the same time, exaggerating the pro-inflammatory response, leading to a worse clinical outcome. Given that increased inflammation and impaired lung function is already seen in asthmatic and

COPD patients, smokers with these diseases may be expected to have the most severe clinical outcomes during viral exacerbations of these lower airway diseases.

### 7.5 Overall Conclusions

This thesis provides the first demonstration that CSE differentially regulates HRV-induced chemokine responses in human airway epithelial cells. HRV-induced CXCL10 is potently inhibited by CSE while the combination of HRV and CSE induces CXCL8 above either stimulus alone. This study also provides the first detailed mechanistic analyses of these effects. The inhibition of CXCL10 is regulated via multiple mechanisms involving the inhibition of transcription factors NF- $\kappa$ B, IRF-1 and STAT-1, as well as inhibition of the viral sensing MDA5 pathway, shown here to be directly linked to HRV-induced CXCL10 induction, and lastly, by inhibiting HRV-induced chromatin accessibility around the CXCL10 transcriptional start site. In contrast, the enhancement of CXCL8 by HRV and CSE is regulated via post-transcriptional mechanisms, chiefly involving mRNA stability and the stabilizing factor HuR. A schematic summarizing this is presented in **Figure 7.1**. If these effects were to be observed *in vivo*, then HRV infection in smokers could ultimately result in decreased recruitment of activated T lymphocytes and NK cells, while at the same time leading to enhanced recruitment of neutrophils. Functional consequences of this could involve decreased viral clearance and antiviral defence, coupled with exaggerated proteolytic tissue destruction mediated by excess neutrophilia. Thus, this thesis provides evidence as to why HRV infections in smokers are longer and more severe compared to non-smokers. Additionally, this study suggests that similar mechanisms may be at play in

both smoking asthmatics and COPD patients during HRV-induced exacerbations and highlight potential future avenues to target for treatment during these exacerbations.

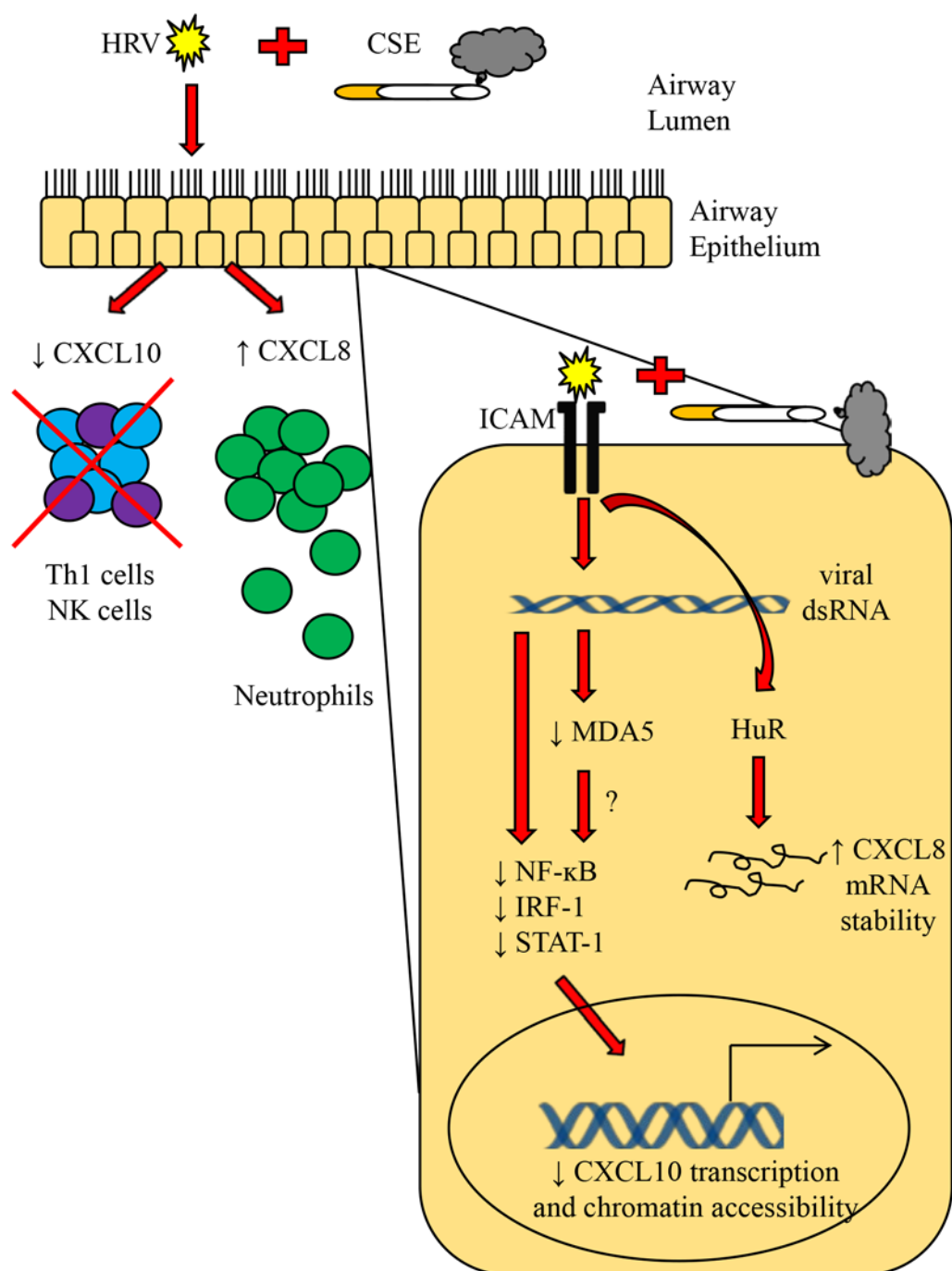


**Figure 7.1: CSE differentially regulates HRV-induced chemokine production in human airway epithelial cells.**

## References

1. Seemungal T, Harper-Owen R, Bhowmik A, et al. Respiratory viruses, symptoms, and inflammatory markers in acute exacerbations and stable chronic obstructive pulmonary disease. *Am. J. Respir. Crit. Care Med.* 2001;164(9):1618–1623.
2. Rohde G, Wiethege A, Borg I, et al. Respiratory viruses in exacerbations of chronic obstructive pulmonary disease requiring hospitalisation: a case-control study. *Thorax.* 2003;58(1):37–42.
3. Greenberg SB, Allen M, Wilson J, Atmar RL. Respiratory viral infections in adults with and without chronic obstructive pulmonary disease. *Am. J. Respir. Crit. Care Med.* 2000;162(1):167–173.
4. Seemungal TA, Harper-Owen R, Bhowmik A, Jeffries DJ, Wedzicha JA. Detection of rhinovirus in induced sputum at exacerbation of chronic obstructive pulmonary disease. *Eur. Respir. J. Off. J. Eur. Soc. Clin. Respir. Physiol.* 2000;16(4):677–683.
5. Johnston SL, Pattemore PK, Sanderson G, et al. Community study of role of viral infections in exacerbations of asthma in 9-11 year old children. *BMJ.* 1995;310(6989):1225–1229.
6. Nicholson KG, Kent J, Ireland DC. Respiratory viruses and exacerbations of asthma in adults. *BMJ.* 1993;307(6910):982–986.
7. To T, Stanojevic S, Moores G, et al. Global asthma prevalence in adults: findings from the cross-sectional world health survey. *BMC Public Health.* 2012;12:204.
8. Patel SN, Tsai C-L, Boudreaux ED, et al. Multicenter study of cigarette smoking among patients presenting to the emergency department with acute asthma. *Ann. Allergy Asthma Immunol. Off. Publ. Am. Coll. Allergy Asthma Immunol.* 2009;103(2):121–127.
9. Silverman RA, Boudreaux ED, Woodruff PG, Clark S, Camargo CA Jr. Cigarette smoking among asthmatic adults presenting to 64 emergency departments. *Chest.* 2003;123(5):1472–1479.
10. Fletcher C, Peto R. The natural history of chronic airflow obstruction. *Br. Med. J.* 1977;1(6077):1645–1648.
11. Broekema M, ten Hacken NHT, Volbeda F, et al. Airway epithelial changes in smokers but not in ex-smokers with asthma. *Am. J. Respir. Crit. Care Med.* 2009;180(12):1170–1178.

12. Althuis MD, Sexton M, Prybylski D. Cigarette smoking and asthma symptom severity among adult asthmatics. *J. Asthma Off. J. Assoc. Care Asthma*. 1999;36(3):257–264.
13. Siroux V, Pin I, Oryszczyn MP, Le Moual N, Kauffmann F. Relationships of active smoking to asthma and asthma severity in the EGEA study. Epidemiological study on the Genetics and Environment of Asthma. *Eur. Respir. J. Off. J. Eur. Soc. Clin. Respir. Physiol*. 2000;15(3):470–477.
14. Venarske DL, Busse WW, Griffin MR, et al. The relationship of rhinovirus-associated asthma hospitalizations with inhaled corticosteroids and smoking. *J. Infect. Dis*. 2006;193(11):1536–1543.
15. Thomson NC, Chaudhuri R, Livingston E. Asthma and cigarette smoking. *Eur. Respir. J. Off. J. Eur. Soc. Clin. Respir. Physiol*. 2004;24(5):822–833.
16. Chalmers GW, Macleod KJ, Little SA, Thomson LJ, McSharry CP, Thomson NC. Influence of cigarette smoking on inhaled corticosteroid treatment in mild asthma. *Thorax*. 2002;57(3):226–230.
17. Chaudhuri R, Livingston E, McMahon AD, Thomson L, Borland W, Thomson NC. Cigarette smoking impairs the therapeutic response to oral corticosteroids in chronic asthma. *Am. J. Respir. Crit. Care Med*. 2003;168(11):1308–1311.
18. Lazarus SC, Chinchilli VM, Rollings NJ, et al. Smoking affects response to inhaled corticosteroids or leukotriene receptor antagonists in asthma. *Am. J. Respir. Crit. Care Med*. 2007;175(8):783–790.
19. Ford ES, Mannino DM, Redd SC, Moriarty DG, Mokdad AH. Determinants of quality of life among people with asthma: findings from the Behavioral Risk Factor Surveillance System. *J. Asthma Off. J. Assoc. Care Asthma*. 2004;41(3):327–336.
20. James AL, Palmer LJ, Kicic E, et al. Decline in lung function in the Busselton Health Study: the effects of asthma and cigarette smoking. *Am. J. Respir. Crit. Care Med*. 2005;171(2):109–114.
21. Eisner MD, Iribarren C. The influence of cigarette smoking on adult asthma outcomes. *Nicotine Tob. Res. Off. J. Soc. Res. Nicotine Tob*. 2007;9(1):53–56.
22. Strine TW, Balluz LS, Ford ES. The associations between smoking, physical inactivity, obesity, and asthma severity in the general US population. *J. Asthma Off. J. Assoc. Care Asthma*. 2007;44(8):651–658.

23. Chalmers GW, MacLeod KJ, Thomson L, Little SA, McSharry C, Thomson NC. Smoking and airway inflammation in patients with mild asthma. *Chest*. 2001;120(6):1917–1922.
24. Cohen S, Tyrrell DA, Russell MA, Jarvis MJ, Smith AP. Smoking, alcohol consumption, and susceptibility to the common cold. *Am. J. Public Health*. 1993;83(9):1277–1283.
25. Gwaltney JM Jr, Hendley JO, Simon G, Jordan WS Jr. Rhinovirus infections in an industrial population. II. Characteristics of illness and antibody response. *Jama J. Am. Med. Assoc.* 1967;202(6):494–500.
26. Blake GH, Abell TD, Stanley WG. Cigarette smoking and upper respiratory infection among recruits in basic combat training. *Ann. Intern. Med.* 1988;109(3):198–202.
27. Marcy TW, Merrill WW. Cigarette smoking and respiratory tract infection. *Clin. Chest Med.* 1987;8(3):381–391.
28. Aronson MD, Weiss ST, Ben RL, Komaroff AL. Association between cigarette smoking and acute respiratory tract illness in young adults. *Jama J. Am. Med. Assoc.* 1982;248(2):181–183.
29. Benseñor IM, Cook NR, Lee IM, et al. Active and passive smoking and risk of colds in women. *Ann. Epidemiol.* 2001;11(4):225–231.
30. Turner RB, Couch RB. Chapter 26: Rhinoviruses. In: Knipe DM, Howley PM, eds. *Fields Virology*. Vol Volume 1. Fifth edition. Lippincott Williams & Wilkins; 2007:896–909.
31. Global Strategy for the Diagnosis, Management and Prevention of COPD. 2013. Available at: <http://www.goldcopd.org/>.
32. The definition of emphysema. Report of a National Heart, Lung, and Blood Institute, Division of Lung Diseases workshop. *Am. Rev. Respir. Dis.* 1985;132(1):182–185.
33. Anderson AE Jr, Foraker AG. Centrilobular emphysema and panlobular emphysema: two different diseases. *Thorax*. 1973;28(5):547–550.
34. Fabbri LM, Luppi F, Beghé B, Rabe KF. Complex chronic comorbidities of COPD. *Eur. Respir. J. Off. J. Eur. Soc. Clin. Respir. Physiol.* 2008;31(1):204–212.
35. Viegi G, Pistelli F, Sherrill DL, Maio S, Baldacci S, Carrozzi L. Definition, epidemiology and natural history of COPD. *Eur. Respir. J. Off. J. Eur. Soc. Clin. Respir. Physiol.* 2007;30(5):993–1013.

36. Stockley RA, Mannino D, Barnes PJ. Burden and pathogenesis of chronic obstructive pulmonary disease. *Proc. Am. Thorac. Soc.* 2009;6(6):524–526.
37. Saetta M, Di Stefano A, Turato G, et al. CD8+ T-lymphocytes in peripheral airways of smokers with chronic obstructive pulmonary disease. *Am. J. Respir. Crit. Care Med.* 1998;157(3 Pt 1):822–826.
38. O’Shaughnessy TC, Ansari TW, Barnes NC, Jeffery PK. Inflammation in bronchial biopsies of subjects with chronic bronchitis: inverse relationship of CD8+ T lymphocytes with FEV1. *Am. J. Respir. Crit. Care Med.* 1997;155(3):852–857.
39. Barnes PJ, Shapiro SD, Pauwels RA. Chronic obstructive pulmonary disease: molecular and cellular mechanisms. *Eur. Respir. J. Off. J. Eur. Soc. Clin. Respir. Physiol.* 2003;22(4):672–688.
40. WHO | Burden of COPD. WHO. Available at: <http://www.who.int/respiratory/copd/burden/en/index.html>. Accessed May 4, 2012.
41. Barnes PJ. Chronic obstructive pulmonary disease: a growing but neglected global epidemic. *Plos Med.* 2007;4(5):e112.
42. Buist AS, McBurnie MA, Vollmer WM, et al. International variation in the prevalence of COPD (the BOLD Study): a population-based prevalence study. *Lancet.* 2007;370(9589):741–750.
43. Decramer M, Janssens W, Miravittles M. Chronic obstructive pulmonary disease. *The Lancet.* 7;379(9823):1341–1351.
44. Miravittles M, Soriano JB, García-Río F, et al. Prevalence of COPD in Spain: impact of undiagnosed COPD on quality of life and daily life activities. *Thorax.* 2009;64(10):863–868.
45. The global burden of disease: 2004 update. 2008.
46. Government of Canada PHA of C. Fast facts about Chronic Obstructive Pulmonary Disease (COPD) 2011. 2011. Available at: <http://www.phac-aspc.gc.ca/cd-mc/publications/copd-mpoc/ff-rr-2011-eng.php#endnote1>. Accessed January 16, 2013.
47. Theriault L, Hermus G, Goldfarb D, Stonebridge C, Fares B. Cost Risk Analysis for Chronic Lung Disease in Canada. 2012. Available at: <http://www.conferenceboard.ca>. Accessed May 31, 2013.
48. Mannino DM, Buist AS. Global burden of COPD: risk factors, prevalence, and future trends. *Lancet.* 2007;370(9589):765–773.

49. Mittmann N, Kuramoto L, Seung SJ, Haddon JM, Bradley-Kennedy C, Fitzgerald JM. The cost of moderate and severe COPD exacerbations to the Canadian healthcare system. *Respir. Med.* 2008;102(3):413–421.
50. Chapman KR, Mannino DM, Soriano JB, et al. Epidemiology and costs of chronic obstructive pulmonary disease. *Eur. Respir. J. Off. J. Eur. Soc. Clin. Respir. Physiol.* 2006;27(1):188–207.
51. WHO | Chronic obstructive pulmonary disease (COPD). WHO. Available at: <http://www.who.int/mediacentre/factsheets/fs315/en/index.html>. Accessed May 8, 2012.
52. Mathers CD, Loncar D. Projections of Global Mortality and Burden of Disease from 2002 to 2030. *Plos Med.* 2006;3(11):e442.
53. Hogg JC, Timens W. The pathology of chronic obstructive pulmonary disease. *Annu. Rev. Pathol.* 2009;4:435–459.
54. Salvi SS, Barnes PJ. Chronic obstructive pulmonary disease in non-smokers. *Lancet.* 2009;374(9691):733–743.
55. Løkke A, Lange P, Scharling H, Fabricius P, Vestbo J. Developing COPD: a 25 year follow up study of the general population. *Thorax.* 2006;61(11):935–939.
56. Fischer BM, Pavlisko E, Voynow JA. Pathogenic triad in COPD: oxidative stress, protease-antiprotease imbalance, and inflammation. *Int. J. Chron. Obstruct. Pulmon. Dis.* 2011;6:413–421.
57. Turino GM. Proteases in copd: A critical pathway to injury. *Chest J.* 2007;132(6):1724–1725.
58. Turino GM. The origins of a concept\*: The protease-antiprotease imbalance hypothesis. *Chest J.* 2002;122(3):1058–1060.
59. MacNee W. OXidants/antioxidants and copd\*. *Chest J.* 2000;117(5\_suppl\_1):303S–317S.
60. Silverman EK, Sandhaus RA. Clinical practice. Alpha1-antitrypsin deficiency. *N. Engl. J. Med.* 2009;360(26):2749–2757.
61. Stoller JK, Aboussouan LS. A review of  $\alpha$ 1-antitrypsin deficiency. *Am. J. Respir. Crit. Care Med.* 2012;185(3):246–259.
62. Stoller JK, Aboussouan LS. Alpha1-antitrypsin deficiency. *Lancet.* 2005;365(9478):2225–2236.

63. Mitchell RS, Silvers GW, Goodman N, Dart G, Maisel JC. Are centrilobular emphysema and panlobular emphysema two different diseases? *Hum. Pathol.* 1970;1(3):433–441.
64. Sapey E, Stockley RA. COPD exacerbations . 2: aetiology. *Thorax.* 2006;61(3):250–258.
65. Celli BR, Barnes PJ. Exacerbations of chronic obstructive pulmonary disease. *Eur. Respir. J. Off. J. Eur. Soc. Clin. Respir. Physiol.* 2007;29(6):1224–1238.
66. Hilleman DE, Dewan N, Malesker M, Friedman M. Pharmacoeconomic evaluation of COPD. 2000. *Chest.* 2009;136(5 Suppl):e30.
67. Rodriguez-Roisin R. Toward a consensus definition for COPD exacerbations. *Chest.* 2000;117(5 Suppl 2):398S–401S.
68. Donaldson GC, Wedzicha JA. COPD exacerbations .1: Epidemiology. *Thorax.* 2006;61(2):164–168.
69. Wedzicha JA, Donaldson GC. Exacerbations of chronic obstructive pulmonary disease. *Respir. Care.* 2003;48(12):1204–1213; discussion 1213–1215.
70. Groenewegen KH, Schols AMWJ, Wouters EFM. Mortality and mortality-related factors after hospitalization for acute exacerbation of COPD. *Chest.* 2003;124(2):459–467.
71. Connors AF Jr, Dawson NV, Thomas C, et al. Outcomes following acute exacerbation of severe chronic obstructive lung disease. The SUPPORT investigators (Study to Understand Prognoses and Preferences for Outcomes and Risks of Treatments). *Am. J. Respir. Crit. Care Med.* 1996;154(4 Pt 1):959–967.
72. Papi A, Bellettato CM, Braccioni F, et al. Infections and airway inflammation in chronic obstructive pulmonary disease severe exacerbations. *Am. J. Respir. Crit. Care Med.* 2006;173(10):1114–1121.
73. Cameron RJ, de Wit D, Welsh TN, Ferguson J, Grissell TV, Rye PJ. Virus infection in exacerbations of chronic obstructive pulmonary disease requiring ventilation. *Intensive Care Med.* 2006;32(7):1022–1029.
74. Sajjan US. Susceptibility to viral infections in chronic obstructive pulmonary disease: role of epithelial cells. *Curr. Opin. Pulm. Med.* 2013;19(2):125–132.
75. Varkey JB, Varkey B. Viral infections in patients with chronic obstructive pulmonary disease. *Curr. Opin. Pulm. Med.* 2008;14(2):89–94.

76. Sethi S, Murphy TF. Infection in the pathogenesis and course of chronic obstructive pulmonary disease. *N. Engl. J. Med.* 2008;359(22):2355–2365.
77. Tsoumakidou M, Tzanakis N, Chrysofakis G, Kyriakou D, Siafakas NM. Changes in sputum T-lymphocyte subpopulations at the onset of severe exacerbations of chronic obstructive pulmonary disease. *Respir. Med.* 2005;99(5):572–579.
78. *GINA Report, Global Strategy for Asthma Management and Prevention.*; 2012.
79. Locksley RM. Asthma and allergic inflammation. *Cell.* 2010;140(6):777–783.
80. Masoli M, Fabian D, Holt S, Beasley R. The global burden of asthma: executive summary of the GINA Dissemination Committee report. *Allergy.* 2004;59(5):469–478.
81. Anandan C, Nurmatov U, van Schayck OCP, Sheikh A. Is the prevalence of asthma declining? Systematic review of epidemiological studies. *Allergy.* 2010;65(2):152–167.
82. Government of Canada SC. Statistics Canada: Canada's national statistical agency. 1995. Available at: <http://www.statcan.gc.ca/start-debut-eng.html>. Accessed May 9, 2013.
83. Bahadori K, Doyle-Waters MM, Marra C, et al. Economic burden of asthma: a systematic review. *Bmc Pulm. Med.* 2009;9(1):24.
84. Lemanske RF Jr, Jackson DJ, Gangnon RE, et al. Rhinovirus illnesses during infancy predict subsequent childhood wheezing. *J. Allergy Clin. Immunol.* 2005;116(3):571–577.
85. Jackson DJ, Gangnon RE, Evans MD, et al. Wheezing rhinovirus illnesses in early life predict asthma development in high-risk children. *Am. J. Respir. Crit. Care Med.* 2008;178(7):667–672.
86. Davies DE. The role of the epithelium in airway remodeling in asthma. *Proc. Am. Thorac. Soc.* 2009;6(8):678–682.
87. Polosa R, Thomson NC. Smoking and asthma: dangerous liaisons. *Eur. Respir. J. Off. J. Eur. Soc. Clin. Respir. Physiol.* 2012.
88. Lange P, Parner J, Vestbo J, Schnohr P, Jensen G. A 15-year follow-up study of ventilatory function in adults with asthma. *N. Engl. J. Med.* 1998;339(17):1194–1200.
89. Jang A-S, Park J-S, Lee J-H, et al. The impact of smoking on clinical and therapeutic effects in asthmatics. *J. Korean Med. Sci.* 2009;24(2):209–214.
90. Neil C Thomson MS. The Role of Cigarette Smoking on Persistent Airflow Obstruction in Asthma.

91. Van Hove CL, Moerloose K, Maes T, Joos GF, Tournoy KG. Cigarette smoke enhances Th-2 driven airway inflammation and delays inhalational tolerance. *Respir. Res.* 2008;9:42.
92. Gangl K, Reininger R, Bernhard D, et al. Cigarette smoke facilitates allergen penetration across respiratory epithelium. *Allergy.* 2009;64(3):398–405.
93. Gallefoss F, Bakke PS. Does smoking affect the outcome of patient education and self-management in asthmatics? *Patient Educ. Couns.* 2003;49(1):91–97.
94. Wark PAB, Johnston SL, Moric I, Simpson JL, Hensley MJ, Gibson PG. Neutrophil degranulation and cell lysis is associated with clinical severity in virus-induced asthma. *Eur. Respir. J. Off. J. Eur. Soc. Clin. Respir. Physiol.* 2002;19(1):68–75.
95. Jackson DJ, Johnston SL. The role of viruses in acute exacerbations of asthma. *J. Allergy Clin. Immunol.* 2010;125(6):1178–1187; quiz 1188–1189.
96. Corne JM, Marshall C, Smith S, et al. Frequency, severity, and duration of rhinovirus infections in asthmatic and non-asthmatic individuals: a longitudinal cohort study. *Lancet.* 2002;359(9309):831–834.
97. Message SD, Laza-Stanca V, Mallia P, et al. Rhinovirus-induced lower respiratory illness is increased in asthma and related to virus load and Th1/2 cytokine and IL-10 production. *Proc. Natl. Acad. Sci. U. S. A.* 2008;105(36):13562–13567.
98. Wark PAB, Johnston SL, Bucchieri F, et al. Asthmatic bronchial epithelial cells have a deficient innate immune response to infection with rhinovirus. *J. Exp. Med.* 2005;201(6):937–947.
99. DeMore JP, Weisshaar EH, Vrtis RF, et al. Similar colds in subjects with allergic asthma and nonatopic subjects after inoculation with rhinovirus-16. *J. Allergy Clin. Immunol.* 2009;124(2):245–252.e3.
100. Hart LA, Krishnan VL, Adcock IM, Barnes PJ, Chung KF. Activation and localization of transcription factor, nuclear factor-kappaB, in asthma. *Am. J. Respir. Crit. Care Med.* 1998;158(5 Pt 1):1585–1592.
101. Pizzichini MMM, Pizzichini E, Efthimiadis A, et al. Asthma and Natural Colds Inflammatory Indices in Induced Sputum: A Feasibility Study. *Am. J. Respir. Crit. Care Med.* 1998;158(4):1178–1184.
102. Gagliardo R, Chanez P, Mathieu M, et al. Persistent activation of nuclear factor-kappaB signaling pathway in severe uncontrolled asthma. *Am. J. Respir. Crit. Care Med.* 2003;168(10):1190–1198.

103. Contoli M, Message SD, Laza-Stanca V, et al. Role of deficient type III interferon-lambda production in asthma exacerbations. *Nat. Med.* 2006;12(9):1023–1026.
104. Lopez-Souza N, Favoreto S, Wong H, et al. In vitro susceptibility to rhinovirus infection is greater for bronchial than for nasal airway epithelial cells in human subjects. *J. Allergy Clin. Immunol.* 2009;123(6):1384–1390.e2.
105. Bochkov YA, Hanson KM, Keles S, Brockman-Schneider RA, Jarjour NN, Gern JE. Rhinovirus-induced modulation of gene expression in bronchial epithelial cells from subjects with asthma. *Mucosal Immunol.* 2010;3(1):69–80.
106. Bullens DMA, Decraene A, Dilissen E, et al. Type III IFN-lambda mRNA expression in sputum of adult and school-aged asthmatics. *Clin. Exp. Allergy J. Br. Soc. Allergy Clin. Immunol.* 2008;38(9):1459–1467.
107. Mackay IM. Human rhinoviruses: the cold wars resume. *J. Clin. Virol. Off. Publ. Pan Am. Soc. Clin. Virol.* 2008;42(4):297–320.
108. Whitton JL, Cornell CT, Feuer R. Host and virus determinants of picornavirus pathogenesis and tropism. *Nat. Rev. Microbiol.* 2005;3(10):765–776.
109. In-Depth-Resources - Facts About the Common Cold | American Lung Association. *Am. Lung Assoc.* Available at: <http://www.lung.org/lung-disease/influenza/in-depth-resources/facts-about-the-common-cold.html>. Accessed January 24, 2013.
110. Bella J, Rossmann MG. Review: rhinoviruses and their ICAM receptors. *J. Struct. Biol.* 1999;128(1):69–74.
111. Rollinger JM, Schmidtke M. The human rhinovirus: human-pathological impact, mechanisms of antirhinoviral agents, and strategies for their discovery. *Med. Res. Rev.* 2011;31(1):42–92.
112. Harris JM 2nd, Gwaltney JM Jr. Incubation periods of experimental rhinovirus infection and illness. *Clin. Infect. Dis. Off. Publ. Infect. Dis. Soc. Am.* 1996;23(6):1287–1290.
113. Monto AS. The seasonality of rhinovirus infections and its implications for clinical recognition. *Clin. Ther.* 2002;24(12):1987–1997.
114. Arruda E, Pitkäranta A, Witek TJ Jr, Doyle CA, Hayden FG. Frequency and natural history of rhinovirus infections in adults during autumn. *J. Clin. Microbiol.* 1997;35(11):2864–2868.

115. Arden KE, Mackay IM. Newly identified human rhinoviruses: molecular methods heat up the cold viruses. *Rev. Med. Virol.* 2010;20(3):156–176.
116. Douglas RG Jr, Cate TR, Gerone PJ, Couch RB. Quantitative rhinovirus shedding patterns in volunteers. *Am. Rev. Respir. Dis.* 1966;94(2):159–167.
117. Winther B, Gwaltney JM Jr, Mygind N, Turner RB, Hendley JO. Sites of rhinovirus recovery after point inoculation of the upper airway. *Jama J. Am. Med. Assoc.* 1986;256(13):1763–1767.
118. Mosser AG, Brockman-Schneider R, Amineva S, et al. Similar frequency of rhinovirus-infectible cells in upper and lower airway epithelium. *J. Infect. Dis.* 2002;185(6):734–743.
119. Jakiela B, Brockman-Schneider R, Amineva S, Lee W-M, Gern JE. Basal cells of differentiated bronchial epithelium are more susceptible to rhinovirus infection. *Am. J. Respir. Cell Mol. Biol.* 2008;38(5):517–523.
120. Gern JE, Galagan DM, Jarjour NN, Dick EC, Busse WW. Detection of rhinovirus RNA in lower airway cells during experimentally induced infection. *Am. J. Respir. Crit. Care Med.* 1997;155(3):1159–1161.
121. Arruda E, Boyle TR, Winther B, Pevear DC, Gwaltney JM Jr, Hayden FG. Localization of human rhinovirus replication in the upper respiratory tract by in situ hybridization. *J. Infect. Dis.* 1995;171(5):1329–1333.
122. Mosser AG, Vrtis R, Burchell L, et al. Quantitative and qualitative analysis of rhinovirus infection in bronchial tissues. *Am. J. Respir. Crit. Care Med.* 2005;171(6):645–651.
123. Hayden FG. Rhinovirus and the lower respiratory tract. *Rev. Med. Virol.* 2004;14(1):17–31.
124. Papadopoulos NG, Johnston SL. Rhinoviruses as pathogens of the lower respiratory tract. *Can. Respir. J. J. Can. Thorac. Soc.* 2000;7(5):409–414.
125. Papadopoulos NG, Bates PJ, Bardin PG, et al. Rhinoviruses infect the lower airways. *J. Infect. Dis.* 2000;181(6):1875–1884.
126. Papadopoulos NG, Sanderson G, Hunter J, Johnston SL. Rhinoviruses replicate effectively at lower airway temperatures. *J. Med. Virol.* 1999;58(1):100–104.

127. Bardin PG, Johnston SL, Sanderson G, et al. Detection of rhinovirus infection of the nasal mucosa by oligonucleotide in situ hybridization. *Am. J. Respir. Cell Mol. Biol.* 1994;10(2):207–213.
128. Winther B, Brofeldt S, Christensen B, Mygind N. Light and scanning electron microscopy of nasal biopsy material from patients with naturally acquired common colds. *Acta Otolaryngol. (Stockh.)*. 1984;97(3-4):309–318.
129. Winther B, Gwaltney JM, Hendley JO. Respiratory virus infection of monolayer cultures of human nasal epithelial cells. *Am. Rev. Respir. Dis.* 1990;141(4 Pt 1):839–845.
130. Turner RB, Hendley JO, Gwaltney JM Jr. Shedding of infected ciliated epithelial cells in rhinovirus colds. *J. Infect. Dis.* 1982;145(6):849–853.
131. Proud D. Chapter 23: Biology of Epithelial Cells. In: Adkinson F, Busse WW, Bochner BS, Holgate ST, Simons ER, Lemanske RF, eds. *Middleton's Allergy: Principles and Practice*. Vol I. Seventh edition. Elsevier Inc; 2009.
132. Proud D, Hudy MH, Wiehler S, et al. Cigarette smoke modulates expression of human rhinovirus-induced airway epithelial host defense genes. *Plos One*. 2012;7(7):e40762.
133. Leigh R, Proud D. The Epithelium as a Regulator of Airway Inflammation. In: Proud D, ed. *The Pulmonary Epithelium in Health and Disease*. John Wiley and Sons; 2008:329–349.
134. Proud D, Leigh R. Epithelial cells and airway diseases. *Immunol. Rev.* 2011;242(1):186–204.
135. Racaniello VR, Knipe DM, Howley PM. Chapter 24: Picornaviridae: The Viruses and Their Replication. In: *Fields Virology*. Vol Volume 1. 5th Edition. Lippincott Williams & Wilkins; 2007:796–838.
136. McErlean P, Shackelton LA, Andrews E, et al. Distinguishing molecular features and clinical characteristics of a putative new rhinovirus species, human rhinovirus C (HRV C). *Plos One*. 2008;3(4):e1847.
137. Bedard KM, Semler BL. Regulation of picornavirus gene expression. *Microbes Infect. Inst. Pasteur*. 2004;6(7):702–713.
138. Palmenberg AC, Rathe JA, Liggett SB. Analysis of the complete genome sequences of human rhinovirus. *J. Allergy Clin. Immunol.* 2010;125(6):1190–1199; quiz 1200–1201.
139. Palmenberg AC, Spiro D, Kuzmickas R, et al. Sequencing and analyses of all known human rhinovirus genomes reveal structure and evolution. *Science*. 2009;324(5923):55–59.

140. Jacobs SE, Lamson DM, George KS, Walsh TJ. Human Rhinoviruses. *Clin. Microbiol. Rev.* 2013;26(1):135–162.
141. Arden KE, Mackay IM. Human rhinoviruses: coming in from the cold. *Genome Med.* 2009;1(4):44.
142. Hao W, Bernard K, Patel N, et al. Infection and Propagation of Human Rhinovirus C in Human Airway Epithelial Cells. *J. Virol.* 2012.
143. Greve JM, Davis G, Meyer AM, et al. The major human rhinovirus receptor is ICAM-1. *Cell.* 1989;56(5):839–847.
144. Staunton DE, Merluzzi VJ, Rothlein R, Barton R, Marlin SD, Springer TA. A cell adhesion molecule, ICAM-1, is the major surface receptor for rhinoviruses. *Cell.* 1989;56(5):849–853.
145. Hofer F, Gruenberger M, Kowalski H, et al. Members of the low density lipoprotein receptor family mediate cell entry of a minor-group common cold virus. *Proc. Natl. Acad. Sci. U. S. A.* 1994;91(5):1839–1842.
146. Staunton DE, Dustin ML, Erickson HP, Springer TA. The arrangement of the immunoglobulin-like domains of ICAM-1 and the binding sites for LFA-1 and rhinovirus. *Cell.* 1990;61(2):243–254.
147. Miller S, Krijnse-Locker J. Modification of intracellular membrane structures for virus replication. *Nat. Rev. Microbiol.* 2008;6(5):363–374.
148. Quiner CA, Jackson WT. Fragmentation of the Golgi apparatus provides replication membranes for human rhinovirus 1A. *Virology.* 2010;407(2):185–195.
149. Kawai T, Akira S. Innate immune recognition of viral infection. *Nat. Immunol.* 2006;7(2):131–137.
150. Guillot L, Le Goffic R, Bloch S, et al. Involvement of toll-like receptor 3 in the immune response of lung epithelial cells to double-stranded RNA and influenza A virus. *J. Biol. Chem.* 2005;280(7):5571–5580.
151. Sajjan US, Jia Y, Newcomb DC, et al. H. influenzae potentiates airway epithelial cell responses to rhinovirus by increasing ICAM-1 and TLR3 expression. *Faseb J. Off. Publ. Fed. Am. Soc. Exp. Biol.* 2006;20(12):2121–2123.
152. Matsukura S, Kokubu F, Kurokawa M, et al. Role of RIG-I, MDA-5, and PKR on the expression of inflammatory chemokines induced by synthetic dsRNA in airway epithelial cells. *Int. Arch. Allergy Immunol.* 2007;143 Suppl 1:80–83.

153. Imaizumi T, Kumagai M, Taima K, Fujita T, Yoshida H, Satoh K. Involvement of retinoic acid-inducible gene-I in the IFN- $\gamma$ /STAT1 signalling pathway in BEAS-2B cells. *Eur. Respir. J. Off. J. Eur. Soc. Clin. Respir. Physiol.* 2005;25(6):1077–1083.
154. Wang Q, Nagarkar DR, Bowman ER, et al. Role of double-stranded RNA pattern recognition receptors in rhinovirus-induced airway epithelial cell responses. *J. Immunol. Baltim. Md 1950.* 2009;183(11):6989–6997.
155. Slater L, Bartlett NW, Haas JJ, et al. Co-ordinated role of TLR3, RIG-I and MDA5 in the innate response to rhinovirus in bronchial epithelium. *Plos Pathog.* 2010;6(11):e1001178.
156. Wang Q, Miller DJ, Bowman ER, et al. MDA5 and TLR3 initiate pro-inflammatory signaling pathways leading to rhinovirus-induced airways inflammation and hyperresponsiveness. *Plos Pathog.* 2011;7(5):e1002070.
157. Triantafilou K, Vakakis E, Richer EAJ, Evans GL, Villiers JP, Triantafilou M. Human rhinovirus recognition in non-immune cells is mediated by Toll-like receptors and MDA-5, which trigger a synergetic pro-inflammatory immune response. *Virulence.* 2011;2(1):22–29.
158. Hewson CA, Jardine A, Edwards MR, Laza-Stanca V, Johnston SL. Toll-like receptor 3 is induced by and mediates antiviral activity against rhinovirus infection of human bronchial epithelial cells. *J. Virol.* 2005;79(19):12273–12279.
159. Chen Y, Hamati E, Lee P-K, et al. Rhinovirus induces airway epithelial gene expression through double-stranded RNA and IFN-dependent pathways. *Am. J. Respir. Cell Mol. Biol.* 2006;34(2):192–203.
160. Edwards MR, Hewson CA, Laza-Stanca V, et al. Protein kinase R, IkappaB kinase-beta and NF-kappaB are required for human rhinovirus induced pro-inflammatory cytokine production in bronchial epithelial cells. *Mol. Immunol.* 2007;44(7):1587–1597.
161. Abraham N, Stojdl DF, Duncan PI, et al. Characterization of transgenic mice with targeted disruption of the catalytic domain of the double-stranded RNA-dependent protein kinase, PKR. *J. Biol. Chem.* 1999;274(9):5953–5962.
162. Edelmann KH, Richardson-Burns S, Alexopoulou L, Tyler KL, Flavell RA, Oldstone MBA. Does Toll-like receptor 3 play a biological role in virus infections? *Virology.* 2004;322(2):231–238.
163. Abe Y, Fujii K, Nagata N, et al. The Toll-Like Receptor 3-Mediated Antiviral Response Is Important for Protection against Poliovirus Infection in Poliovirus Receptor Transgenic Mice. *J. Virol.* 2012;86(1):185–194.

164. Rudd BD, Burstein E, Duckett CS, Li X, Lukacs NW. Differential role for TLR3 in respiratory syncytial virus-induced chemokine expression. *J. Virol.* 2005;79(6):3350–3357.
165. Kato H, Takeuchi O, Sato S, et al. Differential roles of MDA5 and RIG-I helicases in the recognition of RNA viruses. *Nature.* 2006;441(7089):101–105.
166. Takeuchi O, Akira S. Innate immunity to virus infection. *Immunol. Rev.* 2009;227(1):75–86.
167. Yamamoto M, Sato S, Hemmi H, et al. Role of adaptor TRIF in the MyD88-independent toll-like receptor signaling pathway. *Science.* 2003;301(5633):640–643.
168. Meylan E, Curran J, Hofmann K, et al. Cardif is an adaptor protein in the RIG-I antiviral pathway and is targeted by hepatitis C virus. *Nature.* 2005;437(7062):1167–1172.
169. Xu L-G, Wang Y-Y, Han K-J, Li L-Y, Zhai Z, Shu H-B. VISA is an adapter protein required for virus-triggered IFN-beta signaling. *Mol. Cell.* 2005;19(6):727–740.
170. Seth RB, Sun L, Ea C-K, Chen ZJ. Identification and characterization of MAVS, a mitochondrial antiviral signaling protein that activates NF-kappaB and IRF 3. *Cell.* 2005;122(5):669–682.
171. Kawai T, Takahashi K, Sato S, et al. IPS-1, an adaptor triggering RIG-I- and Mda5-mediated type I interferon induction. *Nat. Immunol.* 2005;6(10):981–988.
172. Cate Tr, Couch Rb, Johnson Km. Studies With Rhinoviruses In Volunteers: Production Of Illness, Effect Of Naturally Acquired Antibody, And Demonstration Of A Protective Effect Not Associated With Serum Antibody. *J. Clin. Invest.* 1964;43:56–67.
173. Douglas RG Jr, Fleet WF, Cate TR, Couch RB. Antibody to rhinovirus in human sera. I. Standardization of a neutralization test. *Proc. Soc. Exp. Biol. Med. Soc. Exp. Biol. Med. New York N.* 1968;127(2):497–502.
174. Fox JP, Cooney MK, Hall CE. The Seattle virus watch. V. Epidemiologic observations of rhinovirus infections, 1965-1969, in families with young children. *Am. J. Epidemiol.* 1975;101(2):122–143.
175. Fox JP, Cooney MK, Hall CE, Foy HM. Rhinoviruses in Seattle families, 1975-1979. *Am. J. Epidemiol.* 1985;122(5):830–846.
176. Cate TR, Rossen RD, Douglas RG Jr, Butler WT, Couch RB. The role of nasal secretion and serum antibody in the rhinovirus common cold. *Am. J. Epidemiol.* 1966;84(2):352–363.

177. Yanbaeva DG, Dentener MA, Creutzberg EC, Wesseling G, Wouters EFM. Systemic effects of smoking. *Chest*. 2007;131(5):1557–1566.
178. Arnson Y, Shoenfeld Y, Amital H. Effects of tobacco smoke on immunity, inflammation and autoimmunity. *J. Autoimmun.* 2010;34(3):J258–265.
179. Stämpfli MR, Anderson GP. How cigarette smoke skews immune responses to promote infection, lung disease and cancer. *Nat. Rev. Immunol.* 2009;9(5):377–384.
180. Jha P, Ramasundarahettige C, Landsman V, et al. 21st-century hazards of smoking and benefits of cessation in the United States. *N. Engl. J. Med.* 2013;368(4):341–350.
181. Pryor WA, Stone K. Oxidants in cigarette smoke. Radicals, hydrogen peroxide, peroxyxynitrate, and peroxyxynitrite. *Ann. N. Y. Acad. Sci.* 1993;686:12–27; discussion 27–28.
182. Brunnemann KD, Hoffmann D. Analytical studies on tobacco-specific N-nitrosamines in tobacco and tobacco smoke. *Crit. Rev. Toxicol.* 1991;21(4):235–240.
183. Hoffmann D, Djordjevic MV, Hoffmann I. The changing cigarette. *Prev. Med.* 1997;26(4):427–434.
184. Smith CJ, Hansch C. The relative toxicity of compounds in mainstream cigarette smoke condensate. *Food Chem. Toxicol. Int. J. Publ. Br. Ind. Biol. Res. Assoc.* 2000;38(7):637–646.
185. Bhalla DK, Hirata F, Rishi AK, Gairola CG. Cigarette smoke, inflammation, and lung injury: a mechanistic perspective. *J. Toxicol. Environ. Health B Crit. Rev.* 2009;12(1):45–64.
186. Van der Toorn M, Rezayat D, Kauffman HF, et al. Lipid-soluble components in cigarette smoke induce mitochondrial production of reactive oxygen species in lung epithelial cells. *Am. J. Physiol. Lung Cell. Mol. Physiol.* 2009;297(1):L109–114.
187. Afri M, Gottlieb HE, Frimer AA. Superoxide organic chemistry within the liposomal bilayer, part II: a correlation between location and chemistry. *Free Radic. Biol. Med.* 2002;32(7):605–618.
188. Mao GD, Poznansky MJ. Electron spin resonance study on the permeability of superoxide radicals in lipid bilayers and biological membranes. *Febs Lett.* 1992;305(3):233–236.
189. Nathan C, Cunningham-Bussel A. Beyond oxidative stress: an immunologist's guide to reactive oxygen species. *Nat. Rev. Immunol.* 2013;13(5):349–361.

190. Bernstein D. A review of the influence of particle size, puff volume, and inhalation pattern on the deposition of cigarette smoke particles in the respiratory tract. *Inhal. Toxicol.* 2004;16(10):675–689.
191. Roth MD, Arora A, Barsky SH, Kleerup EC, Simmons M, Tashkin DP. Airway inflammation in young marijuana and tobacco smokers. *Am. J. Respir. Crit. Care Med.* 1998;157(3 Pt 1):928–937.
192. Costabel U, Bross KJ, Reuter C, Rühle KH, Matthys H. Alterations in immunoregulatory T-cell subsets in cigarette smokers. A phenotypic analysis of bronchoalveolar and blood lymphocytes. *Chest.* 1986;90(1):39–44.
193. Hunninghake GW, Crystal RG. Cigarette smoking and lung destruction. Accumulation of neutrophils in the lungs of cigarette smokers. *Am. Rev. Respir. Dis.* 1983;128(5):833–838.
194. Kuschner WG, D'Alessandro A, Wong H, Blanc PD. Dose-dependent cigarette smoking-related inflammatory responses in healthy adults. *Eur. Respir. J. Off. J. Eur. Soc. Clin. Respir. Physiol.* 1996;9(10):1989–1994.
195. Van der Vaart H, Postma DS, Timens W, ten Hacken NHT. Acute effects of cigarette smoke on inflammation and oxidative stress: a review. *Thorax.* 2004;59(8):713–721.
196. Holt PG. Immune and inflammatory function in cigarette smokers. *Thorax.* 1987;42(4):241–249.
197. Amin K, Ekberg-Jansson A, Löfdahl C-G, Venge P. Relationship between inflammatory cells and structural changes in the lungs of asymptomatic and never smokers: a biopsy study. *Thorax.* 2003;58(2):135–142.
198. Tollerud DJ, Clark JW, Brown LM, et al. Association of cigarette smoking with decreased numbers of circulating natural killer cells. *Am. Rev. Respir. Dis.* 1989;139(1):194–198.
199. Mian MF, Lauzon NM, Stämpfli MR, Mossman KL, Ashkar AA. Impairment of human NK cell cytotoxic activity and cytokine release by cigarette smoke. *J. Leukoc. Biol.* 2008;83(3):774–784.
200. Ferson M, Edwards A, Lind A, Milton GW, Hersey P. Low natural killer-cell activity and immunoglobulin levels associated with smoking in human subjects. *Int. J. Cancer J. Int. Cancer.* 1979;23(5):603–609.

201. Hughes DA, Haslam PL, Townsend PJ, Turner-Warwick M. Numerical and functional alterations in circulatory lymphocytes in cigarette smokers. *Clin. Exp. Immunol.* 1985;61(2):459–466.
202. Modestou MA, Manzel LJ, El-Mahdy S, Look DC. Inhibition of IFN-gamma-dependent antiviral airway epithelial defense by cigarette smoke. *Respir. Res.* 2010;11:64.
203. Bauer CMT, Dewitte-Orr SJ, Hornby KR, et al. Cigarette smoke suppresses type I interferon-mediated antiviral immunity in lung fibroblast and epithelial cells. *J. Interf. Cytokine Res. Off. J. Int. Soc. Interf. Cytokine Res.* 2008;28(3):167–179.
204. Wu W, Patel KB, Booth JL, Zhang W, Metcalf JP. Cigarette smoke extract suppresses the RIG-I-initiated innate immune response to influenza virus in the human lung. *Am. J. Physiol. Lung Cell. Mol. Physiol.* 2011;300(6):L821–830.
205. Robbins CS, Bauer CMT, Vujicic N, et al. Cigarette smoke impacts immune inflammatory responses to influenza in mice. *Am. J. Respir. Crit. Care Med.* 2006;174(12):1342–1351.
206. Noah TL, Zhou H, Monaco J, Horvath K, Herbst M, Jaspers I. Tobacco smoke exposure and altered nasal responses to live attenuated influenza virus. *Environ. Health Perspect.* 2011;119(1):78–83.
207. Gualano RC, Hansen MJ, Vlahos R, et al. Cigarette smoke worsens lung inflammation and impairs resolution of influenza infection in mice. *Respir. Res.* 2008;9:53.
208. Feng Y, Kong Y, Barnes PF, et al. Exposure to cigarette smoke inhibits the pulmonary T-cell response to influenza virus and Mycobacterium tuberculosis. *Infect. Immun.* 2011;79(1):229–237.
209. Groskreutz DJ, Monick MM, Babor EC, et al. Cigarette smoke alters respiratory syncytial virus-induced apoptosis and replication. *Am. J. Respir. Cell Mol. Biol.* 2009;41(2):189–198.
210. Castro SM, Kolli D, Guerrero-Plata A, Garofalo RP, Casola A. Cigarette Smoke Condensate Enhances Respiratory Syncytial Virus-Induced Chemokine Release by Modulating NF-kappa B and Interferon Regulatory Factor Activation. *Toxicol. Sci.* 2008;106(2):509–518.
211. Dye JA, Adler KB. Effects of cigarette smoke on epithelial cells of the respiratory tract. *Thorax.* 1994;49(8):825–834.

212. Tamashiro E, Xiong G, Anselmo-Lima WT, Kreindler JL, Palmer JN, Cohen NA. Cigarette smoke exposure impairs respiratory epithelial ciliogenesis. *Am. J. Rhinol. Allergy*. 2009;23(2):117–122.
213. Cohen NA, Zhang S, Sharp DB, et al. Cigarette smoke condensate inhibits transepithelial chloride transport and ciliary beat frequency. *Laryngoscope*. 2009;119(11):2269–2274.
214. Simet SM, Sisson JH, Pavlik JA, et al. Long-term cigarette smoke exposure in a mouse model of ciliated epithelial cell function. *Am. J. Respir. Cell Mol. Biol*. 2010;43(6):635–640.
215. Shao MXG, Nakanaga T, Nadel JA. Cigarette smoke induces MUC5AC mucin overproduction via tumor necrosis factor-alpha-converting enzyme in human airway epithelial (NCI-H292) cells. *Am. J. Physiol. Lung Cell. Mol. Physiol*. 2004;287(2):L420–427.
216. Verra F, Escudier E, Lebargy F, Bernaudin JF, De Crémoux H, Bignon J. Ciliary abnormalities in bronchial epithelium of smokers, ex-smokers, and nonsmokers. *Am. J. Respir. Crit. Care Med*. 1995;151(3 Pt 1):630–634.
217. Petecchia L, Sabatini F, Varesio L, et al. Bronchial airway epithelial cell damage following exposure to cigarette smoke includes disassembly of tight junction components mediated by the extracellular signal-regulated kinase 1/2 pathway. *Chest*. 2009;135(6):1502–1512.
218. Olivera DS, Boggs SE, Beenhouwer C, Aden J, Knall C. Cellular mechanisms of mainstream cigarette smoke-induced lung epithelial tight junction permeability changes in vitro. *Inhal. Toxicol*. 2007;19(1):13–22.
219. Heijink IH, Brandenburg SM, Postma DS, van Oosterhout AJM. Cigarette smoke impairs airway epithelial barrier function and cell-cell contact recovery. *Eur. Respir. J. Off. J. Eur. Soc. Clin. Respir. Physiol*. 2011.
220. Jones JG, Minty BD, Lawler P, Hulands G, Crawley JC, Veall N. Increased alveolar epithelial permeability in cigarette smokers. *Lancet*. 1980;1(8159):66–68.
221. Chang MM-J, Shih L, Wu R. Pulmonary Epithelium: Cell Types and Functions. In: Proud D, ed. *The Pulmonary Epithelium in Health and Disease*. John Wiley and Sons; 2008:1–14.
222. Knight DA, Holgate ST. The airway epithelium: structural and functional properties in health and disease. *Respirol. Carlton Vic*. 2003;8(4):432–446.

223. Barnes PJ. Immunology of asthma and chronic obstructive pulmonary disease. *Nat Rev Immunol.* 2008;8(3):183–192.
224. Lambrecht BN, Hammad H. The airway epithelium in asthma. *Nat. Med.* 2012;18(5):684–692.
225. Bousquet J, Jeffery PK, Busse WW, Johnson M, Vignola AM. Asthma. From bronchoconstriction to airways inflammation and remodeling. *Am. J. Respir. Crit. Care Med.* 2000;161(5):1720–1745.
226. Zlotnik A, Yoshie O. The chemokine superfamily revisited. *Immunity.* 2012;36(5):705–716.
227. Charo IF, Ransohoff RM. The Many Roles of Chemokines and Chemokine Receptors in Inflammation. *N. Engl. J. Med.* 2006;354(6):610–621.
228. Luster AD. Chemokines--chemotactic cytokines that mediate inflammation. *N. Engl. J. Med.* 1998;338(7):436–445.
229. Borish LC, Steinke JW. 2. Cytokines and chemokines. *J. Allergy Clin. Immunol.* 2003;111(2 Suppl):S460–475.
230. Zlotnik A, Yoshie O. Chemokines: a new classification system and their role in immunity. *Immunity.* 2000;12(2):121–127.
231. David J, Mortari F. Chemokine receptors: A brief overview. *Clin. Appl. Immunol. Rev.* 2000;1(2):105–125.
232. Belperio JA, Keane MP, Arenberg DA, et al. CXC chemokines in angiogenesis. *J. Leukoc. Biol.* 2000;68(1):1–8.
233. Allen SJ, Crown SE, Handel TM. Chemokine: receptor structure, interactions, and antagonism. *Annu. Rev. Immunol.* 2007;25:787–820.
234. Baggiolini M, Dewald B, Moser B. Human chemokines: an update. *Annu. Rev. Immunol.* 1997;15:675–705.
235. Baggiolini M. Chemokines and leukocyte traffic. *Nature.* 1998;392(6676):565–568.
236. Rot A, von Andrian UH. Chemokines in innate and adaptive host defense: basic chemokines grammar for immune cells. *Annu. Rev. Immunol.* 2004;22:891–928.

237. Luster AD, Unkeless JC, Ravetch JV. Gamma-interferon transcriptionally regulates an early-response gene containing homology to platelet proteins. *Nature*. 1985;315(6021):672–676.
238. Liu M, Guo S, Hibbert JM, et al. CXCL10/IP-10 in infectious diseases pathogenesis and potential therapeutic implications. *Cytokine Growth Factor Rev*. 2011;22(3):121–130.
239. Vanguri P, Farber JM. Identification of CRG-2. An interferon-inducible mRNA predicted to encode a murine monokine. *J. Biol. Chem*. 1990;265(25):15049–15057.
240. Farber JM. Mig and IP-10: CXC chemokines that target lymphocytes. *J. Leukoc. Biol*. 1997;61(3):246–257.
241. Luster AD, Jhanwar SC, Chaganti RS, Kersey JH, Ravetch JV. Interferon-inducible gene maps to a chromosomal band associated with a (4;11) translocation in acute leukemia cells. *Proc. Natl. Acad. Sci. U. S. A*. 1987;84(9):2868–2871.
242. National Center for Biotechnology Information (NCBI): AceView. Search term: CXCL10.
243. Luster AD, Ravetch JV. Genomic characterization of a gamma-interferon-inducible gene (IP-10) and identification of an interferon-inducible hypersensitive site. *Mol. Cell. Biol*. 1987;7(10):3723–3731.
244. Luster AD, Ravetch JV. Biochemical characterization of a gamma interferon-inducible cytokine (IP-10). *J. Exp. Med*. 1987;166(4):1084–1097.
245. Sauty A, Dziejman M, Taha RA, et al. The T cell-specific CXC chemokines IP-10, Mig, and I-TAC are expressed by activated human bronchial epithelial cells. *J. Immunol. Baltim. Md 1950*. 1999;162(6):3549–3558.
246. Liu L, Callahan MK, Huang D, Ransohoff RM. Chemokine receptor CXCR3: an unexpected enigma. *Curr. Top. Dev. Biol*. 2005;68:149–181.
247. Trifilo MJ, Montalto-Morrison C, Stiles LN, et al. CXC chemokine ligand 10 controls viral infection in the central nervous system: evidence for a role in innate immune response through recruitment and activation of natural killer cells. *J. Virol*. 2004;78(2):585–594.
248. Bonecchi R, Bianchi G, Bordignon PP, et al. Differential expression of chemokine receptors and chemotactic responsiveness of type 1 T helper cells (Th1s) and Th2s. *J. Exp. Med*. 1998;187(1):129–134.
249. Arai K, Liu ZX, Lane T, Dennert G. IP-10 and Mig facilitate accumulation of T cells in the virus-infected liver. *Cell. Immunol*. 2002;219(1):48–56.

250. Kakimi K, Lane TE, Wieland S, et al. Blocking chemokine responsive to gamma-2/interferon (IFN)-gamma inducible protein and monokine induced by IFN-gamma activity in vivo reduces the pathogenetic but not the antiviral potential of hepatitis B virus-specific cytotoxic T lymphocytes. *J. Exp. Med.* 2001;194(12):1755–1766.
251. Loetscher M, Gerber B, Loetscher P, et al. Chemokine receptor specific for IP10 and mig: structure, function, and expression in activated T-lymphocytes. *J. Exp. Med.* 1996;184(3):963–969.
252. Maghazachi AA, Skalhegg BS, Rolstad B, Al-Aoukaty A. Interferon-inducible protein-10 and lymphotactin induce the chemotaxis and mobilization of intracellular calcium in natural killer cells through pertussis toxin-sensitive and -insensitive heterotrimeric G-proteins. *Faseb J. Off. Publ. Fed. Am. Soc. Exp. Biol.* 1997;11(10):765–774.
253. Mahalingam S, Farber JM, Karupiah G. The interferon-inducible chemokines MuMig and Crg-2 exhibit antiviral activity In vivo. *J. Virol.* 1999;73(2):1479–1491.
254. Recombinant human interferon-inducible protein 10 is a chemoattractant for human monocytes and T lymphocytes and promotes T cell adhesion to endothelial cells. *J. Exp. Med.* 1993;177(6):1809–1814.
255. Buttman M, Berberich-Siebelt F, Serfling E, Rieckmann P. Interferon-beta is a potent inducer of interferon regulatory factor-1/2-dependent IP-10/CXCL10 expression in primary human endothelial cells. *J. Vasc. Res.* 2007;44(1):51–60.
256. García-López MA, Sánchez-Madrid F, Rodríguez-Frade JM, et al. CXCR3 chemokine receptor distribution in normal and inflamed tissues: expression on activated lymphocytes, endothelial cells, and dendritic cells. *Lab. Invest. J. Tech. Methods Pathol.* 2001;81(3):409–418.
257. Dufour JH, Dziejman M, Liu MT, Leung JH, Lane TE, Luster AD. IFN-gamma-inducible protein 10 (IP-10; CXCL10)-deficient mice reveal a role for IP-10 in effector T cell generation and trafficking. *J. Immunol. Baltim. Md 1950.* 2002;168(7):3195–3204.
258. Proud D, Turner RB, Winther B, et al. Gene expression profiles during in vivo human rhinovirus infection: insights into the host response. *Am. J. Respir. Crit. Care Med.* 2008;178(9):962–968.
259. Spurrell JCL, Wiehler S, Zaheer RS, Sanders SP, Proud D. Human airway epithelial cells produce IP-10 (CXCL10) in vitro and in vivo upon rhinovirus infection. *Am. J. Physiol. Lung Cell. Mol. Physiol.* 2005;289(1):L85–95.

260. Nie L, Xiang R, Zhou W, Lu B, Cheng D, Gao J. Attenuation of acute lung inflammation induced by cigarette smoke in CXCR3 knockout mice. *Respir. Res.* 2008;9:82.
261. Nie L, Xiang R, Liu Y, et al. Acute pulmonary inflammation is inhibited in CXCR3 knockout mice after short-term cigarette smoke exposure. *Acta Pharmacol. Sin.* 2008;29(12):1432–1439.
262. Wang Z, Chen Y-W, Zhang J-N, Hu X-F, Peng M-J. Pentoxifylline attenuates cigarette smoke-induced overexpression of CXCR3 and IP-10 in mice. *Chin. Med. J. (Engl.)*. 2012;125(11):1980–1985.
263. Pace E, Ferraro M, Siena L, et al. Cigarette smoke increases Toll-like receptor 4 and modifies lipopolysaccharide-mediated responses in airway epithelial cells. *Immunology*. 2008;124(3):401–411.
264. Pace E, Ferraro M, Uasuf CG, et al. Cilomilast counteracts the effects of cigarette smoke in airway epithelial cells. *Cell. Immunol.* 2011;268(1):47–53.
265. Castro SM, Chakraborty K, Guerrero-Plata A. Cigarette smoke suppresses TLR-7 stimulation in response to virus infection in plasmacytoid dendritic cells. *Toxicol. Vitro Int. J. Publ. Assoc. Bibra.* 2011;25(5):1106–1113.
266. Doyle I, Ratcliffe M, Walding A, et al. Differential gene expression analysis in human monocyte-derived macrophages: impact of cigarette smoke on host defence. *Mol. Immunol.* 2010;47(5):1058–1065.
267. Miotto D, Christodoulouopoulos P, Olivenstein R, et al. Expression of IFN-gamma-inducible protein; monocyte chemotactic proteins 1, 3, and 4; and eotaxin in TH1- and TH2-mediated lung diseases. *J. Allergy Clin. Immunol.* 2001;107(4):664–670.
268. Costa C, Rufino R, Traves SL, Lapa E Silva JR, Barnes PJ, Donnelly LE. CXCR3 and CCR5 chemokines in induced sputum from patients with COPD. *Chest.* 2008;133(1):26–33.
269. Ying S, O'Connor B, Ratoff J, et al. Expression and cellular provenance of thymic stromal lymphopoietin and chemokines in patients with severe asthma and chronic obstructive pulmonary disease. *J. Immunol. Baltim. Md 1950.* 2008;181(4):2790–2798.
270. Saetta M, Mariani M, Panina-Bordignon P, et al. Increased expression of the chemokine receptor CXCR3 and its ligand CXCL10 in peripheral airways of smokers with chronic obstructive pulmonary disease. *Am. J. Respir. Crit. Care Med.* 2002;165(10):1404–1409.

271. Medoff BD, Sauty A, Tager AM, et al. IFN-gamma-inducible protein 10 (CXCL10) contributes to airway hyperreactivity and airway inflammation in a mouse model of asthma. *J. Immunol. Baltim. Md 1950*. 2002;168(10):5278–5286.
272. Wark PAB, Bucchieri F, Johnston SL, et al. IFN-gamma-induced protein 10 is a novel biomarker of rhinovirus-induced asthma exacerbations. *J. Allergy Clin. Immunol.* 2007;120(3):586–593.
273. Quint JK, Donaldson GC, Goldring JJP, Baghai-Ravary R, Hurst JR, Wedzicha JA. Serum IP-10 as a biomarker of human rhinovirus infection at exacerbation of COPD. *Chest*. 2010;137(4):812–822.
274. Baggiolini M, Walz A, Kunkel SL. Neutrophil-activating peptide-1/interleukin 8, a novel cytokine that activates neutrophils. *J. Clin. Invest.* 1989;84(4):1045–1049.
275. Yoshimura T, Matsushima K, Tanaka S, et al. Purification of a human monocyte-derived neutrophil chemotactic factor that has peptide sequence similarity to other host defense cytokines. *Proc. Natl. Acad. Sci. U. S. A.* 1987;84(24):9233–9237.
276. Schröder JM, Mrowietz U, Morita E, Christophers E. Purification and partial biochemical characterization of a human monocyte-derived, neutrophil-activating peptide that lacks interleukin 1 activity. *J. Immunol. Baltim. Md 1950*. 1987;139(10):3474–3483.
277. Walz A, Peveri P, Aschauer H, Baggiolini M. Purification and amino acid sequencing of NAF, a novel neutrophil-activating factor produced by monocytes. *Biochem. Biophys. Res. Commun.* 1987;149(2):755–761.
278. Mukaida N. Pathophysiological roles of interleukin-8/CXCL8 in pulmonary diseases. *Am. J. Physiol. Lung Cell. Mol. Physiol.* 2003;284(4):L566–577.
279. Hoffmann E, Dittrich-Breiholz O, Holtmann H, Kracht M. Multiple control of interleukin-8 gene expression. *J. Leukoc. Biol.* 2002;72(5):847–855.
280. Fernandez EJ, Lolis E. Structure, Function, and Inhibition of Chemokines. *Annu. Rev. Pharmacol. Toxicol.* 2002;42(1):469–499.
281. National Center for Biotechnology Information (NCBI): AceView. Search term: CXCL8.
282. Baggiolini M, Clark-Lewis I. Interleukin-8, a chemotactic and inflammatory cytokine. *Febs Lett.* 1992;307(1):97–101.

283. Zhu Z, Tang W, Gwaltney JM Jr, Wu Y, Elias JA. Rhinovirus stimulation of interleukin-8 in vivo and in vitro: role of NF-kappaB. *Am. J. Physiol.* 1997;273(4 Pt 1):L814–824.
284. Winther B, Farr B, Turner RB, Hendley JO, Gwaltney JM Jr, Mygind N. Histopathologic examination and enumeration of polymorphonuclear leukocytes in the nasal mucosa during experimental rhinovirus colds. *Acta Oto-Laryngol. Suppl.* 1984;413:19–24.
285. Naclerio RM, Proud D, Lichtenstein LM, et al. Kinins are generated during experimental rhinovirus colds. *J. Infect. Dis.* 1988;157(1):133–142.
286. Turner RB. The role of neutrophils in the pathogenesis of rhinovirus infections. *Pediatr. Infect. Dis. J.* 1990;9(11):832–835.
287. Turner RB, Weingand KW, Yeh CH, Leedy DW. Association between interleukin-8 concentration in nasal secretions and severity of symptoms of experimental rhinovirus colds. *Clin. Infect. Dis. Off. Publ. Infect. Dis. Soc. Am.* 1998;26(4):840–846.
288. Quint JK, Wedzicha JA. The neutrophil in chronic obstructive pulmonary disease. *J. Allergy Clin. Immunol.* 2007;119(5):1065–1071.
289. Thompson AB, Daughton D, Robbins RA, Ghafouri MA, Oehlerking M, Rennard SI. Intraluminal airway inflammation in chronic bronchitis. Characterization and correlation with clinical parameters. *Am. Rev. Respir. Dis.* 1989;140(6):1527–1537.
290. Stănescu D, Sanna A, Veriter C, et al. Airways obstruction, chronic expectoration, and rapid decline of FEV1 in smokers are associated with increased levels of sputum neutrophils. *Thorax.* 1996;51(3):267–271.
291. Bosken CH, Hards J, Gatter K, Hogg JC. Characterization of the inflammatory reaction in the peripheral airways of cigarette smokers using immunocytochemistry. *Am. Rev. Respir. Dis.* 1992;145(4 Pt 1):911–917.
292. Qiu Y, Zhu J, Bandi V, et al. Biopsy neutrophilia, neutrophil chemokine and receptor gene expression in severe exacerbations of chronic obstructive pulmonary disease. *Am. J. Respir. Crit. Care Med.* 2003;168(8):968–975.
293. Ordoñez CL, Shaughnessy TE, Matthay MA, Fahy JV. Increased neutrophil numbers and IL-8 levels in airway secretions in acute severe asthma: Clinical and biologic significance. *Am. J. Respir. Crit. Care Med.* 2000;161(4 Pt 1):1185–1190.

294. Norzila MZ, Fakes K, Henry RL, Simpson J, Gibson PG. Interleukin-8 secretion and neutrophil recruitment accompanies induced sputum eosinophil activation in children with acute asthma. *Am. J. Respir. Crit. Care Med.* 2000;161(3 Pt 1):769–774.
295. Keatings VM, Collins PD, Scott DM, Barnes PJ. Differences in interleukin-8 and tumor necrosis factor-alpha in induced sputum from patients with chronic obstructive pulmonary disease or asthma. *Am. J. Respir. Crit. Care Med.* 1996;153(2):530–534.
296. Sarir H, Henricks PAJ, van Houwelingen AH, Nijkamp FP, Folkerts G. Cells, mediators and Toll-like receptors in COPD. *Eur. J. Pharmacol.* 2008;585(2-3):346–353.
297. Zaheer RS, Koetzler R, Holden NS, Wiehler S, Proud D. Selective transcriptional down-regulation of human rhinovirus-induced production of CXCL10 from airway epithelial cells via the MEK1 pathway. *J. Immunol. Baltim. Md 1950.* 2009;182(8):4854–4864.
298. Zaheer RS, Proud D. Human rhinovirus-induced epithelial production of CXCL10 is dependent upon IFN regulatory factor-1. *Am. J. Respir. Cell Mol. Biol.* 2010;43(4):413–421.
299. Wu C, Ohmori Y, Bandyopadhyay S, Sen G, Hamilton T. Interferon-stimulated response element and NF kappa B sites cooperate to regulate double-stranded RNA-induced transcription of the IP-10 gene. *J. Interferon Res.* 1994;14(6):357–363.
300. Méndez-Samperio P, Pérez A, Rivera L. Mycobacterium bovis Bacillus Calmette-Guérin (BCG)-induced activation of PI3K/Akt and NF-kB signaling pathways regulates expression of CXCL10 in epithelial cells. *Cell. Immunol.* 2009;256(1-2):12–18.
301. Yeruva S, Ramadori G, Raddatz D. NF-kappaB-dependent synergistic regulation of CXCL10 gene expression by IL-1beta and IFN-gamma in human intestinal epithelial cell lines. *Int. J. Colorectal Dis.* 2008;23(3):305–317.
302. Majumder S, Zhou LZ, Chaturvedi P, Babcock G, Aras S, Ransohoff RM. p48/STAT-1alpha-containing complexes play a predominant role in induction of IFN-gamma-inducible protein, 10 kDa (IP-10) by IFN-gamma alone or in synergy with TNF-alpha. *J. Immunol. Baltim. Md 1950.* 1998;161(9):4736–4744.
303. Nazar AS, Cheng G, Shin HS, et al. Induction of IP-10 chemokine promoter by measles virus: comparison with interferon-gamma shows the use of the same response element but with differential DNA-protein binding profiles. *J. Neuroimmunol.* 1997;77(1):116–127.
304. Clarke DL, Clifford RL, Jindarat S, et al. TNF $\alpha$  and IFN $\gamma$  synergistically enhance transcriptional activation of CXCL10 in human airway smooth muscle cells via STAT-1,

NF- $\kappa$ B, and the transcriptional coactivator CREB-binding protein. *J. Biol. Chem.* 2010;285(38):29101–29110.

305. Villarete LH, Remick DG. Transcriptional and post-transcriptional regulation of interleukin-8. *Am. J. Pathol.* 1996;149(5):1685–1693.

306. Roebuck KA. Regulation of interleukin-8 gene expression. *J. Interf. Cytokine Res. Off. J. Int. Soc. Interf. Cytokine Res.* 1999;19(5):429–438.

307. Kunsch C, Lang RK, Rosen CA, Shannon MF. Synergistic transcriptional activation of the IL-8 gene by NF-kappa B p65 (RelA) and NF-IL-6. *J. Immunol. Baltim. Md 1950.* 1994;153(1):153–164.

308. Matsusaka T, Fujikawa K, Nishio Y, et al. Transcription factors NF-IL6 and NF-kappa B synergistically activate transcription of the inflammatory cytokines, interleukin 6 and interleukin 8. *Proc. Natl. Acad. Sci. U. S. A.* 1993;90(21):10193–10197.

309. D'Aversa TG, Eugenin EA, Berman JW. CD40-CD40 ligand interactions in human microglia induce CXCL8 (interleukin-8) secretion by a mechanism dependent on activation of ERK1/2 and nuclear translocation of nuclear factor-kappaB (NFkappaB) and activator protein-1 (AP-1). *J. Neurosci. Res.* 2008;86(3):630–639.

310. John AE, Zhu YM, Brightling CE, Pang L, Knox AJ. Human airway smooth muscle cells from asthmatic individuals have CXCL8 hypersecretion due to increased NF-kappa B p65, C/EBP beta, and RNA polymerase II binding to the CXCL8 promoter. *J. Immunol. Baltim. Md 1950.* 2009;183(7):4682–4692.

311. Grbic DM, Degagn E, Larrive J-F, et al. P2Y6 receptor contributes to neutrophil recruitment to inflamed intestinal mucosa by increasing CXC chemokine ligand 8 expression in an AP-1-dependent manner in epithelial cells. *Inflamm. Bowel Dis.* 2012;18(8):1456–1469.

312. Liu F, Killian JK, Yang M, et al. Epigenomic alterations and gene expression profiles in respiratory epithelia exposed to cigarette smoke condensate. *Oncogene.* 2010;29(25):3650–3664.

313. Moodie FM, Marwick JA, Anderson CS, et al. Oxidative stress and cigarette smoke alter chromatin remodeling but differentially regulate NF-kappaB activation and proinflammatory cytokine release in alveolar epithelial cells. *Faseb J. Off. Publ. Fed. Am. Soc. Exp. Biol.* 2004;18(15):1897–1899.

314. Krishna M, Narang H. The complexity of mitogen-activated protein kinases (MAPKs) made simple. *Cell. Mol. Life Sci. Cmls.* 2008;65(22):3525–3544.

315. Kyriakis JM, Avruch J. Mammalian MAPK signal transduction pathways activated by stress and inflammation: a 10-year update. *Physiol. Rev.* 2012;92(2):689–737.
316. Turjanski AG, Vaqué JP, Gutkind JS. MAP kinases and the control of nuclear events. *Oncogene.* 2007;26(22):3240–3253.
317. Keshet Y, Seger R. The MAP kinase signaling cascades: a system of hundreds of components regulates a diverse array of physiological functions. *Methods Mol. Biol. Clifton Nj.* 2010;661:3–38.
318. Zhang Y, Dong C. Regulatory mechanisms of mitogen-activated kinase signaling. *Cell. Mol. Life Sci. Cmls.* 2007;64(21):2771–2789.
319. Johnson GL, Lapadat R. Mitogen-activated protein kinase pathways mediated by ERK, JNK, and p38 protein kinases. *Science.* 2002;298(5600):1911–1912.
320. Pearson G, Robinson F, Beers Gibson T, et al. Mitogen-activated protein (MAP) kinase pathways: regulation and physiological functions. *Endocr. Rev.* 2001;22(2):153–183.
321. Chen Z, Gibson TB, Robinson F, et al. MAP kinases. *Chem. Rev.* 2001;101(8):2449–2476.
322. Shaul YD, Seger R. The MEK/ERK cascade: from signaling specificity to diverse functions. *Biochim. Biophys. Acta.* 2007;1773(8):1213–1226.
323. Wiehler S, Proud D. Interleukin-17A modulates human airway epithelial responses to human rhinovirus infection. *Am. J. Physiol. Lung Cell. Mol. Physiol.* 2007;293(2):L505–515.
324. Leigh R, Oyelusi W, Wiehler S, et al. Human rhinovirus infection enhances airway epithelial cell production of growth factors involved in airway remodeling. *J. Allergy Clin. Immunol.* 2008;121(5):1238–1245.e4.
325. Winzen R, Kracht M, Ritter B, et al. The p38 MAP kinase pathway signals for cytokine-induced mRNA stabilization via MAP kinase-activated protein kinase 2 and an AU-rich region-targeted mechanism. *Embo J.* 1999;18(18):4969–4980.
326. Jijon HB, Panenka WJ, Madsen KL, Parsons HG. MAP kinases contribute to IL-8 secretion by intestinal epithelial cells via a posttranscriptional mechanism. *Am. J. Physiol. Cell Physiol.* 2002;283(1):C31–41.
327. Holtmann H, Winzen R, Holland P, et al. Induction of interleukin-8 synthesis integrates effects on transcription and mRNA degradation from at least three different

- cytokine- or stress-activated signal transduction pathways. *Mol. Cell. Biol.* 1999;19(10):6742–6753.
328. Ghosh S, Hayden MS. New regulators of NF- $\kappa$ B in inflammation. *Nat. Rev. Immunol.* 2008;8(11):837–848.
329. Baeuerle PA, Baltimore D. I kappa B: a specific inhibitor of the NF-kappa B transcription factor. *Science.* 1988;242(4878):540–546.
330. Li Q, Verma IM. NF-kappaB regulation in the immune system. *Nat. Rev. Immunol.* 2002;2(10):725–734.
331. Rothwarf DM, Karin M. The NF-kappa B activation pathway: a paradigm in information transfer from membrane to nucleus. *Sci. Stke Signal Transduct. Knowl. Environ.* 1999;1999(5):RE1.
332. Vallabhapurapu S, Karin M. Regulation and function of NF-kappaB transcription factors in the immune system. *Annu. Rev. Immunol.* 2009;27:693–733.
333. Johnson C, Van Antwerp D, Hope TJ. An N-terminal nuclear export signal is required for the nucleocytoplasmic shuttling of IkappaBalpha. *Embo J.* 1999;18(23):6682–6693.
334. Zandi E, Rothwarf DM, Delhase M, Hayakawa M, Karin M. The IkappaB kinase complex (IKK) contains two kinase subunits, IKKalpha and IKKbeta, necessary for IkappaB phosphorylation and NF-kappaB activation. *Cell.* 1997;91(2):243–252.
335. Pasparakis M. Regulation of tissue homeostasis by NF- $\kappa$ B signalling: implications for inflammatory diseases. *Nat. Rev. Immunol.* 2009;9(11):778–788.
336. Chen Z, Hagler J, Palombella VJ, et al. Signal-induced site-specific phosphorylation targets I kappa B alpha to the ubiquitin-proteasome pathway. *Genes Dev.* 1995;9(13):1586–1597.
337. Li ZW, Chu W, Hu Y, et al. The IKKbeta subunit of IkappaB kinase (IKK) is essential for nuclear factor kappaB activation and prevention of apoptosis. *J. Exp. Med.* 1999;189(11):1839–1845.
338. Koetzler R, Zaheer RS, Wiehler S, Holden NS, Giembycz MA, Proud D. Nitric oxide inhibits human rhinovirus-induced transcriptional activation of CXCL10 in airway epithelial cells. *J. Allergy Clin. Immunol.* 2009;123(1):201–208.e9.
339. Honda K, Taniguchi T. IRFs: master regulators of signalling by Toll-like receptors and cytosolic pattern-recognition receptors. *Nat Rev Immunol.* 2006;6(9):644–658.

340. Paun A, Pitha PM. The IRF family, revisited. *Biochimie*. 2007;89(6-7):744–753.
341. Tamura T, Yanai H, Savitsky D, Taniguchi T. The IRF Family Transcription Factors in Immunity and Oncogenesis. *Annu. Rev. Immunol.* 2008;26(1):535–584.
342. Ozato K, Tailor P, Kubota T. The interferon regulatory factor family in host defense: mechanism of action. *J. Biol. Chem.* 2007;282(28):20065–20069.
343. Fujii Y, Shimizu T, Kusumoto M, Kyogoku Y, Taniguchi T, Hakoshima T. Crystal structure of an IRF-DNA complex reveals novel DNA recognition and cooperative binding to a tandem repeat of core sequences. *Embo J.* 1999;18(18):5028–5041.
344. Chen W, Royer Jr. WE. Structural insights into interferon regulatory factor activation. *Cell. Signal.* 2010;22(6):883–887.
345. Koetzler R, Zaheer RS, Newton R, Proud D. Nitric oxide inhibits IFN regulatory factor 1 and nuclear factor-kappaB pathways in rhinovirus-infected epithelial cells. *J. Allergy Clin. Immunol.* 2009;124(3):551–557.
346. Kotla S, Peng T, Bumgarner RE, Gustin KE. Attenuation of the type I interferon response in cells infected with human rhinovirus. *Virology*. 2008;374(2):399–410.
347. Drahos J, Racaniello VR. Cleavage of IPS-1 in cells infected with human rhinovirus. *J. Virol.* 2009;83(22):11581–11587.
348. Levy DE, Darnell JE. STATs: transcriptional control and biological impact. *Nat Rev Mol Cell Biol.* 2002;3(9):651–662.
349. Shuai K, Liu B. Regulation of JAK-STAT signalling in the immune system. *Nat. Rev. Immunol.* 2003;3(11):900–911.
350. Shuai K, Schindler C, Prezioso VR, Darnell JE Jr. Activation of transcription by IFN-gamma: tyrosine phosphorylation of a 91-kD DNA binding protein. *Science*. 1992;258(5089):1808–1812.
351. Horvath CM, Stark GR, Kerr IM, Darnell JE Jr. Interactions between STAT and non-STAT proteins in the interferon-stimulated gene factor 3 transcription complex. *Mol. Cell. Biol.* 1996;16(12):6957–6964.
352. Schindler C, Shuai K, Prezioso VR, Darnell JE Jr. Interferon-dependent tyrosine phosphorylation of a latent cytoplasmic transcription factor. *Science*. 1992;257(5071):809–813.

353. Fu XY, Kessler DS, Veals SA, Levy DE, Darnell JE Jr. ISGF3, the transcriptional activator induced by interferon alpha, consists of multiple interacting polypeptide chains. *Proc. Natl. Acad. Sci. U. S. A.* 1990;87(21):8555–8559.
354. Schindler C, Fu XY, Improtta T, Aebersold R, Darnell JE Jr. Proteins of transcription factor ISGF-3: one gene encodes the 91- and 84-kDa ISGF-3 proteins that are activated by interferon alpha. *Proc. Natl. Acad. Sci. U. S. A.* 1992;89(16):7836–7839.
355. Eddleston J, Lee RU, Doerner AM, Herschbach J, Zuraw BL. Cigarette smoke decreases innate responses of epithelial cells to rhinovirus infection. *Am. J. Respir. Cell Mol. Biol.* 2011;44(1):118–126.
356. Ramaswamy M, Shi L, Varga SM, Barik S, Behlke MA, Look DC. Respiratory syncytial virus nonstructural protein 2 specifically inhibits type I interferon signal transduction. *Virology.* 2006;344(2):328–339.
357. Oshansky CM, Krunkosky TM, Barber J, Jones LP, Tripp RA. Respiratory syncytial virus proteins modulate suppressors of cytokine signaling 1 and 3 and the type I interferon response to infection by a toll-like receptor pathway. *Viral Immunol.* 2009;22(3):147–161.
358. Kong X, San Juan H, Kumar M, et al. Respiratory syncytial virus infection activates STAT signaling in human epithelial cells. *Biochem. Biophys. Res. Commun.* 2003;306(2):616–622.
359. Korpi-Steiner NL, Bates ME, Lee W-M, Hall DJ, Bertics PJ. Human rhinovirus induces robust IP-10 release by monocytic cells, which is independent of viral replication but linked to type I interferon receptor ligation and STAT1 activation. *J. Leukoc. Biol.* 2006;80(6):1364–1374.
360. Xu M, Mizoguchi I, Morishima N, Chiba Y, Mizuguchi J, Yoshimoto T. Regulation of antitumor immune responses by the IL-12 family cytokines, IL-12, IL-23, and IL-27. *Clin. Dev. Immunol.* 2010;2010.
361. Furth PA, Nakles RE, Millman S, Diaz-Cruz ES, Cabrera MC. Signal transducer and activator of transcription 5 as a key signaling pathway in normal mammary gland developmental biology and breast cancer. *Breast Cancer Res. Bcr.* 2011;13(5):220.
362. Barash I. Stat5 in the mammary gland: controlling normal development and cancer. *J. Cell. Physiol.* 2006;209(2):305–313.
363. Barnstein BO, Li G, Wang Z, et al. Stat5 expression is required for IgE-mediated mast cell function. *J. Immunol. Baltim. Md 1950.* 2006;177(5):3421–3426.

364. Shelburne CP, McCoy ME, Piekorz R, et al. Stat5: an essential regulator of mast cell biology. *Mol. Immunol.* 2002;38(16-18):1187–1191.
365. Maier E, Duschl A, Horejs-Hoeck J. STAT6-dependent and -independent mechanisms in Th2 polarization. *Eur. J. Immunol.* 2012;42(11):2827–2833.
366. Chen H, Sun H, You F, et al. Activation of STAT6 by STING Is Critical for Antiviral Innate Immunity. *Cell.* 2011;147(2):436–446.
367. Mullings RE, Wilson SJ, Puddicombe SM, et al. Signal transducer and activator of transcription 6 (STAT-6) expression and function in asthmatic bronchial epithelium. *J. Allergy Clin. Immunol.* 2001;108(5):832–838.
368. Matsukura S, Stellato C, Georas SN, et al. Interleukin-13 upregulates eotaxin expression in airway epithelial cells by a STAT6-dependent mechanism. *Am. J. Respir. Cell Mol. Biol.* 2001;24(6):755–761.
369. Anderson P. Post-transcriptional control of cytokine production. *Nat. Immunol.* 2008;9(4):353–359.
370. Stumpo DJ, Lai WS, Blackshear PJ. Inflammation: cytokines and RNA-based regulation. *Wiley Interdiscip. Rev. Rna.* 2010;1(1):60–80.
371. Hamilton T, Novotny M, Pavicic PJ Jr, et al. Diversity in post-transcriptional control of neutrophil chemoattractant cytokine gene expression. *Cytokine.* 2010;52(1-2):116–122.
372. Chen CY, Shyu AB. AU-rich elements: characterization and importance in mRNA degradation. *Trends Biochem. Sci.* 1995;20(11):465–470.
373. Khabar KSA. Post-transcriptional control during chronic inflammation and cancer: a focus on AU-rich elements. *Cell. Mol. Life Sci.* 2010;67(17):2937–2955.
374. Garneau NL, Wilusz J, Wilusz CJ. The highways and byways of mRNA decay. *Nat. Rev. Mol. Cell Biol.* 2007;8(2):113–126.
375. Stoecklin G, Anderson P. Posttranscriptional mechanisms regulating the inflammatory response. *Adv. Immunol.* 2006;89:1–37.
376. Wilusz CJ, Wilusz J. Bringing the role of mRNA decay in the control of gene expression into focus. *Trends Genet. Tig.* 2004;20(10):491–497.
377. Chen CY, Gherzi R, Ong SE, et al. AU binding proteins recruit the exosome to degrade ARE-containing mRNAs. *Cell.* 2001;107(4):451–464.

378. Wang Z, Kiledjian M. Functional link between the mammalian exosome and mRNA decapping. *Cell*. 2001;107(6):751–762.
379. Mukherjee D, Gao M, O'Connor JP, et al. The mammalian exosome mediates the efficient degradation of mRNAs that contain AU-rich elements. *Embo J*. 2002;21(1-2):165–174.
380. Sandler H, Stoecklin G. Control of mRNA decay by phosphorylation of tristetraprolin. *Biochem. Soc. Trans*. 2008;36(Pt 3):491–496.
381. Fan J, Heller NM, Gorospe M, Atasoy U, Stellato C. The role of post-transcriptional regulation in chemokine gene expression in inflammation and allergy. *Eur. Respir. J. Off. J. Eur. Soc. Clin. Respir. Physiol*. 2005;26(5):933–947.
382. Palanisamy V, Park NJ, Wang J, Wong DT. AUF1 and HuR proteins stabilize interleukin-8 mRNA in human saliva. *J. Dent. Res*. 2008;87(8):772–776.
383. Winzen R, Thakur BK, Dittrich-Breiholz O, et al. Functional analysis of KSRP interaction with the AU-rich element of interleukin-8 and identification of inflammatory mRNA targets. *Mol. Cell. Biol*. 2007;27(23):8388–8400.
384. Suswam EA, Nabors LB, Huang Y, Yang X, King PH. IL-1beta induces stabilization of IL-8 mRNA in malignant breast cancer cells via the 3' untranslated region: Involvement of divergent RNA-binding factors HuR, KSRP and TIAR. *Int. J. Cancer J. Int. Cancer*. 2005;113(6):911–919.
385. Wang S, Zhang J, Zhang Y, Kern S, Danner RL. Nitric oxide-p38 MAPK signaling stabilizes mRNA through AU-rich element-dependent and -independent mechanisms. *J. Leukoc. Biol*. 2008;83(4):982–990.
386. Winzen R, Gowrishankar G, Bollig F, Redich N, Resch K, Holtmann H. Distinct domains of AU-rich elements exert different functions in mRNA destabilization and stabilization by p38 mitogen-activated protein kinase or HuR. *Mol. Cell. Biol*. 2004;24(11):4835–4847.
387. Bhattacharyya S, Gutti U, Mercado J, Moore C, Pollard HB, Biswas R. MAPK signaling pathways regulate IL-8 mRNA stability and IL-8 protein expression in cystic fibrosis lung epithelial cell lines. *Am. J. Physiol. Lung Cell. Mol. Physiol*. 2011;300(1):L81–87.
388. Balakathiresan NS, Bhattacharyya S, Gutti U, et al. Tristetraprolin regulates IL-8 mRNA stability in cystic fibrosis lung epithelial cells. *Am. J. Physiol. Lung Cell. Mol. Physiol*. 2009;296(6):L1012–1018.

389. King EM, Kaur M, Gong W, Rider CF, Holden NS, Newton R. Regulation of tristetraprolin expression by interleukin-1 beta and dexamethasone in human pulmonary epithelial cells: roles for nuclear factor-kappa B and p38 mitogen-activated protein kinase. *J. Pharmacol. Exp. Ther.* 2009;330(2):575–585.
390. Raineri I, Wegmueller D, Gross B, Certa U, Moroni C. Roles of AUF1 isoforms, HuR and BRF1 in ARE-dependent mRNA turnover studied by RNA interference. *Nucleic Acids Res.* 2004;32(4):1279–1288.
391. Gherzi R, Lee K-Y, Briata P, et al. A KH domain RNA binding protein, KSRP, promotes ARE-directed mRNA turnover by recruiting the degradation machinery. *Mol. Cell.* 2004;14(5):571–583.
392. Linker K, Pautz A, Fechir M, Hubrich T, Greeve J, Kleinert H. Involvement of KSRP in the post-transcriptional regulation of human iNOS expression-complex interplay of KSRP with TTP and HuR. *Nucleic Acids Res.* 2005;33(15):4813–4827.
393. Chou C-F, Mulky A, Maitra S, et al. Tethering KSRP, a decay-promoting AU-rich element-binding protein, to mRNAs elicits mRNA decay. *Mol. Cell. Biol.* 2006;26(10):3695–3706.
394. Briata P, Forcales SV, Ponassi M, et al. p38-dependent phosphorylation of the mRNA decay-promoting factor KSRP controls the stability of select myogenic transcripts. *Mol. Cell.* 2005;20(6):891–903.
395. Fan J, Ishmael FT, Fang X, et al. Chemokine transcripts as targets of the RNA-binding protein HuR in human airway epithelium. *J. Immunol. Baltim. Md 1950.* 2011;186(4):2482–2494.
396. Hinman MN, Lou H. Diverse molecular functions of Hu proteins. *Cell. Mol. Life Sci. Cmls.* 2008;65(20):3168–3181.
397. Fan XC, Steitz JA. Overexpression of HuR, a nuclear-cytoplasmic shuttling protein, increases the in vivo stability of ARE-containing mRNAs. *Embo J.* 1998;17(12):3448–3460.
398. Peng SS, Chen CY, Xu N, Shyu AB. RNA stabilization by the AU-rich element binding protein, HuR, an ELAV protein. *Embo J.* 1998;17(12):3461–3470.
399. Lal A, Mazan-Mamczarz K, Kawai T, Yang X, Martindale JL, Gorospe M. Concurrent versus individual binding of HuR and AUF1 to common labile target mRNAs. *Embo J.* 2004;23(15):3092–3102.

400. Bhattacharyya SN, Habermacher R, Martine U, Closs EI, Filipowicz W. Relief of microRNA-mediated translational repression in human cells subjected to stress. *Cell*. 2006;125(6):1111–1124.
401. Brennan CM, Steitz JA. HuR and mRNA stability. *Cell. Mol. Life Sci. Cmls*. 2001;58(2):266–277.
402. Dean JLE, Sully G, Clark AR, Saklatvala J. The involvement of AU-rich element-binding proteins in p38 mitogen-activated protein kinase pathway-mediated mRNA stabilisation. *Cell. Signal*. 2004;16(10):1113–1121.
403. Doller A, Pfeilschifter J, Eberhardt W. Signalling pathways regulating nucleocytoplasmic shuttling of the mRNA-binding protein HuR. *Cell. Signal*. 2008;20(12):2165–2173.
404. Jin SH, Kim TI, Yang KM, Kim WH. Thalidomide destabilizes cyclooxygenase-2 mRNA by inhibiting p38 mitogen-activated protein kinase and cytoplasmic shuttling of HuR. *Eur. J. Pharmacol*. 2007;558(1-3):14–20.
405. Blackshear PJ. Tristetraprolin and other CCCH tandem zinc-finger proteins in the regulation of mRNA turnover. *Biochem. Soc. Trans*. 2002;30(Pt 6):945–952.
406. Lu J-Y, Schneider RJ. Tissue distribution of AU-rich mRNA-binding proteins involved in regulation of mRNA decay. *J. Biol. Chem*. 2004;279(13):12974–12979.
407. Lai WS, Kennington EA, Blackshear PJ. Tristetraprolin and its family members can promote the cell-free deadenylation of AU-rich element-containing mRNAs by poly(A) ribonuclease. *Mol. Cell. Biol*. 2003;23(11):3798–3812.
408. Zhu W, Brauchle MA, Di Padova F, et al. Gene suppression by tristetraprolin and release by the p38 pathway. *Am. J. Physiol. Lung Cell. Mol. Physiol*. 2001;281(2):L499–508.
409. Yang IV, Schwartz DA. Epigenetic Control of Gene Expression in the Lung. *Am. J. Respir. Crit. Care Med*. 2011;183(10):1295–1301.
410. Boffelli D, Martin DIK. Epigenetic inheritance: a contributor to species differentiation? *Dna Cell Biol*. 2012;31 Suppl 1:S11–16.
411. Bell O, Tiwari VK, Thomä NH, Schübeler D. Determinants and dynamics of genome accessibility. *Nat. Rev. Genet*. 2011;12(8):554–564.
412. Adcock IM, Ito K, Barnes PJ. Histone deacetylation: an important mechanism in inflammatory lung diseases. *COPD*. 2005;2(4):445–455.

413. Barnes PJ, Adcock IM, Ito K. Histone acetylation and deacetylation: importance in inflammatory lung diseases. *Eur. Respir. J. Off. J. Eur. Soc. Clin. Respir. Physiol.* 2005;25(3):552–563.
414. Adcock IM, Tsaprouni L, Bhavsar P, Ito K. Epigenetic regulation of airway inflammation. *Curr. Opin. Immunol.* 2007;19(6):694–700.
415. Rajendrasozhan S, Yao H, Rahman I. Current perspectives on role of chromatin modifications and deacetylases in lung inflammation in COPD. *COPD.* 2009;6(4):291–297.
416. Finkel T, Deng C-X, Mostoslavsky R. Recent progress in the biology and physiology of sirtuins. *Nature.* 2009;460(7255):587–591.
417. Breton CV, Byun H-M, Wenten M, Pan F, Yang A, Gilliland FD. Prenatal tobacco smoke exposure affects global and gene-specific DNA methylation. *Am. J. Respir. Crit. Care Med.* 2009;180(5):462–467.
418. Schembri F, Sridhar S, Perdomo C, et al. MicroRNAs as modulators of smoking-induced gene expression changes in human airway epithelium. *Proc. Natl. Acad. Sci. U. S. A.* 2009;106(7):2319–2324.
419. Rajendrasozhan S, Yang S-R, Edirisinghe I, Yao H, Adenuga D, Rahman I. Deacetylases and NF-kappaB in redox regulation of cigarette smoke-induced lung inflammation: epigenetics in pathogenesis of COPD. *Antioxidants Redox Signal.* 2008;10(4):799–811.
420. Barnes PJ. Histone deacetylase-2 and airway disease. *Ther. Adv. Respir. Dis.* 2009;3(5):235–243.
421. Ito K, Ito M, Elliott WM, et al. Decreased histone deacetylase activity in chronic obstructive pulmonary disease. *N. Engl. J. Med.* 2005;352(19):1967–1976.
422. Adenuga D, Yao H, March TH, Seagrave J, Rahman I. Histone Deacetylase 2 Is Phosphorylated, Ubiquitinated, and Degraded by Cigarette Smoke. *Am. J. Respir. Cell Mol. Biol.* 2009;40(4):464–473.
423. Yang S-R, Chida AS, Bauter MR, et al. Cigarette smoke induces proinflammatory cytokine release by activation of NF-kappaB and posttranslational modifications of histone deacetylase in macrophages. *Am. J. Physiol. Lung Cell. Mol. Physiol.* 2006;291(1):L46–57.
424. Ito K, Lim S, Caramori G, Chung KF, Barnes PJ, Adcock IM. Cigarette smoking reduces histone deacetylase 2 expression, enhances cytokine expression, and inhibits glucocorticoid actions in alveolar macrophages. *Faseb J.* 2001;15(6):1110–1112.

425. Marwick JA, Kirkham PA, Stevenson CS, et al. Cigarette smoke alters chromatin remodeling and induces proinflammatory genes in rat lungs. *Am. J. Respir. Cell Mol. Biol.* 2004;31(6):633–642.
426. Rajendrasozhan S, Yang S-R, Kinnula VL, Rahman I. SIRT1, an antiinflammatory and antiaging protein, is decreased in lungs of patients with chronic obstructive pulmonary disease. *Am. J. Respir. Crit. Care Med.* 2008;177(8):861–870.
427. Osoata GO, Yamamura S, Ito M, et al. Nitration of distinct tyrosine residues causes inactivation of histone deacetylase 2. *Biochem. Biophys. Res. Commun.* 2009;384(3):366–371.
428. Churchill L, Chilton FH, Resau JH, Bascom R, Hubbard WC, Proud D. Cyclooxygenase metabolism of endogenous arachidonic acid by cultured human tracheal epithelial cells. *Am. Rev. Respir. Dis.* 1989;140(2):449–459.
429. Reddel RR, Ke Y, Gerwin BI, et al. Transformation of human bronchial epithelial cells by infection with SV40 or adenovirus-12 SV40 hybrid virus, or transfection via strontium phosphate coprecipitation with a plasmid containing SV40 early region genes. *Cancer Res.* 1988;48(7):1904–1909.
430. Fields B, ed. *Fields' Virology*. 3rd Edition. Philadelphia: Lippincott-Raven; 1996.
431. Reed, Muench H. A Simple Method Of Estimating Fifty Per Cent Endpoints. *Am J Epidemiol.* 1938;27(3):493–497.
432. Wirtz HR, Schmidt M. Acute influence of cigarette smoke on secretion of pulmonary surfactant in rat alveolar type II cells in culture. *Eur. Respir. J. Off. J. Eur. Soc. Clin. Respir. Physiol.* 1996;9(1):24–32.
433. Kode A, Yang S-R, Rahman I. Differential effects of cigarette smoke on oxidative stress and proinflammatory cytokine release in primary human airway epithelial cells and in a variety of transformed alveolar epithelial cells. *Respir. Res.* 2006;7:132.
434. Mosmann T. Rapid colorimetric assay for cellular growth and survival: application to proliferation and cytotoxicity assays. *J. Immunol. Methods.* 1983;65(1-2):55–63.
435. Nachlas MM, Margulies SI, Goldberg JD, Seligman AM. The determination of lactic dehydrogenase with a tetrazolium salt. *Anal. Biochem.* 1960;1:317–326.
436. Chomczynski P, Sacchi N. Single-step method of RNA isolation by acid guanidinium thiocyanate-phenol-chloroform extraction. *Anal. Biochem.* 1987;162(1):156–159.

437. Chomczynski P, Sacchi N. The single-step method of RNA isolation by acid guanidinium thiocyanate-phenol-chloroform extraction: twenty-something years on. *Nat. Protoc.* 2006;1(2):581–585.
438. Livak KJ, Schmittgen TD. Analysis of Relative Gene Expression Data Using Real-Time Quantitative PCR and the 2- $^{-\Delta\Delta CT}$  Method. *Methods.* 2001;25(4):402–408.
439. Cuenda A, Rouse J, Doza YN, et al. SB 203580 is a specific inhibitor of a MAP kinase homologue which is stimulated by cellular stresses and interleukin-1. *Febs Lett.* 1995;364(2):229–233.
440. Bulletin\_6050.pdf. Available at: [http://www.biorad.com/webroot/web/pdf/lsr/literature/Bulletin\\_6050.pdf](http://www.biorad.com/webroot/web/pdf/lsr/literature/Bulletin_6050.pdf). Accessed July 24, 2012.
441. Coward WR, Watts K, Feghali-Bostwick CA, Jenkins G, Pang L. Repression of IP-10 by interactions between histone deacetylation and hypermethylation in idiopathic pulmonary fibrosis. *Mol. Cell. Biol.* 2010;30(12):2874–2886.
442. Fridy WW Jr, Ingram RH Jr, Hierholzer JC, Coleman MT. Airways function during mild viral respiratory illnesses. The effect of rhinovirus infection in cigarette smokers. *Ann. Intern. Med.* 1974;80(2):150–155.
443. Sajjan U, Ganesan S, Comstock AT, et al. Elastase- and LPS-exposed mice display altered responses to rhinovirus infection. *Am. J. Physiol. Lung Cell. Mol. Physiol.* 2009;297(5):L931–944.
444. Wang JH, Kim H, Jang YJ. Cigarette smoke extract enhances rhinovirus-induced toll-like receptor 3 expression and interleukin-8 secretion in A549 cells. *Am. J. Rhinol. Allergy.* 2009;23(6):e5–9.
445. Hudy MH, Traves SL, Wiehler S, Proud D. Cigarette smoke modulates rhinovirus-induced airway epithelial cell chemokine production. *Eur. Respir. J. Off. J. Eur. Soc. Clin. Respir. Physiol.* 2010;35(6):1256–1263.
446. Subauste MC, Jacoby DB, Richards SM, Proud D. Infection of a human respiratory epithelial cell line with rhinovirus. Induction of cytokine release and modulation of susceptibility to infection by cytokine exposure. *J. Clin. Invest.* 1995;96(1):549–557.
447. Johnston SL, Papi A, Bates PJ, Mastrorade JG, Monick MM, Hunninghake GW. Low grade rhinovirus infection induces a prolonged release of IL-8 in pulmonary epithelium. *J. Immunol. Baltim. Md 1950.* 1998;160(12):6172–6181.

448. Neville LF, Mathiak G, Bagasra O. The immunobiology of interferon-gamma inducible protein 10 kD (IP-10): a novel, pleiotropic member of the C-X-C chemokine superfamily. *Cytokine Growth Factor Rev.* 1997;8(3):207–219.
449. Government of Canada HC. What makes tobacco so addictive? 2005. Available at: <http://www.hc-sc.gc.ca/hc-ps/tobac-tabac/quit-cesser/now-maintenant/road-voie/addictive-dependance-eng.php>. Accessed May 10, 2013.
450. Benowitz NL. Cigarette smoking and nicotine addiction. *Med. Clin. North Am.* 1992;76(2):415–437.
451. Byrd GD, Davis RA, Ogden MW. A rapid LC-MS-MS method for the determination of nicotine and cotinine in serum and saliva samples from smokers: validation and comparison with a radioimmunoassay method. *J. Chromatogr. Sci.* 2005;43(3):133–140.
452. <http://www.ca.uky.edu/refcig/3R4F/Preliminary/Analysis.pdf>.
453. Rider CF, Miller-Larsson A, Proud D, Giembycz MA, Newton R. Modulation of transcriptional responses by poly(I:C) and human rhinovirus: Effect of long-acting  $\beta$ 2-adrenoceptor agonists. *Eur. J. Pharmacol.* 2013;708(1-3):60–67.
454. Papi A, Johnston SL. Rhinovirus infection induces expression of its own receptor intercellular adhesion molecule 1 (ICAM-1) via increased NF-kappaB-mediated transcription. *J. Biol. Chem.* 1999;274(14):9707–9720.
455. Laan M, Bozinovski S, Anderson GP. Cigarette smoke inhibits lipopolysaccharide-induced production of inflammatory cytokines by suppressing the activation of activator protein-1 in bronchial epithelial cells. *J. Immunol. Baltim. Md 1950.* 2004;173(6):4164–4170.
456. Li Y-T, He B, Wang Y-Z. Exposure to cigarette smoke upregulates AP-1 activity and induces TNF-alpha overexpression in mouse lungs. *Inhal. Toxicol.* 2009;21(7):641–647.
457. Rahman I, Smith CA, Lawson MF, Harrison DJ, MacNee W. Induction of gamma-glutamylcysteine synthetase by cigarette smoke is associated with AP-1 in human alveolar epithelial cells. *Febs Lett.* 1996;396(1):21–25.
458. Zhang Q, Adiseshaiah P, Reddy SP. Matrix Metalloproteinase/Epidermal Growth Factor Receptor/Mitogen-Activated Protein Kinase Signaling Regulate fra-1 Induction by Cigarette Smoke in Lung Epithelial Cells. *Am. J. Respir. Cell Mol. Biol.* 2005;32(1):72–81.
459. Zhao J, Harper R, Barchowsky A, Di YPP. Identification of multiple MAPK-mediated transcription factors regulated by tobacco smoke in airway epithelial cells. *Am. J. Physiol. Lung Cell. Mol. Physiol.* 2007;293(2):L480–490.

460. Di Stefano A, Caramori G, Oates T, et al. Increased expression of nuclear factor-kappaB in bronchial biopsies from smokers and patients with COPD. *Eur. Respir. J. Off. J. Eur. Soc. Clin. Respir. Physiol.* 2002;20(3):556–563.
461. Hellermann GR, Nagy SB, Kong X, Lockey RF, Mohapatra SS. Mechanism of cigarette smoke condensate-induced acute inflammatory response in human bronchial epithelial cells. *Respir. Res.* 2002;3:22.
462. Dhillon NK, Murphy WJ, Filla MB, Crespo AJ, Latham HA, O'Brien-Ladner A. Down modulation of IFN-[gamma] signaling in alveolar macrophages isolated from smokers. *Toxicol. Appl. Pharmacol.* 2009;237(1):22–28.
463. Williams R, Yao H, Dhillon NK, Buch SJ. HIV-1 Tat co-operates with IFN-gamma and TNF-alpha to increase CXCL10 in human astrocytes. *Plos One.* 2009;4(5):e5709.
464. STAT1alpha Monoclonal Antibody | MBL International. 2012. Available at: <http://www.mblintl.com/product/EP-7178>. Accessed April 15, 2013.
465. Guo J-J, Li Q, Zhang J, Huang A-L. Histone deacetylation is involved in activation of CXCL10 upon IFN-gamma stimulation. *Mol. Cells.* 2006;22(2):163–167.
466. Qureshi SA, Salditt-Georgieff M, Darnell JE Jr. Tyrosine-phosphorylated Stat1 and Stat2 plus a 48-kDa protein all contact DNA in forming interferon-stimulated-gene factor 3. *Proc. Natl. Acad. Sci. U. S. A.* 1995;92(9):3829–3833.
467. Kato H, Takeuchi O, Mikamo-Satoh E, et al. Length-dependent recognition of double-stranded ribonucleic acids by retinoic acid-inducible gene-I and melanoma differentiation-associated gene 5. *J. Exp. Med.* 2008;205(7):1601–1610.
468. Barbalat R, Ewald SE, Mouchess ML, Barton GM. Nucleic Acid Recognition by the Innate Immune System. *Annu. Rev. Immunol.* 2011;29(1):185–214.
469. Pichlmair A, Schulz O, Tan CP, et al. RIG-I-mediated antiviral responses to single-stranded RNA bearing 5'-phosphates. *Science.* 2006;314(5801):997–1001.
470. DeWitte-Orr SJ, Mehta DR, Collins SE, Suthar MS, Gale M Jr, Mossman KL. Long double-stranded RNA induces an antiviral response independent of IFN regulatory factor 3, IFN-beta promoter stimulator 1, and IFN. *J. Immunol. Baltim. Md 1950.* 2009;183(10):6545–6553.
471. Schmid S, Mordstein M, Kochs G, García-Sastre A, Tenoever BR. Transcription factor redundancy ensures induction of the antiviral state. *J. Biol. Chem.* 2010;285(53):42013–42022.

472. Elsharkawy AM, Oakley F, Lin F, Packham G, Mann DA, Mann J. The NF-kappaB p50:p50:HDAC-1 repressor complex orchestrates transcriptional inhibition of multiple pro-inflammatory genes. *J. Hepatol.* 2010;53(3):519–527.
473. Yasumoto K, Okamoto S, Mukaida N, Murakami S, Mai M, Matsushima K. Tumor necrosis factor alpha and interferon gamma synergistically induce interleukin 8 production in a human gastric cancer cell line through acting concurrently on AP-1 and NF-kB-like binding sites of the interleukin 8 gene. *J. Biol. Chem.* 1992;267(31):22506–22511.
474. Kim J, Sanders SP, Siekierski ES, Casolaro V, Proud D. Role of NF-kappa B in cytokine production induced from human airway epithelial cells by rhinovirus infection. *J. Immunol. Baltim. Md 1950.* 2000;165(6):3384–3392.
475. Didon L, Barton JL, Roos AB, et al. Lung epithelial CCAAT/enhancer-binding protein- $\beta$  is necessary for the integrity of inflammatory responses to cigarette smoke. *Am. J. Respir. Crit. Care Med.* 2011;184(2):233–242.
476. Miglino N, Roth M, Lardinois D, Sadowski C, Tamm M, Borger P. Cigarette smoke inhibits lung fibroblast proliferation by translational mechanisms. *Eur. Respir. J. Off. J. Eur. Soc. Clin. Respir. Physiol.* 2012;39(3):705–711.
477. Kent L, Smyth L, Clayton C, et al. Cigarette smoke extract induced cytokine and chemokine gene expression changes in COPD macrophages. *Cytokine.* 2008;42(2):205–216.
478. Swenson WG, Wuertz BRK, Ondrey FG. Tobacco carcinogen mediated up-regulation of AP-1 dependent pro-angiogenic cytokines in head and neck carcinogenesis. *Mol. Carcinog.* 2011;50(9):668–679.
479. Herfs M, Hubert P, Poirrier A-L, et al. Proinflammatory cytokines induce bronchial hyperplasia and squamous metaplasia in smokers: implications for chronic obstructive pulmonary disease therapy. *Am. J. Respir. Cell Mol. Biol.* 2012;47(1):67–79.
480. Walters MJ, Paul-Clark MJ, McMaster SK, Ito K, Adcock IM, Mitchell JA. Cigarette smoke activates human monocytes by an oxidant-AP-1 signaling pathway: implications for steroid resistance. *Mol. Pharmacol.* 2005;68(5):1343–1353.
481. Lau C, Castellanos P, Raney D, Wang X, Chow C-W. HRV signaling in airway epithelial cells is regulated by ITAM-mediated recruitment and activation of Syk. *Protein Pept. Lett.* 2011;18(5):518–529.
482. Wang X, Lau C, Wiehler S, et al. Syk is downstream of intercellular adhesion molecule-1 and mediates human rhinovirus activation of p38 MAPK in airway epithelial cells. *J. Immunol. Baltim. Md 1950.* 2006;177(10):6859–6870.

483. Volpi G, Facchinetti F, Moretto N, Civelli M, Patacchini R. Cigarette smoke and  $\alpha,\beta$ -unsaturated aldehydes elicit VEGF release through the p38 MAPK pathway in human airway smooth muscle cells and lung fibroblasts. *Br. J. Pharmacol.* 2011;163(3):649–661.
484. Moretto N, Facchinetti F, Southworth T, Civelli M, Singh D, Patacchini R.  $\alpha,\beta$ -Unsaturated aldehydes contained in cigarette smoke elicit IL-8 release in pulmonary cells through mitogen-activated protein kinases. *Am. J. Physiol. Lung Cell. Mol. Physiol.* 2009;296(5):L839–848.
485. Moretto N, Bertolini S, Iadicicco C, et al. Cigarette smoke and its component acrolein augment IL-8/CXCL8 mRNA stability via p38 MAPK/MK2 signalling in human pulmonary cells. *Am. J. Physiol. Lung Cell. Mol. Physiol.* 2012.
486. Beisswenger C, Platz J, Seifart C, Vogelmeier C, Bals R. Exposure of differentiated airway epithelial cells to volatile smoke in vitro. *Respir. Int. Rev. Thorac. Dis.* 2004;71(4):402–409.
487. Rattenbacher B, Bohjanen PR. Evaluating Posttranscriptional Regulation of Cytokine Genes. In: De Ley M, ed. *Cytokine Protocols*. Vol 820. New York, NY: Springer New York; 2012:71–89.
488. Davies SP, Reddy H, Caivano M, Cohen P. Specificity and mechanism of action of some commonly used protein kinase inhibitors. *Biochem. J.* 2000;351(Pt 1):95–105.
489. Kunsch C, Rosen CA. NF-kappa B subunit-specific regulation of the interleukin-8 promoter. *Mol. Cell. Biol.* 1993;13(10):6137–6146.
490. Atasoy U, Watson J, Patel D, Keene JD. ELAV protein HuA (HuR) can redistribute between nucleus and cytoplasm and is upregulated during serum stimulation and T cell activation. *J. Cell Sci.* 1998;111 ( Pt 21):3145–3156.
491. Shanmugam N, Ransohoff RM, Natarajan R. Interferon-gamma-inducible protein (IP)-10 mRNA stabilized by RNA-binding proteins in monocytes treated with S100b. *J. Biol. Chem.* 2006;281(42):31212–31221.
492. Sheikh AM, Ochi H, Manabe A, Masuda J. Lysophosphatidylcholine posttranscriptionally inhibits interferon-gamma-induced IP-10, Mig and I-Tac expression in endothelial cells. *Cardiovasc. Res.* 2005;65(1):263–271.
493. Sun D, Ding A. MyD88-mediated stabilization of interferon-gamma-induced cytokine and chemokine mRNA. *Nat. Immunol.* 2006;7(4):375–381.

494. Valledor AF, Sánchez-Tilló E, Arpa L, et al. Selective roles of MAPKs during the macrophage response to IFN-gamma. *J. Immunol. Baltim. Md 1950*. 2008;180(7):4523–4529.
495. Vockerodt M, Pinkert D, Smola-Hess S, et al. The Epstein-Barr virus oncoprotein latent membrane protein 1 induces expression of the chemokine IP-10: importance of mRNA half-life regulation. *Int. J. Cancer J. Int. Cancer*. 2005;114(4):598–605.
496. Nagathihalli NS, Massion PP, Gonzalez AL, Lu P, Datta PK. Smoking Induces Epithelial-to-Mesenchymal Transition in Non-Small Cell Lung Cancer through HDAC-Mediated Downregulation of E-cadherin. *Mol. Cancer Ther*. 2012.
497. Smith LA, Paszkiewicz GM, Hutson AD, Pauly JL. Inflammatory response of lung macrophages and epithelial cells to tobacco smoke: a literature review of ex vivo investigations. *Immunol. Res*. 2010;46(1-3):94–126.
498. Korpi-Steiner NL, Valkenaar SM, Bates ME, Evans MD, Gern JE, Bertics PJ. Human monocytic cells direct the robust release of CXCL10 by bronchial epithelial cells during rhinovirus infection. *Clin. Exp. Allergy J. Br. Soc. Allergy Clin. Immunol*. 2010;40(8):1203–1213.
499. Gern JE, Dick EC, Lee WM, et al. Rhinovirus enters but does not replicate inside monocytes and airway macrophages. *J. Immunol. Baltim. Md 1950*. 1996;156(2):621–627.
500. Hall DJ, Bates ME, Guar L, Cronan M, Korpi N, Bertics PJ. The role of p38 MAPK in rhinovirus-induced monocyte chemoattractant protein-1 production by monocytic-lineage cells. *J. Immunol. Baltim. Md 1950*. 2005;174(12):8056–8063.
501. Bartlett NW, Walton RP, Edwards MR, et al. Mouse models of rhinovirus-induced disease and exacerbation of allergic airway inflammation. *Nat. Med*. 2008;14(2):199–204.
502. Newcomb DC, Sajjan US, Nagarkar DR, et al. Human rhinovirus 1B exposure induces phosphatidylinositol 3-kinase-dependent airway inflammation in mice. *Am. J. Respir. Crit. Care Med*. 2008;177(10):1111–1121.
503. Nagarkar DR, Wang Q, Shim J, et al. CXCR2 is required for neutrophilic airway inflammation and hyperresponsiveness in a mouse model of human rhinovirus infection. *J. Immunol. Baltim. Md 1950*. 2009;183(10):6698–6707.
504. Nagarkar DR, Bowman ER, Schneider D, et al. Rhinovirus infection of allergen-sensitized and -challenged mice induces eotaxin release from functionally polarized macrophages. *J. Immunol. Baltim. Md 1950*. 2010;185(4):2525–2535.

505. Ohmori Y, Hamilton TA. A macrophage LPS-inducible early gene encodes the murine homologue of IP-10. *Biochem. Biophys. Res. Commun.* 1990;168(3):1261–1267.
506. Bozic CR, Gerard NP, von Uexkull-Guldenband C, et al. The murine interleukin 8 type B receptor homologue and its ligands. Expression and biological characterization. *J. Biol. Chem.* 1994;269(47):29355–29358.
507. Rosenthal N, Brown S. The mouse ascending: perspectives for human-disease models. *Nat. Cell Biol.* 2007;9(9):993–999.
508. Kips JC, Anderson GP, Fredberg JJ, et al. Murine models of asthma. *Eur. Respir. J. Off. J. Eur. Soc. Clin. Respir. Physiol.* 2003;22(2):374–382.
509. Gueders MM, Paulissen G, Crahay C, et al. Mouse models of asthma: a comparison between C57BL/6 and BALB/c strains regarding bronchial responsiveness, inflammation, and cytokine production. *Inflamm. Res. Off. J. Eur. Histamine Res. Soc. Al.* 2009;58(12):845–854.
510. Takeda K, Gelfand EW. Mouse models of allergic diseases. *Curr. Opin. Immunol.* 2009;21(6):660–665.
511. Zosky GR, Sly PD. Animal models of asthma. *Clin. Exp. Allergy J. Br. Soc. Allergy Clin. Immunol.* 2007;37(7):973–988.
512. Allen JE, Bischof RJ, Suec Chang H-Y, et al. Animal models of airway inflammation and airway smooth muscle remodelling in asthma. *Pulm. Pharmacol. Ther.* 2009;22(5):455–465.
513. Stevenson CS, Birrell MA. Moving towards a new generation of animal models for asthma and COPD with improved clinical relevance. *Pharmacol. Ther.* 2011;130(2):93–105.
514. Mallia P, Message SD, Gielen V, et al. Experimental rhinovirus infection as a human model of chronic obstructive pulmonary disease exacerbation. *Am. J. Respir. Crit. Care Med.* 2011;183(6):734–742.
515. Schneider D, Ganesan S, Comstock AT, et al. Increased cytokine response of rhinovirus-infected airway epithelial cells in chronic obstructive pulmonary disease. *Am. J. Respir. Crit. Care Med.* 2010;182(3):332–340.

## Appendix A: PUBLICATIONS LIST

### Peer Reviewed Journals

**Hudy MH**, Traves SL, Wiehler S, Proud D. Cigarette smoke modulates rhinovirus-induced airway epithelial cell chemokine production. *Eur. Respir. J.* 2010;35(6):1256–1263.

*As primary author I was responsible for carrying out all of the experiments and data analysis. Dr. Suzanne Traves provided the CSE generation protocol and assisted during initial CSE preparation. Shahina Wiehler generated original CXCL10 and CXCL8 promoter-luciferase constructs in a pGL3 plasmid vector, which were transferred by me to the current pGL4 plasmid vector. The first draft of this manuscript was written by me and edited in conjunction with Dr. Suzanne L. Traves, Shahina Wiehler and Dr. David Proud .*

Proud D, **Hudy MH**, Wiehler S, et al. Cigarette smoke modulates expression of human rhinovirus-induced airway epithelial host defense genes. *PLoS ONE.* 2012;7(7):e40762.

*As a co-author, my contribution included carrying out a portion of the experiments and data analysis, specifically including data in Figure 1 (A-D), Figure 2 (A-C) and Figure 5 (D). The manuscript was written in conjunction with Dr. David Proud and Dr. Richard Leigh and edited in conjunction with the remaining authors.*

### Abstracts

**Hudy M.H.**, Proud D. Transcriptional and Epigenetic Modulation of Human Rhinovirus-Induced CXCL10 by Cigarette Smoke Extract. *Am. J. Respir. Crit. Care Med.* Abstract in press, 2013.

**Hudy M.H.**, Proud D. Mechanisms Of Human Rhinovirus-Induced CXCL10 Inhibition By Cigarette Smoke. *Am. J. Respir. Crit. Care Med.* 185: A1435, 2012.

**Hudy M.H.**, Proud D. Mechanisms Of CXCL8 Enhancement By The Combination Of Human Rhinovirus And Cigarette Smoke. *Am. J. Respir. Crit. Care Med.* 185: A2007, 2012.

**Hudy M.H.**, Zaheer R.S., Pelikan J.B., Wiehler S., Proud D. Mechanisms of Human Rhinovirus-Induced CXCL10 Inhibition by Cigarette Smoke. *Am. J. Respir. Crit. Care Med.* 183: A2760, 2011.

Zaheer R.S., **Hudy M.H.**, Pelikan J.B., Wiehler S., Proud D. Modulation of human rhinovirus (HRV)-induced expression of the ubiquitin-like modifier, ISG15, by cigarette smoke extract (CSE) in human bronchial epithelial cells. *Am. J. Respir. Crit. Care Med.* 183: A2758, 2011.

Pelikan J.B., Wiehler S., Zaheer R.S., **Hudy M.H.**, Proud D. Cigarette Smoke Inhibits Human Rhinovirus-Induced Viperin Expression in Airway Epithelial Cells. *Am. J. Respir. Crit. Care Med.* 183: A2759, 2011.

Walker B.L., Zaheer R.S., **Hudy M.H.**, Pelikan J.B., Proud D. Human rhinovirus-induced ISG56 expression is inhibited by cigarette smoke in human airway epithelial cells. *Am. J. Respir. Crit. Care Med.* 183: A2764, 2011.

**Hudy M.H.**, Wiehler S., Traves S.L., Proud D. Modulation Of Human Rhinovirus (HRV)-Induced Airway Epithelial Cell Responses By Cigarette Smoke Extract (CSE). *Am. J. Respir. Crit. Care Med.* **181**: A4234, 2010.

**Hudy M.H.**, Traves S.L., Proud D, Modulation of rhinovirus (HRV)-induced airway epithelial cell responses by cigarette smoke extract (CSE). *Am. J. Respir. Crit. Care Med.* 179: A4262, 2009.

## Appendix B: COPYRIGHT PERMISSION

Copyright permission for data published in:

Hudy MH, Traves SL, Wiehler S, Proud D. Cigarette smoke modulates rhinovirus-induced airway epithelial cell chemokine production. *Eur. Respir. J.* 2010;35(6):1256–1263.

Dear Magda,

Thank you for your enquiry.

We are happy to grant you permission to use our material in your thesis, but unfortunately we cannot allow onward commercial sales and distribution. Permission is granted for the material to be used in a limited way – for instance for your thesis only or for a certain number of reprints only. To accommodate the non-exclusive license required by Library and Archives Canada would mean rescinding our copyright of the material, which is not possible. ERS retains copyright of the material unless the authors of the manuscript were granted non-exclusive copyright at publication.

I am sorry I cannot be of more assistance. If you have any queries please let me know.

Best wishes,

Sarah

On behalf of Kay

Kay Sharpe | European Respiratory Society | Publications Office | 442 Glossop Road | Sheffield | S10  
2PX | UK

Main Tel: +44 1142672860 | Direct Tel: +44 1142672861 | Fax: +44 1142665064 | E-mail:

kay.sharpe@ersj.org.uk

Copyright permission for data published in:

Proud D, Hudy MH, Wiehler S, et al. Cigarette smoke modulates expression of human rhinovirus-induced airway epithelial host defense genes. *PLoS ONE*. 2012;7(7):e40762.

This work was reprinted with permission based on the PLoS open-access license:  
Creative Commons Attribution 2.5 Generic License

(<http://creativecommons.org/licenses/by/2.5/legalcode>).